

Inaugural dissertation
for
obtaining the doctoral degree
of the
Combined Faculty of Mathematics, Engineering and Natural
Sciences
of the
Ruprecht - Karls - University
Heidelberg

presented by
Gnimah Eva Gnouamozi (M.Sc.)
born in: Milan, Italy

Oral examination: 07.03.24

**Characterization of hepatitis delta virus-like agents:
Insights into evolution, replication dynamics,
and host interactions**

Referees: Prof. Dr. Ursula Klingmüller
Prof. Dr. Stephan Urban

The applicant, Gnimah Eva Gnouamozi, declares that she is the sole author of the submitted dissertation and no other sources for help apart from those specifically referred to have been used. Additionally, the applicant declares that he has not applied for permission to enter the examination procedure at another institution, that this dissertation has not been presented to other faculty and has not been used in its current or in any other form in another examination.

Date

Signature

I. ABSTRACT

The human hepatitis delta virus (HDV) is a satellite RNA virus that depends on hepatitis B virus (HBV) surface proteins (HBsAg) to form infectious virions. For the past 40 years, the evolutionary history of HDV has remained largely unknown. Recent discoveries have revolutionized our knowledge of HDV biology. HDV-like agents were identified in a vast and heterogeneous group of vertebrates and invertebrates, highlighting that the evolution of HDV is more complex than previously foreseen and not restricted to humans as primary hosts.

Here, I focused on the characterization of HDV-like agents recently discovered in the woodchuck (*Marmota monax*), the white-tailed deer (*Odocoileus virginianus*), the lesser dog-like bat (*Peropteryx macrotis*) and several species of duck (*Anas gracilis*, *Anas castanea*, *Anas superciliosa*) in terms of replication, viral spreading pathways and cellular permissiveness. Viral replication was initiated by transfecting constructs encoding 1.1-fold over-length antigenomic HDV-like agents (DLA) RNA into human and non-human hepatic and non-hepatic cell lines. A cell-division-mediated viral amplification assay demonstrated the capability of the novel HDV-like agents to replicate and propagate not exclusively in hepatic tissues and without the requirement of envelopment.

To elucidate whether the non-human HDV-like agents can exploit the envelope glycoproteins of hepadna- and other viruses to form infectious particles, I co-transfected cells with the respective expression constructs and plasmids encoding envelope proteins from different viruses. Strikingly, secretion of pseudo-typed virions capable of establishing infection in susceptible target cells was observed.

HDV replication activates interferon (IFN) responses via activation and sensing by MDA5 and LGP2. HDV-induced IFNs and exogenous IFN- α and - γ profoundly suppressed cell division-mediated HDV spread (CDMS) but had only a minor effect on already ongoing

HDV replication in resting cells. The discovery of HDV-like agents provides the chance to investigate the interplay between HDV and IFN response from an evolutionary perspective. However, appropriate cell culture models to investigate replication, host factor dependence and modes of spreading, are lacking.

In my study, I established a robust infection system for the HDV-like agents found in woodchuck (WoDV) and deer (DeDV), overcoming the challenge that they do not express a farnesylated large delta antigen (L-HDAg) and cannot be packaged by HBsAg. After verifying that these agents, as HDV, can propagate efficiently via CDMS, I packaged their genomes with HBsAg by trans-complementation of the HDV L-HDAg. The supernatant was used to infect HepaRG^{NTCP} non-targeted control (NT) and HepaRG^{NTCP} MDA5 and/or LGP2 knock-out (KO) cells always in comparison with HDV. As expected, the HDV replication led to IFN activation in HepaRG^{NTCP}NT but not MDA5/LGP2 KO cells. Accordingly, restriction of CDMS in HepaRG^{NTCP} NT was observed. In contrast, infection with WoDV and DeDV induced minor IFN response in HepaRG^{NTCP}NT cells, and the CDMS of these agents remained efficient independently of MDA5/LGP2 expression. Furthermore, the CDMS of WoDV and DeDV was not significantly affected by exogenous IFN treatment. Therefore, both agents not only lack a strong IFN activation but also display resistance to IFN treatment.

My doctoral thesis on the replication, assembly, transmission, and host tropism of novel HDV-like agents provides insights into the molecular biology, evolution, and virus-host interaction of this unique group of agents.

II. ZUSAMMENFASSUNG

Das humane Hepatitis-Delta-Virus (HDV) ist ein Satelliten-RNA-Virus, das zur Bildung infektiöser Virionen auf Oberflächenproteine des Hepatitis-B-Virus (HBV) angewiesen ist. In den vergangenen 40 Jahren war die Evolutionsgeschichte des HDV weitgehend unbekannt. Jüngste Entdeckungen haben unser Wissen über die HDV-Biologie revolutioniert. HDV-ähnliche Erreger wurden in einer großen und heterogenen Gruppe von Wirbeltieren und Wirbellosen identifiziert, was deutlich macht, dass die Evolution von HDV komplexer ist als bisher angenommen und sich nicht auf den Menschen als Primärwirt beschränkt.

Hier konzentrierte ich mich auf die Charakterisierung der Säugetier-Delta-Erreger die kürzlich im Murmeltier (*Marmota monax*), im Weißwedelhirsch (*Odocoileus virginianus*), in der Zwergfledermaus (*Peropteryx macrotis*) und in mehreren Entenarten *Anas gracilis*, *Anas castanea*, *Anas superciliosa*) entdeckt wurden, im Hinblick auf Replikation, virale Verbreitungswege und zelluläre Permissivität. Ich habe Expressionskonstrukte hergestellt, die für 1,1-fach überlange antigenomische RNA dieser delta-ähnlichen Erreger kodieren. Die virale Replikation wurde durch Transfektion der Konstrukte in menschliche und nicht-menschliche hepatische und nicht-hepatische Zelllinien initiiert. Ein durch Zellteilung vermittelter viraler Amplifikationstest zeigte die Fähigkeit der neuen delta-ähnlichen Erreger, sich nicht ausschließlich in hepatischem Gewebe zu replizieren und zu vermehren, ohne dass eine Umhüllung erforderlich ist.

Um herauszufinden, ob die nicht-menschlichen Delta-Erreger die Hüllglykoproteine von Hepadna- und anderen Viren zur Bildung infektiöser Partikel nutzen können, habe ich Zellen mit den entsprechenden Expressionskonstrukten und Plasmiden, die für Hüllproteine verschiedener Viren kodieren, co-transfiziert. Bemerkenswerterweise wurde die Sekretion von pseudotypisierten Virionen beobachtet, die in der Lage sind, eine Infektion in empfänglichen Zielzellen zu etablieren.

Die HDV-Replikation aktiviert Interferon (IFN)-Reaktionen, die durch MDA5 und LGP2 vermittelt werden. HDV-induzierte IFNs sowie exogenes IFN α und γ unterdrücken die durch Zellteilung vermittelte HDV-Ausbreitung (CDMS) erheblich, haben aber nur eine geringe Wirkung auf die bereits laufende HDV-Replikation in ruhenden Zellen. Die Entdeckung HDV-ähnlicher Erreger bietet die Möglichkeit, das Zusammenspiel zwischen HDV und IFN-Reaktion aus einer evolutionären Perspektive zu untersuchen. Es fehlt jedoch an geeigneten Zellkulturmodellen, um die Replikation, die Abhängigkeit von Wirtsfaktoren und die Ausbreitungsmodalitäten zu untersuchen.

In meiner Studie habe ich ein robustes Infektionssystem für die HDV-ähnlichen Erreger von Murmeltieren (WoDV) und Hirschen (DeDV) entwickelt. Dabei habe ich die Herausforderung gemeistert, dass sie kein farnesyliertes großes Delta-Antigen (L-HDAg) exprimieren und nicht von HBV-Hüllproteinen (HBsAg) verpackt werden können. Nachdem ich mich vergewissert hatte, dass sich diese Erreger wie HDV effizient über CDMS vermehren können, verpackte ich ihre Genome mit HBsAg durch Transkomplementierung des HDV-L-HDAg. Der Überstand wurde verwendet, um HepaRG^{NTCP}NT und HepaRG^{NTCP}-MDA5 und/oder -LGP2-Knock-out (KO) Zellen im Vergleich zu HDV zu infizieren. Wie erwartet, führte die HDV-Replikation zu einer IFN-Aktivierung in HepaRG^{NTCP}NT, nicht aber in -MDA5/LGP2-KO-Zellen. Dementsprechend wurde eine Einschränkung der CDMS in HepaRG^{NTCP} NT beobachtet. Im Gegensatz dazu löste eine Infektion mit WoDV und DeDV eine geringere IFN-Antwort in HepaRG^{NTCP} NT-Zellen aus, und die CDMS dieser Wirkstoffe blieb unabhängig von der MDA5/LGP2-Expression wirksam. Darüber hinaus wurde die CDMS von WoDV und DeDV durch eine exogene IFN-Behandlung nicht wesentlich beeinträchtigt. Daher fehlt beiden Wirkstoffen nicht nur eine starke IFN-Aktivierung, sondern sie sind auch resistent gegenüber einer IFN-Behandlung.

Meine Doktorarbeit über die Replikation, den Aufbau, die Übertragung und den Wirtstropismus neuartiger HDV-ähnlicher Erreger bietet Einblicke in die Molekularbiologie, die Evolution und die Virus-Wirt-Interaktion dieser einzigartigen Gruppe von Viren.

III. TABLE OF CONTENTS

I.	Abstract	7
II.	Zusammenfassung	9
III.	Table of Contents	11
IV.	List of abbreviations	14
1.	Introduction	19
1.1	HEPATITIS VIRUSES	19
1.1.2.	Historical background of hepatitis viruses	25
1.1.3.	Reservoirs for hepatitis viruses in non-human hosts.....	27
1.2	THE HUMAN HEPATITIS DELTA VIRUS.....	30
1.2.1.	The discovery of HDV, much more than just a novel HBV antigen	30
1.2.2.	The genome structure of HDV.....	31
1.2.3.	HDV replication cycle.....	33
1.2.4.	HBV as helper virus.....	36
1.2.5.	An alternative spreading pathway: cell division- mediated spread.....	36
1.2.6.	HDV and innate immunity.....	37
1.2.7.	HDV evolution theories and similarity to viroids.....	41
1.3	DISCOVERIES IN HDV WORLD: HDV-LIKE AGENTS	43
1.3.1	The birth of the kolmioviridae family.....	43
1.3.2	Genome organization and antigen expression	46
1.3.3	Extracellular spread and transmission.....	48
1.3.4	Cellular tropism and tissue range.....	51
1.3.5	HDV-like agents and innate immunity.....	53
1.4	Research Aims and Approaches.....	54
2.	Materials and methods	56
2.1	Materials	56
2.1.1	Cell lines	56
2.1.2	Viruses and pseudoparticles.....	57
2.1.3	Antibodies.....	57
2.1.4	Peptides	59
2.1.5	Plasmids.....	59
2.1.6	Primers and oligos.....	60
2.1.7	Kits.....	62
2.1.8	Chemicals and reagents.....	63

2.1.9	Buffers and solutions.....	65
2.1.10	Enzymes.....	66
2.1.11	Technical devices.....	66
2.1.12	Software.....	66
2.2	Methods.....	67
2.2.1	Molecular cloning.....	67
2.2.2	Cell lines media and maintenance.....	70
2.2.3	Detection of RNA and DNA.....	75
2.2.4	Detection of protein.....	78
2.2.5	Fluorescence-activated cell sorting (FACS) for Atto-stain of hNTCP expressing cell lines.....	79
2.2.6	Taurocholate uptake assay.....	79
2.2.7	Synthesis of myristoylated peptides.....	80
2.2.8	Peptide binding assay binding assay.....	80
2.2.9	Protein prediction using Alpha fold program.....	80
2.2.10	Phylogenetic analysis.....	80
3.	Results.....	81
3.1	Replication, host range, and tissue permissiveness of HDV-like agents.....	81
3.1.1	Establishment of cDNA infectious clones of HDV-like agents.....	81
3.1.2	Generation and characterization of specific antibodies against AvDV antigen.....	85
3.1.3	Design of specific primers and DIG-labeled probes for RNA detection.....	87
3.1.1	Evaluation of genome editing and large delta antigen expression.....	88
3.1.2	HDV and HDV-like agents' replication host range.....	91
3.1.3	Establishment of HDV-like agents' replication in non-hepatocyte-derived cells.....	95
3.1.4	WoDV and DeDV can amplify efficiently via cell division in HuH7 cells.....	96
3.2	Establishment of infection system and characterization of extracellular spread.....	106
3.2.1	Pseudo typing of HDV and HDV-like agents using selected envelope proteins from hepadna- and non-hepadnaviruses.....	106
3.2.2	Effects of HDV-LHDAg expression and prenylation on replication and artificial envelopment of HDV - like agents.....	108
3.2.3	TCID50 of pseudo-typed WoDV and DeDV viral particles.....	115
3.3	Characterization of the interplay between HDV-like agents and the innate immune response.....	119
3.3.1	Infected HepaRG ^{NTCP} cells support WoDV and DeDV replication.....	121
3.3.2	ISGs induction upon WoDV and DeDV infection is lower compared to HDV.....	123
3.3.3	WoDV and DeDV can spread via cell division in HepaRG ^{NTCP} cells.....	126
3.3.4	Interferon treatment does not inhibit cell division-mediated spread of WoDV and DeDV in HuH7 ^{NTCP} cells.....	128
3.3.5	The role of L-HDAg expression in HDV interferon sensitivity.....	130

3.3.5.1	<i>The sensitivity to interferon of the human HDV is not conferred by the emergence of L-HDAg</i>	132
3.3.6	<i>The predominant nuclear localization of HDAg is not conserved among WoDV and DeDV</i>	136
3.3.7	<i>Study of Innate Immune Responses Upon Infection of Lung Carcinoma Epithelial Cells of HDV and HDV-Like Agents.....</i>	138
4.	Discussion	145
5.	Appendix.....	Error! Bookmark not defined.
5.1	<i>Functional analyses of mutations of putative phosphorylation sites in the preS1 domain of Hepatitis B Virus large envelope protein.....</i>	167
5.2	<i>Joint host-pathogen genomic analysis identifies hepatitis B virus mutations associated with human NTCP and HLA class I variation</i>	168
6.	References	170
7.	Publications.....	193
8.	Acknowledgments	195

IV. LIST OF ABBREVIATIONS

ADAR1	Adenosine deaminase acting on RNA 1
ATP	Adenosine triphosphate
ALT	Alanine aminotransferase
N-terminus	Amino terminus
Aa	Aminoacid
APS	Ammonium persulfate
AuAg	Australia antigen
AvDV	Avian delta agent (name from previous publication : avHDV)
Bp	Base pare
BaDV	Bat delta agent (name from previous publication : pmacDV)
IstriDV	Bengalese finch delta agent
BSA	Bovine serum albumin
CsCl	Caesium chloride
C-terminus	Carboxy terminus
LMH	Leghorn chicken hepatoma cell Line
CHO	Chinese hamster ovary cells
CHB	Chronic hepatitis B
CHD	Chronic hepatitis D
cDNA	Complementary DNA
cccDNA	Covalently closed circular DNA
CMV	Cytomegalovirus
Da	Dalton
dpi	Days post infection
dpt	Days post transfection
DeDV	Deer delta agent (name from previous publication : ovirDV)
DAg	Delta antigen
DLA	Delta-like agents
DENV	Dengue virus
dCTP	Deoxycytidine triphosphate
DNA	Deoxyribonucleic acid
DMSO	Dimethylsulfoxide
DTT	Dithiothreitol
ddH2O	Double distilled H2O

dsDNA	Double-stranded linear DNA
DHBV	Duck hepatitis B virus
DMEM	Dulbecco's Modified Eagle Medium
ER	Endoplasmic reticulum
ESCRT	Endosomal sorting complexes required for transport
Env HIV	Envelope glycoprotein
ELISA	Enzyme-linked immunosorbent assay
EGFR	Epidermal growth factor receptor
E. coli	Escherichia coli
EDTA	Ethylenediaminetetraacetic acid
FBS	Fetal bovine serum
fiHDV	Fish delta agent
FACS	Fluorescence-activated cell sorting
For	Forward (primer)
GAPDH	Glyceraldehyde-3-phosphate dehydrogenase
GFP	Green fluorescent protein
HA	Hemagglutinin
HSPG	Heparan sulphate proteoglycan
HAV	Hepatitis A virus
HBc	Hepatitis B core protein
HBeAg	Hepatitis B e antigen
HBsAg	Hepatitis B surface antigen
HBV	Hepatitis B virus
HCV	Hepatitis C virus
HDAg	Hepatitis delta antigen
HDV	Hepatitis delta virus
HEV	Hepatitis E virus
HCC	Hepatocellular carcinoma
HuH7	Human Hepatoma-Derived Cell Line
HIV	Human immunodeficiency virus
IF	Immunofluorescence
IVT	In Vitro Transcription
IAV	Influenza A virus
IFI27	Interferon alpha inducible protein 27
IFI44	Interferon alpha inducible protein 44
ISG	Interferon Stimulated Gene
ISG15	Interferon Stimulated Gene 15
IFN-α	Interferon- α
IFN-β	Interferon- β

IFN-λ1	Interferon-λ1
IU/mL	International unit per millilitro
JAK	Janus kinase
kb	Kilobase
KD	Knock down
KO	Knock out
L-HBsAg	Large hepatitis B surface antigen
L-HDAg	Large hepatitis delta antigen
LB	Lysogeny broth
MDA5	Melanoma differentiation-associated protein 5
mRNA	Messenger RNA
M-HBsAg	Middle hepatitis B surface antigen
MAVS	Mitochondrial antiviral-signaling protein
M	Molar
mge	Multiplicity of genome equivalents
MVB	Multivesicular body
Mx1	MX dynamin like GTPase 1
MyrB	Myrcludex B
amHDV	Newt delta agent
NB	Northern blot
NLS	Nuclear localisation signal
NPC	Nuclear pore complex
NUC	Nucleos(t)ide analogue
nt	Nucleotide
ORF	Open reading frame
PFA	Paraformaldehyde
PBS	Phosphate buffered saline
PAGE	Polyacrylamide gel electrophoresis
PEG	Polyethylenglycol
PCR	Polymerase chain reaction
pi	Post infection
pt	Post transfection
pgRNA	Pregenomic RNA
PHH	Primary human hepatocytes
qPCR	Quantitative PCR
RSAD2	Radical S-adenosyl methionine domain containing 2
RIG-I	Retinoic acid inducible gene I
RDeV	Spiny rat delta agent
Rev	Reverse

RT	Reverse transcription
RT-qPCR	Reverse transcription quantitative PCR
rpm	Revolutions per minute
RNA	Ribonucleic acid
RNP	Ribonucleoprotein
roDV	RodentDV
RT	Room temperature
shNT	Short hairpin non-targeting
D-DAg	Small delta antigen
S-HBsAg	Small hepatitis B surface antigen
S-HDAg	Small hepatitis delta antigen
sHDV	Snake delta agent
SDS	Sodium dodecyl sulfate
NTCP	Sodium taurocholate cotransporting polypeptide
SSC	Standard saline citrate
SVP	Subviral particle
tHDV	Termite HDV
TEMED	Tetramethylethylene-diamine
tfHDV	Toad delta agent
TLR	Toll-like receptor
tRNA	Transfer RNA
TBS	Tris buffered saline
TBS-T	Tris buffered saline - tween 20
Tris	Tris(hydroxymethyl)-aminomethane
TAE	Tris-acetate-EDTA buffer
TE	Tris-EDTA buffer
TN	Tris-NaCl buffer
UV	Ultraviolet
U	Unit
VSV	Vesicular stomatitis virus
vge	Viral genome equivalent
WB	Western blot
WGA	Wheat germ agglutinin
WT	Wild-type
WoDV	Woodchuck delta agent (name from previous publication : mmDV)
WHO	World health organization

1. INTRODUCTION

1.1 HEPATITIS VIRUSES

Hepatitis, a term derived from the Greek words "*hepar*" (liver) and "*itis*" (inflammation), is a significant healthcare burden worldwide and refers to a condition of liver damage and inflammation. The most common cause of hepatitis is infection by hepatotropic viruses, namely hepatitis A virus (HAV), hepatitis B virus (HBV), hepatitis C virus (HCV), hepatitis D virus (HDV) and hepatitis E virus (HEV). While some forms of hepatitis are acute and self-limiting, HBV, HCV, HDV and HEV can become chronic. The potential for chronicity may vary by virus type and sub-genotype, as well as by geographic location and distribution (Castaneda et al., 2021).

Worldwide, viral hepatitis and related complications are responsible for around 1.5 million deaths annually (Lancet, 2022; WHO, 2023). Most deaths are caused by HBV and HCV infections. Treatment and therapeutic goals differ depending on the viral agent and include prevention of transmission, improved early detection, and medical management (Loader et al., 2019).

Human hepatitis viruses are assigned to various virus families and genera (Table 1.1). Specifically, HAV is classified into the *Picornaviridae* family, *Hepatovirus* genus, HBV belongs to the *Hepadnaviridae* family, *Orthohepadnavirus* genus, HCV is assigned to the *Flaviviridae* family, *Hepacivirus* genus, HDV to the *Kolmioviridae*, *Deltavirus* genus and finally HEV belongs to the *Hepeviridae* family, *Orthohepevirus* genus.

Although all five hepatitis viruses cause primary clinical symptoms in the liver, they differ greatly in terms of genome characteristics, modes of transmission, endemicity, and clinical outcomes (Table 1.1).

	HAV	HBV	HCV	HDV	HEV
Virus family	<i>Picornaviridae</i> , <i>Hepatitis virus</i>	<i>Hepadnaviridae</i> , <i>Orthohepadnavirus</i>	<i>Flaviviridae</i> , <i>Hepaciviridae</i>	<i>Kolmioviridae</i> <i>Deltavirus</i>	<i>Heperviridae</i> <i>Orthohepevirus</i>
Genome type	Positive sense linear ssRNA	Circular, partially dsDNA (full-length negative sense, partial positive sense (replication via reverse transcription)	Positive-sense linear ssRNA	Viroid-like, negative-sense circular ssRNA	Positive-sense linear ssRNA
Genome length	7,500	3,200	9,600	1,700	7,200
Virion diameter	27-32	42	55-5	36-43	30-34
Envelope	No/quasi- enveloped	Yes	Yes	Yes	No/quasi- enveloped
Course of infection	Acute (Lemon et al., 2017)	Acute/chronic (children 30-90%, adults <5%) (Paganelli et al., 2012)	Acute/chronic (80- 85%) (Webster et al., 2015)	Acute/chronic (>80 if superinfection) (Pascarella & Negro, 2011)	Acute/chronic (<1%) (Pischke et al., 2014)
Predominant transmission	Mainly fecal-oral, parental (Das et al., 2017)	Vertical, parental, sexual	Parental	Parental, sexual	Fecal-oral, food-borne, parental
Cellular receptor	Unknown	NTCP, Heparan sulfate proteoglycans (Schulze et al., 2007; Yan et al., 2012)	CD81, SR-B1, LDL receptor, claudin-1, occludin (Catanese et al., 2010; Pileri et al., 1998; Yamamoto et al., 2016)	NTCP, Heparan sulfate proteoglycans (Lamas Longarela et al., 2013; Yan et al., 2012)	Unknown

Table 1.1 Molecular and clinical characteristics of all human hepatitis viruses. dsDNA, double-stranded DNA; nt, nucleotide; NTCP, sodium taurocholate co-transporting polypeptide; ssRNA, single-stranded RNA. Adapted from (Rasche et al., 2019).

1.1.1. Etiology, epidemiology, and treatment

HAV is transmitted primarily through contaminated water and food or with direct contact with an infected person (WHO, 2023a). The infection is usually sporadic and rarely causes epidemics. Developing countries, mainly in Africa, Asia, and South and Central America, with inadequate sanitation are considered endemic regions (Miguereles et al., 2021). Fulminant hepatitis is rare and HAV infection usually resolves on its own, thus current treatment options are primarily supportive (Gabrielli et al., 2023; Lemon et al., 2017; Miguereles et al., 2021). An inactivated HAV vaccine has been licensed in Europe since

1991 (Herzog et al., 2021), while a live attenuated vaccine has been in use in China since 1992 (Cui et al., 2014).

In 2019, HBV resulted in an estimated 820 000 deaths, mostly from cirrhosis and hepatocellular carcinoma (HCC) (WHO, 2023b). HBV can be transmitted through sexual contact via body fluids, through blood, via injection drug use or unsafe medical practices, and through close person-to-person contact. The highest burden of HBV infection is observed in sub-Saharan Africa and the Western Pacific. In countries with high rates of chronic HBV infection, transmission typically occurs in early childhood or vertically from mother to child. This is the period when the risk of developing chronic disease is highest (Table 1.1) (Cibangu & Onoya Onaluwa, 2021; Hou et al., 2005; Yang et al., 2019).

The best form of prevention is via vaccination ("Hepatitis B vaccines: WHO position paper – July 2017," 2017). While supportive care is the primary approach to managing acute HBV infection, chronic infection can be treated with pegylated interferon- α (IFN- α) and several nucleos(t)ide analogues (NUCs): Tenofovir disoproxil, Tenofovir alafenamide, Entecavir, Telbivudine, Adefovir dipivoxil and Lamivudine (Pan et al., 2023). These therapies can help alleviate symptoms and improve daily life. However, these treatments do not fully eradicate the infection.

Individuals with chronic HBV infection are at higher risk of HDV infection. HDV is defined as satellite virus because it relies on the HBV surface antigen (HBsAg) for extracellular spread. HDV is primarily transmitted through intravenous drug use, contaminated healthcare equipment, and sexual contact. Although it is still a problem in resource-poor countries, transmission through blood transfusions is now less of a concern, thanks to increased monitoring techniques (Yang et al., 2019). HDV is endemic in regions such as the Middle East, Asia, Africa, the Amazon Basin, and the Pacific Islands (Stockdale et al., 2020).

Currently available treatments aim to prevent complications associated with HDV chronic infection (Table 1.2).

Pegylated interferon-alpha (Peg-IFN- α) is the preferred treatment for HDV infection. While it has shown some promising results in virological response rates, low rates of HDV RNA negativity have been observed 24 weeks after stopping treatment. It's also common for patients to experience late relapses (Heidrich et al., 2014; Wedemeyer et al., 2011). Moreover, Peg-IFN- α treatment can lead to significant adverse effects, including flu-like symptoms, depression and cytopenia (Elazar & Glenn, 2022).

Bulevirtide (Hepcludex®, formerly Myrcludex B) is a 47-amino acid long peptide adapted from the HBsAg PreS1 sequence. Bulevirtide competitively inhibits HBV and HDV binding to NTCP, preventing virus entry into hepatocytes. As a monotherapy, patients have shown good responses to Bulevirtide, with significant reductions in HDV RNA levels (Bogomolov et al., 2016). However, most patients do not achieve undetectable HDV RNA levels, and some experience a rebound after the end of treatment.

Bulevirtide has also shown promising outcome when used in combination with Peg-IFN- α , with 50% of patients having undetectable HDV RNA at 24 weeks follow-up (Lampertico et al., 2022; Wedemeyer & Negro, 2019). This is due to the synergistic effect of inhibiting both extracellular and cell division-mediated spread of HDV. Bulevirtide has been approved in the EU as a monotherapy HDV chronic infected patients (Kang & Syed, 2020).

Peg-IFN-lambda (Peg-IFN- λ) is a type III interferon, correlated with fewer side effects compared to Peg-IFN- α . This is because the receptors for type III interferons are only expressed on epithelial cells, mostly in the liver and lungs. In contrast, the receptors for type I interferons are expressed ubiquitously in the body (Muir et al., 2014). Studies have demonstrated that Peg-IFN- λ has a better virological response at 24 weeks after treatment compared to Peg-IFN- α (36% versus 28%). It is currently undergoing phase III trials.

Lonafarnib (LNF) is a small molecule that inhibits prenylation of HDV L-HDAg. By blocking this process, LNF interferes with the packaging of HDV RNP by HBsAg.

LNF has been studied as a monotherapy as well as in combination with ritonavir (a protease inhibitor used for the treatment of HIV/AIDS) and/or Peg-IFN- α . The combination of LNF with Peg-IFN- α was found to work synergistically, resulting in improved antiviral responses (Koh et al., 2015). Moreover, low doses of oral LNF were found to be more effective with better tolerated adverse effects when compared to high-dose regimens. Currently, LNF with several combinations therapies is in phase III trials. Phase II trials is also on-going for LNF with Peg-IFN- λ . The adverse effects observed during these trials were mostly mild to moderate.

The mechanism of action of nucleic acid polymers (NAPs) is still unclear, but entry and HBsAg secretion inhibition are probably involved. A clinical trial in combination with Peg-IFN- α showed that after 3.5 years, 75% of patients were HDV RNA negative (Bazinet et al., 2017). Importantly the treatment had a good safety profile and tolerable side effects.

Drug	Substance	Mode of action	Availability
Peg-IFN-α	<i>Protein</i>	<i>Cytokine activates the innate immune system</i>	<i>Approved for HBV, off-label use for HDV</i>
Bulevirtide	<i>PreS1 peptide</i>	<i>NTCP binding, blocking HBV/HDV entry</i>	<i>Phase II, CMA by EMA in July 2020</i>
Peg-IFN-λ	<i>Protein</i>	<i>Cytokine activates the innate immune system</i>	<i>Phase II</i>
Lonafarnib	<i>Small molecule</i>	<i>Inhibiting L-HDAg prenylation and HDV secretion</i>	<i>Phase III</i>
REP2139	<i>Nucleic acid polymer (NAPs)</i>	<i>Inhibiting HBsAg secretion, possibly also HBV/HDV entry</i>	<i>Phase II</i>

Table 1.2. Approved and investigational HDV drugs. CMA, conditional marketing authorization; Peg-IFN pegylated interferon; NTC, human sodium taurocholate co-transporting polypeptide. Adapted from (Zhang & Urban, 2021).

Before the introduction of blood screening protocols, HCV was a major adverse event associated with blood transfusion. HCV infection is prevalent in Africa and Asia, with a mortality rate of 7.0 unit per 100,000 in 2019 (Figure 1.1). Acute HCV infections are usually asymptomatic, and around 30% of infections are cleared within 6 months (Webster et al., 2015). The remaining 70% will develop chronic HCV infection. For chronic infected HCV

patients, the risk of cirrhosis and HCC goes from 15% to 30% within 20 years (Organization, 2023b).

The most effective treatments for HCV infection are IFN α , ribavirin, and direct acting antivirals (DAAs). When treated with DAAs more than 95% of people with HCV can clear the infection, although the main obstacle is to diagnosis and treatment (Cornberg & Manns, 2022).

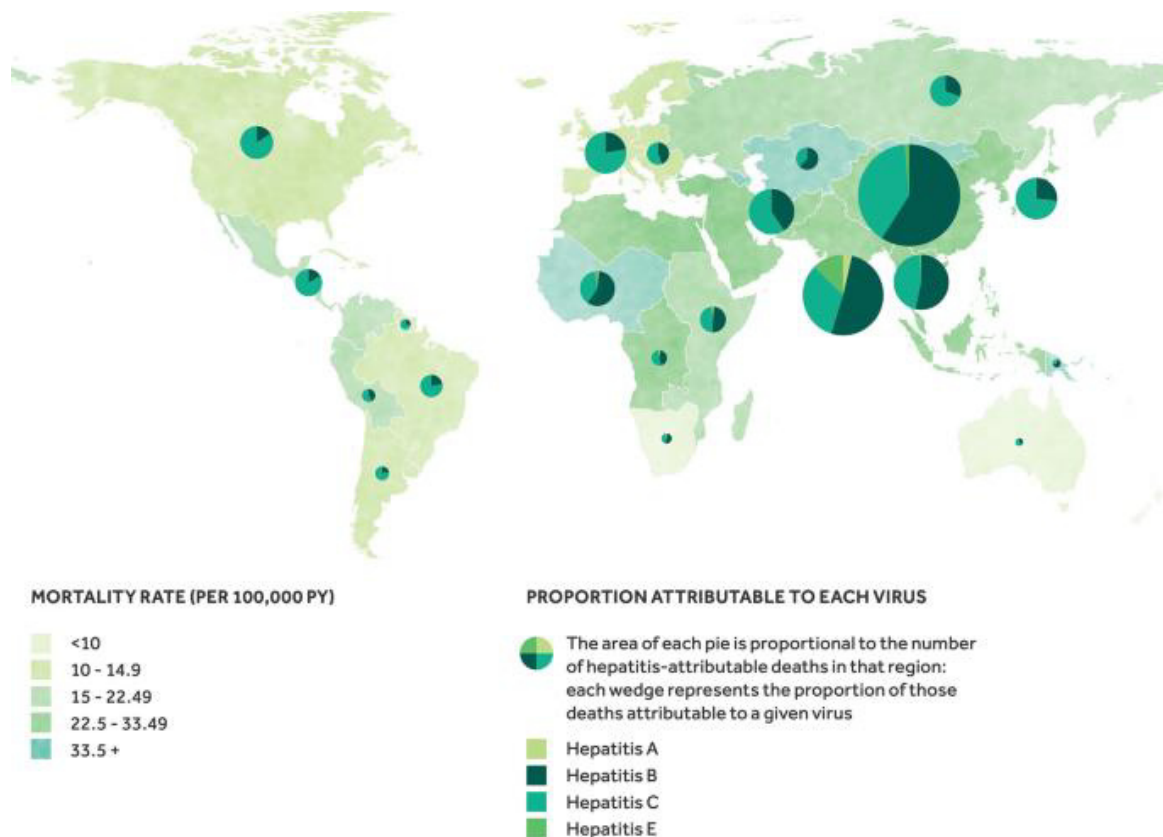


Figure 1.1. Map of viral hepatitis-related mortality. The pie charts indicate each virus type's contribution to the total hepatitis-related mortality. HDV is not included. From (Yang et al., 2019)

The main route of transmission for HEV is via contaminated food and water. It can also spread through zoonotic and transfusional transmission. Consumption of raw or undercooked animal products can lead to HEV infection. Moreover, HEV can be

transmitted from an infected mother to her fetus, although the likelihood is low (WHO, 2023b). HEV is found mainly in developing countries with inadequate sanitary conditions and is endemic in Asia, Africa, the Middle East, and Central America. Supportive care and symptomatic therapies are the primary treatment options for acute and self-limiting illness (Aslan & Balaban, 2020; Gabrielli et al., 2023).

1.1.2. Historical background of hepatitis viruses

The first definition of epidemic jaundice dates back to Hippocrates (460-375 B.C.) in ancient Greece. Hippocrates observed the clinical syndrome of fulminant hepatitis and described it as: *“The bile contained in the liver is full of phlegm and blood and erupts (out of the liver). After such an eruption, the patient soon raves, becomes angry, talks nonsense, and barks like a dog. Most patients die within the space of eleven days”* (Oon, 2012).

However, it was not until the last century that advances in molecular biology and virology led to identifying the causative agents of each type of hepatitis. At *Willowbrook State School* in New York, unethical experiments were conducted on mentally disabled children infected with blood samples from hepatitis patients. These experiments confirmed previous studies (Findlay & Willcox, 1945; Neefe et al., 1944) identifying two different forms of hepatitis. These forms differed in incubation time, clinical outcome, and immunologic profile. The first type of infectious hepatitis, called hepatitis A, had a shorter incubation period and was highly contagious. The second type, hepatitis B, was less contagious and had a more extended incubation period (Krugman et al., 1967).

While studying genetic polymorphisms in the Australian Aboriginal population in 1965, Blumberg discovered an antigen (Blumberg et al., 1965). This antigen, named the Australian antigen (AuAg), was found to be associated with a high incidence of leukemia. This discovery led to the hypothesis that the antigen might be associated with viral induced cancer. However, it wasn't until the 1970s that advances in electron microscopy

techniques allowed Dane et al. to identify 42 nm particles in sera that tested positive for the AuAg (Dane et al., 1970).

The so-called "Dane" particles were found to be associated with infectivity and serum hepatitis. The antigenic structure and viral components, including viral DNA polymerase, were subsequently identified (Hirschman et al., 1971; Robinson & Greenman, 1974). Soon after, the cloning and sequencing of the HBV genome were rapidly accomplished (Charnay et al., 1979; Sninsky et al., 1979; Vaudin et al., 1988).

Feinstone et al. were the first to identify the 27 nm viral protein of HAV in stool samples from patients with acute hepatitis (Feinstone et al., 1973). Cloning, genome sequencing, and propagation in cell culture systems have allowed the development of vaccines against the etiologic agents that cause fulminant hepatitis (Provost & Hilleman, 1979; Provost et al., 1986; Ticehurst et al., 1983).

After the identification of HAV, cases of post-transfusion hepatitis were classified as non-A, non-B (NANBH), as no viral markers for HAV or HBV were identified in the patients (Alter et al., 1978). Chimpanzee transmission experiments led to the identification of an enveloped virus 45-60 nm in diameter (Bradley et al., 1985). However, it was not until 1989 that the etiologic agent of NANBH was identified and renamed HCV (Choo et al., 1989; Kato et al., 1990).

HEV was first identified during an epidemic in the Kashmir Valley of India. The disease primarily affected pregnant women and caused high rates of jaundice. The epidemic affected more than 200 villages with a population of more than 600,000 (Khuroo, 1980; Khuroo et al., 1981). Evidence of a new human hepatitis virus distinct from post-transfusion non-A, non-B hepatitis has been found.

Soon after, an outbreak of non-A, non-B hepatitis occurred in a military camp in Afghanistan. A team from the Institute of Poliomyelitis in Moscow, USSR, led by Dr. M.S. Balayan and Dr. A.G. Andjaparidze, was sent to investigate the epidemic (Balayan et al., 1983). Dr. Balayan himself ingested pooled stool extracts from 9 Afghan epidemic hepatitis

patients and developed typical clinical signs and symptoms of acute non-A, non-B hepatitis. Stool samples from infected individuals contained 27-30 nm spherical virus-like particles (VLPs). Inoculation of macaques with virus-containing stool extracts from 2 patients resulted in histopathology, enzymatically confirmed hepatitis, secretion of viral particles, and antibody responses (Bradley & Balayan, 1988).

Between 1983 and 1990, no further molecular studies of HEV were conducted due to the lack of viral particles in stool samples needed for viral genome cloning and sequencing. However, large quantities of VLPs were obtained from bile samples of experimentally infected cynomolgus macaques. In 1990, Reyes et al. partially cloned the HEV cDNA (Reyes et al., 1990), and the full-length HEV genome was sequenced in 1991 (Tam et al., 1991), followed by the development of an enzyme immunoassay to detect antibodies to HEV (Goldsmith et al., 1992).

1.1.3. Reservoirs for hepatitis viruses in non-human hosts

The discovery of hepatitis viruses in humans inevitably drew attention to the zoonotic potential of these hepatic pathogens. HBV was the first human hepatitis virus for which an animal homologue was identified in woodchucks and ducks in 1978 and 1980, respectively (Mason et al., 1980; Summers et al., 1978). These discoveries were immediately followed by the identification of the first hepatitis in non-human primates (Lanford et al., 1998; Vaudin et al., 1988) and other mammals, since bats were also discovered to be an animal reservoir for HBV-like viruses (Diakoudi et al., 2022; Drexler, Geipel, et al., 2013; He et al., 2015; Piewbang et al., 2022; Ratti et al., 2023). Three studies identified domestic cats and dogs infected with hepadnaviruses (Aghazadeh et al., 2018; Diakoudi et al., 2022; Piewbang et al., 2022; Ratti et al., 2023), shedding a light on the potential for host shifting through close contact with domesticated animals. This theory would be supported by the report of HBV-like viruses causing chronic infections in several equine species (Walter et al., 2017). To further complicate the riddle, a surprising finding of hepadnaviruses in animal species distant from humans, such as fish, reptiles, and amphibians, suggests a

possible non-human evolution for HBV (Dill et al., 2016; Hahn et al., 2015; Lauber et al., 2017).

Unlike HBV, HAV seems to possess a preference for many non-human primates and other mammalian species, since naturally infection has been described in tamarins, owl monkeys, African green monkeys, cynomolgus monkeys, rhesus monkeys, and seals (Anthony et al., 2015; de Oliveira Carneiro et al., 2018; Nainan et al., 1991).

The history of non-human HCV dates back to 1995 when a virus distantly related to HCV was identified in a laboratory tamarin (Robertson, 2001; Simons et al., 1995). Since then, HCV-like agents have been identified in horses, dogs, bats, rodents, cattle, and monkeys (Corman et al., 2015; Drexler, Corman, et al., 2013; Harvey et al., 2023; Lyons et al., 2014; Quan et al., 2013; Walter et al., 2017).

However, among all human hepatitis viruses, zoonotic transmission has been documented indeed only for HEV. Domestic pigs have been considered a natural reservoir for HEV since the discovery of an infected pig in 1997 (Meng et al., 1998). Interestingly, an avian HEV strain was able to cause liver damage in farmed chickens. The alert for a form of hepatitis causing pathologies in farm animals, grease the wheels for following research showing HEV infect in various animals, including farmed rabbits, wild rats, camels, bats, and deers (Drexler et al., 2012; Johne et al., 2010; Meng et al., 1998; Raj et al., 2012; Rasche et al., 2016; Woo et al., 2014).

Since it was discovered over 40 years ago, HDV has been thought to only infect humans. However, in 2018, the first HDV-like sequences were identified in snake and duck species (64, 65), paving the way for many more discoveries to come.

The discoveries of hepatitis viruses in non-human reservoirs are shown chronologically in Figure 2 (Rasche et al., 2019).

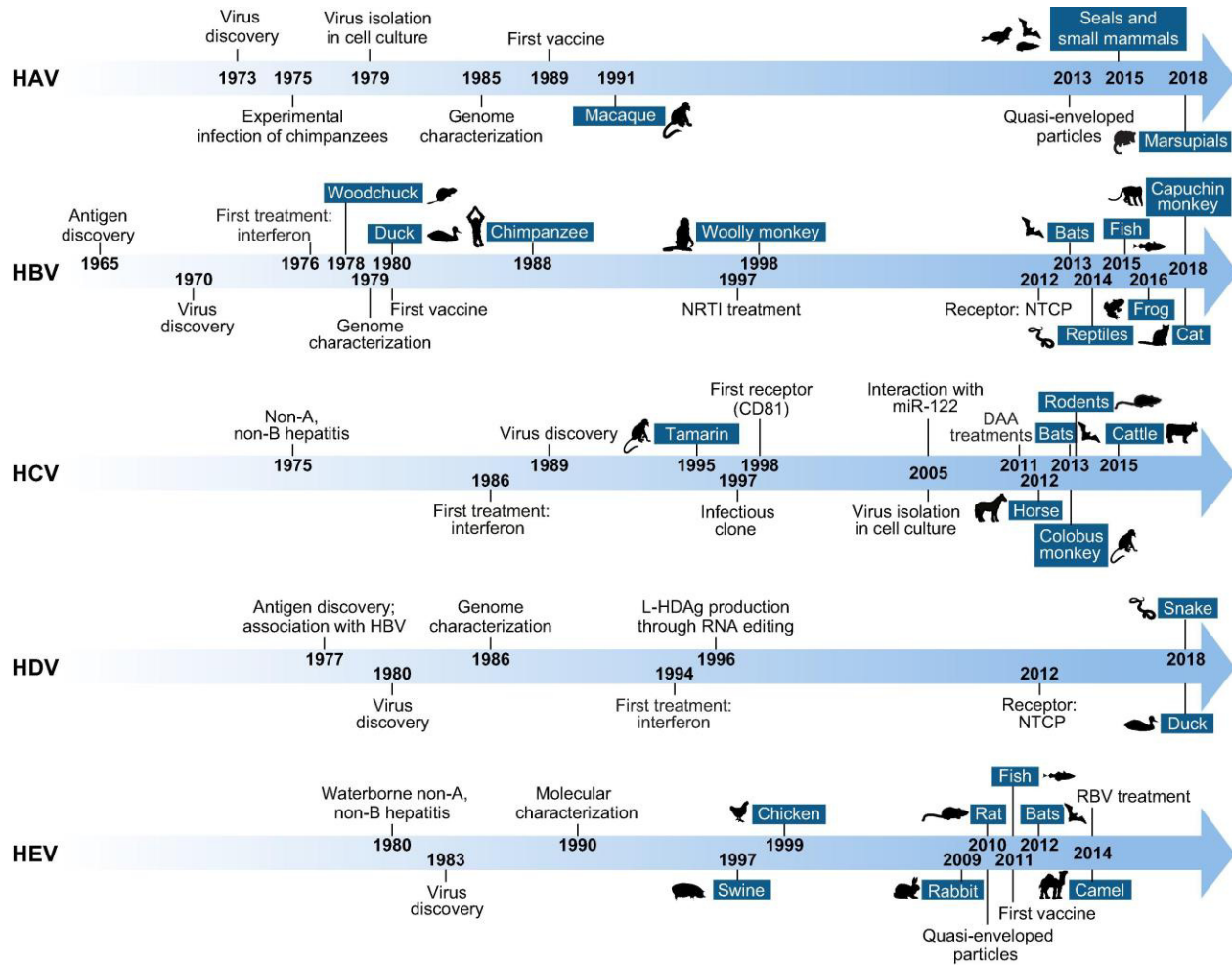


Figure 1.2. Milestones and discovery of Hepatitis viruses in human and non-human hosts. Adapted from (Rasche et al., 2019).

1.2 THE HUMAN HEPATITIS DELTA VIRUS

1.2.1. *The discovery of HDV, much more than just a novel HBV antigen*

The discovery of HBV in the late 1960s was an incredible milestone for virology and hepatitis viruses. With the discovery of new viral agents came the need for new tools to detect and monitor these pathogens in patients and patient-derived samples. This is where Dr. Mario Rizzetto, a postdoctoral researcher in charge of identifying molecular assays to determine HBV replication activity, came into play (Rizzetto, 2020). Rizzetto investigated the expression of HBV core antigen (HBcAg) in liver cells by using a fluorescein FITC-labeled anti-core reagent from the IgG fraction of an HBsAg seropositive patient. Certain HBsAg+ biopsies contained elements that could fix complement but did not respond to the reference FITC-conjugated anti-HBc. A new antigen was identified, which was only present in the nuclei of infected liver cells. This new antigen-antibody system was immunologically distinct from the nuclear HBsAg antigen-antibody complex (Figure 1.3). The novel antigen was designated as HBV nuclear antigen (HBnAg), and the discovery was submitted to a major medical journal for publication (Rizzetto et al., 1977). In the meantime, Dr. Christian Trepo, a virologist studying HBV in Lyon, identified the envelope antigen of HBV (HBeAg) in a biopsy sample taken from an HBV patient. Immunological staining revealed that HBeAg was localized in the nucleus, which suggested that HBeAg and HBnAg were the same antigen. However, after further collaboration, the two antigens were confirmed as distinct. Since the letter *N* was already used for an HBsAg variant, the new antigen was renamed *delta* according to the Greek alphabet. At first, the scientific community expressed skepticism and disbelief about the identification of a new HBV antigen. However, the US National Institutes of Health (NIH) awarded Rizzetto a grant to investigate the nature of delta antigen. While working at NIH, Rizzetto collaborated with Drs. John Gerin and Robert Purcell to create a serological assay to detect anti-delta antibodies in serum. After performing transmission experiments using the NIH colony of

chimpanzees, they discovered that the new pathogen was a defective virus that relies on the helper function of HBV for viral particle formation.

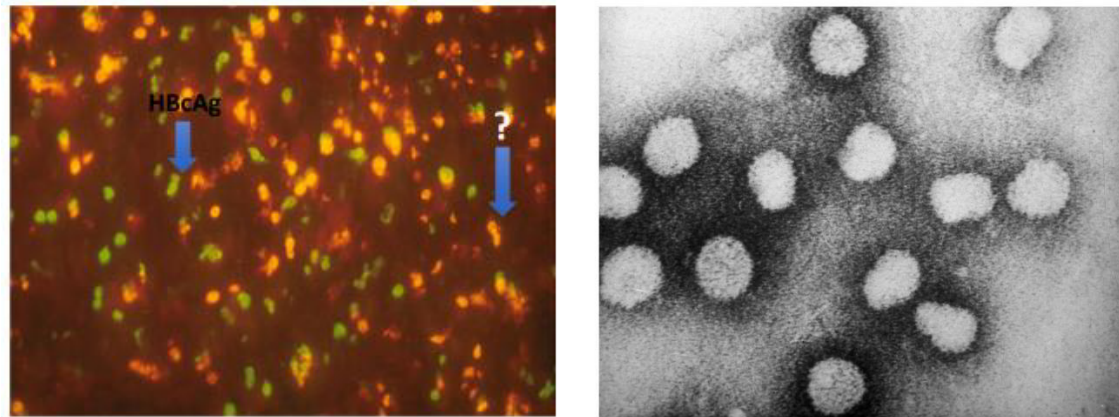


Figure 1.3. First fluorescent picture and EM of HDV antigen and virion. (Left) HBcAg in green fluorescence and delta antigen in red fluorescence in a human liver containing both antigens. (Right) EM of a 36-nm delta particle, negatively stained with 1% phosphotungstic acid, the HDV virion, seen in the delta-positive serum. Unpublished figure from the author's laboratory. Adapted from (Rizzetto, 2020)

The identification of a novel hepatitis RNA agent that replicates independently of HBV led to a change in the name from the Greek letter delta to the Latin letter D. The Hepatitis delta virus or HDV was "born". Soon after, three independent groups have sequenced the complete HDV genome using RNA isolated from chimpanzee serum (Wang et al., 1986), woodchuck liver (Kuo et al., 1988) or human serum (Makino et al., 1987).

1.2.2. The genome structure of HDV

HDV is the smallest RNA virus that is known to infect humans. The virion contains a circular, single-stranded negative-sense RNA molecule of approximately 1700 nucleotides (nt) (Kos et al., 1986). HDV RNA is tightly packed by two viral proteins - small delta antigen (S-HDAg) and large delta antigen (L-HDAg) - both derived from the translation of a single open reading frame (ORF) (Figure 1.4A). The RNA genome and viral proteins form together the ribonucleoprotein complex (RNP). Due to the high base pair self-complementation (74%), the HDV genome forms a tight rod-like structure, which increases

RNA stability (Wang et al., 1986). During replication, anti-genome molecules, complementary to the genome sequence, and an 800 nt mRNA, serving as a template for viral antigen expression, are generated (Figure 1.4B) (Lo et al., 1998; Luo et al., 1990). The S-HDAg is required for RNA replication (Yamaguchi et al., 2001), whereas the L-HDAg is necessary for virion assembly and has an inhibitory effect on late HDV replication (Glenn et al., 1992; Hwang & Lai, 1993, 1994; Lee et al., 1994; Modahl & Lai, 2000).

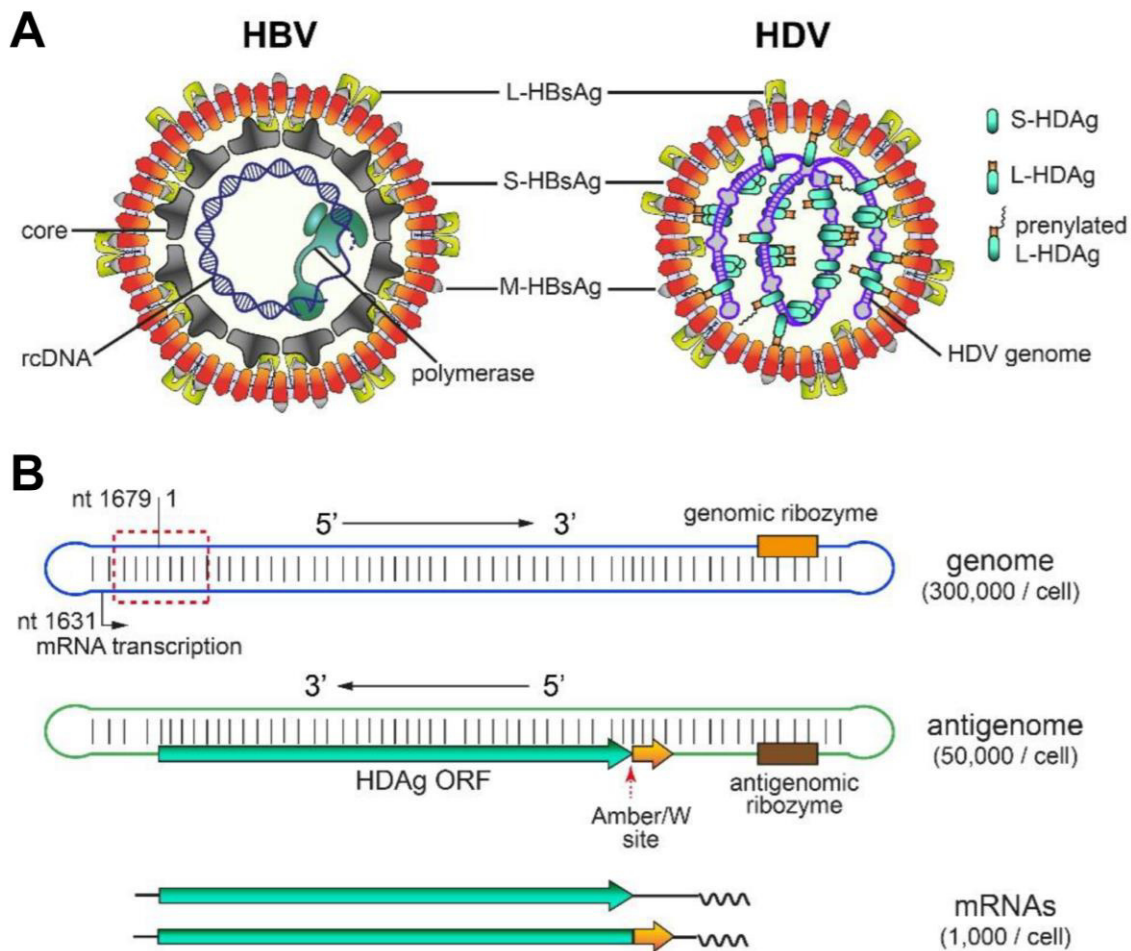


Figure 1.4. Structure of the HDV virion and genome. (A) Schematic representation of the viral structure of HBV and HDV. HDV is a small RNA virus packaged by HBV surface antigens (HBsAg). HBsAg is present in 3 forms: small (s-HBsAg), medium (M-HBsAg) and large (L-HBsAg). The HDV genome is surrounded by small (S) and large (L) isoforms of the hepatitis delta antigen (HDAg). Part of the L-HDAg is prenylated enabling the binding with S-HBsAg. (B) Schem of HDV genome, antigenome and mRNAs. The small, negative-sensed, circular ssRNA genome is highly base-paired forming a rod-like structure. mRNAs

encoding for S- and L-HDAg are transcribed from the genome oriented-strand. The antigenome sequence, complementary to the genome, can be edited at the Amber/W site by ADAR1e enzyme leading to modified genomes in the next replication round and subsequently an extended mRNA encoding for L-HDAg. Adapted from (Zhang & Urban, 2020).

1.2.3. HDV replication cycle

The helper function of HBV involves sharing its envelope proteins with HDV, resulting in a common entry pathway. The entry process begins with a non-specific interaction with heparan sulfate proteoglycans (HSPGs) expressed on the surface of hepatocytes (Lamas Longarela et al., 2013; Leistner et al., 2008; Schulze et al., 2007; Sureau & Salisse, 2013). This step facilitates the secondary specific binding to the cellular receptor and bile acid transporter sodium-taurocholate co-transporting polypeptide (NTCP) (Yan et al., 2013; Yan et al., 2014; Yan et al., 2012).

In addition to NTCP, epidermal growth factor receptor (EGFR) has recently been described as a cofactor for HBV/HDV entry via endocytosis processes (Figure 1.5) (Iwamoto et al., 2019; Verrier et al., 2016). The HDV virion uncoats in the cytoplasm, and its RNP is transported to the nucleus of the infected cell. A nuclear localization signal present in the S-HDAg is essential for this process (Chou et al., 1998).

Although HDV depends on HBV envelope proteins for assembly and entry, HDV RNA replication occurs independently of HBV. HDV relies on host polymerases for replication because it lacks its own polymerase-coding capacity. Studies indicate that HDV mRNA synthesis is mediated by DNA-dependent RNA Polymerase II (Pol-II) (Filipovska & Konarska, 2000; Macnaughton et al., 2002; Modahl et al., 2000). HDV exploits a DNA-dependent polymerase for RNA synthesis, probably thanks to the rod-like structure of its genome, which resembles double-stranded DNA conformation (Cao et al., 2009; Lai, 2005).

Replication occurs via a rolling circle amplification (RCA) mechanism involving the transcription of antigenomic RNAs (AG) that are complementary to the genome (G) (Figure 1.5) (Chen et al., 1986; de la Pena et al., 2021; Taylor, 2006). The antigenomic

strand encodes a viral ribozyme that cleaves the resulting multimers into monomers (Sharmeen et al., 1988; Webb & Luptak, 2011; Wu et al., 1989). The monomers assemble into circular antigenomic molecules, serving as a template for the genomic strand progeny (Sharmeen et al., 1989). In the second step of rolling circle replication, multiple genome copies with the same polarity are transcribed using antigenomic templates. They are then cleaved by a second viral ribozyme encoded in the genomic strand. The HDV mRNA, which has the same polarity as the antigenome, contains an open reading frame (ORF) encoding the S-HDAg protein.

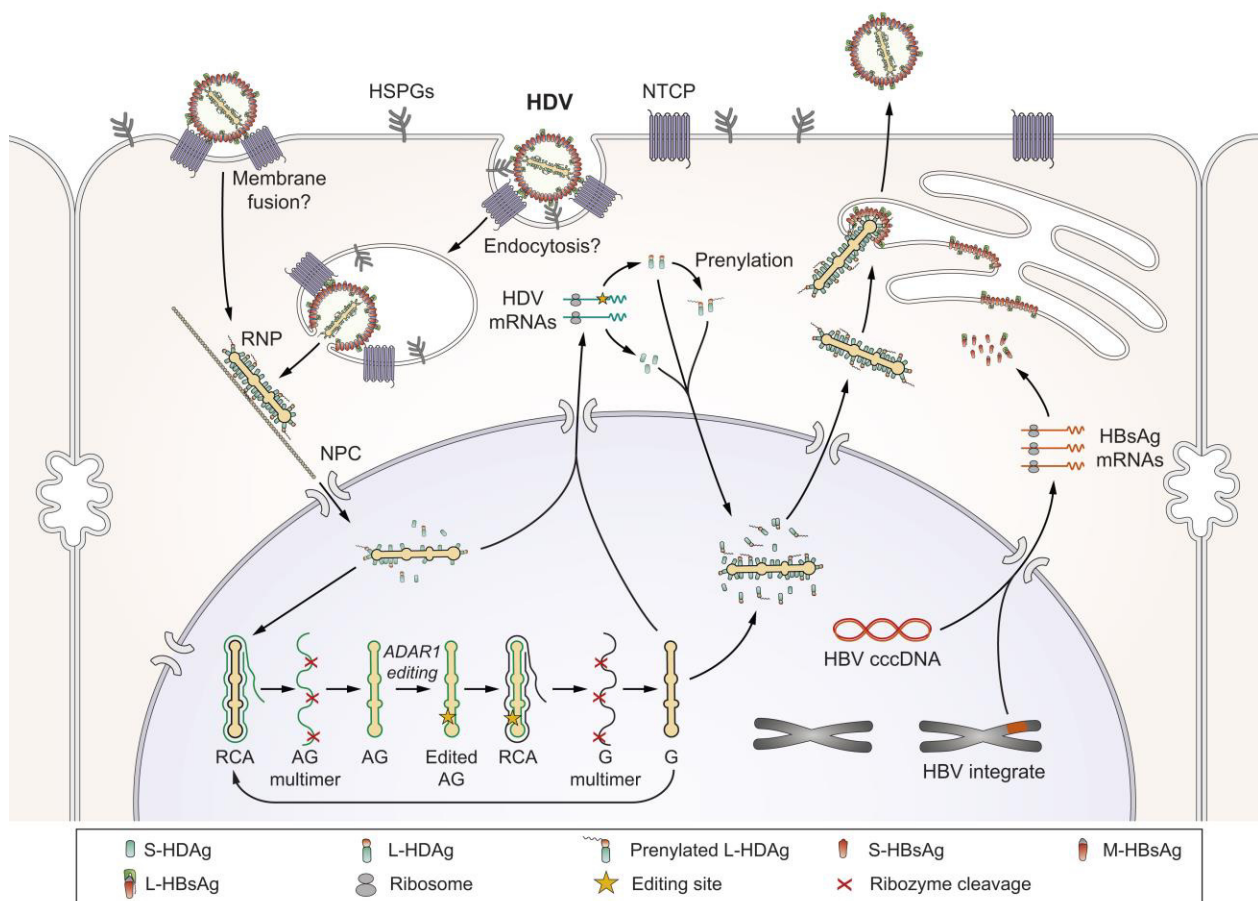


Figure 1.5. HDV Replication Cycle. HDV particles attach to heparan sulfate proteoglycans (HSPGs) and then to the viral receptor NTCP to enter host cells. Once inside, the ribonucleoprotein (RNP) is released and transported to the nucleus to initiate RNA replication. The incoming genome (G) serves as the initial template for rolling circle amplification. The resulting antigenome (AG) multimers are cleaved in the cis configuration by the intrinsic ribozyme and then ligated to form circular monomers. A second round of rolling circle amplification using the AG as the template, results in the synthesis of HDV G multimers, which are subsequently cleaved to produce monomers. ADAR1 may edit the HDV AG, generating an extended HDAg

ORF that makes L-HDAg. A portion of L-HDAg undergoes prenylation. Both S-HDAg and L-HDAg, are transported to the nucleus to regulate virus replication or bind to HDV RNA to form RNP. The RNP containing G can be exported to the cytoplasm and packaged into the HBV envelope via the interaction between L-HDAg and S-HBsAg. HDV virions are released via the ER-Golgi secretory pathway. From (Zhang & Urban, 2021).

During replication, the cellular enzyme Adenosine Deaminase Acting on RNA-1 (ADAR1) edits the antigenomic RNA. This results in the mutation of the S-HDAg ORF stop codon (UAG) adenosine to Inosine (UIG), which is recognized as Guanosine, resulting in the formation of a tryptophan codon (UGG) (Casey, 2002; Casey & Gerin, 1995; Polson et al., 1998; Savva et al., 2012; Wong & Lazinski, 2002). This event leads to the expression of L-HDAg through a C-terminal extension of the S-HDAg ORF by 19-20 amino acids, depending on the genotype (Figure 1.6). The extension contains a CXXQ motif, which can be post-translationally farnesylated by a cellular farnesyltransferase (Glenn et al., 1992). Farnesylation of the L-HDAg is a critical factor in down-regulating viral replication and promoting viral assembly by interacting with the cytosolic loop of HBsAg (Hwang & Lai, 1993, 1994; Lee et al., 1994).

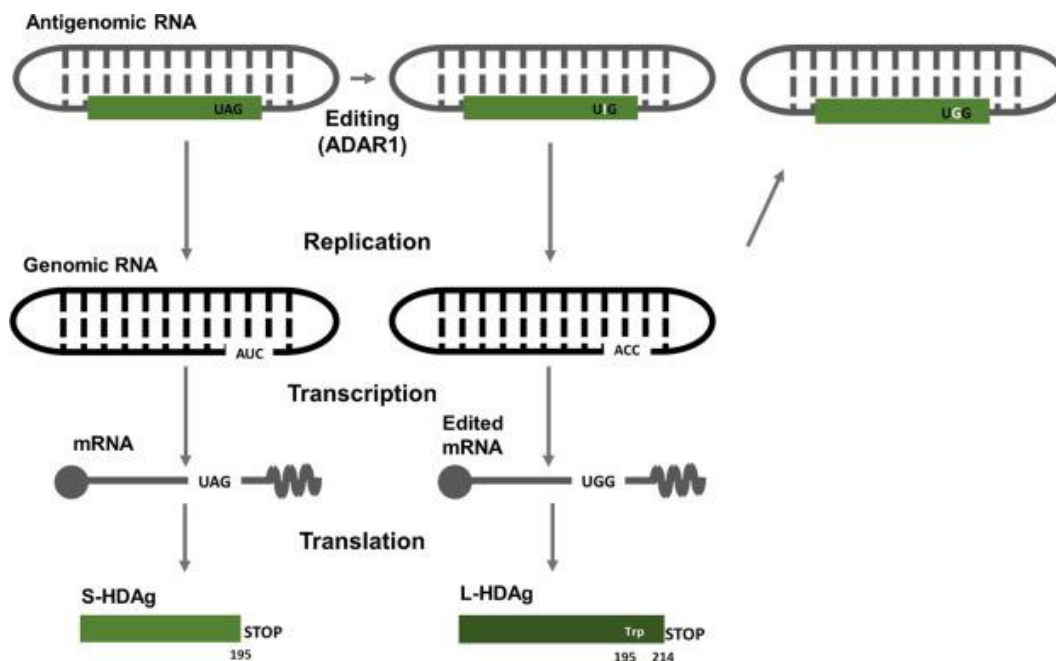


Figure 1.6. HDV antigenome editing by ADAR-1. HDV RNA contains a single open reading frame in its antigenomic RNA, which produces two isoforms of HDAg. Adenosine deaminase acting on RNA-1 (ADAR1) is responsible for editing the amber/W site on the antigenomic HDV RNA by converting adenosine to inosine. After mRNA replication and transcription, the initial stop codon (AUG) that signals the end of S-HDAg synthesis is changed to UGG, which codes for a tryptophan (Trp) residue. This modification allows for translation to continue until the subsequent stop codon, resulting in the addition of 19 amino acids (L-HDAg). From (Mentha et al., 2019).

1.2.4. HBV as helper virus

HBsAg expression is derived from both covalently closed circular DNA (cccDNA) in HBV infected cells and HBV DNA integrates in the host genome (Figure 1.5). As a result, HDV can use HBsAg for packaging and virion formation even in the absence of active HBV replication (Freitas et al., 2014).

For proper cell entry and binding to NTCP, HBsAg requires post-translational modification by the addition of a myristoyl group to its N-terminal extremity (Abou-Jaoude et al., 2007; Blanchet & Sureau, 2007).

The L-HDAg extension also contains a nuclear export signal (NES), which has been shown to contribute significantly to the export of HDV RNP from the nucleus to the cytoplasm, allowing HBsAg packaging (Lee et al., 2001). HDV virion is now a fully infectious particle and can exit the infected cell, possibly via the ER-Golgi secretory pathway.

1.2.5. An alternative spreading pathway: cell division-mediated spread

HDV can spread extracellularly through HBsAg packaging and *de novo* infection of NTCP-expressing cells, as well as intracellularly through cell division, in cell culture and the human liver chimeric mouse model, independently of HBV (Giersch et al., 2019; Zhang et al., 2022).

The observed phenotype of this alternative spreading pathway is the formation of clusters of HDAg-positive cells indicating the transmission of HDV RNA from mother to daughter cells, via clonal expansion. This spreading pathway allows the persistence of HDV in the liver, even without HBV co-infection, as observed in liver transplant patients still infected

with HDV, in absence of HBsAg expression (Mederacke et al., 2012; Samuel et al., 1995). However, the spread of HDV through cell division in vitro could be inhibited by both exogenous IFN and HDV-induced innate immunity response.

1.2.6. HDV and innate immunity

1.2.6.1 Sensing by innate immunity

In contrast to HBV, a stealth virus that does not induce innate immunity during infection (Mutz et al., 2018; Wieland et al., 2004), HDV triggers a cellular antiviral response. HDV replication is sensed via the recognition of viral RNA by pattern recognition receptors (PRRs) as retinoid acid-inducible gene 1 (RIG-1)-like receptors (RLRs) (Figure 1.7). Specifically, the melanoma differentiation antigen 5 (MDA5) has been identified as the primary sensor of HDV replication, working synergistically with a second PRR, Laboratory of Physiology and Genetics 2 (LGP2) (Gillich et al., 2023; Zhang et al., 2018). Indeed, LGP2 has been shown to stabilize the binding of MDA5 with RNA to ensure an efficient mounting of the innate immune response (Sato et al., 2010).

Additionally, previous research has demonstrated that the Mitochondrial antiviral-signaling protein (MAVS) plays a crucial role in HDV detection, enhancing innate responses by the adaptive immune system in mice (Suarez-Amaran et al., 2017).

Upon sensing of HDV replication, downstream transcription factors, namely IFN regulatory factor (IRF) 3/7 and nuclear factor- κ B (NF κ B) are activated, thereby translocating to the nucleus and starting transcription of interferons (IFNs).

These IFNs bind to their specific receptors (*IFNAR1/IFNAR2* for *IFN- α/β* and *IFNLR1/IL10R2* for *IFN- λ*) expressed on the cell membrane. This binding activates the JAK-STAT pathway, via their association with Janus kinase (JAK) 1/2 and tyrosine kinase (TYK) 2. These kinases mediated the phosphorylation of the transcription factors *signal transducer and activator of transcription* (STAT) 1/2 and IRF9 allowing their dimerization

and nuclear translocation. In the nucleus they activate the expression of IFN-stimulated genes (ISGs), crucial in the establishment of the cellular antiviral state.

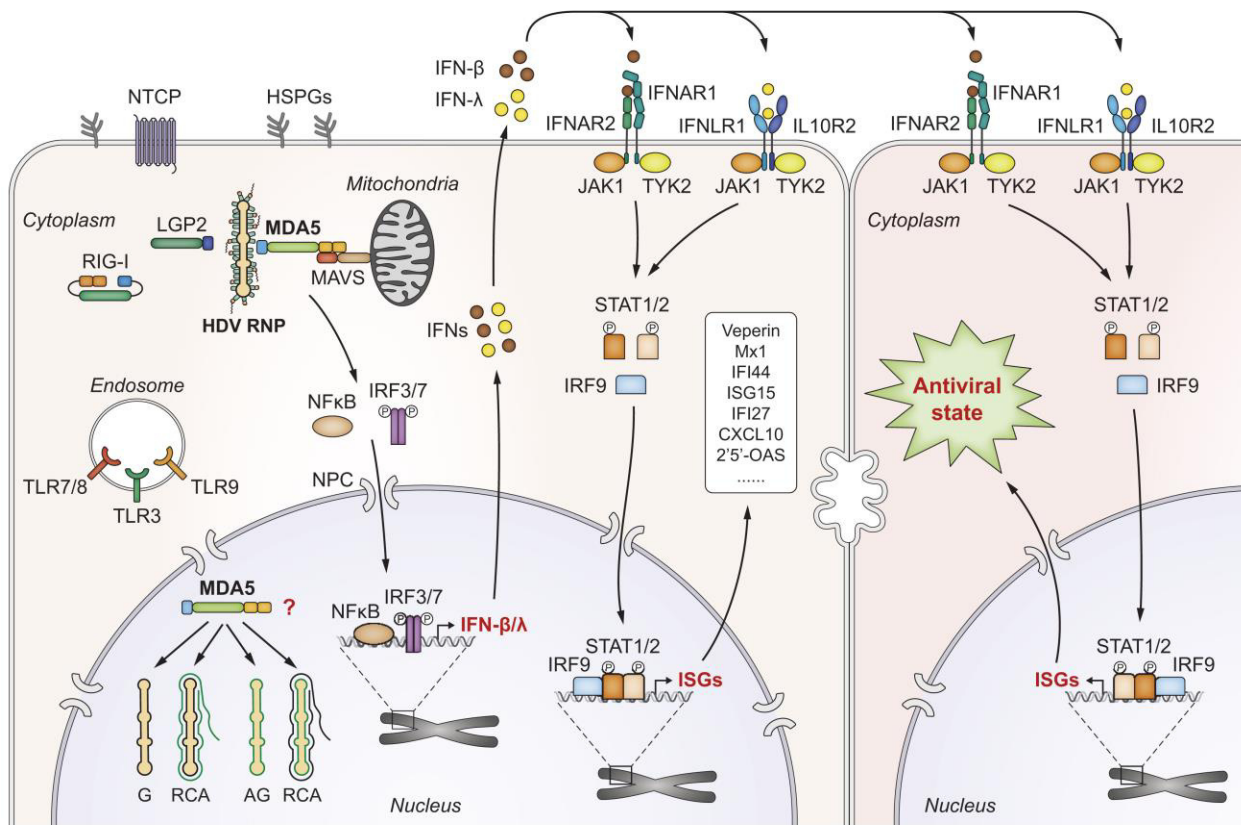


Figure 1.7. Innate immune sensing upon HDV infection. HDV RNP localizes in the cytoplasm where is possibly recognized by the pattern recognition receptor (PRR) MDA5. This recognition activates the mitochondrial antiviral signaling protein (MAVS) and downstream transcription factors, namely IFN regulatory factor (IRF) 3/7 and nuclear factor- κ B (NF κ B). The activated transcription factors are translocated into the nucleus and initiate the transcription of IFN- β/λ . Secreted IFN- β/λ bind to their receptors (IFNAR1/IFNAR2 for IFN- α/β and IFNLR1/IL10R2 for IFN- λ) on the infected cell or neighboring cells, which further activates Janus kinases (JAK) 1/2, tyrosine kinase (TYK) 2, and transcription factors signal transducer and activator of transcription (STAT) 1/2 and IRF9. STAT1/2 and IRF9 are translocated into the nucleus and activate hundreds of IFN-stimulated genes (ISGs), which directly inhibit HDV replication and protect the uninfected cells against subsequent infection. From (Zhang & Urban, 2021).

However, how the recognition of HDV replication occurs remains unclear. HDV replicates in the nucleus of infected cells, but the PRRs that sense the HDV RNA intermediates are mainly located in the cytoplasm (Loo & Gale, 2011). One hypothesis is that a small fraction

of MDA5 may localize in the nucleus, allowing better sensing of mRNA intermediates resulting from HDV replication (Zhang & Urban, 2020).

1.2.6.2 Innate immunity and cell division-mediated spread

Innate immunity responses to HDV infection trigger the production and upregulation of IFNs and ISGs, respectively. However, IFN stimulation has a limited effect on HDV replication in resting non-dividing cells (Zhang et al., 2018; Zhang & Urban, 2021).

HDV-induced interferon responses and exogenous interferon treatment specifically target cell division-mediated spread of HDV (Figure 1.8). The mechanisms by which IFN specifically targets cell division-mediated spread are still poorly understood. HDV replicates in the nuclei, but during mitosis, nuclear membrane disruption could expose the HDV replication intermediates and render the viral RNA susceptible to PRR recognition and consequential degradation (Zhang & Urban, 2021). However, further investigations are needed to fully understand and confirm the exact mechanism behind the IFN mode of action.

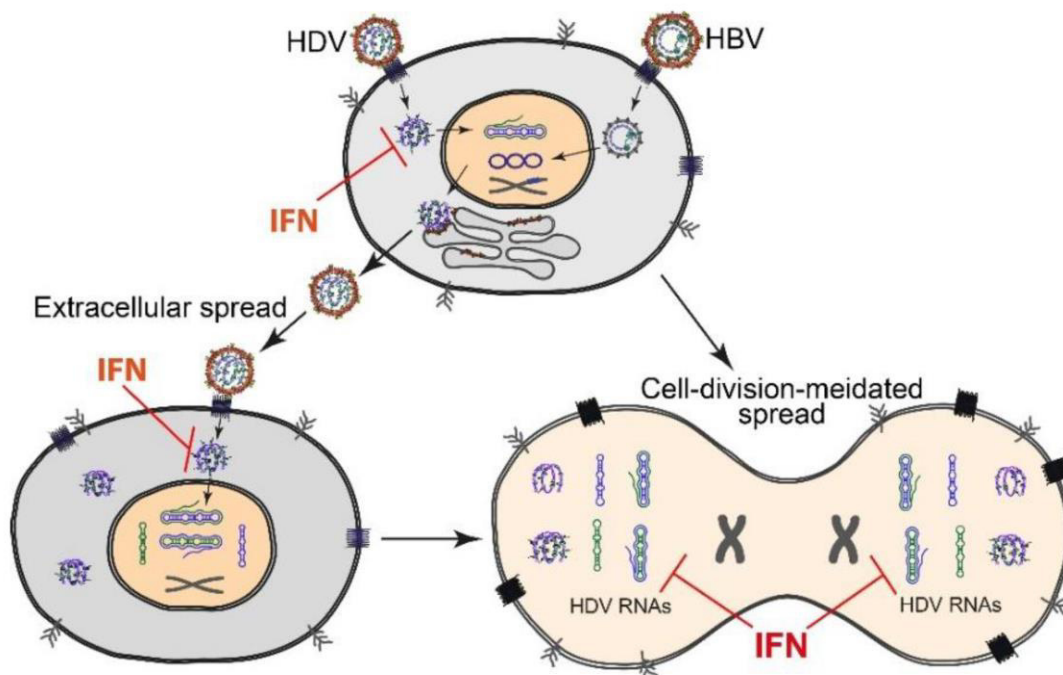


Figure 1.8. Impact of interferon induction on cell division-mediated spread. HDV can spread via two distinct pathways. The first pathway occurs via de novo infection-mediated extracellular spreading, whereby the co-infection of HBV/HDV results in the production of HDV progeny that infects neighboring hepatocytes. Although the IFN response inhibits the early stages of HDV infection, it does not significantly impair HDV RNA replication. The second pathway occurs through cell division-mediated spread, where HDV survives cell division and effectively replicates in both daughter cells. The IFN response causes HDV RNA to be efficiently degraded during cell division, which also prevents the re-establishment of replication in daughter cells. From (Zhang & Urban, 2020).

1.2.6.3 Innate immunity response and HDV genome editing

L-HDAg expression can have an inhibitory effect on HDV replication (Chao et al., 1990; Modahl & Lai, 2000). The ADAR1 enzyme, which catalyzes the transition to L-HDAg expression, exists in two isoforms that differ in length, cellular localization, and induction pathways. While the short ADAR1 (110kDa) localizes only in the nucleus, the large isoform (150kDa) can be found both in the nucleus and cytoplasm and its activation is IFN-dependent (George et al., 2005; Patterson & Samuel, 1995; Savva et al., 2012). Hartwig et al. demonstrated that the activity of the IFN-induced ADAR1-L isoform could enhance the editing of the S-HDAg into L-HDAg (Hartwig et al., 2004; Hartwig et al., 2006), resulting in a reduction of HDV replication.

Although tempting, this putative role of L-HDAg expression in HDV sensitivity to IFN is still debated, as a previous study disproves an upregulation in HDV genome editing upon IFN treatment (Zhang et al., 2022).

1.2.6.4 Viral countermeasures to HDV-induced IFN responses

IFN stimulation targets the cell division-mediated spread of HDV, but only has a minor effect on HDV replication in resting cells. HDV must have adopted countermeasures to prevent elimination upon both viral-induced IFN responses and IFN treatment. Replicating viral RNA might be highly protected within the nuclear membrane, where cytoplasmic PRR have no access (Sato et al., 2010).

Some viruses have been shown to be able to use viral proteins to actively counteract innate immune responses by i) shielding RNA intermediates from degradation or ii) directly binding to key PRRs or other components of the innate immune cascade (Childs et al., 2009; Sui et al., 2023; Zhang et al., 2017). Little is known about HDV, but a potential role for S-HDAg in the resistance could be speculated (Xu et al., 2021). Indeed, S-HDAg not only lacks IFN induction potential when expressed in the absence of replicating RNA (Lucifora et al., 2023), but it has been shown to slightly improve resistance to IFN stimulation upon treatment with Polyinosinic:polycytidylic acid (Poly I:C), a potent immune stimulant interacting with toll-like receptor 3 (TLR3) (Han et al., 2011).

1.2.7. HDV evolution theories and similarity to viroids

The evolutionary history of HDV remains largely unknown. Since its discovery in 1977, several theories have been proposed to elucidate the origin of HDV.

First, HDV shares several characteristics with viruses infecting plants, so-called viroids (Elena et al., 1991).

Viroids are the smallest infectious entities, whose taxonomy includes about 30 viroid species divided into two families: *Pospiviroidae* and *Avsunviroidae* (Figure 1.9) (Giguere & Perreault, 2017).

Members of the *Pospiviroidae* family possess a rod-shaped RNA genome and replicate in the nucleus using the asymmetric rolling-circle mechanism, but they lack intrinsic ribozyme activity. In contrast, the members of *Avsunviroidae* have a highly branched structure; they use a symmetric rolling-circle mechanism to replicate and have hammerhead ribozymes (Ding, 2009; Flores et al., 2014; Wang, 2021). Sharing a small RNA genome, catalytic ribozyme sequences, and viral replication mechanism (de la Pena & Gago-Zachert, 2022; Flores et al., 2011; Lasda & Parker, 2014; Taylor, 2014) hints at the possible origin of HDV from a viroid sequence that transferred from plants to an herbivore reservoir and adapted to replicate in the liver, possibly in co-evolution with HBV.

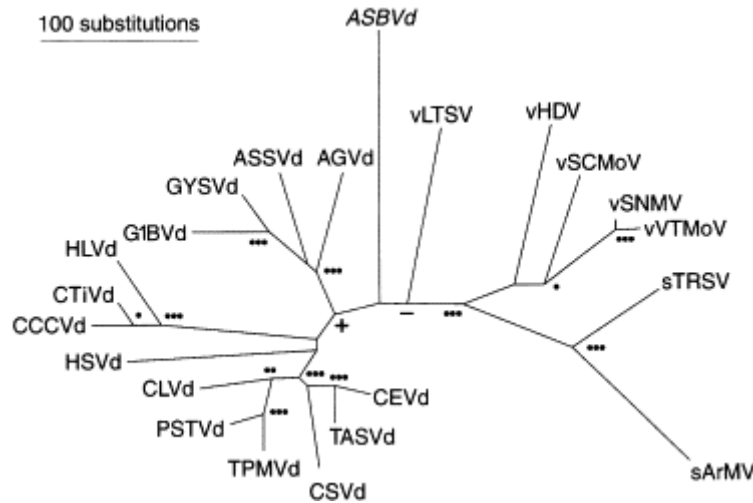


Figure 1.9. Consensus phylogenetic tree containing viroids, viroid-like satellite RNAs, and the viroid-like domain of hepatitis delta virus RNA. From (Elena et al., 1991).

Moreover, viroids, as noncoding RNAs, depend on host factors for replication. Studies have demonstrated the ability of *Pospiviroidae* to hijack host cellular ligase 1 (Nohales et al., 2012) as HDV can redirect a host DNA dependent RNA polymerase for replication.

A second, less plausible theory suggests that HDV is derived from the cellular transcriptome. A ribozyme RNA encoded in the intron region of the CPEB3 gene has a structure similar to the ribozyme encoded in the HDV genome (Salehi-Ashtiani et al., 2006). In addition, in 1996, Brazas et al. identified a protein capable of interacting with S-HDAg and renamed it Delta-interacting protein A (DIPA) (Brazas & Ganem, 1996). This protein, which has a high homology with S-HDAg, was found to influence HDV replication. The hypothesis that HDV originated from a cellular transcript is intriguing. However, the recent discovery of novel HDV-like agents in several animal species adds more complexity to the theory of the cellular origin of HDV. In fact, these findings demonstrate how HDV-like agents can replicate in various animal species, indicating that the evolution of HDV cannot be restricted to humans.

1.3 DISCOVERIES IN THE HDV WORLD: HDV-LIKE AGENTS

For the past 40 years, human HDV has been the only member of the genus *Deltavirus* (Rizzetto et al., 1977).

The human HDV genome is highly variable, with a 16 % difference within the same genotype and up to 40% variation between different genotypes (Le Gal et al., 2017; Stockdale et al., 2020). This heterogeneity is contained within the L-HDAg C-terminal extension (Wang et al., 1986; Wang et al., 2009), which likely allows a differential packaging preference of the HDV RNP by HBsAg (Wang et al., 2021).

This genomic divergence allows the differentiation into 8 clades, namely HDV-1 to HDV-8 (Figure 1.9). However, the ribozyme region is highly conserved among these different genotypes (Pacin-Ruiz et al., 2022).

HDV genotype 1 is distributed worldwide (Braga et al., 2012; Casey et al., 1993; Shakil et al., 1997; Stockdale et al., 2020; Viana et al., 2005). Genotype 2 is predominant in countries in East Asia, such as Japan and Russia (Ivaniushina et al., 2001; Wu et al., 1998). Genotypes 3 and Genotype 4 have been documented in the Amazon basin and Japan, respectively (Alvarado-Mora et al., 2011; Sakugawa et al., 1999).

Genotypes from 5 to 8 are all found in central Africa (Radjef et al., 2004). In 2008, Barros et al. identified genotype 8 infected individuals in the indigenous population of Brazil (Barros et al., 2011).

1.3.1 *The birth of the kolmioviridae family*

Recent advances in the field of metagenomics have led to the discovery of HDV-like agents in the transcriptome libraries of a wide range of non-human vertebrates and invertebrates, such as termites, bats, snakes, deers, and woodchucks (Figure 1.9&10).

In 2018, sequences of HDV-like agents or (delta-like agents, DLAs) were identified in oropharyngeal and cloacal samples collected from several duck species, including Grey

duck, Chestnut teal, and Pacific black duck. Novel HDV-like agents were also found in various tissues of boa constrictors and water pythons (Hetzl et al., 2019; Wille et al., 2018).

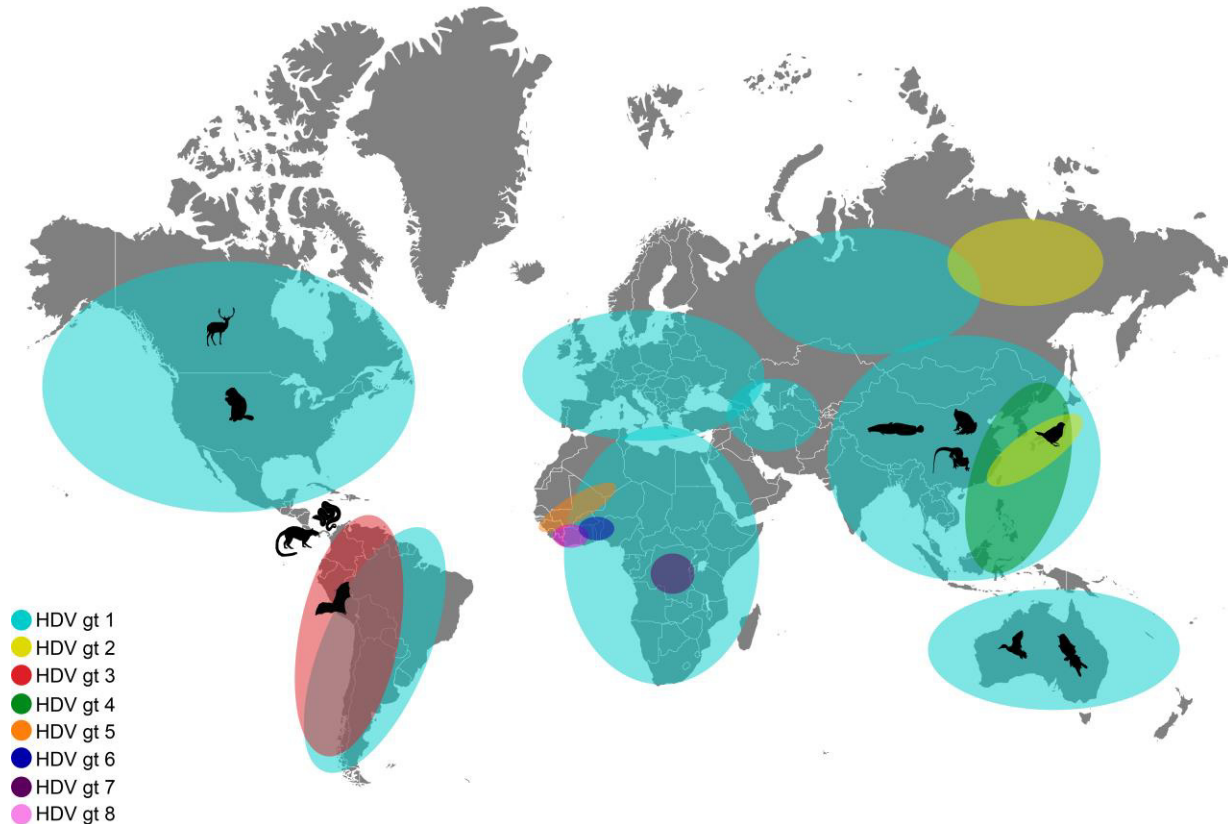


Figure 1.10. Geographic distribution of HDV and HDV-like agents. HDV-like agents identified in Ducks (*avHDV*), Newt (*amHDV*) Toad (*tfHDV*) Fish (*fiHDV*) Termite (*tHDV*), Snake (*sHDV*), Woodchuck (*mmdDV*), Deer (*ovirDV*), Bat (*pmacDV*), Bengalese finch (*lstriDV*) and RodentDV (*roDV*) are depicted in correlation with human HDV (genotypes 1-8) as distribution of animal hosts in which they were identified.

Further discoveries in fish, amphibians, and invertebrates followed in 2019 (168). These DLAs were isolated from samples where no accompanying hepadnaviruses were found, as was the case for the avian delta agent (AvDV).

Potentially bridging the evolutionary gap between human HDV and the HDV-like agents mentioned above, several novel HDV-like viruses have been discovered in different tissues and organs of mammalian species, such as woodchuck, white-tailed deer, Tome's spiny rat, and two species of bats (lesser dog bat and common vampire bat) (Bergner et al.,

2021; Iwamoto et al., 2021; Paraskevopoulou et al., 2020). A more recent discovery identified HDV-like agents in two marsupial species (Harvey et al., 2023).

The discovery of these non-human HDV-like agents has led to the creation of a new taxonomic family named *Kolmioviridae*. The name is derived from the Finnish word "kolmio" meaning triangle, which is a reference to the Greek letter Δ (delta), used to denote the genus *Deltavirus* within the *Ribozyviria* realm (Viruses, 2020).

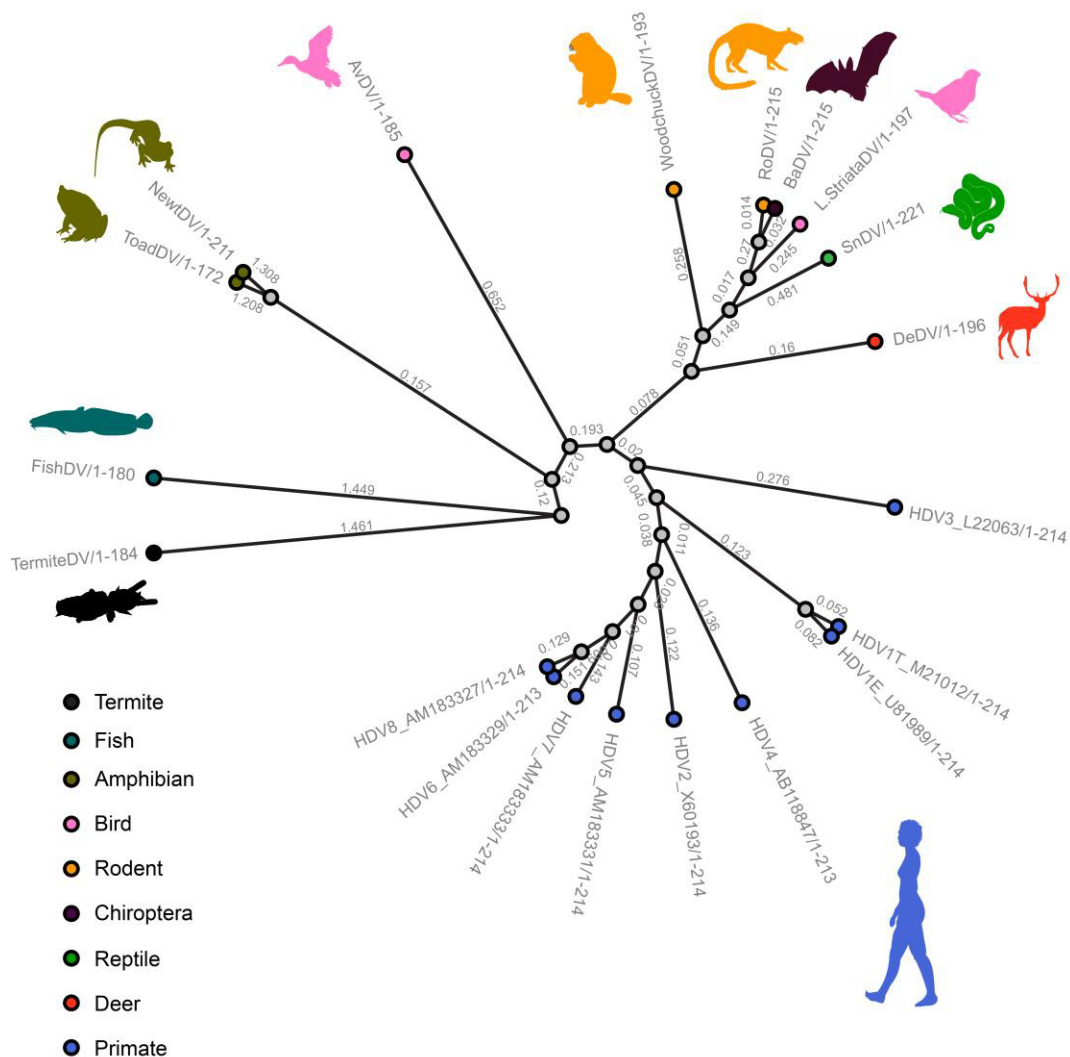


Figure 1.11. Phylogeny of HDV-like agents. Phylogenetic analysis of the S-HDAg from the human HDV (genotypes 1-8) and small delta antigens (SDAg) of HDV-like agents. Color codes refer to host species taxa.

Values along the branches represent Bayesian posterior probabilities (PP) indicating the probability (=1) that the tree is correct.

1.3.2 Genome organization and antigen expression

Due to the novelty of these discoveries, detailed characterization and in-depth *in vitro* data are currently lacking. The primary source of information on genome characteristics and viral antigen expression comes from *in silico* prediction models. These models show typical features of HDV, such as the presence of genomic and antigenomic ribozymes, a high degree of self-complementarity of the circular genome, and an ORF encoding a small delta antigen (S-DAg) (de la Pena et al., 2021; Wille et al., 2018) (Figure 1.11).

AvDV and snake (SnDV) HDV-like agents share 53% and 32% genomic identity with human HDV genotype 1, respectively (Hetzl et al., 2019; Wille et al., 2018). The viral antigen of toad, newt, fish, and termite agents share 26%, 23%, 23%, and 26% amino acid identity with S-HDAg, respectively, as expected given the phylogenetic distance between the hosts (Chang et al., 2019).

The DAgs of HDV-like agents identified in mammalian species share higher identity with human HDAg (56% to 63%) (Bergner et al., 2021; Iwamoto et al., 2021; Paraskevopoulou et al., 2020). This could indicate a potential common ancestor shared with HDV (Perez-Vargas et al., 2021).

HDV relies on its prenylated L-HDAg to exploit HBsAg for virion formation, but little is known about non-human HDV-like agents.

Interestingly, an UAG stop codon that could potentially be edited by ADAR1 is present in the snake, deer, and bat HDV-like agents genome sequence but only in the snake and bat DLAs genomes, the editing could lead to the addition of 22 and 18 amino acids, respectively.

A plus one (+1) frameshift event in the AvDV and woodchuck delta agent (WoDV) DAgs would result in the addition to their S-DAg of 18 and 1 amino acids, respectively. None of

these putative ADAR1 editing events or frameshift mutations could lead to the expression of a prenylation motif.

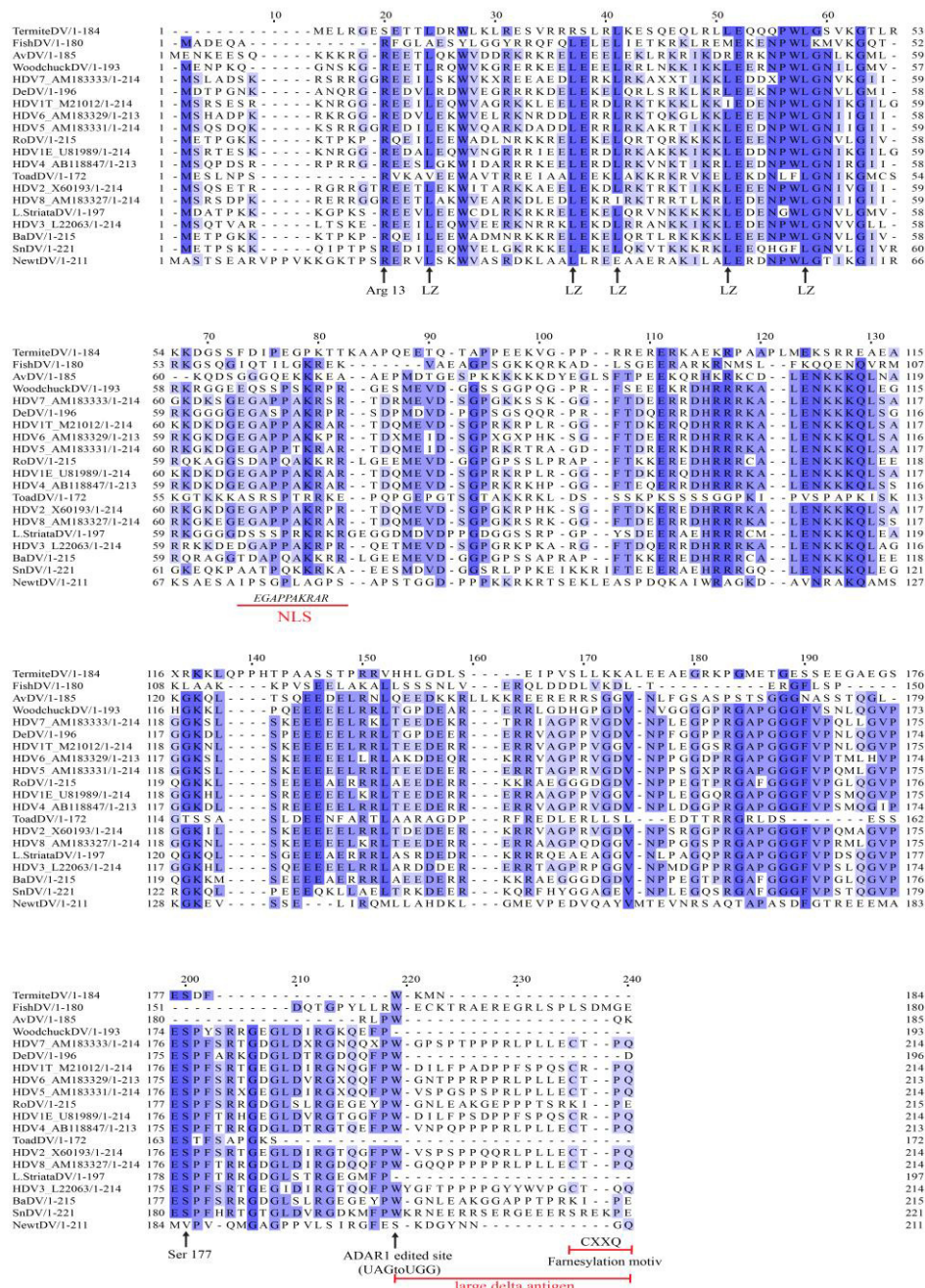


Figure 1.12. Alignment of L-HDAG sequences of HDV and putative L-DAg originated by editing of HDV-like agents genomes. The translated genome of human HDV is compared with the putative L-DAg of newly discovered delta agents. The translations of the L-DAg proteins were aligned using MUSCLE and visualized using Jalview. Conserved regions sharing similar signatures between different

DAGs are marked in blues. The consensus sequence was obtained considering a threshold of $\geq 50\%$ of amino acid identity.

The lack of a prenylation motif supports the hypothesis that the association between HDV and HBV is not evolutionarily conserved and that these agents may spread via alternative pathways. The novel HDV-like agents may indeed be capable of being packaged by different envelope glycoproteins in a farnesylation-independent manner.

1.3.3 Extracellular spread and transmission

1.3.3.1 Co-infection and putative helper virus

Bergner et al. sought to investigate the putative helper virus co-infection for the mammalian HDV-like agents identified in woodchuck, deer, and bat (Bergner et al., 2021) (Table 1.4). A screen to identify candidate helper associations revealed no trace of hepadnaviruses, while poxviruses, hepaciviruses, and retroviruses were present. The authors of the AvDV report identified sequences of the influenza A virus genome in the same swabs (Wille et al., 2018); similarly, SnDV was shown to replicate and spread using envelope proteins of both reptarenaviruses and hartmanviruses *in vitro* (Hetzl et al., 2019; Szirovicza et al., 2022; Szirovicza et al., 2020). Furthermore, HDV-like agents identified in bat species were found to co-infect with poxviruses, hepaciviruses, and retroviruses, with no trace of hepadnaviruses (Bergner et al., 2021; Iwamoto et al., 2021; Paraskevopoulou et al., 2020).

These data led to the hypothesis that the novel DLAs may have evolved to use various hepadna-unrelated enveloped viruses as helpers.

Given these genomic peculiarities of HDV-like agents, we could further speculate that their primary spread pathway may be even different from the cell-free spread used by HDV.

Delta agent	Putative L-DAG	Identified Co-infection	References
Avian (avHDV)	yes (no CxxQ)	Influenza virus	(Wille et al., 2018)
Newt HDV (amHDV)	no	Newt astrovirus	(Chang et al., 2019)
Toad HDV (tfHDV)	no	Influenza virus, toad astrovirus	(Chang et al., 2019)
Fish HDV (fiHDV)	no	Frogfish arenavirus, goosefish hantavirus, batfish reovirus	(Chang et al., 2019)
Termite HDV (tHDV)	no	Flavi-like virus	(Chang et al., 2019)
SnakeHDV (sHDV)	yes (no CxxQ)	Reptarenavirus, Hartmanivirus	(Hetzel et al., 2019; Szirovicza et al., 2020)
Woodchuck DV (mmoDV)	no	Hepadnavirus ?	(Bergner et al., 2021; Iwamoto et al., 2021)
Deer DV (ovirDV)	no	Poxviridae	(Bergner et al., 2021; Iwamoto et al., 2021)
BatDV (pmacDV)	yes (no CxxQ)	Bat HCV, Pegivirus	(Bergner et al., 2021; Iwamoto et al., 2021)
Bengalese finchDV (IstriDV)	no	/	(Iwamoto et al., 2021)
RodentDV (roDV)	yes (no CxxQ)	/	(Paraskevopoulou et al., 2020)

Table 1.4. HDV-like agents, potential genome editing and identified co-infections.

1.3.3.2 Autonomous extracellular cell-to-cell spread

The spread and transmission pathways of the new HDV-like agents are still undefined. Human HDV shares specific characteristics with viroids (Flores et al., 2011; Taylor, 2014). It is well understood how these plant viruses can spread from cell to cell through nanochannels called *plasmodesmata*, which are physiologically used to transport small molecules and nutrients between neighboring cells (Kumar et al., 2015). Although this is not the primary route of HDV spread, things may have been different before the co-evolution that allowed HDV to exploit the HBV surface protein to egress and *de novo* infect cells.

It has been described how many viruses can spread from infected to uninfected cells by exploiting physiological cell-cell contacts or by establishing *de novo* ones by subverting

the cellular adhesion machinery. For example, HCV has been shown to spread even in the presence of neutralizing antibodies that block both the viral glycoprotein and the cellular receptor required for cell attachment and entry (Timpe et al., 2008). Measle virus can induce cell-cell fusion and syncytia formation as an alternative to cell-free spread (Duprex et al., 1999). HIV requires CD4 as a primary receptor on the surface of immune cells but can also use virological synapsis to spread between neighboring cells (Groot et al., 2008). The strategy of spreading by direct cell-to-cell infection has several advantages. It allows for rapid transmission without binding to a specific receptor on the target cell surface, simplifying the entry process. In addition, this method may require a lower level of viral replication to establish a new infection. Finally, movement without leaving the intracellular *milieu* could protect the virus from external factors (Mothes et al., 2010; Sattentau, 2008).

1.3.3.3 Host-to-host transmission

In contrast to HBV, vertical transmission of HDV from mother to offspring is rare (Aliasi-Sinai et al., 2023). Among the HDV-like agents, the case of SnDV provides interesting insights into host-to-host spread. Indeed, evidence of infection has been reported in a boa constrictor and its offspring, as well as in a water python sharing the same environment (Hetzl et al., 2019). This may indicate both horizontal and vertical transmission. WoDV, which was found replicating in a newborn woodchuck without woodchuck hepatitis virus (WHV) co-infection, would further support the hypothesis of vertical or/and parenteral transmission.

The discovery of these novel HDV-like agents in different animal species highlights the likelihood of inter-taxon transmission and the zoonotic potential of the delta virus genus. The spiny rat delta agent (RDeV) described by Paraskevopoulou et al. (Paraskevopoulou et al., 2020) shares a high degree of genomic identity with the lesser dog-like bat delta agent (PmacDV), suggesting putative interspecies host shifts (Bergner et al., 2021) and hinting towards a potential transmission between these two hosts.

1.3.4 Cellular tropism and tissue range

The hepatic tropism of HDV is mainly due to its strong correlation with HBV co-infection, which was previously thought to be exclusive. This understanding has been completely undermined by a recent study reporting that HDV can utilize envelope glycoproteins of viruses other than HBV (e.g., HCV, VSV, DENV) to produce infectious particles (Perez-Vargas et al., 2019). This observation opened intriguing epidemiological perspective, especially in term of HCV infection, considering the high prevalence and death rate of this hepatic virus. However, epidemiological evidence of this putative transmission are lacking, since only one patient was reported with circulating HDV RNA in absence of HBV infection markers (Chemin et al., 2021), and no further studies corroborated this observation (Cappy et al., 2021; Pfluger et al., 2021; Roggenbach et al., 2021).

Since no helper virus has been identified to suggest a specific cellular tropism, it is not surprising that these agents have been found in different organs (Table 3). Wille *et al.* reported HDV-like agent sequences found in a pool of oropharyngeal and cloacal samples from several duck species (Wille et al., 2018).

The novel SnDV was found in various tissues of two snake species, such as the liver, spleen, kidney, lung, and brain, indicating a broad cellular tropism (Hetzl et al., 2019) (Table 3).

In addition, HDV-like agents identified in fish, amphibians, and invertebrates were detected predominantly in the intestines, livers, lungs, and gills of these species (Chang et al., 2019).

Mammalian HDV-like agents have also been detected in the liver, heart, lung, intestine, and kidney of a spiny rat (Paraskevopoulou et al., 2020), in the liver and blood of a woodchuck, in the pedicle of a white-tailed deer, and in the liver of two species of bats (Bergner et al., 2021; Iwamoto et al., 2021).

Delta agent	Genome Size (bp)	GC content (%)	Host species	Host Organ	References
Avian (avHDV)	1706	50	<i>Anas gracilis, Anas castanea, Anas superciliosa</i>	Cloaca, respiratory tract	(Wille et al., 2018)
Newt HDV (amHDV)	1735	56	<i>C.orientalis</i>	Gut, liver	(Chang et al., 2019)
Toad HDV (tfHDV)	1547	56	<i>B.gargarizas</i>	Lung	(Chang et al., 2019)
Fish HDV (fiHDV)	1583	46	<i>Macroramphosusscolopax, Ophidion sp., Eptatretus burgeri, Okamejei acutispina, Proscyllium habereri, Lophius litulon, Eleutheronema tetradac tylum, Zeus faber, Antennarius striatus, Halieutaea stellata, Gonorynchus abbreviatus</i>	Gill	(Chang et al., 2019)
Termite HDV (tHDV)	1589	56	<i>S.intermedius</i>	Whole body	(Chang et al., 2019)
SnakeHDV (sHDV)	1711	53	<i>Boa constrictor, Liasis mackloti savuensis</i>	Brain, liver, lung, kidney, spleen	(Hetzel et al., 2019; Szirovicza et al., 2020)
Woodchuck DV (mmoDV)	1712	56	<i>Marmota monax</i>	Liver, PBMC	(Bergner et al., 2021; Iwamoto et al., 2021)
Deer DV (ovirDV)	1690	55	<i>Odocoileus virginianus</i>	Pedicle	(Bergner et al., 2021; Iwamoto et al., 2021)
BatDV (pmacDV)	1669	54	<i>Peropteryx macrotis</i>	Liver	(Bergner et al., 2021; Iwamoto et al., 2021)
Bengalese finchDV (lstriDV)	1708	56	<i>Lonchura striata</i>	Blood	(Iwamoto et al., 2021)
RodentDV (roDV)	1669	54	<i>Proechimys guirae</i>	Liver, kidney, lung, heart, small intestine	(Paraskevopoulou et al., 2020)

Table 1.5. HDV-like agents and identification species and organs. HDV-like agents are represented in correlation to their genome size (in bp), genome GC content (in percentage , %), the host species and the organs in which RNA sequences were identified.

With the discovery of new DLAs, it has become clear that the strong liver tropism proper of HDV, is not strictly conserved among the *Deltavirus* genus.

1.3.5 HDV-like agents and innate immunity

So far, there is a lack of studies on the interaction between HDV-like agents and the respective host immune system. However, in line with what was previously discussed for HDV, the role of IFN in the replication and persistence of HDV-like agents could be speculated.

Paraskevopoulou et al. evaluated the immune response in *P. semispinosus* by indirect immunofluorescence assay in serum samples (Paraskevopoulou et al., 2020). Both RDeV RNA-positive and RDeV RNA-negative samples tested positive for anti-RDeAg antibodies, suggesting the potential role of the adaptive immune response in viral clearance. In addition, hydrodynamic delivery of cDNA of the RDeV genome induced upregulation of several ISGs in an *in vivo* mouse model (Khalfi et al., 2023).

Studying the induction of innate immunity upon infection with HDV-like agents may play a critical role in better understanding host-to-host transmission and putative evasion mechanism (Bean et al., 2013; Mandl et al., 2015)

1.4 RESEARCH AIMS AND APPROACHES

This project aims to characterize HDV-like agents in terms of their replication, viral spreading pathways, and cellular permissiveness.

Aim 1: Investigation of replication, host range and cellular permissiveness

The goal here is to establish cell culture and detection systems in order to better understand and identify cellular permissiveness and potential cell-to-cell spreading pathways.

First, infectious clones encoding 1.1-fold antigenomic RNAs of the HDV-like agents will be generated. It is expected that viral replication will begin upon transfection of different cell lines. Assays will be developed to detect HDV-like agent antigens in transfected and infected cells using generated antibodies for immunofluorescence (IF) and western blot (WB) analysis. In addition, viral RNA will be detected by northern blot (NB) and quantitative reverse transcription polymerase chain reaction (RT-qPCR) in intracellular and supernatant samples. These tools will be used to characterize the replication of HDV-like agents. In addition, the replication competence of HDV-like agents will be assessed by cell division-mediated viral amplification assay (CDMAA), as recent studies have shown HDV replication to spread and persist even after cell division.

The efficiency of viral replication in tissues other than the liver will be evaluated, as some HDV-like agents have been isolated from non-hepatic tissues and may use envelope proteins from non-hepadnaviruses. Replication assays will be performed in various human and non-human cell lines. After analyzing their tissue tropism, the transmission efficiency of HDV-like agents in different cell lines will be evaluated via two transmission pathways: envelope-mediated *de novo* infection and cell division-mediated spread (CDMS).

Aim 2: Virion pseudo-typing and extracellular spread

This study aims to investigate the ability of newly found HDV-like agents to use envelope glycoproteins from hepadnaviruses and non-hepadnaviruses to generate infectious particles. To achieve this goal, infectious clones of HDV-like agents will be co-transfected with plasmids that encode envelope proteins from different viruses, including HCV and vesicular stomatitis virus (VSV). Viral secretion validation in cell culture media will be performed by measuring viral genome copies and conducting infection assays on susceptible cell lines. The outcome of this approach will provide insight into the release of pseudo-typed viruses and their capability to enter cells based on specific cellular tropism conferred by diverse envelope glycoproteins.

Aim 3: Role of innate immunity in the replication of HDV-like agents

Previous research has shown that HDV replication activates the innate immune sensor MDA5, stimulating a robust type I IFN response (Zhang et al., 2018).

In this study, to characterize the innate immune response against HDV-like agents, an infectious cell culture system including HDV-like agent pseudo-particles and NTCP-expressing human cell lines derived from liver (HuH7, HepaRG) and lung (A549), will be established. These tools will be used to study the IFN response upon HDV-like agents infection, and the impact of the innate immune response on their spread and replication.

This data will provide novel insights into the host-pathogen interface of HDV-like agents and propose HDV-like agents as a tool for investigating the role of the L-HDAg in HDV replication, spread, and interplay with immune system.

Overall, this project aims to provide a comprehensive understanding of the evolution of the *Deltavirus* genus while elucidating the complex co-evolutionary relationship between satellite and helper viruses.

2. MATERIALS AND METHODS

2.1 Materials

2.1.1 Cell lines

Cell line name	Specification	Reference
HuH7	Human hepatocarcinoma cells	
HuH7 ^{NTCP}	Subclone derived from HuH7 cells by lentiviral overexpression of NTCP	Zhang et al., (2018)
HepG2	Human liver carcinoma-derived cells line	Aden et al., (1979)
HepG2 ^{NTCP}	Subclone derived from HuH7 cells by lentiviral overexpression of NTCP	Zhang et al., (2018)
HEK293T	Human embryonic kidney cell line	DuBridge et al., (1987)
HeLa	Uterus adenocarcinoma cells	Scherer et al., 1953
A549	Lung adenocarcinoma cells	Gillich et al., (2023)
A549 ^{NTCP}	Subclone derived from HuH7 cells by lentiviral overexpression of NTCP	Gillich et al., (2023)
A549 MDA5 KO	MDA5 knock out	Gillich et al., (2023)
HepaRG	Human hepatoma cell line	Gripon et al., (2002)
HepaRG ^{NTCP} shNT		Zhang et al., (2018)
HepaRG ^{NTCP} shMDA5	Subclone derived from HuH7 cells by lentiviral overexpression of NTCP	Zhang et al., (2018)
HepaRG ^{NTCP} MDA5KO	MDA5 knock out	Gillich et al., (2023)
HepaRG ^{NTCP} LGP2KO	LGP2 knock out	Gillich et al., (2023)
HepaRG ^{NTCP} MDA5/LGP2DKO	MDA5/LGP2 double knock out	Gillich et al., (2023)
Vero E6	African green monkey kidney cells	Prof. Ralf Bartenschlager, Heidelberg
CHO	Chinese hamster ovary cells	Schulze et al., (2007)
PaKi	Bat kidney cells	Prof. Martin Schwemmle, Freiburg
LMH	Chicken hepatoma cells	Urban et al., (1998)
WHC-17	Woodchuck hepatoma cells	Dr. Carla Coffin, Calgary
HuH7 TtA L-HDAg	HuH7 cells with TtA promoter for inducible expression of L-HDAg	Zhenfeng Zhang
HepG2 ^{HA-NTCP}	Subclone derived from HepG2 cells by lentiviral overexpression of HA-NTCP	This thesis

HepG2 ^{HA-NTCP S267F}	Subclone derived from HepG2 cells by lentiviral overexpression of HA-NTCP S267F	This thesis
--------------------------------	---	-------------

Table 2.1. Cell lines used in this study.

2.1.2 Viruses and pseudoparticles

Virus	Viral (pseudo) particle for infection assay	Source
HBV	Cell-culture derived, produced in HuH7 cells by co-transfection and purified via PEG precipitation or heparin affinity chromatography	This Thesis
HDV	Cell-culture derived, produced in HuH7 cells by co-transfection and purified via PEG precipitation or heparin affinity chromatography.	This Thesis
WoDV/ HBsAg	Cell-culture derived, produced in HuH7 cells by co-transfection and L-HDAg complementation and purified via PEG precipitation or heparin affinity chromatography.	This thesis
DeDV/ HBsAg	Cell-culture derived, produced in HuH7 cells by co-transfection and L-HDAg complementation and purified via PEG precipitation or heparin affinity chromatography.	This Thesis
HCV	Strain: J6/JFH1 chimera (gt2a)	Prof. Dr. Volker Lohman Heuss, Rothhaar et al., (2022)
DENV	Strain : New Guinea C (NGC)	Amplified from cDNA clone (Dr. Alessia Ruggeri)

Table 2.2. Viruses and pseudo particles used in this study.

2.1.3 Antibodies

2.1.3.1 Primary antibodies

Name	Dilution	Reference	Supplier	Cat. No.	Clone no.
HDAg	IF 1:3000 WB 1:3000	Wang W et al., (2021)	Kerafast	EHD001	FD3A7
SnDAg	IF 1:1000 WB 1:1000	This thesis			
AvDAg	IF 1:1000 WB 1:1000	This thesis			

β -actin	WB 1:5000	Zhang et al., (2018)	Sigma-Aldrich	A5441	AC15
Mx1	IF 1:500 FACS 1:500	Flohr et al., (1999) FEBS Lett. 463, 24-28	Dr. Georg Kochs, Germany	/	M143
pSTAT1	IF 1:500	Mutz et al., (2018)	BD	562072	
MDA5	WB 1:1000		Enzo Life Sciences	ALX-210-935	
LGP2	WB 1:100		IBL		
HBsAg		Lempp et al., (2019)	Davide Cortin, Humans Biomed	Human anti HBsAg monoclonal antibody	HBD87
HCV NS5A		Lindenbach et al., (2005)			9E10
DENV NS4B	IF 1:100	/	GeneTex	GTX124250	
WGA	IF 1:1000	Goellner et al. (2023)	Thermo Fisher Scientific	W11261	
ADAR1	WB 1:1000		Cell Signaling	14175	

Table 2.3. Primary antibodies used in this study.

2.1.3.2 Secondary antibodies

Name	Dilution	Supplier	Cat. No.
Goat anti-mouse AlexaFluor 488	IF 1:1000	Thermo Fisher Scientific	A11001
Goat anti-rabbit AlexaFluor 488	IF 1:1000	Thermo Fisher Scientific	A11008
Goat anti-human AlexaFluor 488	IF 1:1000	Thermo Fisher Scientific	A1013
Goat anti-human AlexaFluor 555	IF 1:1000	Thermo Fisher Scientific	A21433
Goat anti-rabbit AlexaFluor 546	IF 1:1000	Thermo Fisher Scientific	A11010
Goat anti-rabbit AlexaFluor 647	IF 1:1000	Thermo Fisher Scientific	A21244
Goat anti-rabbit IRDye 800CW	WB: 1:10000	Licor	
Goat anti-mouse IRDye 680CW	WB: 1:10000	Thermo Fisher Scientific	A21057
Goat anti-mouse IRDye 800CW	WB: 1:10000	Licor	A21244

Table 2.4. Secondary antibodies used in this study.

2.1.4 Peptides

Name	Sequence	Source
Myrcludex B (MyrB)	MyrGTNLSVPNPLGFFPDHQLDPAFGANSNNPDWDF NPNKDHWEANKVG	Walter Mier
MyrB Atto565	MyrGTNLSVPNPLGFFPDHQLDPAFGANSNNPDWDF NPNKDHWEANKVG - Atto565	Walter Mier

Table 2.5. Peptides used in this study.

2.1.5 Plasmids

Plasmid name	Description	Reference
pJC126	Eukaryotic expression vector encoding an overlength (1.1) antigenome of Hepatitis Delta Virus genotype 1	Gudima et al., (2002)
pcDNA3.1/Zeo(+) SnDV 1.1(-)	Eukaryotic expression vector encoding an overlength (1.1) antigenome of snake delta agent	This thesis
pcDNA3.1/Zeo(+) AvDV 1.1(-)	Eukaryotic expression vector encoding an overlength (1.1) antigenome of avian delta agent	This thesis
pcDNA3.1/Zeo(+) WoDV 1.1(-)	Eukaryotic expression vector encoding an overlength (1.1) antigenome of woodchuck delta agent	This thesis
pcDNA3.1/Zeo(+) DeDV 1.1(-)	Eukaryotic expression vector encoding an overlength (1.1) antigenome of deer delta agent	This thesis
pcDNA3.1/Zeo(+) BaDV 1.1(-)	Eukaryotic expression vector encoding an overlength (1.1) antigenome of bat delta agent	This thesis
pcDNA3.1/Zeo(+)-HDVgt5Senegal (defect)	Eukaryotic expression vector encoding an overlength (1.1) antigenome of Hepatitis Delta Virus genotype 5, replication defective	Wang et al., (2021)
pcDNA3.1/Zeo(+)-L-HDAg	Eukaryotic expression vector encoding the large HDAg with the editing mutation	Christina Filzmayer
pLX304-WH2.8 (WHV 2564-2105) env	Eukaryotic expression vector encoding the envelope proteins of Woodchuck hepatitis B virus	Wenshi Wang
pWPI_spE1E2J6_Zeo-HCVEnv	Eukaryotic expression vector encoding the envelope proteins of HCV	Prof.Ralf Bartenschlager, Heidelberg
pMD2.G (vsv-g)	VSV-G expression construct for pseudotyping of Lentiviruses	Didier Trono
psPAX2 (gag-pol)	Lentiviral packaging vector expressing HIV gag, pol, tat and rev	Didier Trono
pWPI Puro DVs prM-E	Eukaryotic expression vector encoding the surface proteins of DENV	Prof.Ralf Bartenschlager,

		Heidelberg
pWPI Puro HA-hNTCP	Bicistronic lentiviral vector encoding human NTCP with HA tag at N-terminus	Yi Ni
pWPI Puro HA-hNTCP-C800T	Bicistronic lentiviral vector encoding human NTCP S267F variant with HA tag at N-terminus	Yi Ni
pJC126 HDV gt1 Taylor 2xUAA pSVLD3	pJC126 with two TAA stop mutations Eukaryotic expression vector encoding a head-to-tail trimer of the Hepatitis Delta Virus antigenome (genotype 1)	Benno Zehnder Kuo et al., (1989)
pT7HB2.7	Plasmid encoding a 2700 bp subgenomic fragment of HBV including the L, M, S & X ORFs under the authentic promoter	Sureau et al., (2003)
pcDNA3.1/Zeo(+) empty	Eukaryotic expression empty vector	
pcDNA3.1/Zeo(+)-pcDNA-L-HDAg C211S	Eukaryotic expression vector encoding the large HDAg with the editing mutation and a mutation at position C211	This thesis
pcDNA3.1/Zeo(+)-pcDNA-L-HDAgQ214Stop	Eukaryotic expression vector encoding the large HDAg with the editing mutation and a mutation at position S214	This thesis
pcDNA-S-HDAg	Eukaryotic expression vector encoding the small HDAg	Christina Filzmayer
pcDNA3.1/Zeo(-) HuL S98A	Eukaryotic expression vector encoding HBV mutated L protein	This thesis
pcDNA3.1/Zeo(-) HuL S98D	Eukaryotic expression vector encoding HBV mutated L protein	This thesis
pcDNA3.1/Zeo(-) HuL S67A	Eukaryotic expression vector encoding HBV mutated L protein	This thesis
pcDNA3.1/Zeo(-) HuL S67D	Eukaryotic expression vector encoding HBV mutated L protein	This thesis
pcDNA3.1/Zeo(-) HuL S6A	Eukaryotic expression vector encoding HBV mutated L protein	This thesis
pcDNA3.1/Zeo(-) HuL S6D	Eukaryotic expression vector encoding HBV mutated L protein	This thesis

Table 2.6. Plasmids used in this study.

2.1.6 Primers and oligos

Name	Sequence (5' to 3')	Source
NheI_for	TCAATGGGAGTTTGTTTTGGCACC	This Thesis
EcoRI_rev	GTAGTCAGAACAGGGTTTACTGTT	
S98A_for	CCTACCCCGCTGGCCCCACCTTTGAGAAACT	This Thesis
S98A_rev	TCTCAAAGGTGGGGCCAGCGGGTAGGCTGCCT	

S98D_for	CCTACCCCGCTGGACCCACCTTTGAGAAACACT	This Thesis
S98D_rev	TCTCAAAGGTGGGTCCAGCGGGGTAGGCTGCCT	
S67A_for	CTTTTGGGGTGGGCCCTCAGGCTCAGGGCATA	This Thesis
S67A_rev	CTGAGCCTGAGGGGCCACCCCAAAGGCCTCC	
S67D_for	CTTTTGGGGTGGGACCCTCAGGCTCAGGGCATA	This Thesis
S67D_rev	CTGAGCCTGAGGGTCCCACCCCAAAGGCCTCC	
S6A_for	GGGCAGAATCTTGCCACCAGCAATCCTCTGGGA	This Thesis
S6A_rev	AGGATTGCTGGTGGCAAGATTCTGCCCATGCT	
S6D_for	GGGCAGAATCTTGACACCAGCAATCCTCTGGGA	This Thesis
S6D_rev	AGGATTGCTGGTGTCAAGATTCTGCCCATGCT	
HDV-Ferns_for	GCGCCGGCYGGGCAAC	Ferns et al., (2012)
HDV-Ferns_rev	TTCCTCTTCGGGTCGGCATG	
HDV_for	ATGAGCCGGTCCGAGTCGAGGAAGA	This Thesis
HDV_rev	TTCTTTCTTCGGCCACCCACTGC	
WoDV_for	CCTGGCTGGGGAACATCCTGGGAAT	This Thesis
WoDV_rev	TTCTCCTCGTGGTCTCTTGGACGGG	
DeDV_for	AATCCCTGGCTGGGAAACGTCTCTCG	This Thesis
DeDV_rev	ATCCGATCTTGGTCTCTTGGCCGGG	
BaDV_for	AACCCATGGCTGGGGAACGTTCTTG	This Thesis
BaDV_rev	GCGTCTTTTCTTAGCCTGGGGAGCG	
hIFNb_for	ACCAACAAGTGTCTCCTCCA	Zhang et al., (2018)
hIFNb_rev	AAGCCTCCCATTCAATTGCC	

hIFN1_for	CGCCTTGGAAGAGTCACTCA	Zhang et al., (2018)
hIFN1_rev	GAAGCCTCAGGTCCCAATTC	
RSAD2_for	CGTGAGCATCGTGAGCAATG	Zhang et al., (2018)
RSAD2_rev	TCTTCTTTCCTTGGCCACGG	
MxA_for	AAGAGCCGGCTGTGGATATG	Zhang et al., (2018)
MxA_rev	GCGGTTCTGTGGAGGTTA	
ISG15_for	GATCACCCAGAAGATCGGCG	Zhang et al., (2018)
ISG15_rev	GTTCTGTCGCATTTGTCCACC	
Mx1_for	AAGAGCCGGCTGTGGATATG	Zhang et al., (2018)
Mx1_rev	GCGGTTCTGTGGAGGTTAA	
IFI27_for	TGCTCTCACCTCATCAGCAG	Zhang et al., (2018)
IFI27_rev	GGCCACAACCTCCTCCAATCA	
IFI44_for	TGAGTGAGAAAGAAGGCGGC	Zhang et al., (2018)
IFI44_rev	GTCCTTCAGCGATGGGGAAT	
hIFNa_for	GACTCCATCTTGGCTGTGA	Zhang et al., (2018)
hIFNa_rev	TGATTTCTGCTCTGACAACCT	
hGAPDH_for	GAAGGTGAAGGTCGGAGTC	Zhang et al., (2018)
hGAPDH_rev	GAAGATGGTGATGGGATTTTC	
hNTCP_for	GGACATGAACCTCAGCATTGTG	Appelman et al.,(2017)
hNTCP_rev	GCCGTTTGGATTTGAGGACG	
HA tag_for	CACCATGTACCCATACGATGTT	Appelman et al.,(2017)
HA tag_rev	ATGATGCCATACTGTGCCAC	

Table 2.7. Oligos used in this study.

2.1.7 Kits

Name	Provider	Cat. No
High-capacity cDNA reverse transcription kit	Thermo Fisher	362271
GeneJET gel extraction kit	Thermo Scientific	K0691
GeneJET PCR purification kit	Thermo Scientific	K0701
Nucleospin RNA kit	Thermo Scientific	740955.250
Nucleospin tissue kit	Thermo Scientific	740952.29
Plasmid plus mini kit	Qiagen	12143
Plasmid plus midi kit	Qiagen	12943

DIG RNA Labeling Mix	Roche	11 277 073 910
Viral RNA mini kit	Qiagen	52906
Digoxin (DIG) Luminescent Detection Kit for Nucleic Acids	Roche	11363514910
DIG Easy Hyb™	Roche	11603558001
DIG Wash and Block Buffer Set	Roche	11585762001

Table 2.8. Kits used in this study.

2.1.8 Chemicals and Reagents

Chemical	Company/provider	Cat.no.
[α -P32] deoxycytidine 5'-triphosphate (dCTP)	Hartmann Analytic	SRP-205
Acetic acid	Sigma-Aldrich	33209
Acrylamide/Bisacrylamide(30% w/v)	SERVA electrophoresis	10687
Adenosine 5'-Triphosphate (ATP)	New England Biolabs	P0756
Agarose	Biozym Scientific	840004
Ammonium persulfate (APS)	Thermo Fisher Scientific	10744171
Ampicillin	Carl Roth	K029
B. Braun Aqua ad iniectabilia (H2O)	University Hospital Heidelberg	
Bovine serum albumin (BSA)	Carl Roth	8076.2
Bovine Serum Albumin (BSA) Fraction V, IgG free	Carl Roth	3737.2
Bromophenol blue	Waldeck	4F-057
Caesium chloride (CsCl)	Invitrogen	15507023
Carrier RNA	Qiagen	52906
Cutsmart buffer	New England Biolabs	B7204S
Dimethylsulfoxide (DMSO)	Merck	102950
Dithiothreitol (DTT)	Sigma-Aldrich	D0632
Dulbecco's Modified Eagle Medium (DMEM)	Thermo Fisher Scientific	41965039
Dulbecco's Modified Eagle Medium F12 (DMEM F12)	Thermo Fisher Scientific	31330038
Dulbecco's Phosphate Buffered Saline (PBS)	Sigma-Aldrich	D8537
Ethanol (EtOH)	Sigma-Aldrich	32205
Ethidium bromide	Sigma-Aldrich	E7637
Ethylenediaminetetraacetic acid (EDTA)	SERVA electrophoresis	39760.01
Fetal bovine serum (FBS)	Sigma-Aldrich	S0615
Ficoll PM70	Sigma-Aldrich	F2878
Fluoromount G	Life technologies, Invitrogen	4958-02
GeneRuler DNA Ladder Mix	Thermo Fisher Scientific	SM0331
Glutamine, L-	Life technologies, Invitrogen	25030024

Glycerol	Thermo Fisher Scientific	G/0650/15
Glycine	Sigma-Aldrich	G8898
GlycoBlue Coprecipitant	Thermo Fisher Scientific	AM9516
Heparin sodium salt	Sigma-Aldrich	H3149
HEPES 1M	Thermo Fisher Scientific	12509079
Hoechst 33342	Life technologies, Invitrogen	H3570
Hydrochloric acid (HCl)	Sigma-Aldrich	30721
Hydrocortisone hemisuccinate	Sigma-Aldrich	H4881
Insulin	Sigma-Aldrich	91077C
Interferon α 2A	PBL Assay science	11100-1
Isopropanol	Sigma-Aldrich	33539
Lamivudine (3TC)	Sigma-Aldrich	L1295
LB broth (Lennox)	Sigma-Aldrich	L3022
LB broth with agar (Lennox)	Sigma-Aldrich	L2897
Lonafarnib	Selleckchem	S2797
Methanol	Sigma-Aldrich	34860
Midori Green Advance	Biozym Scientific	617004
Milk powder	Carl Roth	T145.2
Opti-MEM	Thermo Fisher Scientific	Iris Biotech
PageRuler Plus prestained protein ladder	Thermo Fisher Scientific	26619
Paraformaldehyde (PFA)	Sigma-Aldrich	P6148
Penicillin/Streptomycin Life technologies	Invitrogen	15140-122
Polyethylenglycol (PEG 8000)	Sigma-Aldrich	89510
Puromycin	Invivogen	ant-pr-1
RNase inhibitor	Thermo Fisher Scientific	N8080119
RNAzol RT	Sigma-Aldrich	R4533
Ruxolitinib	Invivogen	tlr-rux
Sodium azide (NaN ₃)	Sigma-Aldrich	8591
Sodium chloride (NaCl)	Sigma-Aldrich	S7653
Sodium citrate	AppliChem	131.655.121
Sodium dodecyl sulfate (SDS)	SERVA electrophoresis	20765
Sodium hydroxide (NaOH)	Sigma-Aldrich	30620
β -Mercaptoethanol	Sigma-Aldrich	M6250
Sucrose	Carl Roth	4621.1
Tetramethylethylene-diamine (TEMED)	Carl Roth	2367.3
TransIT-LT1	Mirus Bio	MIR2300
Tris	Carl Roth	4855.2
Triton X-100	Merck	108603

Tween-20	Carl Roth	9127.1
Western lightning Plus-ECL	PerkinElmer	NEL103001EA
William's E	Life technologies, Invitrogen	22551-022

Table 2.9. Reagents used in this study.

2.1.9 Buffers and solutions

Buffer Composition	
Media for bacteria cultivation	
LB medium	20 g LB broth in 1000 ml H ₂ O, autoclaved, with or without 100 µg/ml Ampicillin
LB agar plate	35 g LB broth with agar in 1000 ml H ₂ O, autoclaved, 100 µg/ml Ampicillin
Agarose gel electrophoresis	TAE buffer (50X) 2 M Tris, 1 M glacial acetic acid, 500 mM EDTA (pH 8.0)
Heparin affinity chromatography	TN buffer 20 mM Tris, 140 mM NaCl (pH 7.4)
	TN400 buffer 20 mM Tris, 400 mM NaCl (pH 7.4)
	TN600 buffer 20 mM Tris, 600 mM NaCl (pH 7.4)
	TN2140 buffer 20 mM Tris, 2.14 M NaCl (pH 7.4)
CsCl density gradients	CsCl solutions : 1.2 g/ml (28.9 g CsCl and 100 g H ₂ O), 1.3 g/ml (40.3 g CsCl and 100 g H ₂ O), 1.4 g/ml (54.5 g CsCl and 100 g H ₂ O), 20% sucrose 2 g sucrose and 8 g PBS
DNA dot blot	Soak I 1.5 M NaCl, 500 mM NaOH
	Soak II 3 M NaCl, 500 mM Tris (pH7.4)
	SSC buffer (20X) 3 M NaCl, 300 mM sodium citrate (pH 7.0)
	Wash buffer 1X SSC, 0.5% SDS
SDS PAGE	SDS sample buffer (2X) 0.1 mg/ml bromophenol blue, 10% DTT, 20% glycerol, 6% SDS, 200 mM Tris (pH 6.8)
	Resolving gel buffer (4X) 1.5 M Tris, 0.4% SDS, 0.01% NaN ₃ (pH 8.8)
	Stacking gel buffer (4X) 500 mM Tris, 0.4% SDS, 0.01% NaN ₃ (pH 6.8)
	SDS running buffer (10X) 250 mM Tris, 1.92 M glycine, 1% SDS (pH 8.3)
Western blot	Blotting buffer 48 mM Tris, 39 mM glycine, 0.04 % SDS, 10% methanol
	TBS (10X) 200 mM Tris, 1.37 M NaCl (pH 8.0)
	TBS-T 1X TBS, 0.05% Tween-20
Northern blot	Soak I 1.5 M NaCl, 0.05 M NaOH
	SSC buffer (20X) 3 M NaCl, 300 mM sodium citrate (pH 7.0)
	SSC buffer (2X) , 0.5 % SDS
	SSC buffer (0.2X). 0.5 % SDS
DEPC water	MilliQ water 1 L
	DEPC 1 mL (0.1%)

10x MOPS	DEPC water 900 ml 41.9 g MOPS (200 mM) 4.1 g Na acetate (50 mM) 3.7 g EDTA (10 mM)
Digoxigenin (DIG) detection	DIG-wash buffer Blocking solution Detection buffer CSPD
FACS	0.5% BSA 0.02% Sodium azide in 1x PBS

Table 2.10. Buffers and solution used in this study.

2.1.10 Enzymes

Enzyme	Provider	Cat.No.
DNA restriction enzymes (various)	New England Biolabs	
Phusion DNA polymerase	New England Biolabs	M0530
PNGase F	New England Biolabs	P0704S
Taq Universal SYBR Green Supermix	Bio-Rad	1725124
RQ1 RNase-Free DNase	Promega	M6101
T4 DNA ligase	New England Biolabs	M0202
Trypsin EDTA	Bio&Sell	L2143

Table 2.11. Enzymes used in this study.

2.1.11 Technical devices

Machine	Supplier
PCR Flexcycler ²	Analytik
CFX96™ Real time system	BioRad
LI-COR Odyssey M	Licor
Microscope Leica	Leica
Microscope Nikon	Nikon
Cell Discoverer 7	Zeiss
FACS Canto	BD Biosciences

Table 2.12. Specific devices used in this study.

2.1.12 Software

Name	Application	Provider	Version
ImageJ	Image processing	Open source	
GraphPad Prism	Graphs preparation	GraphPad software LLC	9.3.14.71
Adobe Illustrator	Content preparation	Adobe Inc.	27.6
Cell Profiler	IF pictures analysis	Broad Institute	4.2.6

Ilastik	IF pictures analysis	Open source	1.4.0
FlowJo	FACS data analysis	FloJo LLC	10.7.2
Vector NTI	Vector analysis and visualization	Life Technologies	
SnapGene	Vector analysis and visualization	GSL Biotech	7.0.3
Jalview	Phylogenetic analysis	University of Dundee	2.11.3.0
FigTree	Phylogenetic analysis	GitHub	1.4.4
EndNote	Reference management	Clarivate Analytics	21.2.0.17387
Empiria Studio	Western blot analysis	LI-COR	2.3
CFX Manager	RT qPCR analysis	Biorad	
Quantity One	Dot-blot and Southern blot analysis	Biorad	
NIS-Elements	Microscopy	Nikon	
Alpha Fold	Molecule editor and visualization		
JaCoP	IF pictures analysis		
PyMOL	Molecule editor and visualization	Schrodinger Inc.	2.5.4

Table 2.13. Software used in this study.

2.2 Methods

2.2.1 Molecular cloning

2.2.1.1 HDV-like agents plasmids

Plasmid pJC126 harboring 1.1 copy of the HDV-genotype 1 antigenome was kindly provided by Prof. Dr. John Taylor. Plasmids pcDNA3.1/Zeo(+) containing 1.1 copies of the antigenome of HDV-like agents were generated by insertion of a synthetic 1.1-HDV antisense sequence into plasmid pcDNA3.1 Zeo (+). Cloning was performed by Dr. Stefan Seitz.

2.2.1.2 DNA digestion and ligation

DNA digestion was carried out using restriction enzymes and buffer systems from NEB, following the manufacturer's protocol. NEB cloner was used to determine the appropriate buffer conditions in double digests. For cloning purposes, approximately 10 µg plasmid DNA and 1 µl enzyme were incubated in the appropriate 1x reaction buffer for at least 2 hours at 37°C. After digestion, the DNA was purified by agarose gel electrophoresis and with GeneJET. The backbone and the generated insert were mixed at a ratio of 1:3 and ligated overnight at 16°C using T4 ligase (NEB). As control for re-ligated empty backbones, a ligation without insert was performed.

Reagent	25 μ l	50 μ l	Final concentration
5X Phusion HF or GC Buffer	5 μ l	10 μ l	1X
10 mM dNTPs	0.5 μ l	1 μ l	200 μ M
10 μ M Forward (or Reverse) Primer	1.25 μ l	2.5 μ l	0.5 μ M
DMSO (optional)	(0.75 μ l)	(1.5 μ l)	(3%)
Phusion DNA Polymerase	0.25 μ l	0.5 μ l	1.0 units/ 50 μ l PCR
Template DNA	variable	variable	< 200 ng
Nuclease-Free Water	to 25 μ l	to 50 μ l	

Table 2.14. PCR mixture using Phusion polymerase. Adapted from Phusion protocol.

Step	Temperature	Time
Initial Denaturation	98°C	30 seconds
25–35 Cycles	98°C	5–10 seconds
	45–72°C	10–30 seconds
	72°C	15–30 seconds/kb
Final Extension	72°C	5–10 minutes
Hold	4°C	

Table 2.15. PCR cycles using Phusion polymerase.

2.2.1.3 Point mutation using overlapping PCR

Two overlapping fragments were amplified from the plasmid pcDNA3.1/Zeo(-)HuLWT using PCR. The first fragment was amplified using forward primer NheI_for and separate reverse primer for each point mutation, while the second fragment was amplified using separate forward primer for each point mutation and reverse primer EcoRI_rev. Phusion DNA polymerase was used for PCR, and the PCR cycle is depicted in Table 2.15. . After agarose gel electrophoresis analysis and purification , the two fragments were annealed and amplified in a second PCR round using primers NheI for and EcoRI rev as described for the first step. The PCR product and the backbone plasmid were digested with NheI and EcoRI enzymes. After isolation and purification, the PCR product with the inserted mutation was ligated back into the pcDNA3.1/Zeo(-) vector using T4 DNA ligase.

pcDNA3.1/Zeo(+)-pcDNA-L-HDAgC211S and pcDNA3.1/Zeo(+)-pcDNA-L-HDAgQ214Stop farnesylation site mutants were also generated using overlapping PCR methodology as described above. Fragments containing the single mutation were

amplified from plasmid pcDNA3.1/Zeo(+)-L-HDAg, digested with NheI and NotI, and ligated back into pcDNA3.1/Zeo(+)-L-HDAg.

2.2.1.4 Agarose gel electrophoresis

For 1 % concentrated agarose gel, 1 g of agarose was dissolved in 100 mL of 1xTAE buffer and mixed with 5 µl of ethidium bromide. DNA samples were mixed with 6x DNA loading dye and loaded onto the gel, which was run in 1x TAE buffer at 130 V for 20 – 30 min. Bands were checked under UV-light and acquired for documentative purposes.

2.2.1.5 Plasmid preparation Midi and Mini prep

For transformation and quick re-transformation of plasmids, the chemically competent bacterial E. coli strain DH5α was used. DH5α were thawed on ice for around 10 minutes. Plasmid DNA (1 µg total) was added to the bacteria, mixed and incubated for 30 minutes on ice. Bacteria were then heat-shocked for 60 seconds at 42°C and immediately put on ice for 2 minutes before the addition of antibiotic-free LB medium. Cells were incubated for 1 hour at 37°C on a shaking thermomixer and then plated on LB-agar plates with the proper selection antibiotic (ampicillin: 0.1 mg/ml; gentamycin: 7 µg/ml; kanamycin: 0.3 mg/ml). Plates were incubated overnight at 37°C. Bacterial colonies were picked the next day and incubated in either 4 ml (for mini preparation) or 200 ml (for midi preparation) of LB medium containing the appropriate antibiotic selection overnight at 180 rpm and at 37°C. Plasmids were isolated using mini preparation or midi preparation (Plasmid plus mini kit, Qiagen and Plasmid plus midi kit, Qiagen, respectively) or according to the manufacturer's instructions.

2.2.1.6 Sequencing of plasmids

To check the correct identity after (re-) transformation, Plasmids were sequenced via Sanger methodology by GATC Services of Eurofins Genomics (Germany). 5 µl of plasmid DNA (with a concentration of around 100 ng/µl) were mixed with 5 µl of the appropriated sequencing primer (5 µM) in a 1.5 ml reaction tube labeled with an identification barcode sticker. Sequencing results were obtained online and were analyzed by Vector NTI.

2.2.2 Cell lines media and maintenance

HuH7 (parental and derived), HEK293T, A549, HeLa, and VeroE6 cells were maintained in Dulbecco's Modified Eagle Medium (DMEM), supplemented with 10% of FBS, 2 mM L-glutamine, 50 U/mL penicillin, 50 µg/mL streptomycin. CHO, PaKi and LMH cells were kept in culture with F12 DMEM medium supplemented with 10% of FBS, 2 mM L-glutamine, 50 U/mL penicillin, 50 µg/mL streptomycin, Pyruvate and NEAA.

HepaRG (parental and derived) cells were cultured in Williams E medium supplemented with 10% FCS, 5 mg/mL insulin, 50 mM hydrocortisone, mM L-glutamine, 50 U/ml penicillin, and 50 µg/ml streptomycin.

2.2.2.1 Cryopreservation and revival

Cultured cells were detached with trypsin and centrifuge for 5 minutes at 500 rpm at RT. The medium was aspirated, and cells were resuspended in cryo-medium (60% DMEM,30% FCS, 10% DMSO) distributed to freezing vials (3 tubes for one full T75 flask) and frozen at -80°C for at least 2 days before storage in a liquid nitrogen tank. For the revival of frozen cells, vials were put into a water bath of 37°C until thawed. Cells were then rapidly added to 5 ml medium and centrifuged for 10 minutes at 500 rpm at RT. The cell pellet was resuspended into pre-warmed medium and seeded into a T25 flask. When confluency was reached, cells were transferred into a T75 flask for maintenance.

2.2.2.2 Cell counting

Cells were detached with trypsin and resuspended into complete medium pipetting up and down, to avoid cells aggregates. 10 µl of cell suspension was mixed with 10 µl of trypan blue and inserted in the counting chamber to determine the cell number per ml and cell viability.

2.2.2.3 *Plasmid transfection in eukaryotic cell lines*

For plasmid DNA transfection were seeded depending on the plate format used as indicated in Table 2.16 . The next day, 100 to 1,000 ng DNA was mixed with OptiMEM in the amount indicated in Table 2.16, and lastly LT1 reagent was added into the mix. After 20 minutes of incubation at RT the mixture was added to the cells dropwise. After 24 hours of incubation, cells were washed once with PBS and medium was added.

Culture format	96-well	48-well	24-well	12-well	6-well	10-cm dish
Surface area	0.35 cm ²	1.0 cm ²	1.9 cm ²	3.8 cm ²	9.6 cm ²	59 cm ²
Complete growth medium	92 µl	263 µl	0.5 ml	1.0 ml	2.5 ml	15.5 ml
Serum-free medium	9 µl	26 µl	50 µl	100 µl	250 µl	1.0 ml
DNA (1µg/µl stock)	0.1 µl	0.26 µl	0.5 µl	1 µl	2.5 µl	5 µl
TransIT-LT1 Reagent	0.3 µl	0.78 µl	1.5 µl	3 µl	7.5 µl	15 µl

Table 2.16. Transfection mixture with LT1 reagent based on format used. Adapted from TransIT®-LT1 Transfection Protocol.

2.2.2.4 *Lentivirus production*

For lentivirus production HEK293T were seeded in 10 cm dished at a concentration of 2x10⁶/mL. The next day, the culture medium was exchanged to fresh pre-warmed medium around 1 hour before transfection. Transfection mix was prepared using 9 µg of psPAX2 (gag-pol) , 6 µg of pMD2.G (VSV-g) and 9 µg of pWPI vector encoding the gene of interest . The solution was added dropwise onto the cells and the medium was changed to 24 hours post transfection. The supernatant containing the lentiviruses was collected at 2 different timepoints (48 hours and 72 hours after transfection), filtered through a 0.45 µm pore-size filter and either concentrated via ultracentrifugation or directly used to transduce target cells.

2.2.2.5 *Generation of stable cell line*

For the generation of stable cell lines, target cells were seeded in a 6 well plate and after 24 hours , transduced 1 ml of non-concentrated lentiviral particles or 100 µl if concentrated. For non-concentrated lentiviral particles , transduction was repeated 2 times (24 and 48 hours post seeding). Transduced cells were then selected using culture medium complemented with the proper antibiotics. As negative control, medium with antibiotic selection was also applied to untransduced cells. After negative control cells were completely dead, transduced cells were split in T75 flasks and maintained in culture until used or frozen as described in 2.2.2.1.

2.2.2.6 *Virus production and precipitation using Polyethylene glycol 8000 (PEG)*

For production of HDV and HDV-like agents stock , HuH7 cells were seeded at a density of 5×10^6 per 10 cm dish and the day after they were transfected with 2,5 µg of HDV-agents' plasmids and 2.5 µg of plasmid expressing HBV envelope proteins (pT7HB2.7, pLX304-HB2.7) using LT1 Transfection reagent (prod. No. MIR 2305). 24 hours post transfection cells were washed with PBS once and medium was replaced. Supernatant was collected at day 7, 10 and 13 after transfection and viral HDV particles were precipitated using Polyethylene glycol 8000 (PEG8000) in PBS. PEG8000 (40% stock solution) was added to 10% final concentration to the collected supernatant and the solution was incubated overnight (ON) at 4 °C and then centrifuged for 1 hour at 10000 x g, at 4°C. The precipitate was recovered in 100 µl (for 10 mL of initial supernatant) of 10% FCS /PBS and incubated by shaking at 4 °C ON to allow complete resuspension of viral particles. After resuspension, the viral stock was centrifuged twice at 3000 xg for 10 minutes at RT to eliminate the insoluble portion. Virus preparation was aliquoted and stored at -20 or -80 °C for longer periods.

2.2.2.7 Virus production and purification using heparin column chromatography.

Transfection of producers cells was performed as described in 2.2.2.6. Supernatants were pooled and applied to heparin affinity chromatography using a 5-ml heparin-Sepharose column: column was equilibrated with 3 column volumes (CVs) TN buffer at 2 ml/min, followed by sample application at 1 ml/min. Unbound sample was washed out from the column with 5 CVs TN buffer (2 ml/min). The virus was eluted from the column with a linear gradient of TN2140 over 10 CVs, during which fractions à 2.5 ml were collected. The column was re-equilibrated with a 5 CVs TN buffer. Virus-containing fractions were pooled (7.5 ml), mixed with ddH₂O and 1.8 ml of FCS, aliquoted and stored at -80 °C.

2.2.2.8 Infection

For infection experiments, cells were seeded in 24-well plates at different concentrations depending on the cell line used (*Table 2.17*). The following day infection medium was prepared containing precipitated virus, DMSO and PEG8000 (4% final concentration). After 16 hours cells were washed twice with PBS, and medium was changed at day 1 and 3 post infection (pi). As an entry inhibition control, the cells were treated with 500 nM Hepcludex (former Myrcludex B), 15 minutes prior and during infection. On day 7 pi, cells were washed 3 times with PBS and fixed for immunofluorescence (IF) analysis.

Cell line	Seeding Density
HuH7 ^{NTCP}	2.5 x10 ⁵ /mL
HepG2 ^{NTCP}	5 x10 ⁵ /mL
HepaRG ^{NTCP}	5 x10 ⁵ /mL
A549 ^{NTCP}	2.5x10 ⁵ /mL

Table 2.17. Cellular seeding density for infection experiments.

2.2.2.9 IU/mL calculation for infection

HuH7^{NTCP} cells were then infected with HDV/HBsAg, WoDV/HBsAg, or DeDV/HBsAg using the same international Unit per mL (IU/mL) calculated as follows:

$$IU/ml \text{ virus} = (IU/ml \text{ reference} \times \text{copies/ml virus}) / (\text{copies/ml reference})$$

The term "reference" refers to the laboratory - established HDV viral stock with known IU/ml values.

2.2.2.10 TCID50 for assessment of virus infectivity

To determine TCID50 values for the produced viral pseudo-particles, HuH7^{NTCP} cells were seeded in 96 well plates and infected with 20 µl of concentrated virus serially diluted (every dilution had a factor of 1:10) in quadruplicates. Each dilution is performed in DMSO and PEG containing media as performed in session 2.2.2.8. 24 hours post infections, medium was replaced by fresh medium implemented with DMSO (1% , final concentration). 6 days post infection cells were washed and fixed for IF and staining of DAg using FD3A7 antibody. Wells containing DAg positive cells were noted and the values were inserted in a premade Excel sheet for automatic TCID50 values calculations.

2.2.2.11 Cell division-mediated viral amplification assay (CDMAA)

Different cell lines were transfected with the plasmids encoding the antigenome of HDV and HDV-like agents. At day 6 post transfection (passage 0=P0) cells were split at different dilution factors depending on the cell line used, to allow clonal expansion. At every split cells were in parallel fixed, and DAg expression was visualized by immunofluorescence using the FD3A7 monoclonal antibody raised by S-HDAg.

2.2.2.12 Interferon treatment

ISG expression was stimulated via IFNα2A treatment. Cells were incubated with medium with IFN2a (final concentration 200 IU/mL) for 24 hours. Cells were harvested and lysed for protein quantification via western blot (WB) or intracellular RNA quantification via RT-qPCR.

2.2.3 Detection of RNA and DNA

2.2.3.1 RNA purification from precipitated virus and RT-qPCR detection.

To determine the concentration of the virus in PEG precipitated or AKTa purified supernatant the QiAMP Viral RNA Mini kit was used, following the manufacturer's instructions. Total viral RNA was extracted from 50 μL of virus. To remove residual plasmid, 40 μL of the eluate was digested with DNase I (2 U/ μL) at 37°C for 15 min. To inactivate DNase and to break the secondary structure of HDV RNA, the RNA was incubated for 5 minutes for heat shock at 95°C. Samples were immediately put in frozen metal racks and stored at -80°C until use.

2.2.3.2 RNA purification of intracellular RNA.

Intracellular RNA extraction from harvested cells was carried out using the NucleoSpin RNA Kit following the manufacturer's instructions . RNA concentration was measured by Nanodrop.

2.2.3.3 Reverse transcription (RT) and Quantitative PCR (RT-qPCR) for supernatant and intracellular mRNA detection

Reverse transcription was performed according to the High-capacity cDNA reverse transcription kit using as indicated by Table 2.18 and Table 2.19.

Reagent	μl
RNA	X (1 μg)
H2O	13.2-X
10x Buffer	2
10x Random primer	2
100 mM dNTP	0.8
RNase inhibitor	1
RTase	1
Total	20

Table 2.18. Reverse transcription mixture.

Step	Temperature	Time
------	-------------	------

1	25 °C	10 min
2	37 °C	120 min
3	85 °C	5 min
4	4 °C	hold

Table 2.19. Reverse transcription steps and temperature cycles.

The obtained cDNA was diluted 1: 2.5 with Braun water for RT- Quantitative PCR (qPCR) analysis. RT-qPCR was performed using iTaq universal SYBR Green Supermax on a CFX96 thermocycler as indicated by Table 2.20 and Table 2.21. Copy numbers were quantified using pJC126 for HDV or plasmids containing the respective HDV-like agents genome. For ISGs detection, the values for each gene were normalized on GAPDH as housekeeping gene.

Reagent	µl
2x SYBR green mix	7.5
Forward primer (10 µM)	0.6
Reverse primer (10 µM)	0.6
H2O	3.3
Template	3
Total	15

Table 2.20. RT-qPCR mixture.

Step		Temperature	Time
1	Polymerase activation and DNA denaturation	95 °C	3 min
2	Amplification	Denaturation	95 °C
3	(40 cycles)	Annealing/Extension/Plate read	60 °C
4	Denaturation	95 °C	10 sec
5	Melt-Curve analysis	65-95 °C	Default setting

Table 2.21. RT-qPCR steps and temperature cycles.

2.2.3.4 Northern Blot.

RNA extraction was performed as mentioned above in section 2.2.3.2. The total RNA was then quantified using Nanodrop and diluted to achieve the same final RNA concentration a total of 10 µg RNA/sample was loaded on an agarose/paraformaldehyde (PFA) gel. RNA was run in a 1.5% MOPS agarose gel containing 2.2M formaldehyde. After denaturation (50mM NaOH for 5min), RNAs were transferred to a nylon membrane by capillary transfer using 20× SSC buffer. Membranes were dried and fixed by UV crosslinking. Virus specific

probes were synthesized via IVT using the Digoxigenin (DIG) RNA labeling Mix, 10 x conc. protocol as indicated in Table 2.22. Membranes were hybridized at 60 °C overnight singularly. The following day the probe was removed, and the membrane was washed 2 times with 20 ml 2X SSC/0.1% SDS for 5min at RT. After 2 additional washes with 20 ml 0.2X SSC/0.1% SDS, for 15-20min at 60°C in the hybridization oven and washed with 20 ml 1×DIG-wash buffer for 5min at RT. The membrane was then blocked with 20 ml blocking solution for 30-60min at RT and incubated with antibody solution for 1h. After 3 washed with 20 ml 1xDIG wash buffer (3x10 min at RT), membrane was equilibrated with 15 ml 1×detection buffer for 2-5min incubated with detection solution for 10-30min at 37°C. Signal was detected by INTAS instrument at 1 min for 30 sequential acquisition.

Reagent	Volume
1 µg linearized plasmid DNA or appropriate amount of PCR product	x µl
DIG RNA labeling mix, 10 ×	2 µl
Transcription buffer, 10 ×	2 µl
Sterile RNase free ddH ₂ O	X µl
RNA polymerase 20 U/µl	2 µl
Total volume	20 µl

Table 2.22. RNA labeling with digoxigenin-UTP by *in vitro* transcription with T7 RNA polymerase.

2.2.3.5 Caesium chloride (CsCl) density gradient centrifugation and HBV DNA dot blot

The Caesium chloride (CsCl) density gradient was prepared using buffer described in Table 1.10. and using a 4ml Beckman Coulter Ultra-Clear Centrifuge tubes (SW60, 11x60mm). 500µl 1.4 g/ml CsCl solution was added to the bottom of the centrifuge tube followed by 500µl 1.3 g/ml CsCl, 500µl 1.2 g/ml and 500 µl 20% sucrose carefully applied using a cut 500 µl piper tip.

The samples (50µl PEG precipitate virus) was loaded at the top and the tubes were filled up with 1xPBS. All of the tubes were carefully tared (0.01g precision) and centrifuged at 58'000 rpm, for 3.hours , at 20 °C.

Fractionation was carried out using Beckman Fraction Recovery System in 96 well plate (6 drops per fraction, 12 fractions per sample) and fraction density was measured using a refractometer.

For DNA dot blot collected samples and 50µl of the standard (DNA H1-H6) were loaded on dot blot machinery and transferred on nylon membrane thought vacuum. After 2 washes with 1xPBS , the membrane was soaked in Soak I buffer 2 times for 90s and in Soak II buffer 2x for 60s. Nylone membrane was transferred to dry Whatman paper and auto crosslinked 2x in UV Stratalinker 1800.

2.2.4 Detection of protein

2.2.4.1 Immunofluorescence

Cells were washed once with PBS, then fixed with 4% PFA at RT for 20 min. After three washing steps with PBS, permeabilization buffer (Triton X 100 , 0,5%) was added, the cells were permeabilized at RT for 10 min and washed thrice with PBS. The cells were incubated with primary antibody at the proper dilution in 2% BSA/PBS at RT for 1 hour. After three washing steps with PBS, cells were incubated with 1:1000 diluted secondary antibody and 2 µg/mL Hoechst stain in the same solution as the secondary antibody for 1 hour at RT while shaking, protected from light. Until imaging, the stained cells were stored in the dark at 4°C. Cells seeded on coverslips were stained as described above. Then, the coverslips were once washed in de-ionized H2O and mounted on glass slides with 10 µL of Fluor mount-G mounting medium. The cells were imaged at inverted microscopes. For sub-cellular localization, images were taken at 20x magnification.

2.2.4.2 Western blot

For western blot analysis, the cells were cultured in 24 well plates until desired timepoint. Cells were washed once with PBS, then lysed in 75 µL 2x SDS sample buffer. The lysates were stored at -20°C. Before loading the SDS gel, the samples were vortexed, heated to

95°C for 10 min, and the liquid was centrifuged at maximum speed for 20 minutes. For SDS PAGE, a resolving gel containing 15% polyacrylamide was combined with a 3% stacking gel. For each well, 3 µl of lysate was added. After resolving in SDS running buffer at 60 V for 20 min then at 120 V, the proteins were transferred from the gel to a nitrocellulose membrane using a semi-dry system at 25 V for 30 min. Directly after blotting, the membrane was incubated in blocking buffer for 1 hour at RT. The membrane was incubated with primary antibody solution at the appropriate dilution (Table 2.3) in blocking buffer at 4°C, ON. After washing thrice with TBST for 10 min, 10 mL of the peroxidase secondary antibodies (goat anti rabbit 800 and goat anti mouse 680 both 1:10,000 in blocking buffer) was applied for 1 h at RT, acquisition was performed using Licor.

2.2.5 Fluorescence-activated cell sorting (FACS) for Atto-stain of hNTCP expressing cell lines

Cells were seeded at maximum 50% confluence and the following day medium was aspirate and cells were washed 1 time with 1x PBS. Cells were then trypsinized and resuspended in 500µl medium. After centrifugation at 300xg for 5min, cells were resolved in FACS-Buffer and centrifuge again at 300xg for 5 min. After supernatant was removed, cells were resuspended in FACS Buffer and separated using a cell strainer to isolate single cells . On ice, Myr-Atto 656 peptide was added to the cells at the desired concentration and after 15 minutes incubation cell were centrifuged to remove the peptides. Fluorescence was measured by flow cytometry using Cell Sorter BD FACS Celesta.

2.2.6 Taurocholate uptake assay

Cells were seeded in 24-well plates and incubated overnight at 37 °C. The following day, cells were incubated in basal medium in the presence or absence of 200 nM MyrB for 15 min at 37 °C. A mix of 50 µM cold TC and 10 nM [3H] TC was added for co-incubation of another 15 min at 37 °C. Then, cells were chilled on ice, washed extensively, and lysed in

lysis buffer (PBS/0.05 % SDS/0.25 M NaOH). [3H] scintillation counts were determined using the LS 6000 liquid scintillation counter .

2.2.7 Synthesis of myristoylated peptides

WT and ARP myristoylated peptides were synthesized by solid phase peptide synthesis employing the Fmoc/tBu strategy with HBTU/DIPEA activation in an Applied Biosystems 433A peptide synthesizer. Atto565-maleimide was linked to the lysine (K) at position 59. The identity of the peptides was controlled by mass spectrometry.

2.2.8 Peptide binding assay binding assay

Cells were incubated with 200 nM MyrcludexB-Atto565 diluted in basal medium for 30 min at 37 °C, washed 3 times for 5 min with 2 % BSA/PBS and once with PBS. For fixed cell imaging, cells were fixed with 1,25 % PFA for 10 min and nuclei were stained with 1 µg/ml Hoechst for 10 min.

2.2.9 Protein prediction using Alpha fold program

The aminoacidic sequences were analyzed using the online software Alpha Fold 2 (<https://colab.research.google.com/github/sokrypton/ColabFold/blob/main/AlphaFold2.ipynb>) and output files were analyzed and displayed using PyMOL.

2.2.10 Phylogenetic analysis

Aminoacidic sequences in FASTA format were aligned using Multiple Sequence Comparison by Log-Expectation (MUSCLE) online tool (<https://www.ebi.ac.uk/Tools/msa/muscle/>) and output alignment was visualized and modified using Jalview or FigTree software.

3. RESULTS

3.1 REPLICATION, HOST RANGE, AND TISSUE PERMISSIVENESS OF HDV-LIKE AGENTS

Given the novelty of the discovery of HDV-like agents, specific commercially available tools to study the *in vitro* and *in vivo* replication of these agents are currently lacking. The main aim of this study was to establish appropriate assays and methods to detect viral markers such as viral RNA and viral antigen. These markers could indicate *in vitro* replication of HDV-like agents, which have been identified in several animal species. This study focused on DLAs identified in woodchuck (WoDV), deer (DeDV), bat (BaDV), and various duck species (AvDV).

3.1.1 Establishment of cDNA infectious clones of HDV-like agents

To study and characterize the replication, host, and cellular range of non-human HDV-like agents, namely WoDV, DeDV, BaDV and AvDV, infectious clones were generated by cDNA synthesis of the corresponding antigenome (Figure 3.1A).

A 1.1-fold antigenomic sequence was inserted into a pcDNA3.1/Zeo (+) vector (Figure 3.1B). To determine the correct identity, each plasmid was sequenced by the Sanger method using human cytomegalovirus promoter (CMV) primers and digested with enzymes flanking the antigenomic sequences. After agarose gel run of digested plasmids, a band could be observed at around 2000 bp for all pcDNA3.1. This band indicated the antigenome insert of 1910 bp, 1887 bp, 1865 bp and 1890 bp, for WoDV, DeDV, BaDV and AvDV respectively (Figure 3.1C).

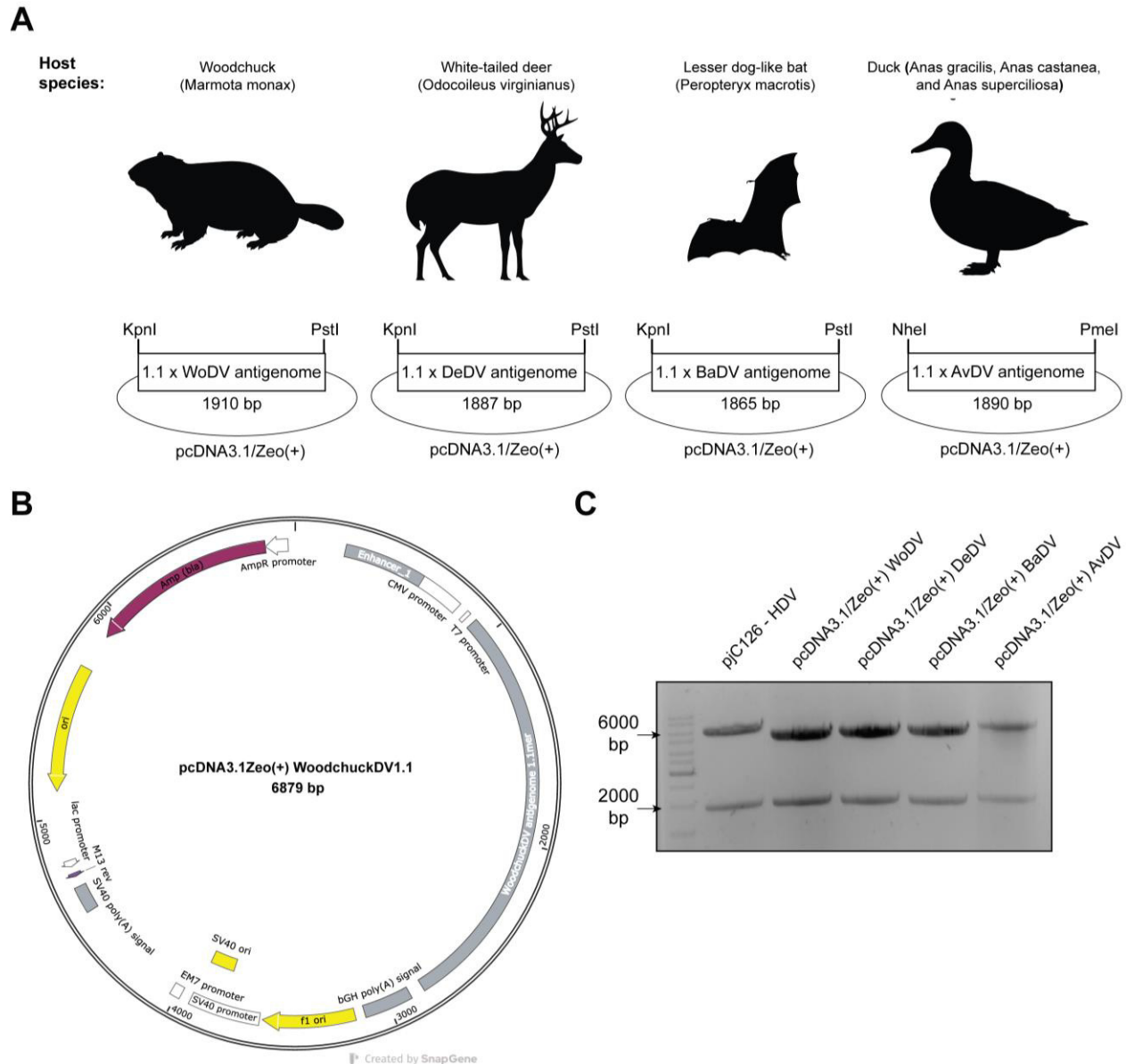


Figure 3.1. Cloning of pcDNA3.1 plasmids encoding 1.1 mer antigenome sequences of HDV-like agents. Antigenome constructs of HDV-like agents were generated via the insertion of 1.1-fold antigenomic cDNA into a pcDNA3.1 vector (A). The final plasmid harbors antigenome sequences under CMV promoted and contains a T7 promoter for RNA IVT and ampicillin resistance for bacterial selection, as represented by the WoDV construct (B). Plasmids were digested with the indicated restriction enzymes and run on agarose gel for identity check (C).

3.1.1.1 *Assessment of replication capacity of generated cDNA clones in human and chicken hepatoma cells*

Having confirmed the identity of the cDNA sequences, the replication competence of these constructs was evaluated. Considering the broad host range in which these HDV-like agents were discovered, as well as the phylogenetic genome distance between human HDV and AvDV, two different cell lines - human hepatoma-derived cell lines (HuH7) and chicken hepatoma cell line (LMH), were used. These cells were transfected with the antigenomes constructs, and 5 days post-transfection (pt), viral antigen was detected via IF and WB analysis. Given the novelty of these delta agents, no antibodies against the respective delta antigen (DAg) were commercially available. However, I took advantage of the commonly used antibody against the human HDV DAg (FD3A7 monoclonal α rabbit) to evaluate antibody cross-reactivity among the antigens of HDV-like agents. To provide a comparison between HDV and HDV-like agents, cells were transfected with a pcDNA3.1/Zeo (+) plasmid harboring 1.1mer antigenomic sequence of HDV (pJC126, kind gift from J. Taylor), used as replication competent control, while an HDV genotype 5 replication defective clone (HDV defect) was used as negative control to define lack of replication capacity (Wang et al., 2021).

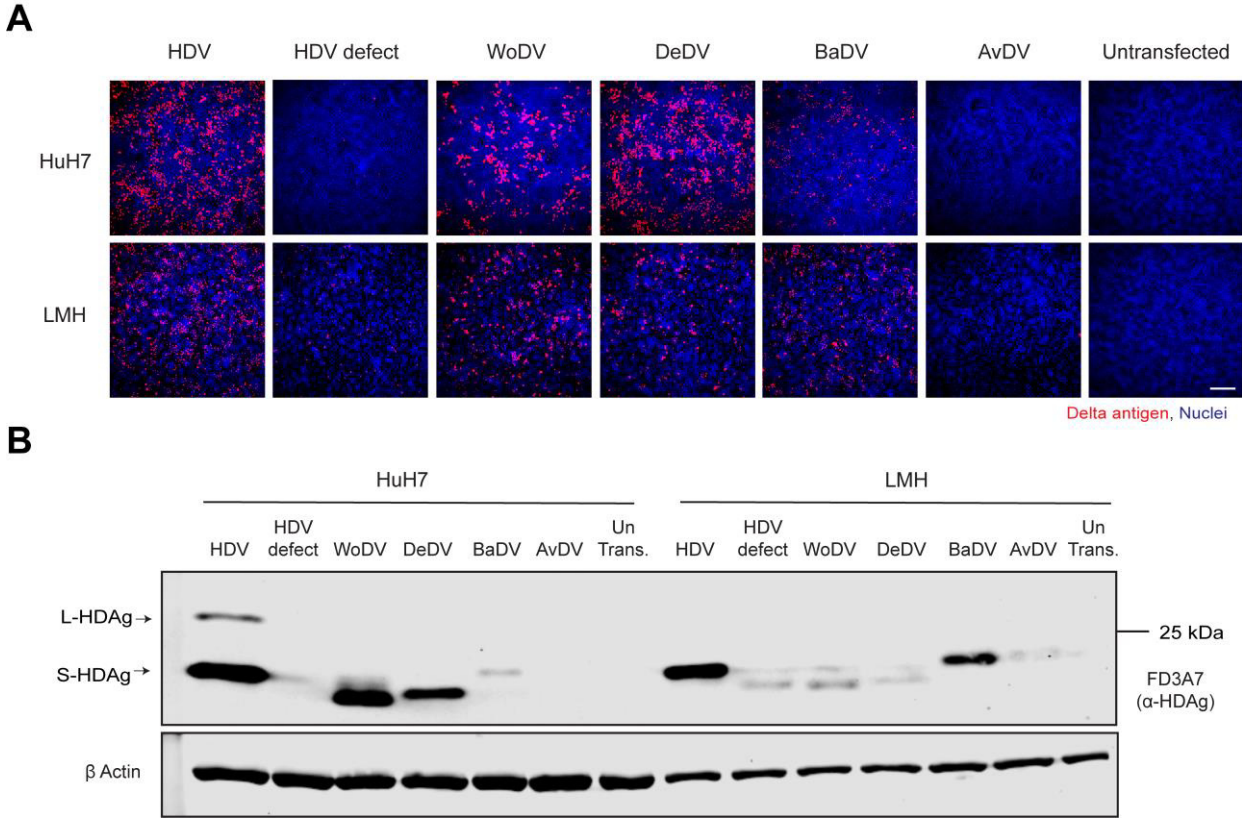


Figure 3.2. Immunostaining of delta antigen upon transfection of HuH7 and LMH cells reveals antibody cross-reactivity. HuH7 and LMH cells were transfected with cDNA constructs, and 5 days post-transfection (pt), cells were either fixed and stained for IF analysis (A) or lysed for WB (B). For both techniques, the delta antigens (DAg) were stained using the commercially available monoclonal antibody FD3A7 a rabbit coupled with goat α rabbit Alexa Fluor 546 (IF) or goat α rabbit IRDye 800CW (WB). Scale bar : 200 μ m.

Transfected cells were stained for DAg visualization via IF (Figure 3.2A) or lysed for DAg-specific WB analysis (Figure 3.2B). 5 days pt, a robust antigen signal was observed for HDV. In contrast, only a weak signal was detected for HDV defect, indicating a reduced antigen expression derived solely from plasmid transfection and not from replication.

Interestingly, WoDV, DeDV, and BaDV DAgs could be detected using FD3A7 antibody anti-H-DAg, demonstrating species cross-reactivity (Figure 3.2A). However, no DAg detection was observed for AvDV in HuH7 and LMH. This could be due to the amino acid divergence of the AvDV antigen in comparison to the H-DAg, as shown in Figure 1.11. The results from the IF were further confirmed by WB analysis, where antigen expression was

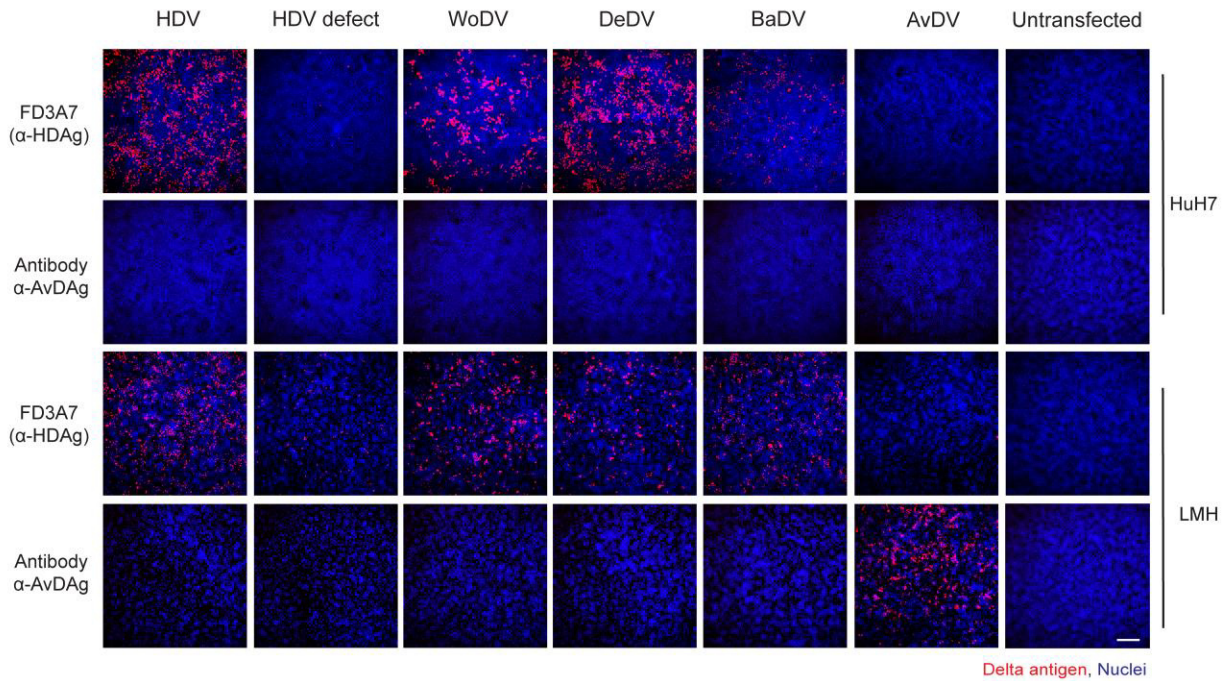
observable for HDV, WoDV, and DeDV but not for AvDV in HuH7 cells. In comparison, the signal intensity in LMH cells was lower than in HuH7 for all mammalian HDV-like agents' Ags, except BaDAg. These findings highlighted the requirement for AvDV antigen-specific antibody to fully elucidate the replication and spread capability of this distantly phylogenetic agent.

3.1.2 Generation and characterization of specific antibodies against AvDV antigen

Due to the inefficient detection of AvDV antigens using the H-DAg antibody FD3A7, a specific antibody for AvDAg was generated by expressing the N-terminal polyhistidine-tagged DAg in BL21(DE3) pLysS competent bacteria. Subsequently, the respective DAg was purified through Ni-NTA affinity chromatography, and then used for immunization in rabbits. Antigen production and purification were carried out by Angga Prawira (M.Sc.).

For the *in vitro* analysis of this newly generated antibody, HuH7 and LMH cells were transfected with cDNA antigenome constructs of all HDV-like agents. IF and WB analysis were performed to identify viral Ag expression at day 5 pt. The specific AvDAg antibody allowed for the detection of AvDAg in LMH cells but not in HuH7 cells. These results suggest a potential lack of efficient antigen expression in human hepatoma cells (Figure 3.3A&B). The AvDag antibody exhibited high specificity towards the corresponding antigen. Detection of H-DAg, WoDAg, DeDAg, and BaDAg was restricted and less effective when compared to FD3A7 antibody in both cell lines and read-outs employed. Notably, the AvDV-specific antibody failed to detect AvDag in HuH7 cells, while the signal was strong in LMH cells, implying the necessity of identifying the most suitable host and cell line for replicating each agent.

A



B

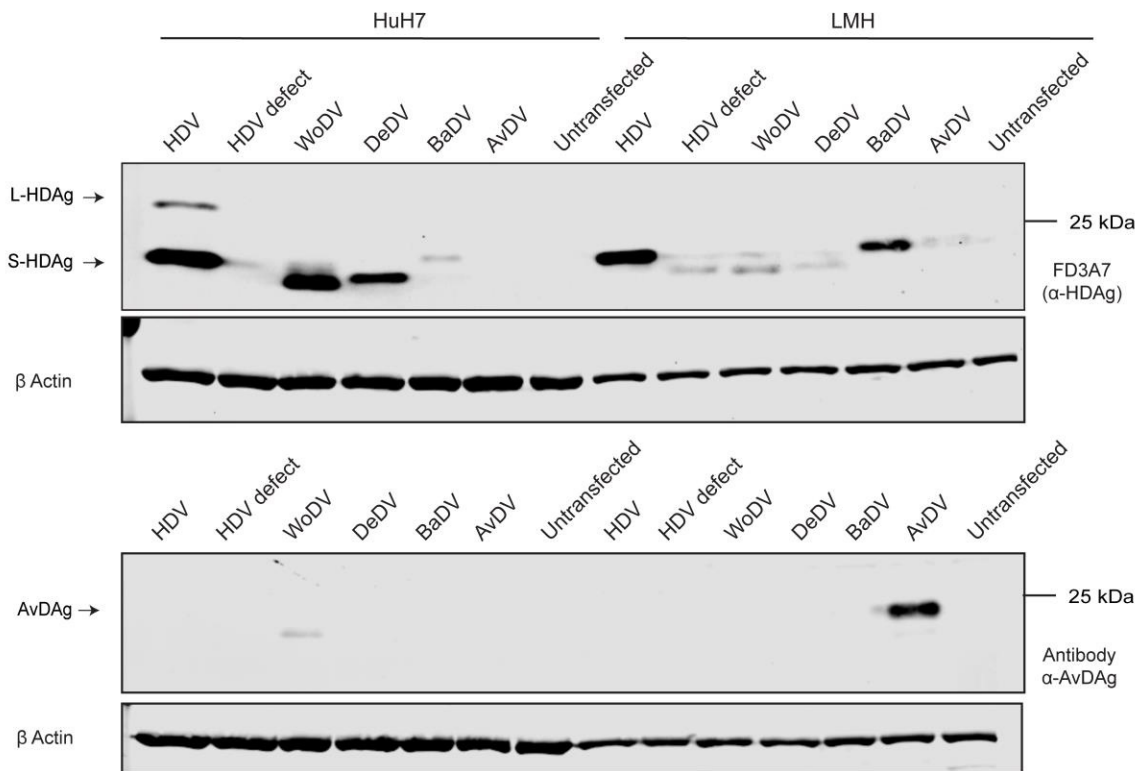


Figure 3.3. Analysis of specific antibodies against Avian antigen and cross-reactivity studies. For antibody cross-reactivity studies, HuH7 and LMH cells were transfected with pJC126 or pcDNA3.1/Zeo (+)

vectors containing the 1.1mer antigenome of WoDV, DeDV, BaDV, and AvDV and harvested at day 5 pt for IF (A) and WB (B) analysis. Transfected HuH7 and LMH cells were immuno-stained for IF using FD3A7 or α -AvDAg antibody and counterstained with Hoechst. For WB, samples were incubated with FD3A7 and α -AvDAg antibody and β actin antibody used as housekeeping gene. Scale bar: 200 μ m.

3.1.3 Design of specific primers and DIG-labeled probes for RNA detection

RT-qPCR primers tailored to a non-coding genome region were designed to obtain a more precise characterization of viral replication and persistence. Additionally, RNA genome-specific probes were generated using the non-radioactive Digoxigenin (DIG)-labeling method for Northern blot (NB) analysis of viral RNA. Each probe was produced by In vitro transcription (IVT) of RNA labeled with DIG nucleotides, allowing RNA binding and visualization post-staining with α DIG antibodies. HuH7 cells were transfected with an antigenome vector and harvested for RNA extraction on days 2, 6, 12, and 18 pt.

Following HDV transfection of HuH7 cells, viral RNA was increased in both qPCR and NB analysis, reaching a plateau by day 6 pt (Figure 3.4). In comparison to HDV, WoDV and DeDV RNA levels increased earlier, and replication remained strong and continued to increase until day 12 pt. Notably, BaDV replication was significantly lower than that of other mammalian HDV-like agents, as evidenced by lower RNA levels and lower DIG signals in NB (Figure 3.4).

The two used methodologies showed good correlation in terms of RNA content and replication kinetics.

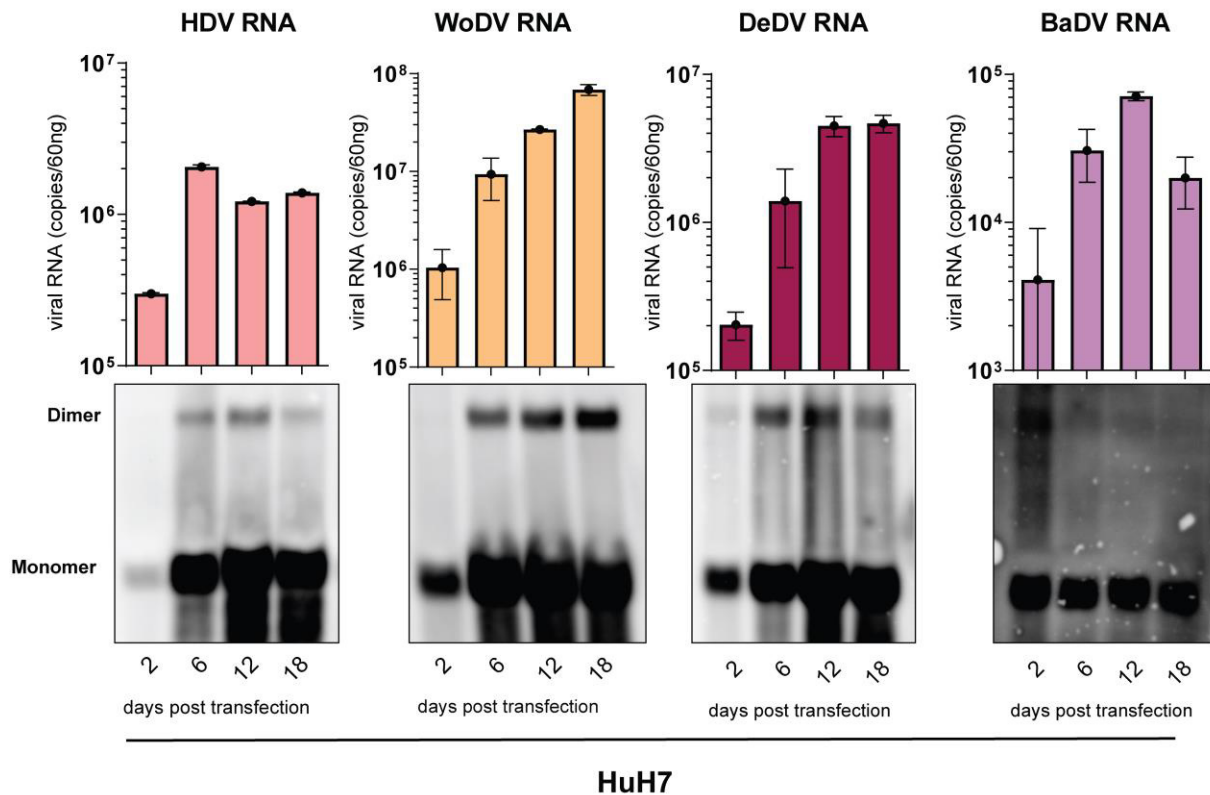


Figure 3.4. Characterization of specific primers and DIG-labeled probes for RNA detection. HuH7 cells were transfected with pcDNA3.1 of HDV and HDV-like agents' antigenomes. RNAs were analyzed via RT-qPCR and NB at day 2, 6, 12, or 18 pt.

3.1.1 Evaluation of genome editing and large delta antigen expression

In *silico* prediction data revealed no UAG stop codon at the end of the S-DAg ORF of HDV-like agents. This would prevent the emergence of a functional L-DAg through the editing of the cellular enzyme ADAR1. Indeed, the expression of the human HDV large antigen (L-HDAg) is dependent on the editing by this cellular enzyme. To verify the *in silico* predicted data, HuH7 and LMH cells were transfected with HDV-like agents antigenomes, and viral Ag expression kinetics was assessed via WB and IF using the pan-agents antibody FD3A7 for mammalian HDV-like agents and the newly generated antibody for AvDV.

HDV L-HDAg was expressed from d6 pt until day 12 pt (Figure 3.5A). On day 12 pt, a decreased S-HDAg expression was observed, likely due to the suppressive impact of L-HDAg on HDV replication. Interestingly, no expression of L-DAg was observed for the mammalian HDV-like agents, even at later time points (12 days pt), despite the successful establishment of replication as indicated by the increase in S-DAg expression (Figure 3.5A).

The replication of HDV, WoDV, and DeDV in HuH7 cells was robust as confirmed by IF, through the increase in viral antigen expression (Figure 3.5B). The strong signal on day 12 could suggest later replication kinetics of WoDV and DeDV compared to the human HDV. AvDVAg expression was evaluated in LMH cells. AvDAg expression was observed in both IF and WB until day 12 pt (Figure 3.5C&D). Notably, a faint second band above the smaller AvDAg band was observed in the WB analysis starting from day 6 pt.

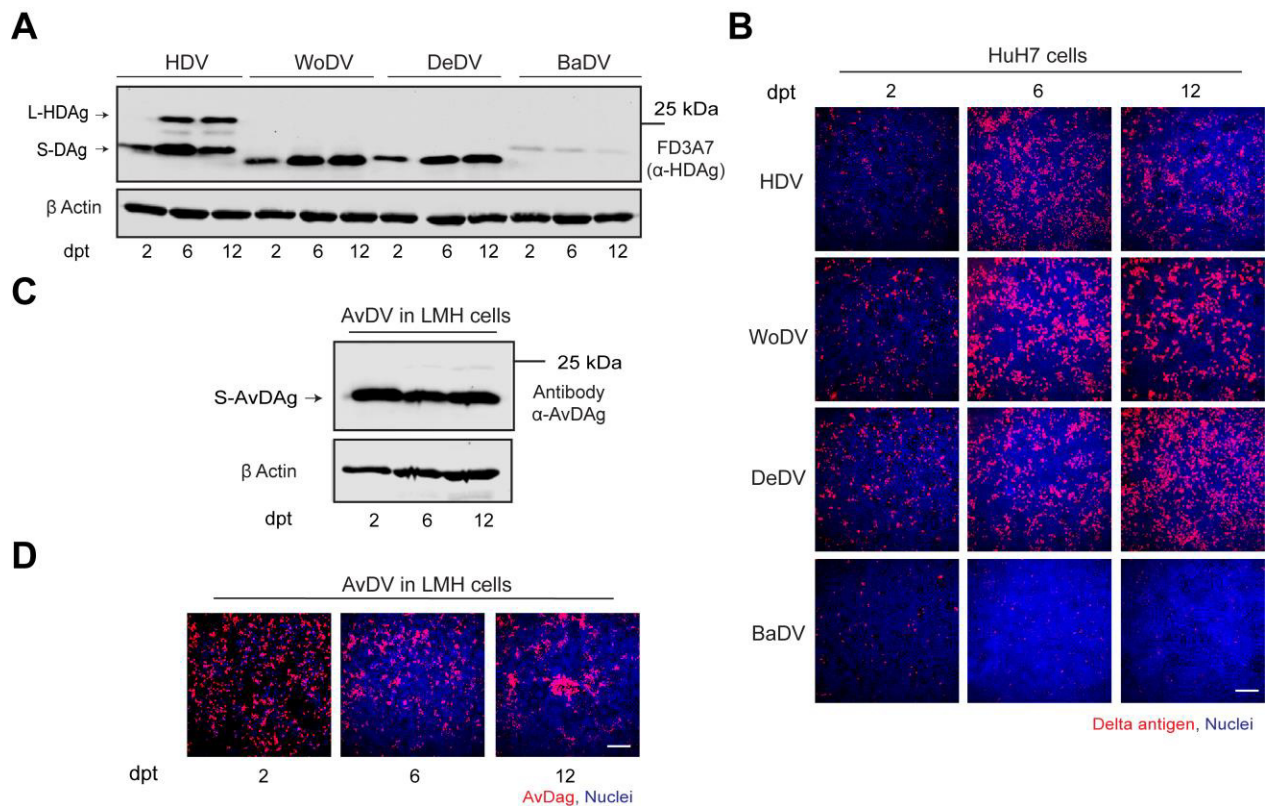


Figure 3.5. Replication kinetics and L-DAG expression. HuH7 (A&B) and LMH (C&D) cells were transfected with plasmids harboring a 1.1-fold DLA antigenome and harvested on day 2, 6 and 12pt. Viral antigen expression and putative editing-DAG expression were assessed via WB analysis (A) or IF (B) using FD3A7 anti-S-HDAg antibody or anti-AvDAg antibody. AvDAg kinetics expression was evaluated in LMH cell line via WB (C) and IF (D). Scale bar 200 μ m.

Based on *in silico* prediction data, the AvDV genome does not contain a recognition site for editing by ADAR1. However, a frameshift event (+1) in the AvDAg can result in an extension of 17 amino acids in the S-DAG. This extension resembles in length of the one generated by ADAR1 editing in the human HDV genome (Figure 3.6). However, no farnesylation site is present. The mechanism for the expression and functional characterization of this L-AvDAg is currently under investigation.

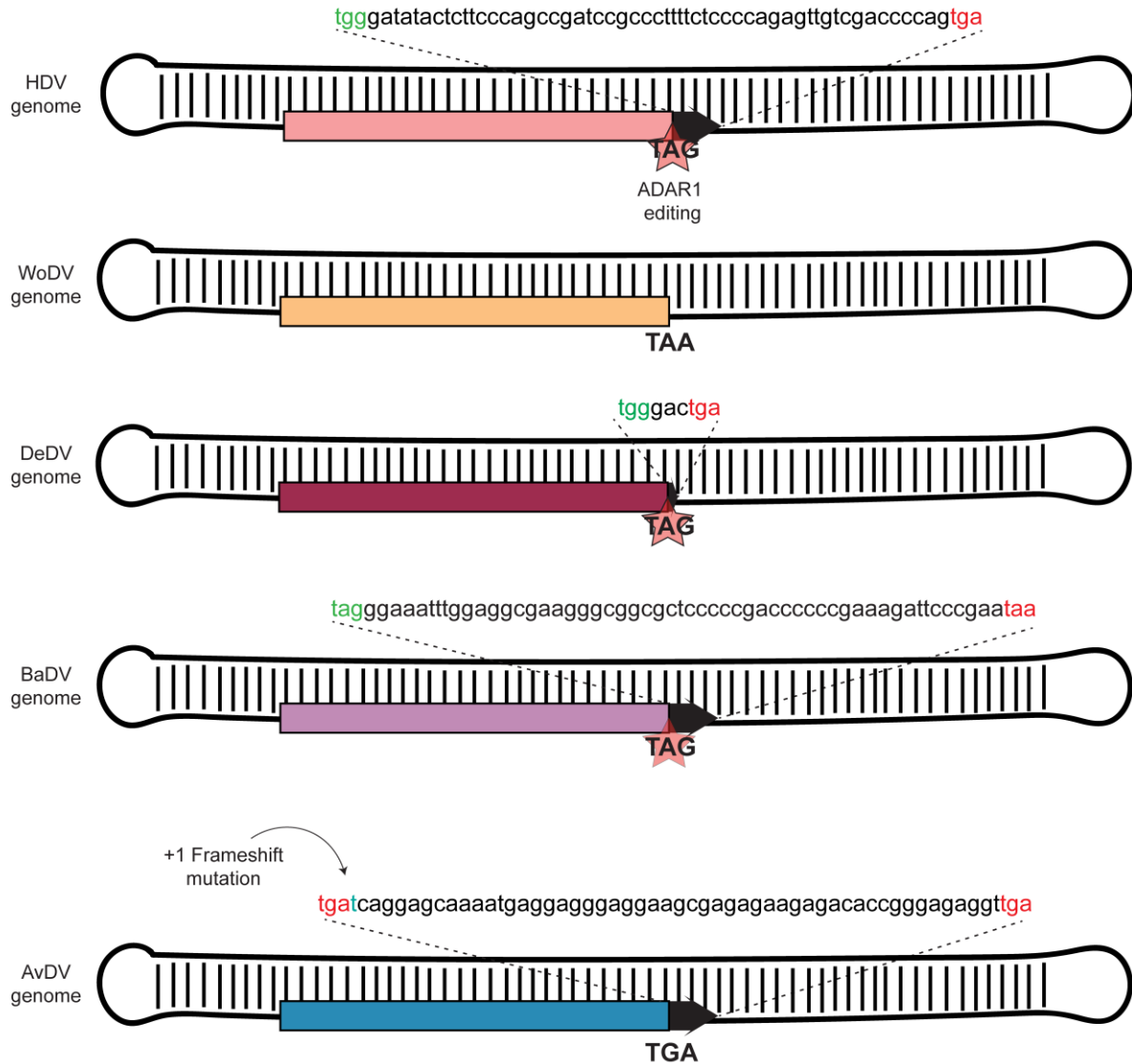
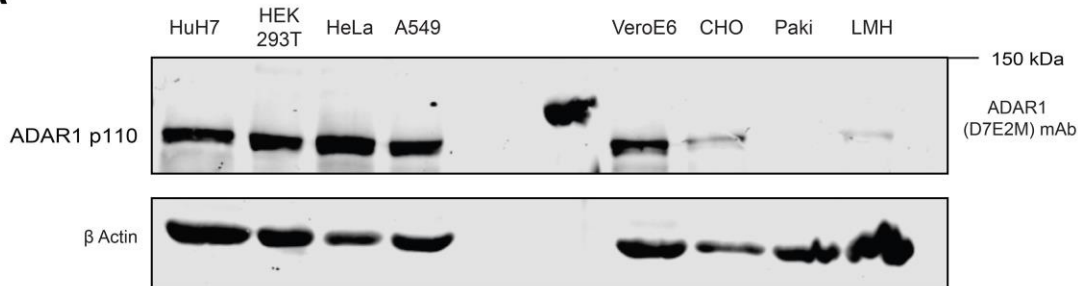


Figure 3.6. Schematic representation of the putative large delta antigen generated by ADAR1 editing or alternative frameshift mutation.

3.1.2 HDV and HDV-like agents' replication host range

Given the significance of host factors in determining the outcome of viral establishment and replication success, it was essential to characterize genome editing and replication mechanisms in a wide range of host-derived cell lines. To achieve this objective, cell lines

sourced from various animal species and organs were employed. Vero E6 (African Green Monkey – Kidney), CHO (Hamster – Ovary), PaKi (Black Flying Fox Bat – Kidney), and LMH (Chicken – Liver) cell lines were analyzed to assess and evaluate the expression and conservation of ADAR1 enzyme, which is a critical host factor in HDV life cycle. A human ADAR1 antibody was used in WB for protein detection in HuH7 cells, as well as other human-derived cell lines (HEK293T, HeLa, and A549) (Figure 3.7A). Efficient detection in VeroE6 may be attributed to the close positioning of human and monkey ADAR1 sequences (Figure 3.7B&C).

A**B**

	Identity (%)	
	Protein	DNA
H.sapiens		
vs. P.troglodytes	99.7	99.7
vs. M.mulatta	96.8	97.5
vs. C.lupus	82.4	83.0
vs. B.taurus	85.1	87.0
vs. M.musculus	80.1	81.8
vs. R.norvegicus	80.1	82.2
vs. G.gallus	59.5	62.9

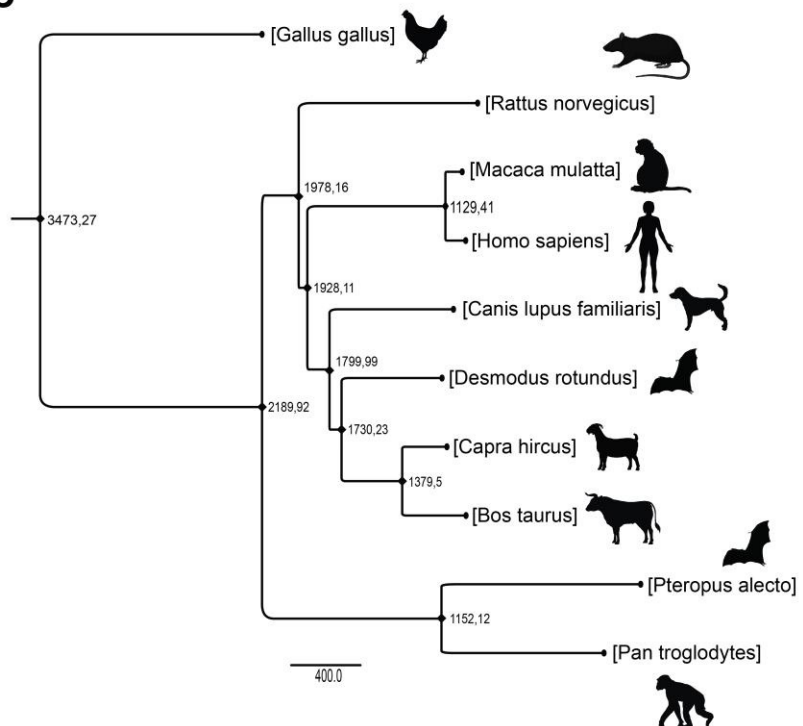
C

Figure 3.7. ADAR1 expression and conservation. HuH7, HEK293T, HeLa, A549, Vero E6, CHO, PaKi, and LMH cells were tested for ADAR1 expression via WB analysis using monoclonal antibody against the human ADAR1, D7E2M (A). A comparison of ADAR1 orthologs is represented as a percentage of protein and DNA sequence identity (B) and phylogenetic distance (C).

Notably, low protein detection was observed in cell lines derived from hamsters, bats, and chickens.

To comprehensively assess the replication and genome editing potential of HDV-like agents, as well as their host range, the above-mentioned cell lines derived from these different animal species were transfected (Figure 3.8A). Transfection efficiency was tested by transfecting each cell line with a plasmid encoding GFP and assessing the signal 3 days post (Figure 3.8B). For the analysis of viral Ag expression, cells were harvested on days 2, 6, and 12 and analyzed via WB (Figure 3.8C) and IF (Figure 3.8D) to detect DA_g.

The expression of HDV S- and L-HDA_g was observed in VeroE6 and CHO cells, while the signal was weak in Paki and absent in LMH cells (Figure 3.8C). HDV, WoDV, and DeDV showed excellent replication in VeroE6 and CHO cells, but no L-Ag expression was observed for WoDV or DeDV, confirming results in HuH7 cells. BaDV Ag expression increased over time only in CHO cells but was still at a lower level when compared to other mammalian HDV-like agents. No expression increase of BaDA_g was found in Paki cells, suggesting the need to validate the replication of this agent in a broader selection of Bat-derived cell lines. AvDA_g expression was observed in VeroE6 and CHO but only until day 2 and day 6 post, respectively. Only LMH cells allowed AvDA_g expression until 12 post, confirming AvDV replication solely in a cell line derived from a species closer to its original host. Both methods, WB, and IF, demonstrated a good correlation regarding DA_g expression kinetics and signal intensity. Therefore, the following experiments were by me based on WB analysis.

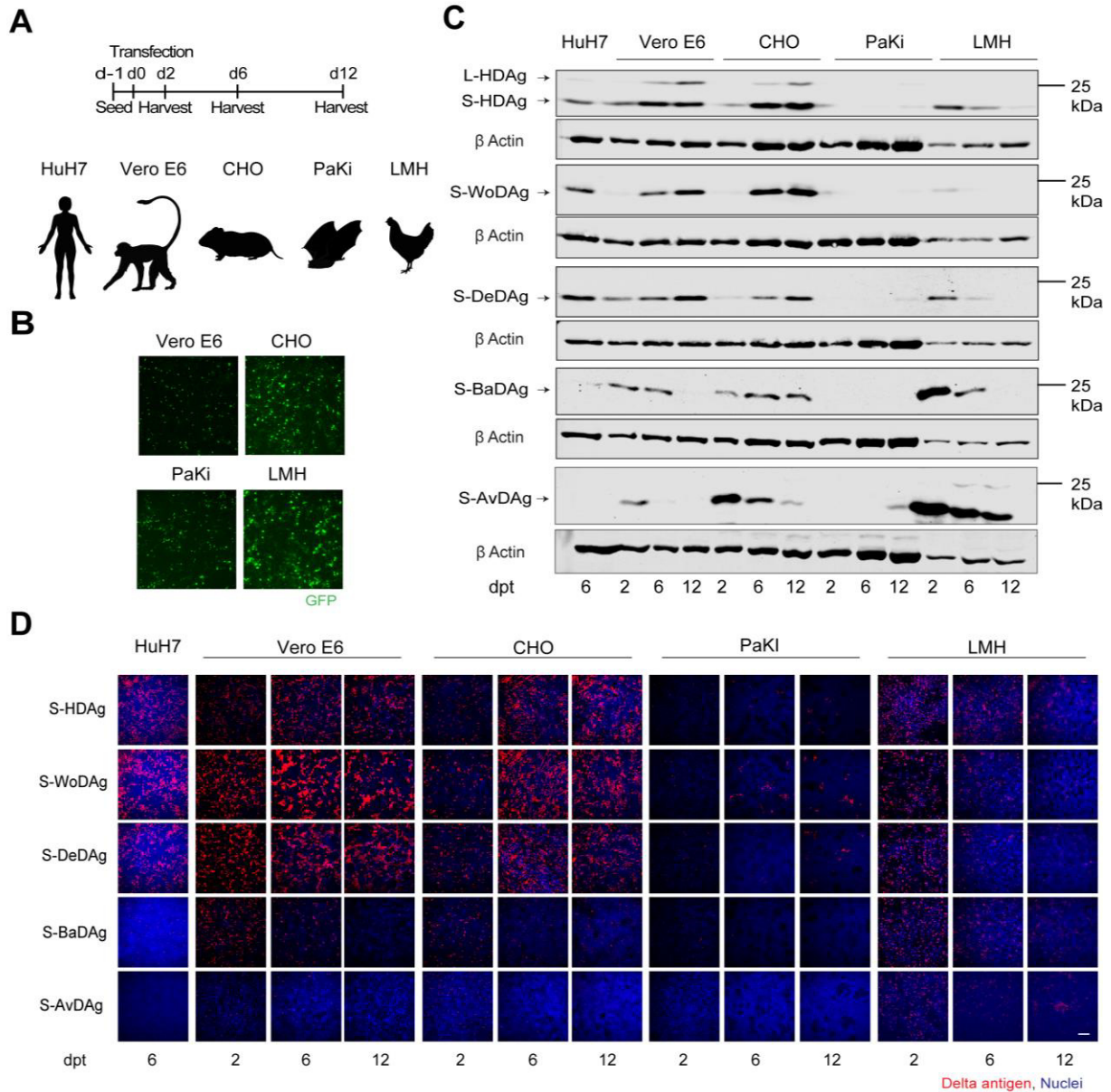


Figure 3.8. Antigen expression and replication in Vero E6, CHO, PaKi, and LMH cells. Vero E6, CHO, PaKi, and LMH cells were transfected with HDV-like agent constructs and harvested on days 2, 6, and 12 pt (A) and with a GFP plasmid to check transfection efficiency of each cell line (B). Viral antigen expression and putative genome editing were assessed via WB analysis (C) and IF (D) using FD3A7 anti-S-HDAg antibody or specific α -AvDAg antibody.

3.1.3 Establishment of HDV-like agents' replication in non-hepatocyte-derived cells

Given that replication of HDV-like agents may not be limited to hepatocytes, I examined the ability of various non-hepatoma-derived cell lines to support replication. To this goal, cervical adenocarcinoma (HeLa), embryonic kidney (HEK293T), and epithelial lung carcinoma (A549) cells, were transfected and assessed for viral Ag expression (Figure 3.9A). All mammalian tested DLAs could establish replication in HeLa cells. However, a significant decrease of Ag expression was observed at day 12 pt, probably due to cell viability issues, as indicated by a decreased level of β -actin signal (Figure 3.9B). However, replication was efficient in HEK293T cells, as indicated by the high editing rate for HDV and late expression of S-WoDAg and S-DeDAg (Figure 3.9B). In A549 cells, an increase of S-HDAg was observed for HDV, but only a faint band for L-HDAg was detected, indicating a lack of efficient replication in this lung-derived cell line. Both WoDV and DeDV S-DAg were expressed and still present at day 12 pt, although the signal was much lower when compared to HeLa and HEK293T cell lines.

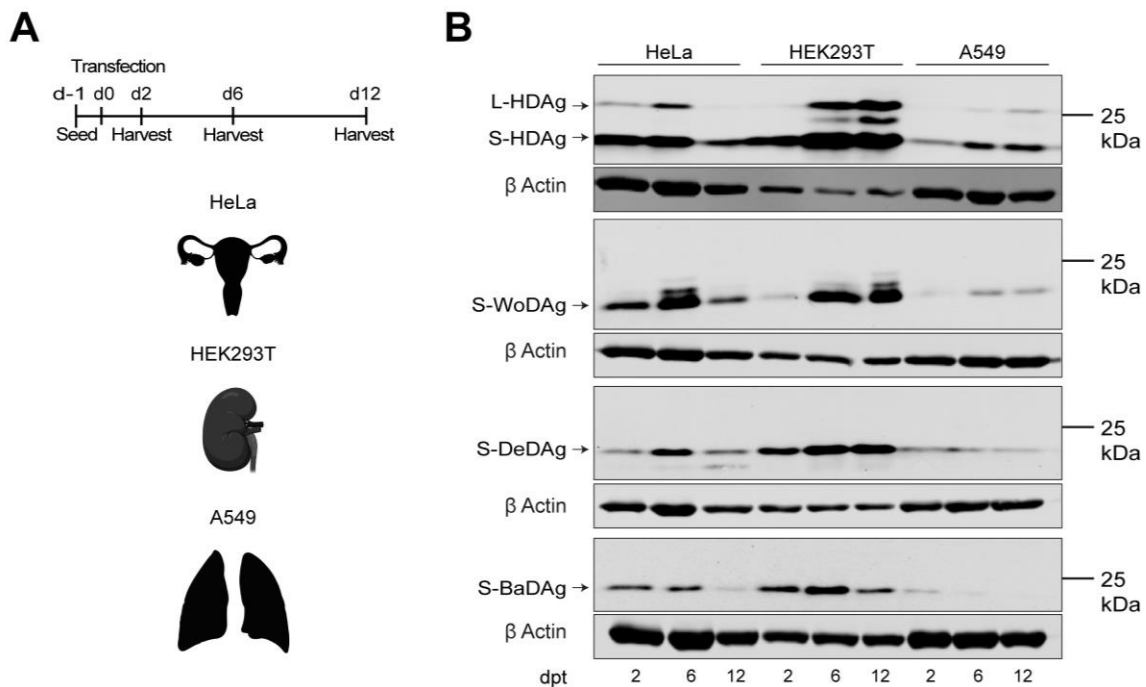


Figure 3.9. Antigen expression in non-hepatic human cell lines. HeLa, HEK293T, and A549 cells were transfected and harvested on day 2, 6 or 12 pt (A). For each time point, cells were lysed, and delta antigen expression was visualized by WB using the FD3A7 antibody (B).

The expression of BaDV S-DAG reached its highest level at day 6 pt only in HeLA and HEK293T cells and then decreased by day 12 pt (Figure 3.9B). These results show replication of DLA non only in hepato-derived cell lines, opening a possibility of intra-host spread that could be broader, compared to the hepatotropic HDV. However, consider the strong relevance of cell-to-cell spread in HDV, and the lack of these studies for DLAs, before delving into intra-host spread examination, I investigated the possibility of CDMS for DLAs too

3.1.4 WoDV and DeDV can amplify efficiently via cell division in HuH7 cells

It is already well characterized how the human HDV can spread and persist intracellularly from mother to daughter cell after cell division (Giersch et al., 2019; Zhang et al., 2022). To investigate if this spreading pathway is conserved among HDV-like agents, a cell-division-mediated viral amplification assay (CDMAA) was established and performed first in human hepatoma cells. HuH7 cells were transfected with 1.1mer antigenome constructs and split when confluency was reached, with a 1:100 dilution factor. Transfected cells were fixed in parallel at every split and stained for DAG visualization (Figure 3.10A). When viral spread occurs by cell division, a cluster of DAG-positive cells may be observed due to the expansion of viral replication through cell mitosis originating from a single infected cell. As expected, clusters of Ag-positive cells were observed for the human HDV WT but not for HDV defect, indicating specificity of the assay for replication-dependent cell division-mediated spread (Figure 3.10B).

Interestingly, clusters were detected for WoDV and DeDV from passage 1 (P1) (Figure 10 B) to passage 3 (P3 data not shown) with an intensity that was comparable to the human

HDV. Clusters of positive cells were also detected for BaDV but required more sensitive microscopy methods, suggesting that BaDV replication is maintained weakly in human hepatoma cells.

Cell division-mediated spread of AvDV was also evaluated in HuH7 cells. Consistent with previous data on AvDV replication in HuH7, CDMS of this agent is absent in this hepatoma cell line (Figure 3.10B), probably due to a lack of replication in human cells.

For a more quantitative overview of CDMS efficiency in HuH7 cells, clusters were quantified using the Cell Profiler software. For quantification, clusters were analyzed in terms of size, number of cells per cluster, and intensity of single cell signal. These factors were multiplied to obtain a value indicating the ability to spread by cell division and the strength of intracellular replication (Figure 3.10C).

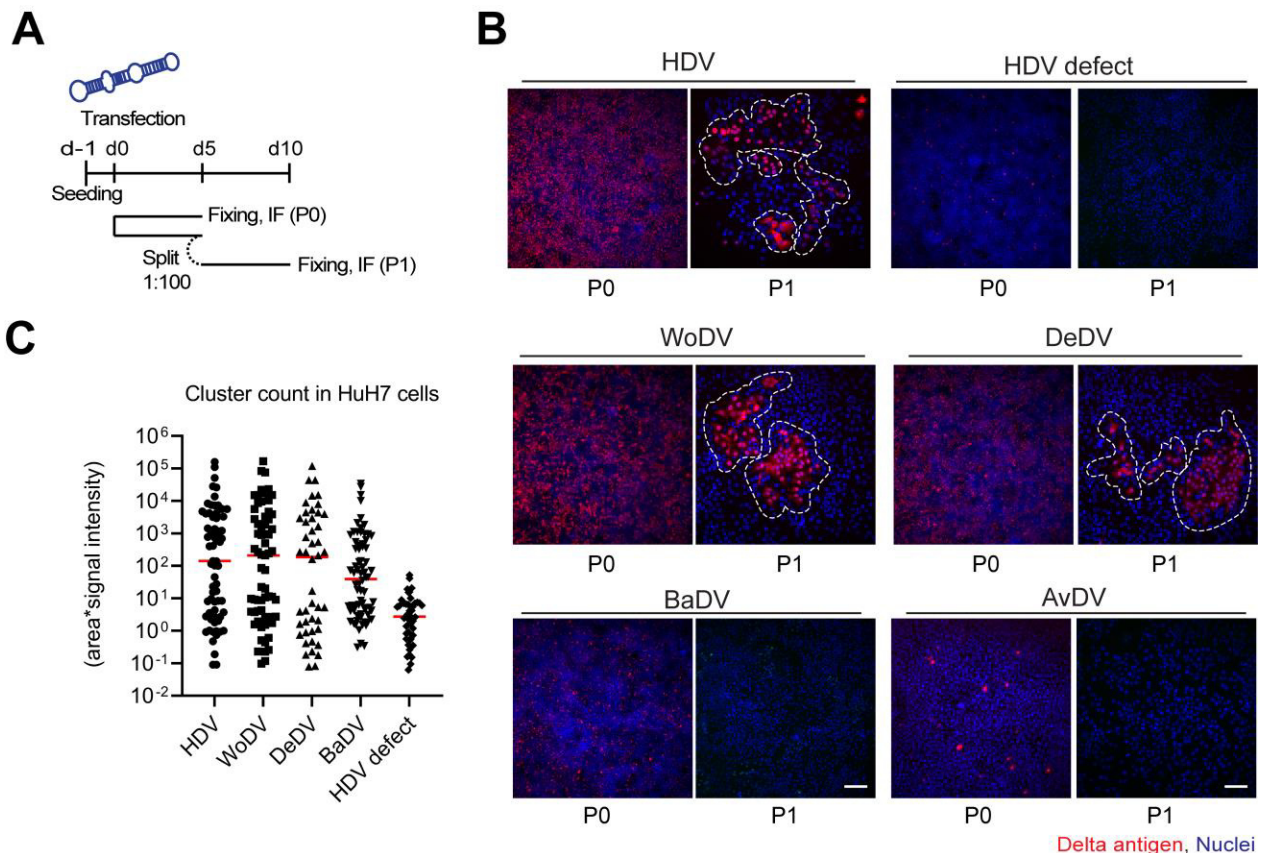


Figure 3.10. Mammalian DLA can spread via cell division in human hepatoma cells. HuH7 were transfected with HDV-like agent constructs and, on day 5, pt, were split at a high dilution factor of 1:100

(passage 0=P0) (A). On day 5 *pt* and day 5 post passage (P1), cells were fixed, and DAg expression was visualized by IF using FD3A7 antibody or α AvDAg antibody (B). Delta antigen-positive cells were then quantified using Cell Profiler (C). Scale bar: 200 μ m.

Confirming the IF staining, HDV, WoDV, and DeDV had a comparable cluster count level, indicating comparable CDMS efficiency. Compared to the negative control, HDV defect, BaDV displayed higher values, confirming a weaker replication for this agent.

However, the phenotype observed in CDMAA cannot be distinguished from the putative extracellular cell-to-cell spread in the absence of envelopment. To investigate this phenotype further, I had to establish a novel cell culture system.

3.1.7.1 HDV-like agents cannot spread autonomously to neighboring cells

It has already been well-characterized how viruses can use cellular junctions to spread from one adjacent cell to another, bypassing the entry pathway receptor-dependent method (Mothes et al., 2010). This possible spreading pathway may appear phenotypically similar to the one observed in the context of cell division-mediated spread. To differentiate between CDMS and envelope-independent cell-to-cell spread, I established a co-culture system using fluorescent protein expression. Following lentiviral transduction, HuH7 cells expressing either mScarlet or GFP were generated via lentiviral transduction (Figure 3.11A-left panel). mScarlet-positive HuH7 cells were transfected with the antigenome constructs on day 0, and after 3 days, the transfected cells were co-cultured with untransfected GFP-HuH7 cells. Maintenance of the co-culture system was carried out for a total of 10 days (Figure 3.11A-right panel). After 10 days of co-culture, the cells were fixed and stained to visualize the expression of DAg.

DAg-positive mScarlet cells were observed in close proximity to GFP cells, therefore, the cell-to-cell transmission would result in DAg-positive GFP cells. However, no co-localization between the GFP and DAg signal was observed, as shown by IF (Figure 3.11B).

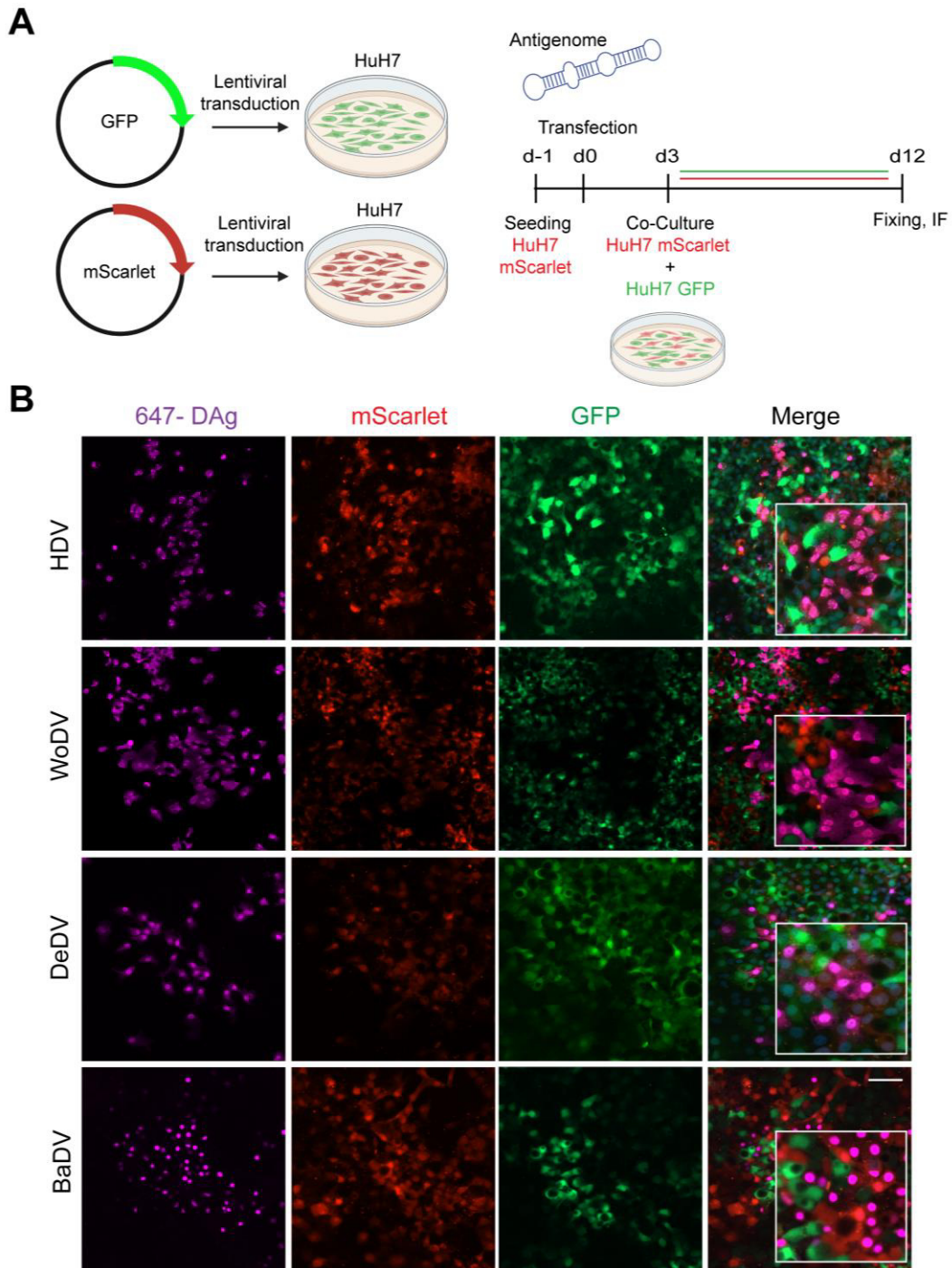


Figure 3.11. Autonomous extracellular spread of HDV-like agents is rare. HuH7 cells were transduced to express mScarlet or GFP and maintained under antibiotic selection for several passages. mScarlet - HuH7 cells were transfected with HDV-like agent constructs, and after 3 days, they were co-cultured with HuH7 GFP cells in the presence of DMSO, to prevent overgrowth (A). After 10 days, cells were fixed and stained for delta antigen (magenta) visualization (FD3A7 anti-S-HDAg and Alexa Fluor 647-labeled anti-rabbit antibody) (B). Images were acquired using ZEISS Cell Discoverer 7 microscopy Scale: 50 μ m.

Having established the capacity of DLA to undergo cell division-mediated spread in human hepatoma cells, animal- and non-liver-derived cell lines were also evaluated and assessed from CDMS permissiveness.

3.1.7.2 *The spread of HDV-like agents through cell division is not limited to human or liver-derived cells*

To obtain a more reliable measure of viral replication and intracellular spread, CDMS was assessed in previously investigated non-human derived cell lines, namely Vero E6, CHO, PaKi and LMH cells. As performed for HuH7 cells, non-human-derived cell lines were transfected and split at a high dilution factor to allow clonal expansion. When confluence was reached, cells were fixed and stained for DA_g visualization.

Vero E6 and CHO cells exhibited efficient CDMS of HDV, WoDV, and DeDV, consistent with the pattern observed for Ag expression kinetics. Clustering was not observed in PaKi cells for HDV, WoDV, and DeDV, as indicated by the single-cell level signal. Interestingly, no cluster was formed by BaDV in the bat-derived cell line (Figure 3.12A).

The staining of AvDA_g with a specific antibody revealed high replication and efficient cluster formation in LMH cells (Figure 3.12B), indicating an efficient cell division-mediated spread for AvDV exclusively in avian cells. IF visual results were confirmed by cluster quantification data (Figure 3.12C).

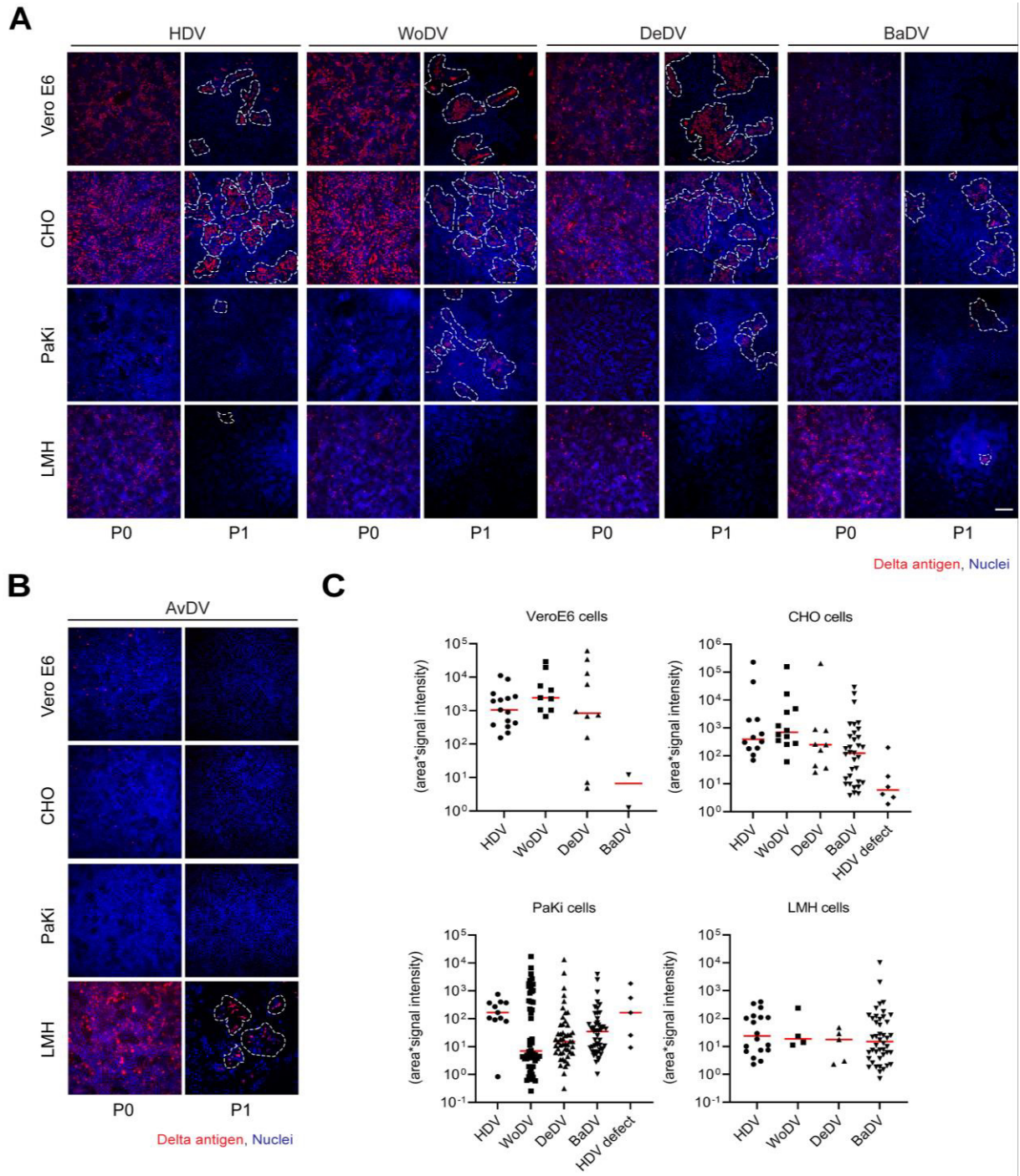


Figure 3.12. HDV and HDV-like agents' cell division-mediated spread in different animal cell lines. Vero E6, CHO, PaKi, and LMH cells were transfected and then split (dilution factor 1:100) at day 5 pt (passage 0=P0). After confluency was reached, cells were fixed, and DAg expression was visualized by IF

using FD3A7 antibody (A) or antibody α -AvDAg (B). Clusters of DAg -positive cells were quantified using the Cell Profiler program (C). Scale bar: 200 μ m.

The new HDV-like agents are characterized by their apparent lack of a strong liver tropism, which applies to human HDV. To investigate CDMS in human cell lines that are not derived from the liver, HeLa (uterus), HEK293T (kidney), and A549 (lung) cells were transfected. After passaging, viral Ag expression was analyzed via IF.

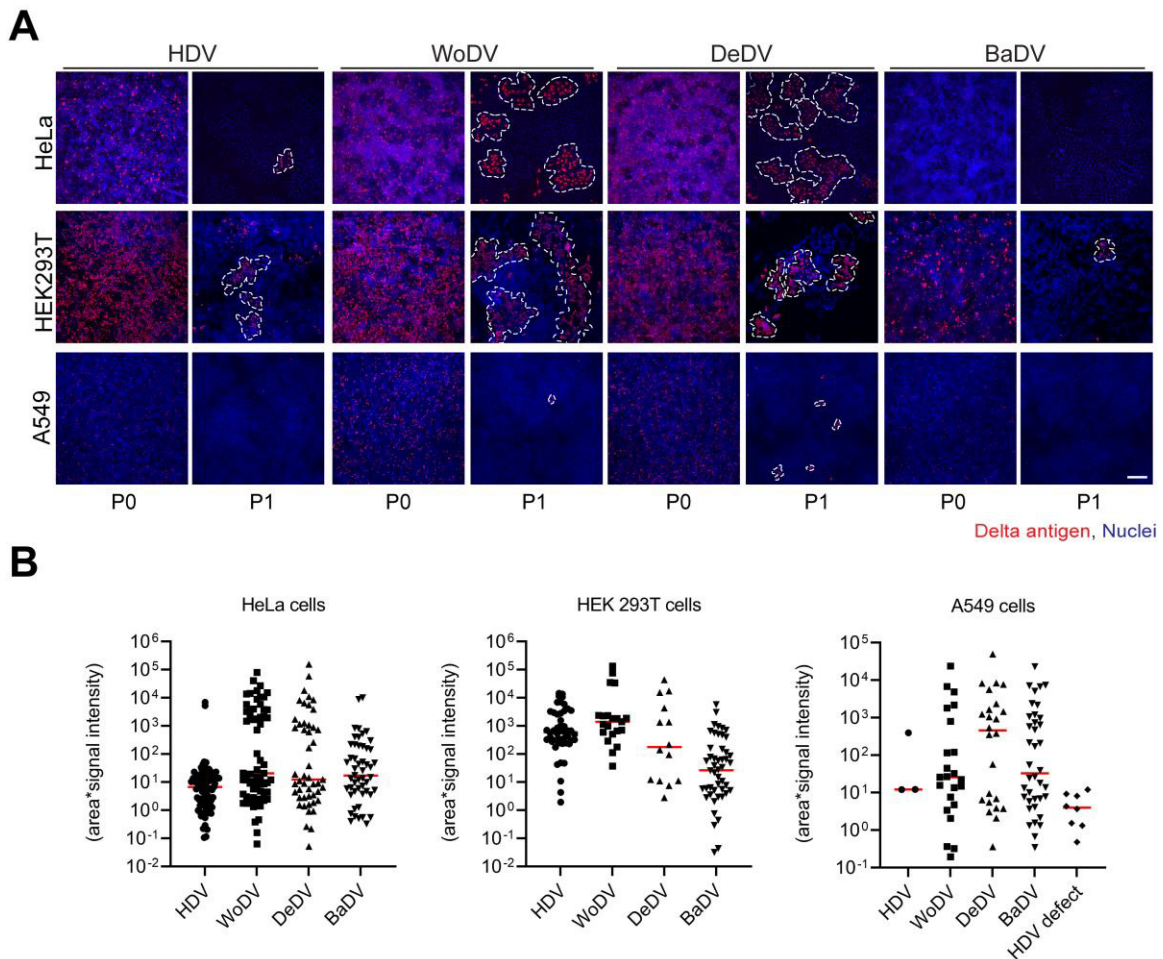


Figure 3.13. Cell division mediated spread in non-hepatic human cell lines. HeLa, HEK293T, and A549 cells were transfected with delta-like agent constructs and split (dilution factor 1:100) at day 5 post-transfection (passage 0=P0). Cells were fixed at day 5 post-transfection or day 5 post passage (P1), and

delta antigen expression was visualized by immunofluorescence using FD3A7 antibody (A). Delta antigen-positive cells were then quantified using Cell Profiler program (B). Scale bar: 200 μ m.

Interestingly, CDMS of WoDV and DeDV was more efficient than HDV in HeLa and HEK293T cells (Figure 3.13A&B). In addition, no cluster formation was observed in A549 cells for all HDV-like agents (Figure 3.13A&B). The lack of tissue-specific host factors may hinder efficient replication in lung-derived cell lines. Another potential factor to consider in the initiation of viral replication is the role of the innate immune system, given the proficient innate immunity of A549 cells and the susceptibility of HDV to interferon stimulation. To test this hypothesis, CDMS in A549 was evaluated in the context of IFN signaling inhibition.

3.1.7.3 Cell division-mediated spread in A549 cells is enhanced upon Ruxolitinib treatment

Of all the cell lines analyzed for DLA replication, A549 cells have already been shown to be able to mount immune activation upon pathogen infection (Dias et al., 2021; Hartman et al., 2007; Urban et al., 2020). The contribution of innate immunity in establishing viral replication and spread was assessed, given the low effectiveness of viral replication and cell division-mediated spread in this cell line. In the first instance, the antiviral state following transfection of A549 cells was evaluated. This was achieved by measuring the ISG15 upregulation after 5 days pt. The transfected cells were treated in parallel with the JAK1/JAK2 inhibitor, Ruxolitinib, to prevent the induction IFNs stimulation (Figure 3.14A). The results showed a significant decreased of ISG15 upregulation upon Ruxolitinib treatment in A549 cells and for all the carried-out transfections (Figure 3.14B). Moreover, Dag expression of HDV and all DLAs tested, was increased upon Ruxolitinib treatment (Figure 3.14C). Innate immunity and IFN activation highly impact on HDV CDMS but have little effect on its intracellular replication once established (Gillich et al., 2023; Zhang et al., 2022). CDMAA was conducted on A549, with and without Ruxolitinib treatment, to

investigate the role of innate immunity in blocking viral maintenance and CDMS. No efficient CDMS was observed in A549 for HDV and BaDV, even upon Ruxolitinib treatment. However, using the inhibitor, an increase in cluster formation was observed for WoDV and DeDV. These data might suggest a possible implication of interferon induction in HDV-like agents persistence.

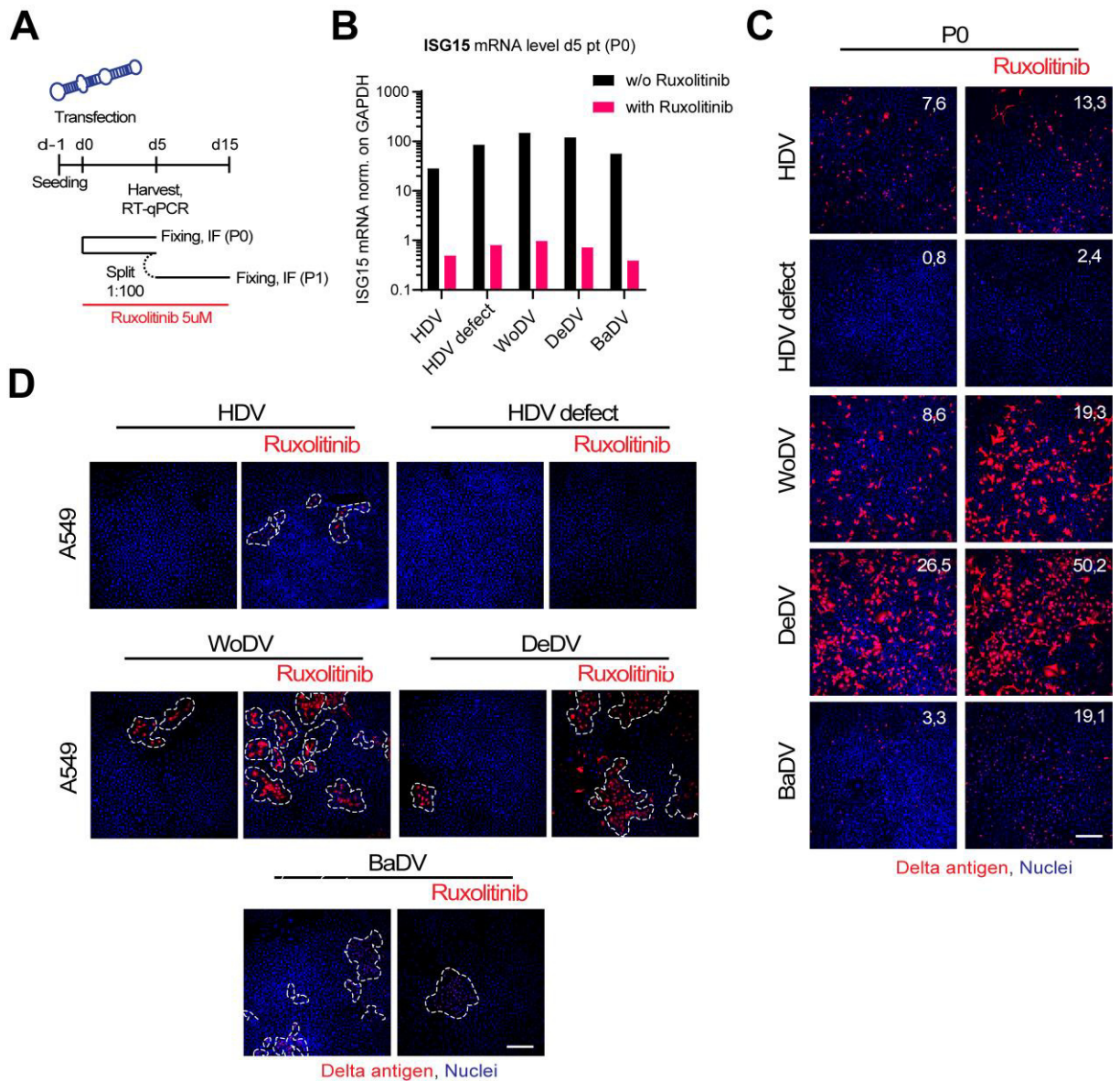


Figure 3.14. Ruxolitinib treatment increases the CDMS of WoDV and DeDV in A549 cells. Ruxolitinib treated or untreated A549 cells were transfected with viral constructs, and 5 days pt cells were lysed for ISGs induction measurement or split for viral amplification assay (A). At Passage 0 = P0), cells were lysed

for ISG15 mRNA level measurement (B) or stained for DAg detection via IF (C). When, after splitting, cellular confluence was reached, cells were fixed and stained for Ag visualization via IF (D). Scale bar: 200 μ m.

In summary, HDV-like agents were able to establish replication in several human (HuH7, HeLa, HEK293T) and non-human (VeroE6, CHO) cell lines. Interestingly, HDV-like agents could efficiently spread via cell division, underpinning the importance of this spreading pathway not only in the context of HDV. However, among all tested cell line , PaKi, LMH and A549 seems not to be permissive for efficient viral replication.

To properly study the interplay between HDV-like agents and innate immune regulation, an infection system is required. Potential methods for DLA pseudo-typing were evaluated, with the aim of establishing an infection system.

3.2 ESTABLISHMENT OF INFECTION SYSTEM AND CHARACTERIZATION OF EXTRACELLULAR SPREAD

3.2.1 *Pseudo typing of HDV and HDV-like agents using selected envelope proteins from hepadna- and non-hepadnaviruses*

A recent study reports that HDV may be packaged and spread via envelope glycoproteins of several non-hepadna viruses (Perez-Vargas et al., 2019). However, this observation has limited clinical evidence, and it remains a subject of debate. To date, the HDV-like agents investigated in this study have not been identified as satellite viruses of any known helper virus (Bergner et al., 2021; Iwamoto et al., 2021).

Given the broad range of cellular replication and the absence of L-HDAg expression, I aimed to determine whether novel HDV-like agents could exploit hepadna and non-hepadnaviruses' envelope glycoproteins for extracellular propagation. To this end, HuH7 were used as viral particles producers' cells and transfected with cDNAs of HDV-like agents together with plasmids containing envelope proteins derived from HBV (HBsAg), Hepatitis C virus (HCV-E1E2), Dengue virus (DENV-PrME) and Vesicular stomatitis virus (VSV-g) (Figure 3.15A). HDV and HBsAg co-transfection was used as positive control for efficient virus production and packaging. The supernatant was collected, and the secretion of virions was measured via RT-qPCR of viral genome copies. Infectivity was assessed through the infection of HuH7^{NTCP} cells (HDV-like agents pseudotyped using DENV-PrME and VsV-g) and HuH7 Lunet^{CD81h} cells (HDV-like agents pseudotyped using HCV-E1E2). For the co-transfection of HCV-E1E2 and DENV-PrME, RT-qPCR analysis indicated no significant increase in the viral RNA level in the supernatant compared to mono-transfected cells (antigenome-only transfection) (Figure 3.15B). Using VSV-g as packaging glycoprotein, a higher extracellular RNA level was observed. Infection using HDV/VSV-g pseudoparticles resulted in extremely low infection rate, with only few positive cells each well (Figure 3.15C). However, IF analysis demonstrated higher % of DAg-positive HuH7-NTCP cells infected with the pseudotyped WoDV/VSV-g and DeDV/VSV-g

particles (Figure 3.15C), compared to HDV. To evaluate the susceptibility of HuH7 Lunet^{CD81h} cells and HuH7^{NTCP} cells to HCV-E1E2 and DENV-PrME binding, control infections were conducted using HCV and DENV, respectively (Figure 3.15D).

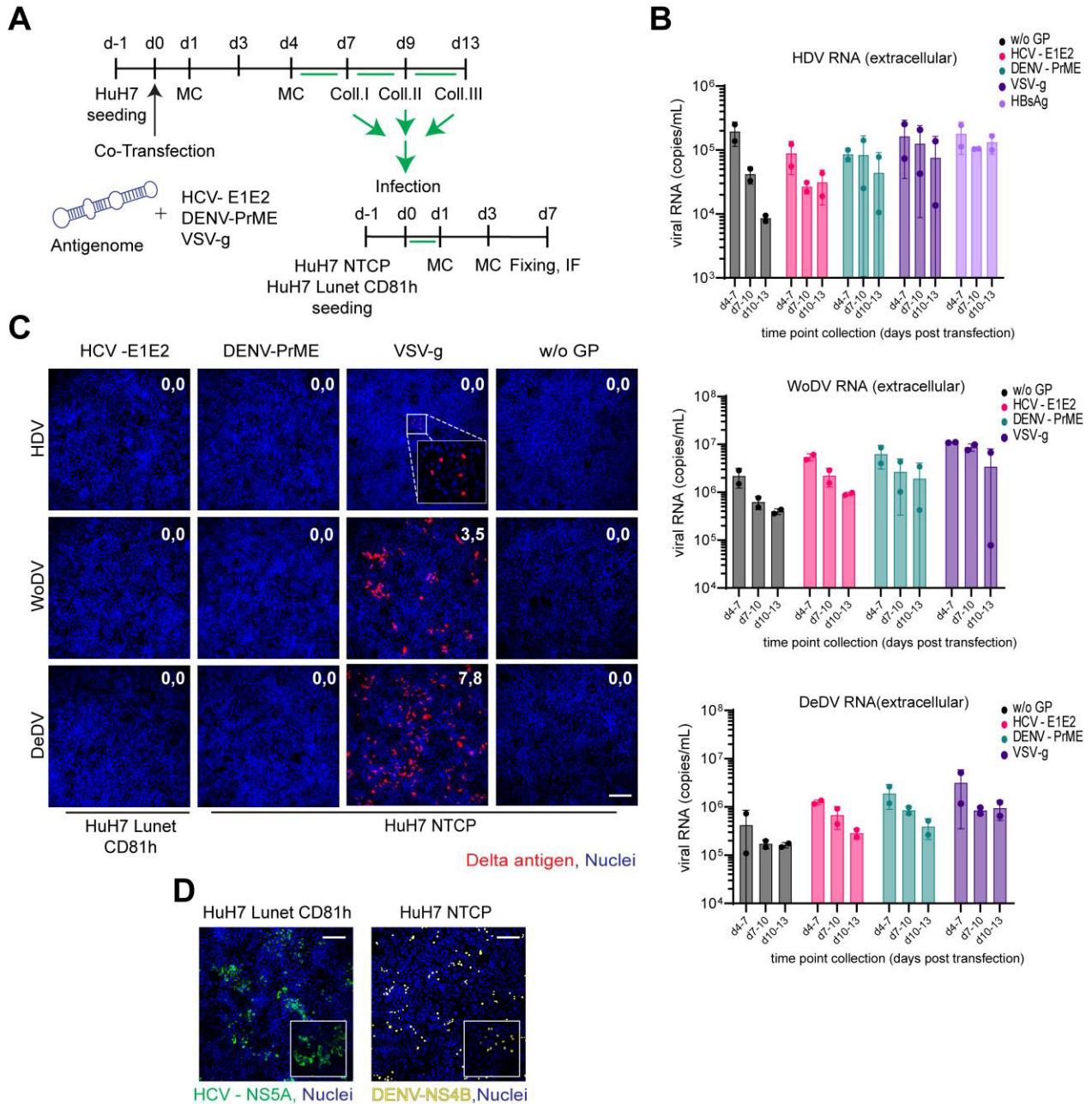


Figure 3.15. Finding a helper virus for WoDV and DeDV. HuH7 cells were co-transfected with delta-like agent constructs and envelope glycoproteins derived from hepadna (HBsAg) and non-hepadnaviruses

(HCV-E1E2, DENV-PrME and VSV-g) (A). The supernatant was collected on days 7, 10, and 13 *pt*, and viral load was measured via RT-qPCR (B). PEG-precipitated supernatant was used to infect HuH7^{NTCP} and HuH7 Lunet^{CD81h} cells. After 7 days, cells were fixed and stained for viral delta antigen (C). HuH7 Lunet CD81h and HuH7 NTCP were infected using HCV and DENV, respectively, and infection was evaluated via IF staining of the respective NS5A viral protein expression (D). Scale bar: 200 μ m.

Considering the discrepancy between HDV and DLA pseudo-typing using VSV glycoproteins, a more consistent pseudo-typing technique needed to be established. To this aim, the interaction of WoDV and DeDV RNP with the human HDV L-HDAg was evaluated.

3.2.2 Effects of HDV-LHDAg expression and prenylation on replication and artificial envelopment of HDV - like agents

3.2.2.1 The human HDV L-HDAg has an inhibitory effect on WoDV and DeDV replication

The human HDV L-HDAg is responsible for the interaction with HBV envelope proteins and, therefore, crucial for HDV secretion (Hwang & Lai, 1993; Sureau et al., 1993). Alongside this function, L-HDAg also has an inhibitory effect on HDV replication (Hartwig et al., 2006; Hwang & Lai, 1994; Modahl & Lai, 2000). Farnesylation has an essential role in both functions. As previously shown, HDV-like agents lack expression of an L-DAg and do not encode a prenylation recognition motif. The impact of L-HDAg expression on the replication of WoDV and DeDV was then investigated, focusing specifically on the role of prenylation. HuH7 cells were transfected with a plasmid expressing HDV-like agents antigenomic cDNA together with a plasmid containing the human HDV L-HDAg. To evaluate the impact of L-HDAg farnesylation on replication, the farnesyl transferase inhibitor LNF was employed (Figure 3.16A). Co-expression of L-HDAg resulted in decreased levels of intracellular viral RNA for HDV and all HDV-like agents tested (Figure 3.16B). The abrogation of farnesylation significantly reversed the inhibitory effect on HDV replication. However, LNF could not fully restore WoDV and DeDV replication (Figure 3.16B).

To authenticate the role of farnesylation in the inhibitory process, an L-HDAg farnesylation mutant was produced. Mutation of the cysteine residue located in position 211 to a serine residue (C211S) abrogated the prenylation motif within the L-HDAg (Bordier et al., 2002). To assess the role of the expression level on the L-HDAg-mediated inhibitory effect on viral replication, WT or mutant L-HADg plasmids were transfected at different ratios relative to DLA antigenomes plasmids (Figure 3.17A). The co-transfection of WT L-HDAg led to inhibition of HDV replication, independent of the co-transfection ratio (Figure 3.17B), indicating a robust inhibitory effect even at lower L-HDAg expression levels. L-HDAg C211S could inhibit replication only at higher expression levels, as shown by the increasing HDV replication when lower C211S L-HDAg is co-transfected (33.3% and 20%). For DLA, WT L-HDAg could profoundly inhibit the replication of both WoDV and DeDV and only a partial restoration of DeDV replication was observed (Figure 3.17B). WoDV was highly inhibited, even in co-expression with lower unfarnesylated L-HDAg amounts (33.3% and 20%).

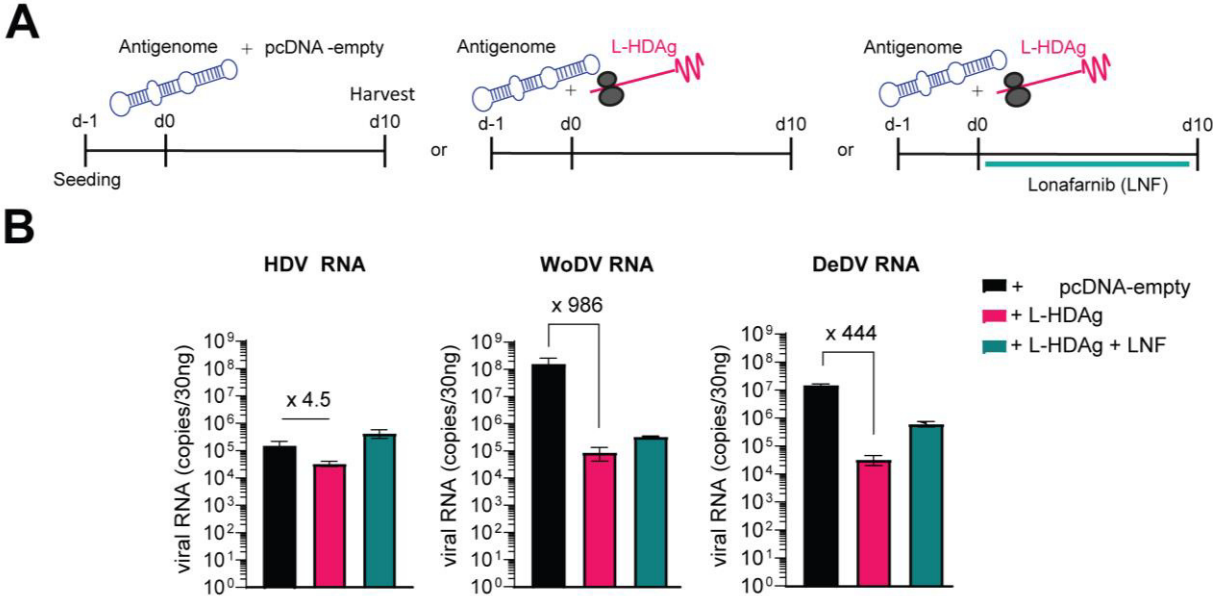


Figure 3.16. WoDV and DeDV replication are inhibited by exogenous expression of HDV L-HDAg. HuH7 cells were transfected with HDV-like agents 1.1 mer antigenome constructs together with a plasmid encoding for the L-HDAg of the human HDV. In parallel, Lonafarnib (LNF) treatment was performed to

prevent L-HDAg farnesylation (A). At day 10 pt, viral RNA levels were quantified via RT-qPCR using specific primers for each agent (B).

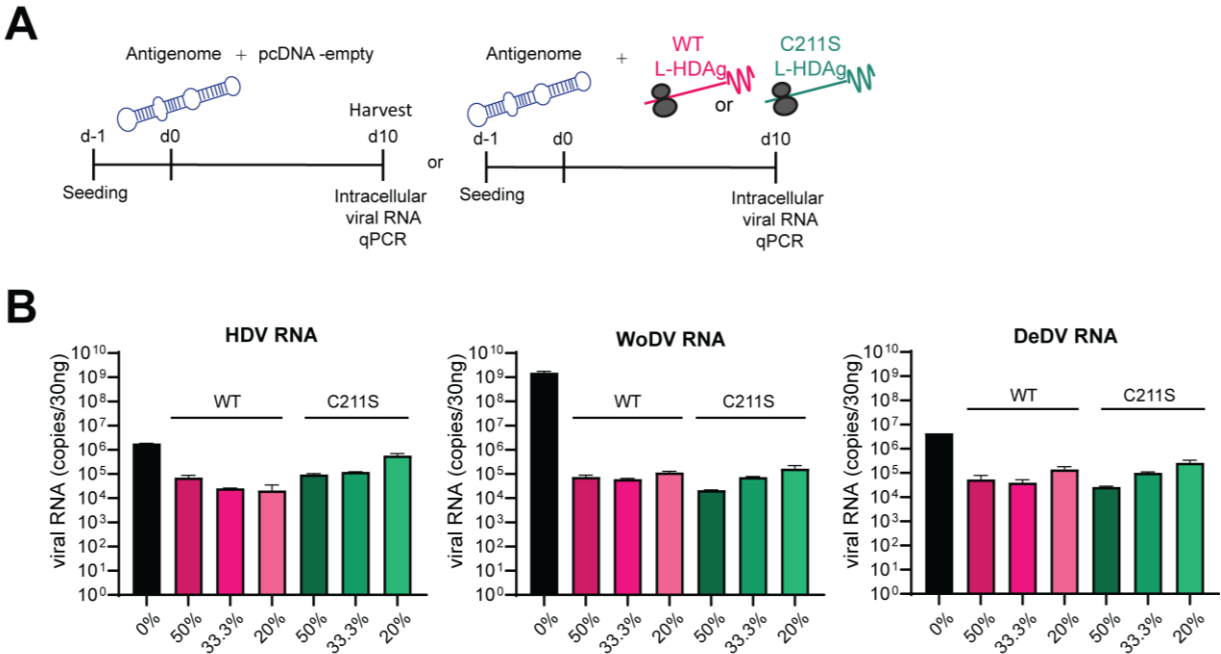


Figure 3.17. Unfarnesylated L-HDAg can inhibit WoDV and DeDV replication. HuH7 cells were transfected with HDV-like agents 1.1 mer antigenome and different amounts of plasmid encoding for WT L-HDAg and L-HDAg farnesylation mutant (C211S) (A). At day 10 pt, viral RNA was quantified via RT-qPCR (B).

These data might indicate that, unlike for HDV, the farnesylation status of L-HDAg might not be necessary for viral inhibition.

3.2.2.2 Exogenous S-HDAg expression inhibits the replication of HDV-like agents

Since unfarnesylated L-HDAg had a more pronounced negative effect on viral replication of HDV-like agents compared to the human HDV (Figure 3.16&17), I aimed to explore the possible impact of the human S-HDAg on viral replication. HDV-like agent antigenomes were co-transfected with a plasmid encoding human S-HDAg (Figure 3.18A), and viral replication was assessed 10 days pt via RT-qPCR. Interestingly, the co-transfection of S-

HDAg resulted in a significant inhibition of both WoDV and DeDV replication. This inhibition observed during co-transfection is independent of the antigen farnesylation status. This indicates that when co-expressed with WoDV or DeDV antigenomes, both L-HDAg and S-HDAg can inhibit replication, emphasizing that, unlike for HDV, farnesylation status of L-HDAg is dispensable for the inhibitory effect on HDV-like agent replication.

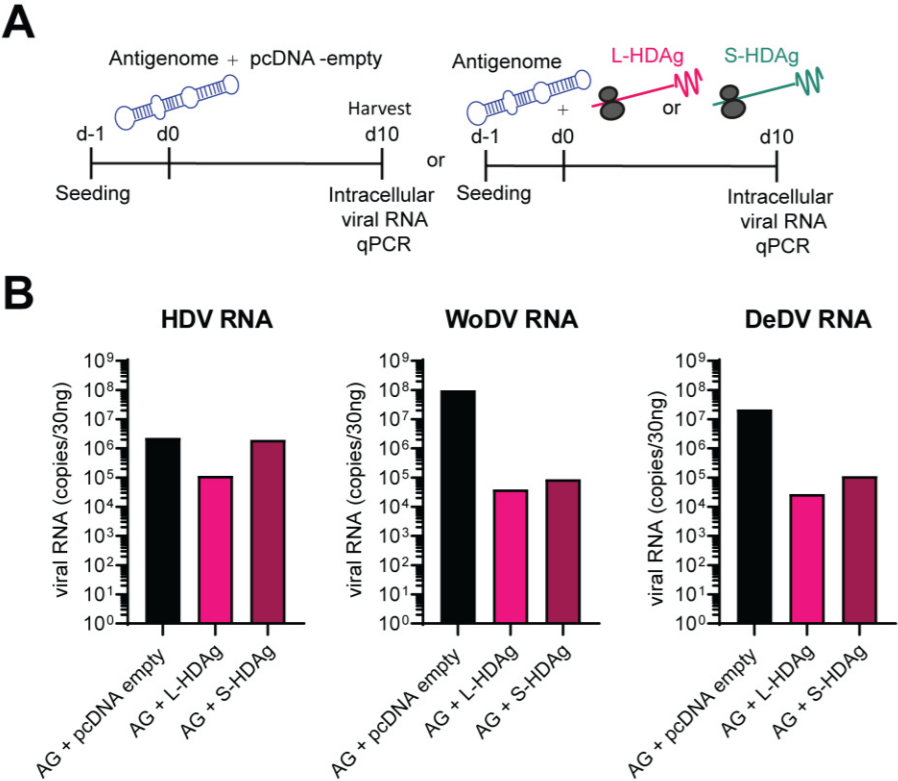


Figure 3.18. Expression of HDV S-HDAg inhibits WoDV and DeDV replication. HuH7 cells were transfected with HDV-like agents 1.1 mer antigenome constructs together with a pcDNA3.1 empty plasmid, as negative control, or a plasmid encoding for the S-HDAg or the L-HDAg of the human HDV (A). 10 dpt, viral RNA levels were quantified via RT-qPCR (B).

3.2.2.3 Late L-HDAg trans-complementation has no inhibitory effect on viral replication

To establish an infection system that exploits the interaction between WoDV and DeDV S-HDAg with L-HDAg, L-HDAg was trans-complemented at later time points. Day 3 and day 6 post-antigenome transfection were selected to assess the impact on viral replication and

antigen expression (Figure 3.19A). As previously observed, co-transfection of antigenomes and L-HDAg abolished replication and antigen expression of HDV and HDV-like agents (Figure 3.19B).

Efficient viral replication, shown as DAg antigen expression, was observed when L-HDAg was trans-complemented at days 3 and 6 post-antigenome transfection, imitating L-HDAg expression during natural HDV infection. These results indicate that L-HDAg had a suppressive effect on the replication of WoDV and DeDV only when L-HDAg was in surplus and viral replication had not yet been established.

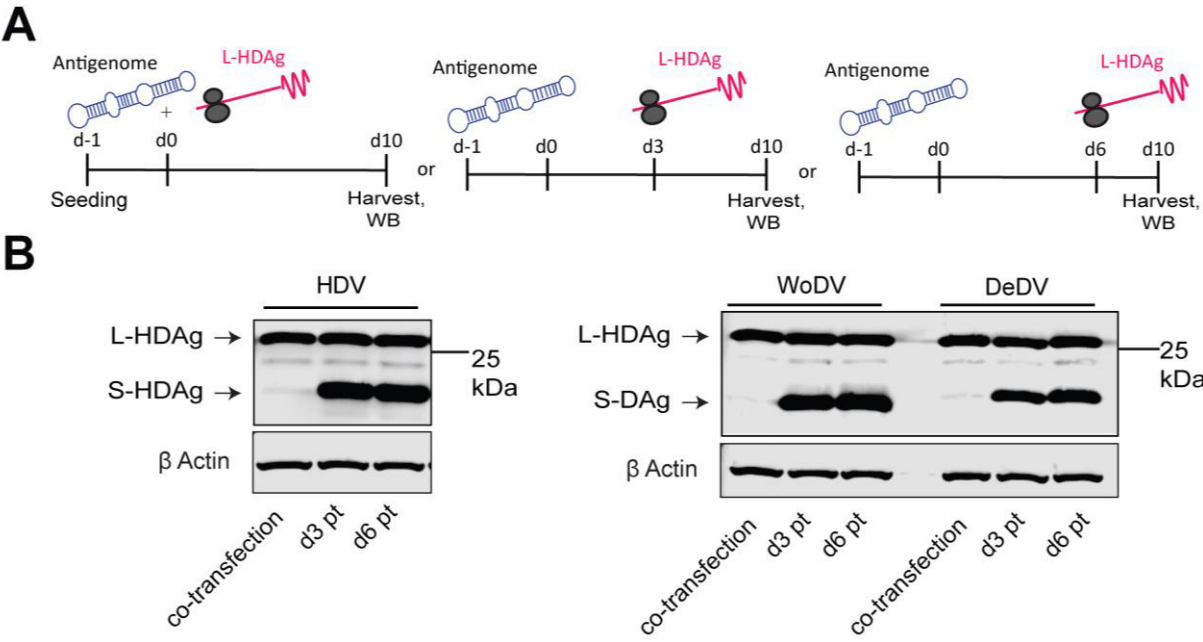


Figure 3.19. Effect of late L-HDAg trans-complementation on viral antigen level. HuH7 cells were transfected with HDV-like agent 1.1 mer antigenome constructs. L-HDAg was co-transfected or trans-complemented 3 or 6 days later (A). 10 dpt, as indicator of viral replication, viral antigen expression was assessed via WB (B).

Taken together, co-expression studies revealed an inhibitory role for L-HDAg exogenous expression in the replication of WoDV and DeDV. This enlightened the interaction between WoDV and DeDV RNP with L-HDAg, which could be exploited for pseudo-typing purposes.

3.2.2.4 *Trans-complemented L-HDAg promotes the packaging of WoDV and DeDV RNP by HBsAg*

To investigate if the non-human DLA can exploit interaction with L-HDAg for packaging by the envelope glycoproteins of HBV, viral particles were produced through co-transfection and trans-complementation in HuH7 cells as producer cells. HuH7 cells were initially transfected with the antigenome plasmid and a plasmid containing the HBV envelope, HBsAg. After 3 days, the human L-HDAg was trans-complemented (Figure 3.20A). To demonstrate that envelopment was specifically mediated by the interaction between HBsAg and exogenous farnesylated L-HDAg, virus production was also performed under LFN treatment, which inhibits farnesylation, and consequentially viral particle formation.

L-HDAg trans-complementation for WoDV and DeDV DLA led to increase in viral RNA release into the supernatant, which was reduced under LFN treatment (Figure 3.20B). To test the infectivity of pseudo-typed viral particles, the same amount of PEG-precipitated virus (in μl) was used for infecting HuH7^{NTCP} cells. While co-transfection of HDV with HBsAg resulted in the secretion of infectious particles, WoDV and DeDV could not produce infectious particles, confirming previous findings from Iwamoto et al. (Figure 3.20C-left panel). Remarkably, the trans-complementation of L-HDAg yielded a high infection rate for WoDV and DeDV (Figure 3.20C-middle panel). The entry inhibitor BLV proficiently blocked the infection, indicating an authentic NTCP-dependent virus entry. No infection events could be observed when producing cells were treated with LFN (Figure 3.20C-right panel).

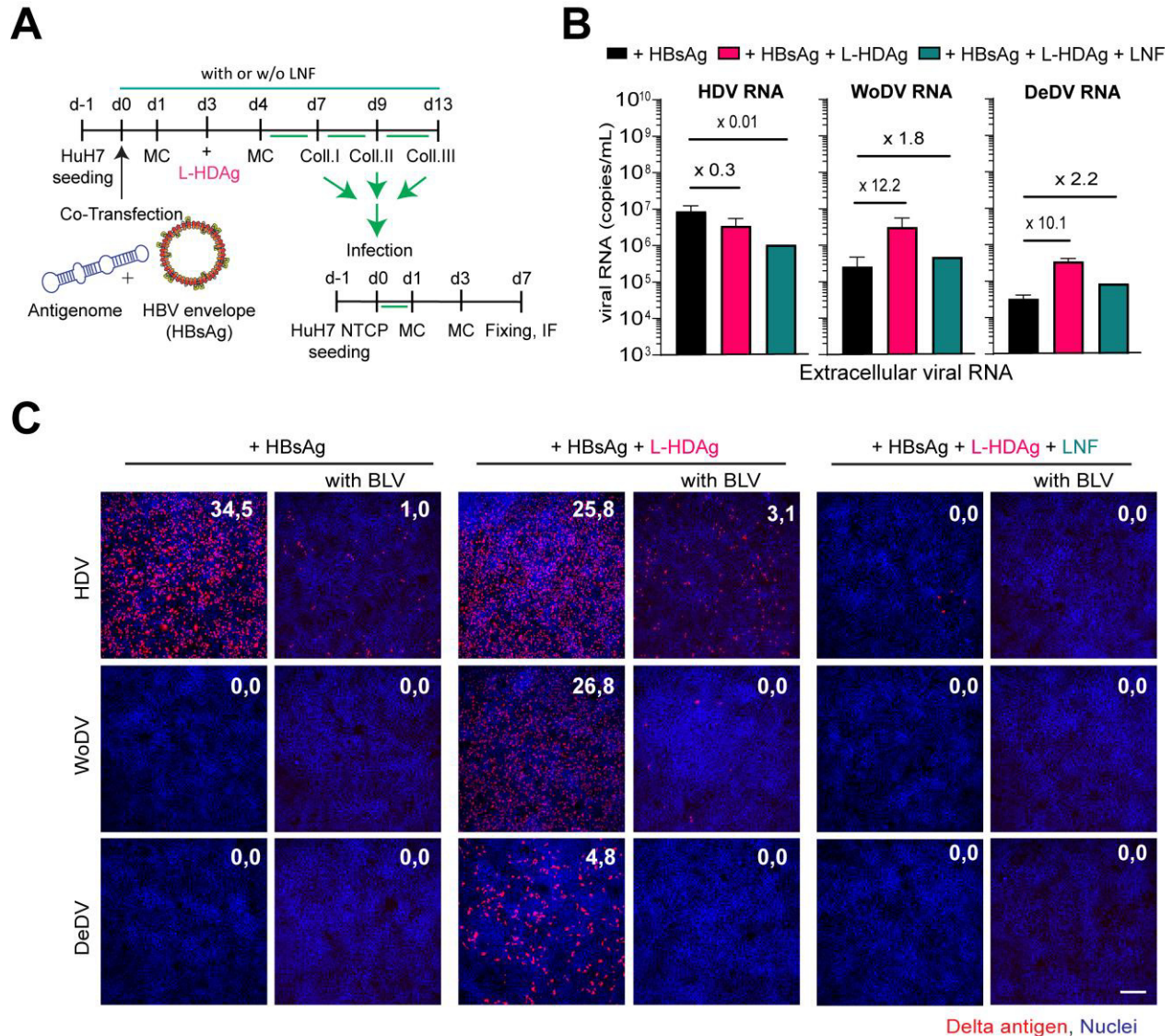


Figure 3.20. L-HDAg complementation and packaging by HBV envelope proteins. HuH7 cells were co-transfected with delta-like agent 1.1 mer antigenome constructs and pLX304-HB2.7 plasmid with or without L-HDAg trans-complementation. Virus production was also performed under LNF treatment (A). Supernatant from transfection was collected, and after PEG precipitation, the viral load was measured via RT-qPCR (B). PEG precipitated virus was used to infect HuH7^{NTCP} cells, and after 7 days, cells were fixed and stained for DAg visualization (C). The first column represents infection performed with virus produced without L-HDAg complementation. Bulevirtide (BLV) treatment was used as a control (second column). The third and fourth columns depict infection with L-HDAg complemented virus with or without BLV treatment, respectively. The fifth and sixth columns represent infection with L-HDAg complemented virus and LNF treatment (1 μ M) to prevent farnesylation, with or without BLV treatment, respectively. DAg-positive cells were quantified using Ilastik program and are shown as percentages in each image. Scale bar: 200 μ m.

As mentioned above, the Infection of HuH7^{NTCP} was carried out using an equal volume for each virus without considering the actual RNA content in the supernatant or the infectivity of different agents. For a more precise evaluation of pseudo-typing efficiency and viral infectivity, an infectious system was established based on the quantification of released viral RNA and Tissue Culture Infectious Dose (TCID₅₀) assays.

3.2.3 TCID₅₀ of pseudo-typed WoDV and DeDV viral particles

To determine the infectivity and titer of WoDV and DeDV pseudo-typed particles, a TCID₅₀ assay was performed (Figure 3.21A). At 5 days post-infection (pi), cells were fixed and stained for IF analysis. For each dilution, wells with positive cells were numbered for automatic TCID₅₀/mL calculation (Figure 3.21B). In parallel, RNA from the same virus production was extracted and quantified via RT-qPCR using agent-specific primers. The human HDV WT and human HDV defect were used as positive and negative controls for efficient packaging and infectivity. HuH7^{NTCP} cells were then infected with HDV/HBsAg, WoDV/HBsAg, or DeDV/HBsAg using the same international Unit per mL (IU/mL) calculated as Indicated in paragraph 2.2.2.9.

Infection using IU/mL as a reference showed a discrepancy in infection rate between different agents represented by % of DAg-positive cells (Figure 3.21C-left column), although the same IU was used to perform the infection. The variation in infectivity levels could be attributed to the different amounts of free viral RNA released during viral production, as well as the RNA particles that are infectious due to being enveloped by HBsAg. Moreover, a set of agent-specific primers was used for each DLA RNA quantification, leading to potential differences. Infection using TCID₅₀ values as a benchmark led to a more consistent and comparable infection rate across various agents (Figure 3.21C-right column).

For further infection experiments, TCID₅₀ values were used as a reference to achieve a comparable infection rate between HDV and HDV-like agents.

In summary, for HDV and all the HDV-like agents tested, the co-expression of WT L-HDAg reduced intracellular viral RNA levels and S-DAg expression. The abrogation of farnesylation strongly reversed the inhibitory effect on HDV replication. However, in the presence of non-farnesylated L-HDAg, replication of WoDV and DeDV was still inhibited, as well as in the context of human HDV S-DAg co-transfection.

Interestingly, L-HDAg exogenous expression allowed the packaging of WoDV and DeDV RNP by HBsAg. The viral pseudo-particles produced established infection in HuH7^{NTCP} cells via NTCP receptor binding.

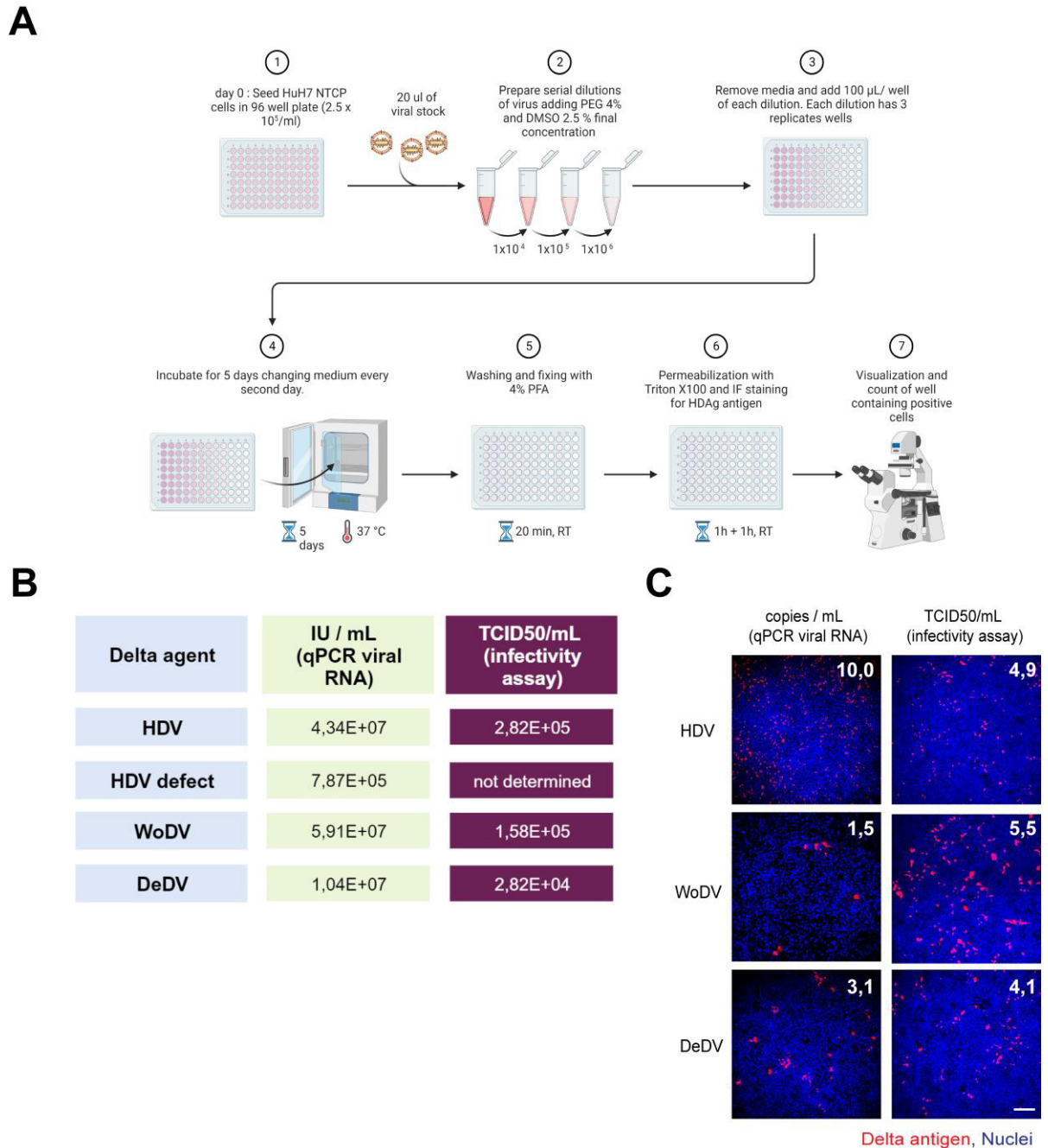


Figure 3.21. Infection using TCID50 as quantification method, resulting in a comparable infection rate in HuH7^{NTCP}. Experimental setup for quantification of TCID50 values of HDV, WoDV and DeDV pseudoparticles (A). Titers [IU/ ml] of HDV and HDV-like agents were quantified by RT-qPCR or TCID50 measurement (B). HuH7^{NTCP} cells were infected either with 1 IU/ cell of HDV, WoDV, or DeDV or with 1MOI using TCID50 as the reference value. 6 days pi DA_g-positive cells were stained by IF and quantified via Ilastik software(C). Scale bar: 200 µm.

Having established an infection system in NTCP-expressing cell lines, the following steps were to evaluate innate immunity induction in infected human-derived- cell lines.

3.3 CHARACTERIZATION OF THE INTERPLAY BETWEEN HDV-LIKE AGENTS AND THE INNATE IMMUNE RESPONSE

HDV replication activates IFN responses, mediated by two main PRRs, MDA5 and LGP2 (Gillich et al., 2023; Zhang et al., 2018). HDV-induced IFNs, as well as exogenous IFNs, profoundly suppress HDV CDMS but have only a minor effect on already ongoing HDV replication in resting cells (Zhang et al., 2022). The discovery of HDV-like agents in different animal species provides the chance to investigate the interplay between HDV and IFN response from an evolutionary perspective. To this end, a well-established, innate immune-competent, hepato-derived cell line, HepaRG, was used for infection experiments (Gillich et al., 2023; Zhang et al., 2018). The overexpression of NTCP renders this cell line susceptible to HBsAg envelope-mediated HDV infection, even without differentiation into hepatocyte-like and biliary-like cells.

All previous infection experiments were performed using PEG precipitate viral particles, which might contain impurities. Before assessing innate immunity induction upon DLA infection, ISG upregulation was assessed upon HDV stock infection purified via PEG precipitation or heparin affinity chromatography (Figure 3.22A). ISG15 and Mx1 mRNA expression in infected HepaRG^{NTCP} non-targeting (NT) and HepaRG^{NTCP} shMDA5 (MDA5 knock-down-KD) were compared at 2-, 5-, and 9-days pi (Figure 3.22B). Overall, ISG15 and Mx1 showed similar expression patterns, and ISG upregulation peaked at day 5 pi and decreased partially until day 9 pi. As expected, HepaRG^{NTCP}NT displays a much higher ISG expression than HepaRG^{NTCP} shMDA5, here used as a negative control for HDV-induced antiviral response. A more pronounced ISG induction in HepaRG^{NTCP} shMDA5 was observed during infection using a PEG-precipitated virus. Considering this higher background in ISG upregulation, all the following experiments were conducted using stock purified by heparin affinity chromatography via Äkta machinery.

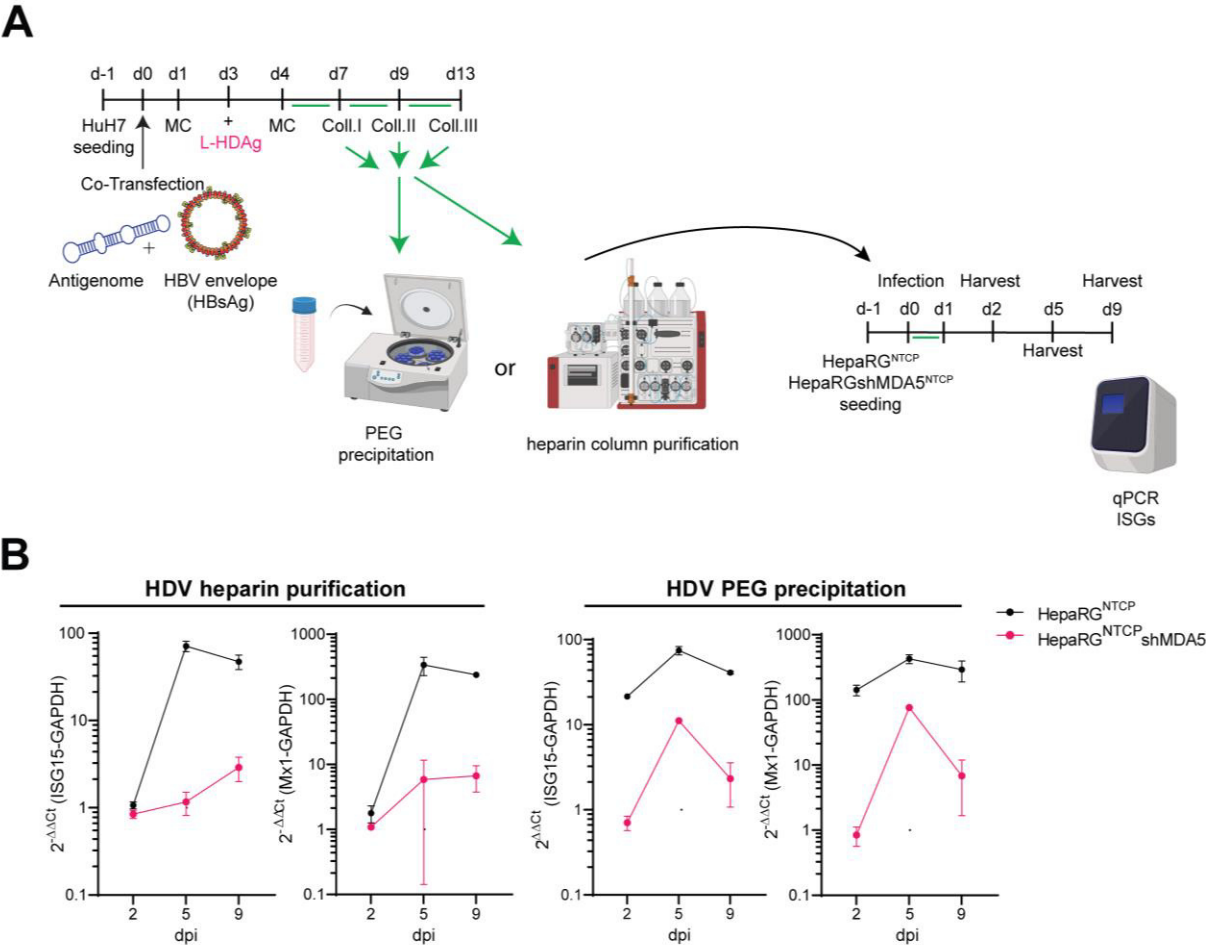


Figure 3.22. Comparison between PEG precipitation and his chromatography virus purification in ISGs induction. HDV stocks were concentrated either by heparin affinity chromatography or PEG precipitation and used to infect HepaRG^{NTCP}NT and HepaRG^{NTCP} shMDA5 (A). ISG15 and Mx1 expression in infected cells was measured on mRNA level by RT-qPCR. Measurements were performed on days 2, 5, and 9 pi (B). Data are normalized to GAPDH and displayed as fold change to an uninfected condition. Values are shown as mean \pm SD.

Moreover, to avoid possible background ISG activation in the context of KD cells (HepaRG^{NTCP} shMDA5 cells), further experiments were conducted using knock-out (KO) cell lines already available in my research group (Gillich et al., 2023; Zhang et al., 2018; Zhang et al., 2022) . Considering the central role of MDA5 and LGP2 in HDV sensing, in addition to HepaRG^{NTCP} NT cells, HepaRG^{NTCP} MDA5 or LGP2 KO cells were used.

Before proceeding with the innate immunity study using HepaRG^{NTCP}NT and HepaRG^{NTCP} MDA5 or LGP2 KO, the PRR KO efficiency upon IFN α stimulation was assessed. Cells were treated with 200 IU/mL of IFN α 2A for 24 hours and harvested for lysis and RT-qPCR analysis of MDA5 and LGP2 mRNA levels. Even upon IFN α stimulation, MDA5 and LGP2 expression remained lower in HepaRG^{NTCP} MDA5 and HepaRG^{NTCP} LGP2KO cells, respectively, when compared to HepaRG^{NTCP}NT cells (Figure 3.23). In unstimulated HepaRG^{NTCP} MDA5 KO cells, a KO of 97% was achieved, while for HepaRG^{NTCP} LGP2KO, the KO level reached 35%.

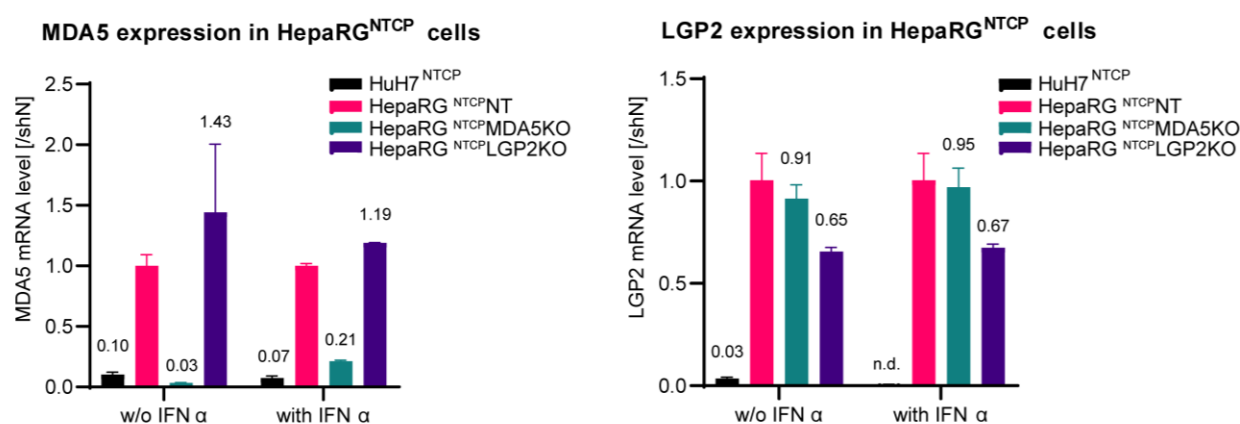


Figure 3.23. Confirmation of MDA5 and LGP2 KO level in HepaRG^{NTCP}NT. Efficiency of MDA5 and LGP2 KO in HepaRG^{NTCP} NT, MDA5 or LGP2 KO and expression of MDA5 upon IFN α 2A stimulation was evaluated on mRNA level. Results were normalized on values obtained from HepaRG^{NTCP} NT.

3.3.1 Infected HepaRG^{NTCP} cells support WoDV and DeDV replication

Viral stocks of HDV, WoDV, and DeDV were titrated by using the TCID₅₀ methodology (Figure 3.21). HuH7^{NTCP}, HepaRG^{NTCP} NT, and HepaRG^{NTCP} MDA5 or LGP2 KO were mono-infected with HDV, WoDV, or DeDV, and either fixed at day 6 pi for Ag visualization or harvest for intracellular viral RNA quantification via RT-qPCR on day 3 or 6 pi (Figure 3.24A). In all cell lines tested, HDV and HDV-like agents were able to establish replication, as indicated by the increase of intracellular viral RNA from day 3 to day 6 pi (Figure 3.24B) and by % of positive cells visualized via IF at day 6 pi (Figure 3.24C).

Notably, the infection rate was comparable among agents and cell lines.

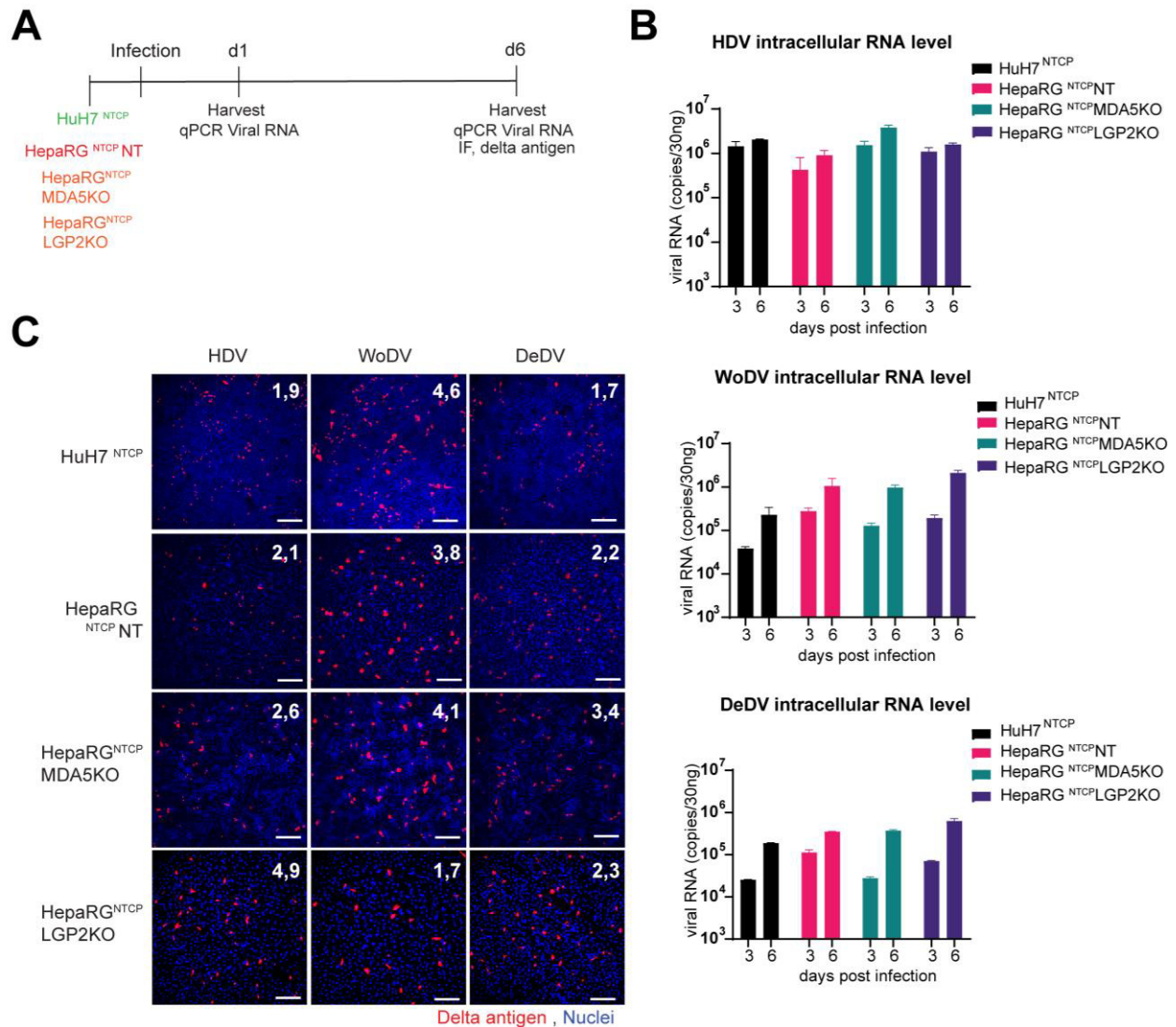


Figure 3.24. Quantification of intracellular viral RNA and % of DAg-positive cells upon infection. *Huh7^{NTCP}*, *HepaRG^{NTCP} NT*, and *HepaRG^{NTCP} MDA5* or *LGP2* KO cells were infected with HDV and HDV-like agents and harvested at days 3 and 6 pi for viral RNA detection via RT-qPCR (A&B). In parallel, DAg-positive cells were visualized via IF after FD3A7 antibody staining at day 6 post-infection (C). Viral RNA was quantified along a plasmid standard and is displayed in reference to BLV treatment conditions. Values are shown as mean \pm SEM. The % of delta antigen-positive cells was calculated using Ilastik software. Scale bar: 200 μ m.

Considering the successful establishment of viral replication upon HDV-like agents infection, the next step was to evaluate the upregulation of differential ISGs in infected cells.

3.3.2 ISGs induction upon WoDV and DeDV infection is lower compared to HDV

Since IF staining and RT-qPCR showed similar infection rates across agents and cell lines, the innate immune response upon HDV-like agents was evaluated. Among all the ISGs tested, the expression of RSAD2 was chosen as representative, considering the high level of upregulation of this gene in the context of HDV infection (Lucifora et al., 2023; Zhang et al., 2018). RSAD2 mRNA was measured in Huh7^{NTCP}, HepaRG^{NTCP} NT, and HepaRG^{NTCP} MDA5 or LGP2 KO upon mono-infection with HDV, WoDV, or DeDV at 3 and 6 pi. In parallel, cells were also infected in the presence of BLV, which blocks viral entry, providing a background threshold. As anticipated, neither HDV nor HDV-like agents elicited ISG expression in Huh7^{NTCP} due to IFN production deficiency. However, in HepaRG^{NTCP} NT cells, which are IFN-competent, it is known that HDV triggers MDA5/LGP2-mediated RSAD2 induction expression (Zhang et al., 2018; Zhang et al., 2022). Strikingly, here WoDV and DeDV caused only a minor RSAD2 induction, with no significant difference between HepaRG^{NTCP}NT and HepaRG^{NTCP} MDA5 or LGP2 KO cells (Figure 3.25). Only a minor increase in RSAD2 was observed for DeDV at day 6 pi, indicating striking differences in ISG induction compared to HDV.

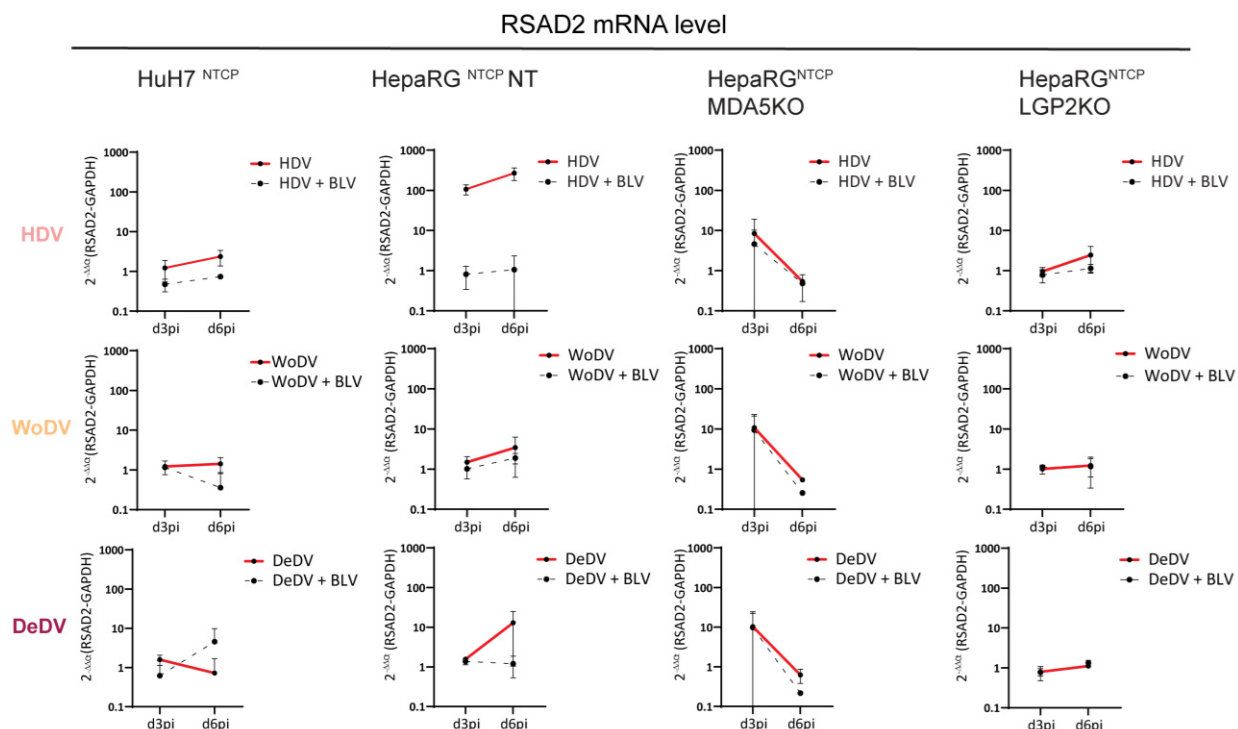


Figure 3.25. HDV-like agents induce a mild ISGs upregulation in HepaRG^{NTCP} cells. Huh7^{NTCP}, HepaRG^{NTCP} NT, and HepaRG^{NTCP} MDA5 or LGP2 KO were infected in the absence or presence of BLV. Copy numbers of RSAD2 mRNAs at day 3 and 6 pi were quantified using RT-qPCR. Data were normalized to GAPDH and displayed as fold change to uninfected condition. Values are shown as mean \pm SEM.

To confirm results from bulk ISGs measurement, ISGs upregulation was evaluated via IF analysis. To this goal, virus-induced IFN stimulation was assessed by IF staining of Mx1, one of the most upregulated ISGs upon HDV infection (Zhang et al., 2018). Considering the late induction observed in DeDV-infected HepaRG^{NTCP} NT, d9 pi was introduced as an additional time point. HepaRG^{NTCP} NT were infected with HDV, WoDV, or DeDV and fixed at day 3, 6 or 9 pi for IF staining of DAG and Mx1. As a control of the specificity of the Mx1 induction signal, HepaRG^{NTCP} MDA5KO were also infected and stained (Figure 3.26A).

Viral DAGs were detected from day 3 onwards in both HepaRG^{NTCP} NT and HepaRG MDA5KO (Figure 3.26B). Interestingly, although good infection was established for WoDV and DeDV, Mx1 expression was detectable only for HDV infected- HepaRG^{NTCP} NT cells, reaching a peak at day 6 pi. Mx1 upregulation was observed in DeDV-infected cells at d9

pi, although the signal was weak when compared to the induction observed during HDV infection.

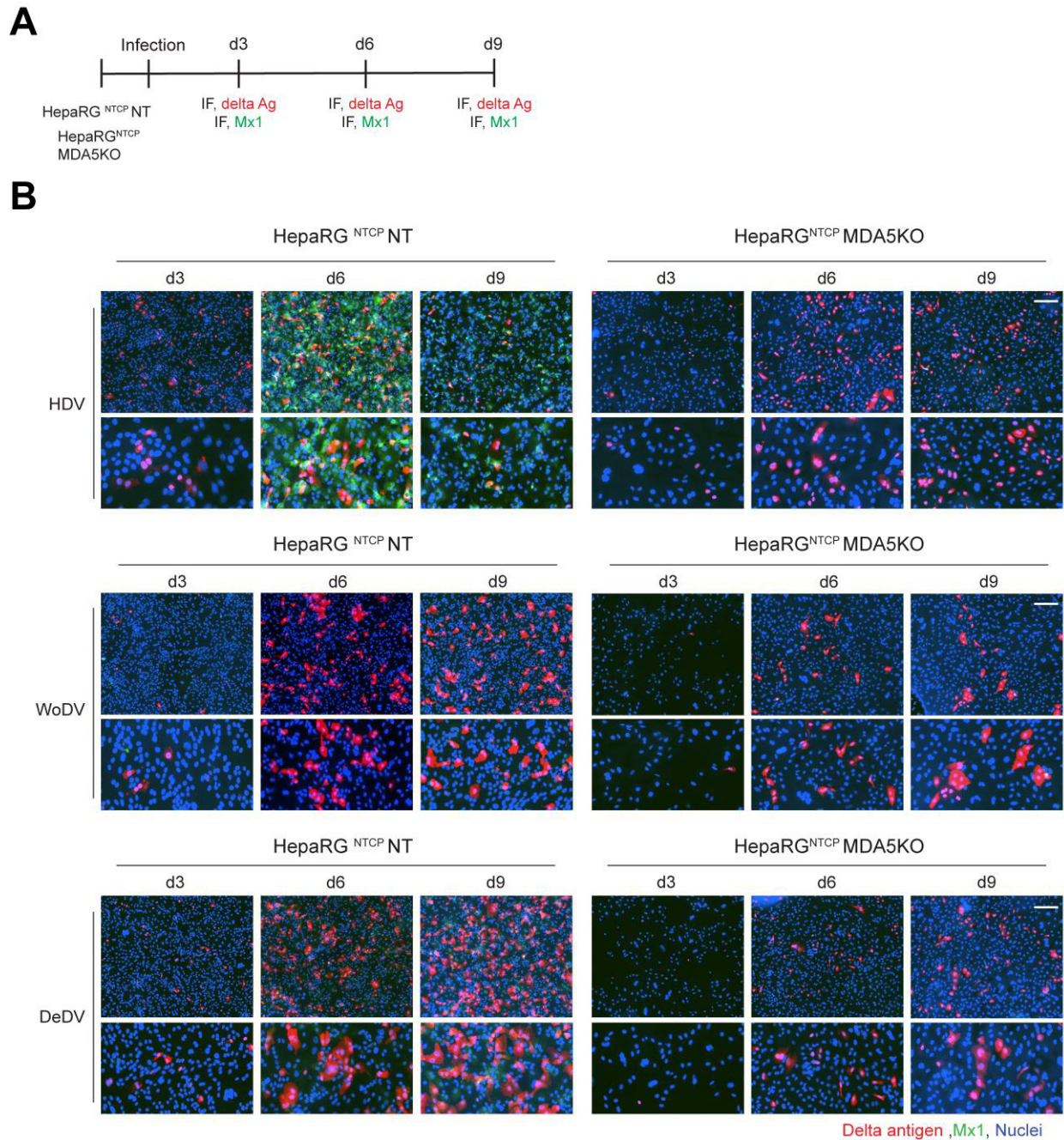


Figure 3.26. HDV, but not WoDV and DeDV infection efficiently activates Mx1 expression in HepaRG^{NTCP} cells. HepaRG^{NTCP} and HepaRG^{NTCP} MDA5KO cells were infected with HDV, WoDV, or DeDV (A). On day 3, d6 or d9 pi, infection efficiency was analyzed by IF detecting DAG and activation of the IFN response was

determined by IF detecting Mx1 (B). Scale bars: 200 μ m. Lower panels show zoom-in sections of the FOV above.

These results confirmed the bulk measurement where DeDV induced a later and lower ISGs induction when compared to HDV. As a result of limited innate immunity stimulation, WoDV and DeDV infection rates still increased at day 9 pi, while HDV reached a plateau at day 6 pi, suggesting an active counteraction of innate immunity by HDV but not by WoDV and DeDV replication.

Considering the lack of profound innate immunity stimulation upon WoDV and DeDV infection, I evaluated the impact of this phenotype in the context of CDMS.

3.3.3 WoDV and DeDV can spread via cell division in HepaRG^{NTCP} cells

To examine the impact of reduced ISGs induction on CDMS, innate immune competent cells were infected with either HDV, WoDV, or DeDV, and on day 6 pi cells were split at 1:50 dilution factor to allow cell division. When confluence was reached, cells were fixed and stained for DAg visualization (Figure 3.27A)

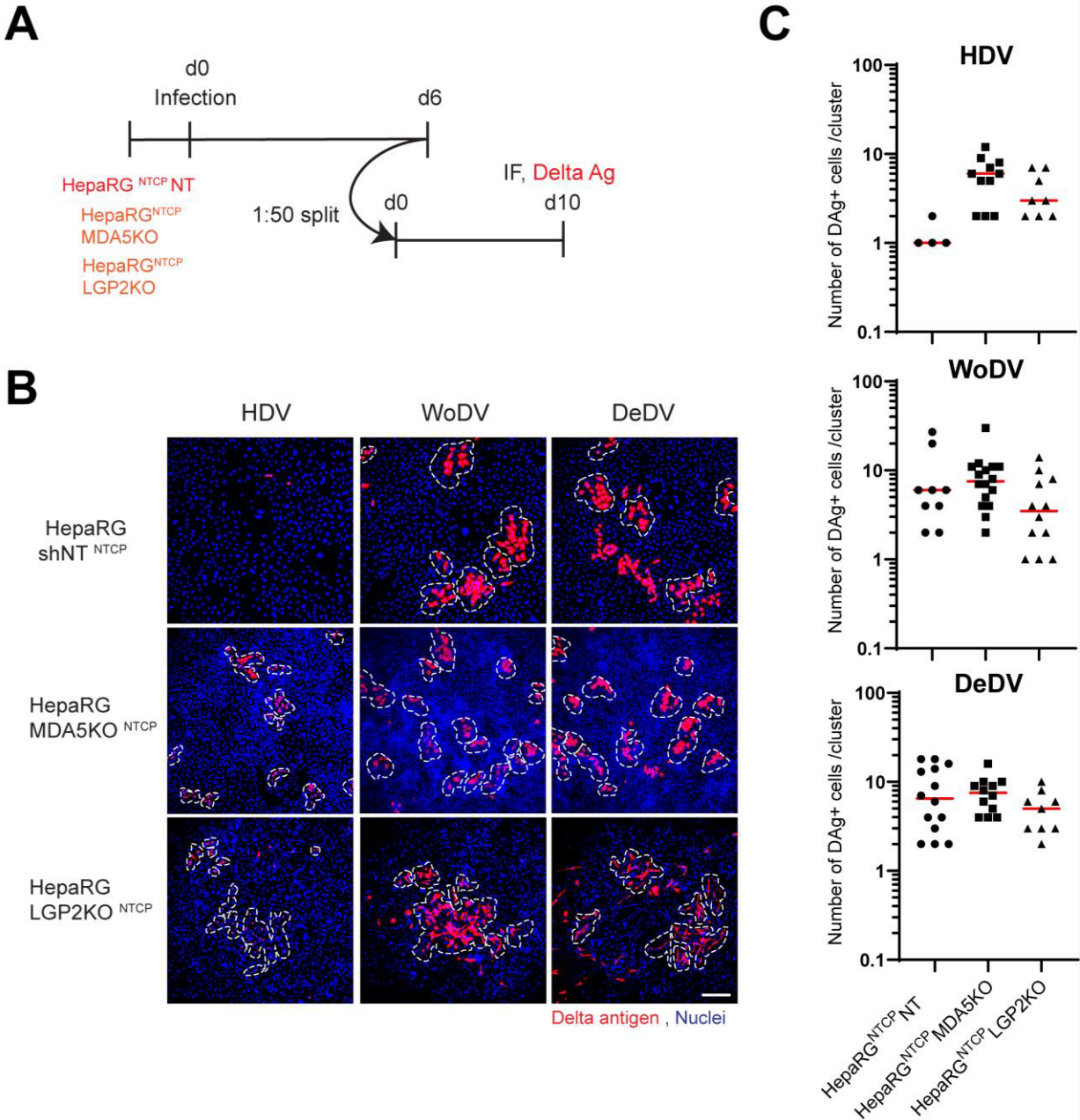


Figure 3.27. HepaRG^{NTCP} NT cells allow WoDV and DeDV to spread via cell division. Innate immune competent HepaRG^{NTCP} NT and MDA5 or LGP2 KO cells were infected, and after 6 days, cells were split at 1:50 dilution factor to allow clonal expansion (A). At confluence, cells were fixed, and clusters of infected cells were visualized by IF staining of DAAG (B) and quantified using Cell Profiler (C). Scale bar: 200 μ m.

As predicted, HDV replication induced IFN activation in HepaRG^{NTCP} NT but not MDA5 KO or LGP2 KO cells. Consequently, only HepaRG^{NTCP} NT showed restriction of CDMS (Figure

3.27B). In contrast, WoDV and DeDV CDMS remained efficient in HepaRG^{NTCP} cells and independently of LGP2 or MDA5 expression (Figure 3.27B). The persistence of WoDV and DeDV via cell division in innate immune competent cells might be due to the lack of ISGs induction upon these DLAs infection. To test this hypothesis, CDMS of WoDV and DeDV was further evaluated under exogenous IFN treatment conditions.

3.3.4 Interferon treatment does not inhibit cell division-mediated spread of WoDV and DeDV in HuH7^{NTCP} cells

The CDMS of the human HDV is sensitive not only to viral replication-induced IFN responses but also to IFN treatment (Zhang et al., 2022). Therefore, the impact of exogenous IFN treatment on CDMS of WoDV and DeDV was investigated. HuH7^{NTCP} cells were infected, and on day 5 pi, cells were split (dil.1:100), and IFN-alpha (IFN α 2A) was added to the culture medium (Figure 3.28A). 5 days post-splitting, clusters of DAg positive cells were visualized via IF staining. While the human HDV completely lost the capability to persist after cell division, WoDV and DeDV DAg were still detectable in clusters of DAg-positive cells after splitting (Figure 3.28B&C). This indicated that the CDMS of WoDV and DeDV was not significantly affected by exogenous IFN treatment. To determine if these DLAs had an active role in repressing innate immunity upregulation in infected cells, a co-staining of the DAg and Mx1 gene was performed (Figure 3.28D). In contrast to the human HDV, CDMS of WoDV and DeDV was still strong even with high Mx1 expression at the single cell level, not affecting the antiviral state within the cell (Figure 3.28E).

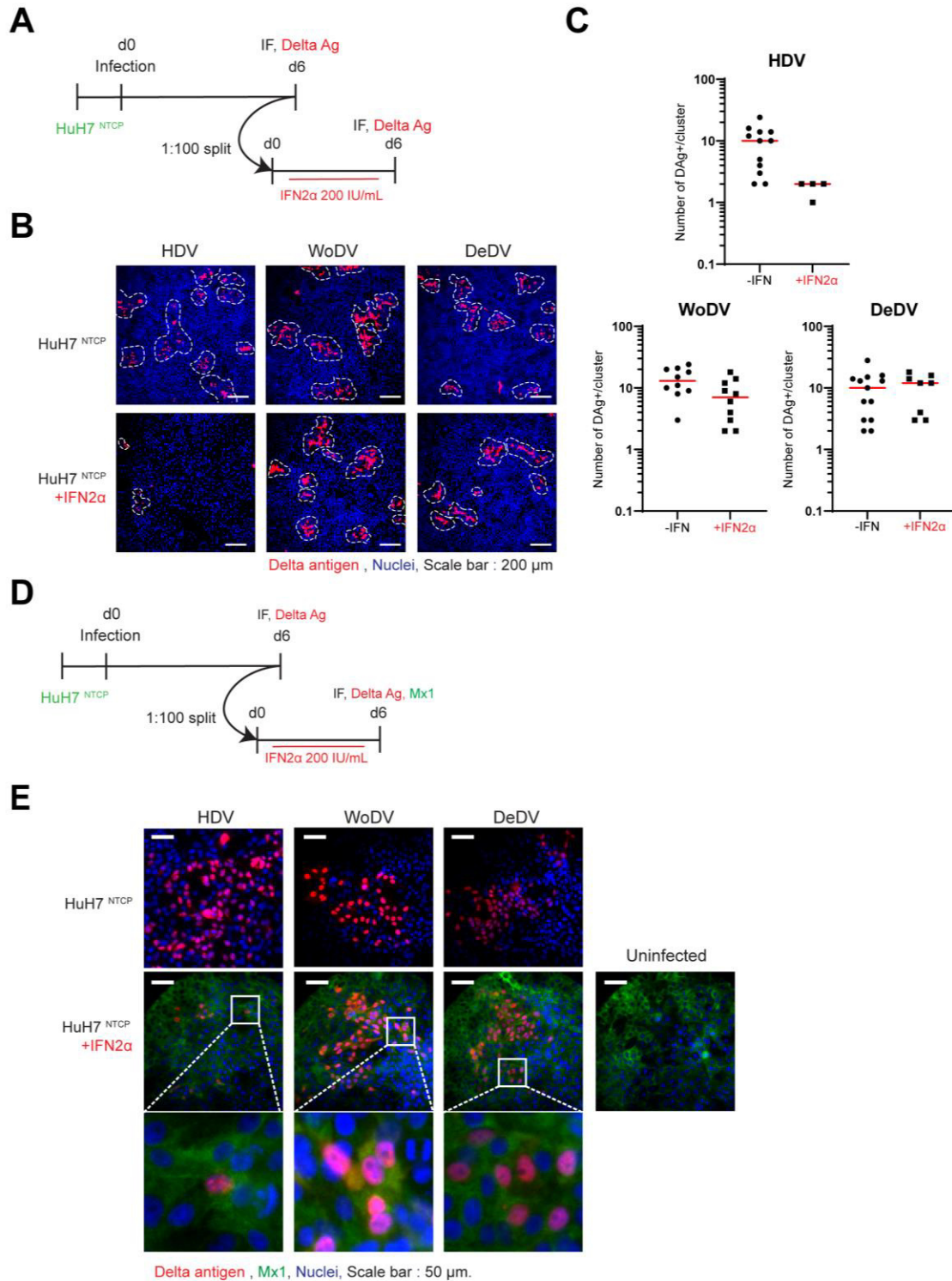


Figure 3.28. *IFN treatment does not inhibit the cell division-mediated spread of WoDV and DeDV in infected HuH7^{NTCP} cells.* HuH7^{NTCP} cells were infected with HDV, WoDV, and DeDV and passaged (1:100 dilution) at day 5 pi (A). Cells were then treated with 200 U/ml of IFN- α 2A for 5 days, and DA α -positive cells

were visualized by IF staining (B) and quantified using Cell profiler (C). Scale bar: 200 μ m. Infected HuH7^{NCT} cells were treated with 200 U/ml of IFN- α 2A during a clonal expansion (D). 5 days post-splitting, cells were stained for DAg and Mx1 visualization (E). Scale bar: 50 μ m.

Taken together, these results indicated that both WoDV and DeDV HDV-like agents lack a strong IFN activation, and their spread was not significantly affected by IFN α treatment.

Next, the potential mechanisms behind the decrease in IFN sensitivity of WoDV and DeDV CDMS was examined, starting from the potential role of L-HDAg expression in IFN-induced replication inhibition.

3.3.5 The role of L-HDAg expression in HDV interferon sensitivity

The ADAR1 enzyme, which is responsible for HDV antigenome editing and L-HDAg expression, exists in two isoforms: the short isoform (ADAR1-S, 110kDa) localizes only in the nucleus, and the large isoform (ADAR1-L, 150kDa) can be found both in the nucleus and cytoplasm and its activation is IFN dependent (Savva et al., 2012). Hartwig *et. al* demonstrated that the activity of the IFN-induced ADAR1-L isoform could enhance the editing of the S-HDAg into L-HDAg, leading to the consequential reduction of HDV replication (Hartwig et al., 2004; Hartwig et al., 2006). Given that human L-HDAg has a role in viral replication and its connection to IFN induction, I sought to investigate the role of artificial L-HDAg expression on the impact of IFN signaling on WoDV and DeDV replication. To achieve this aim, I utilized a hepatoma cell line, HuH7, expressing L-HDAg under the Tet-off system (HuH7tTA L-HDAg). The intracellular L-HDAg expression is initiated by removing Doxycycline from the culture medium (Figure 3.29A). HuH7tTA L-HDAg cells were transfected with HDV and HDV-like agent constructs. After 6 days post-transfection, cells were either harvested for lysis and RT-qPCR analysis or split at a high dilution factor (1:50). During cell division, cells were treated with IFN α , with or without Doxycycline in the culture media (Figure 3.29B) until confluence was reached (7 days post-split-7dps).

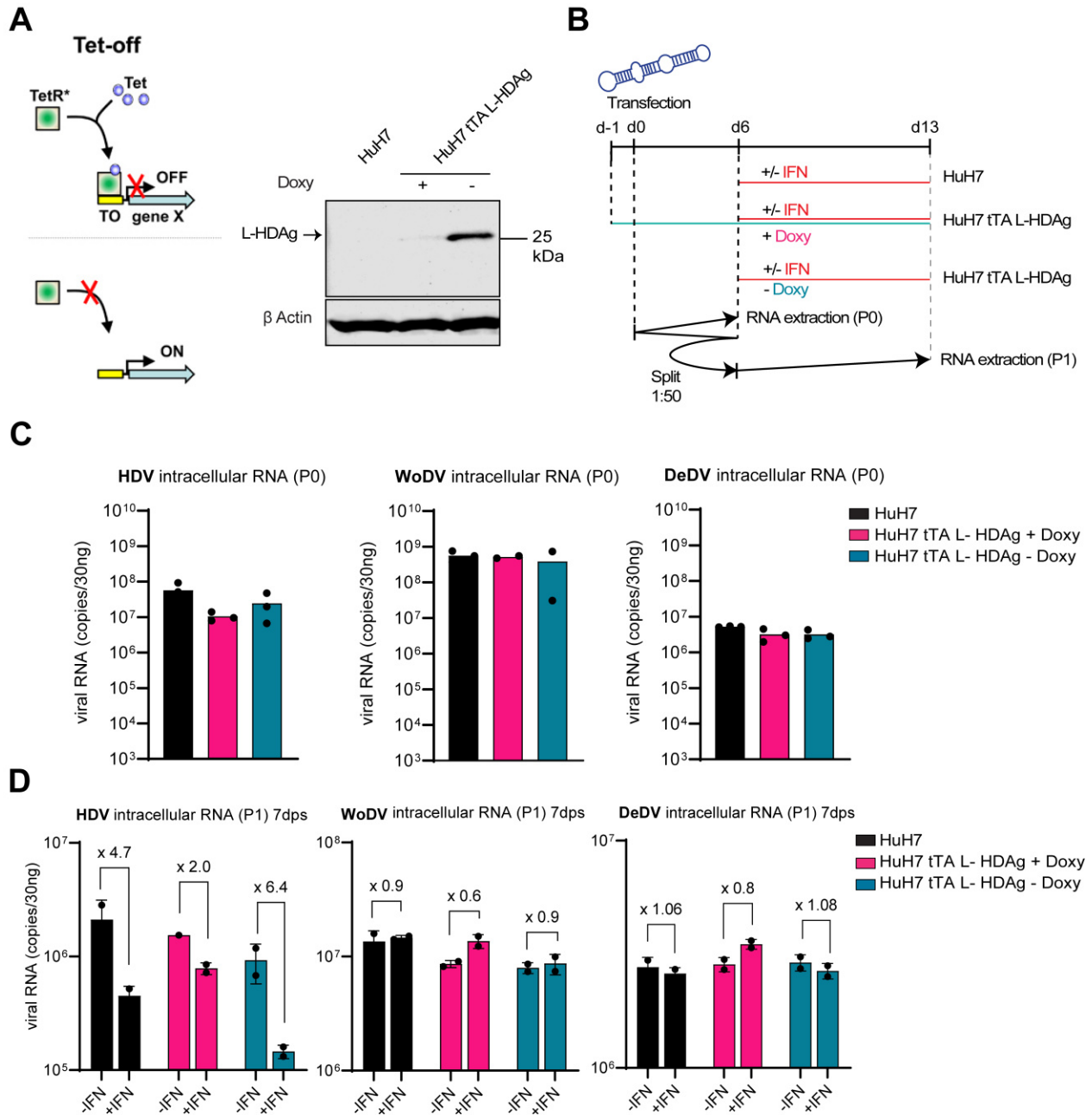


Figure 3.29. WoDV and DeDV sensitivity to IFN in the presence of artificial L-HDAg expression. Schematic representation of the Tet-off system, which allows the inducible expression of L-HDAg when doxycycline is removed from the culture medium, as shown in WB where L-HDAg is expressed in HuH7tTA L-HDAg cells only in absence of Doxycycline (A). HuH7tTA L-HDAg were transfected with HDV, WoDV and DeDV antigenomes and, 6 days post-transfection were split with a dilution factor of 1:50 (B). Split cells were treated with IFN α 2A and kept in culture with or without Doxycycline in the culture medium. Intracellular viral RNA was measured via RT-qPCR, 6 days post-transfection (C) or 7 days post-split (D).

For HDV and HDV-like agents tested, the induced expression of L-HDAg did not result in replication inhibition (Figure 3.29C), confirming my previous data that L-HDAg did not significantly impact viral replication when trans-complemented (Figure 3.19). With an initial comparable RNA level among different conditions, the effect of IFN treatment on WoDV and DeDV replication was evaluated. RNA replication of HDV decreased during IFN treatment, regardless of artificial L-HDAg expression (Figure 3.29D). Notably, WoDV and DeDV did not exhibit inhibition upon treatment with IFN, or upon artificial expression of L-HDAg (Figure 3.29D).

These results suggested that L-HDAg did not play a significant role in WoDV and DeDV susceptibility to IFN. I then pursued a cloning approach to confirm this finding and further assess the impact of the absence of L-HDAg on the immune sensitivity of HDV.

3.3.5.1 *The sensitivity to interferon of the human HDV is not conferred by the emergence of L-HDAg*

Considering the inhibitory effect of L-HDAg on HDV replication and its connection to IFN induction, the next step was to determine whether the absence of L-HDAg was the primary factor contributing to HDV sensitivity to IFN. A human HDV mutant was created containing a double UAA stop codon at the end of the S-HDAg ORF, with abolished expression of L-HDAg (Figure 3.30A). Analysis of transfected cells via WB and IF revealed a clear HDV 2xUAA mutant phenotype, in which no L-HDAg expression was detected (Figure 3.30B&C). In order to study innate immunity induction, infectious particles were generated via packaging of HDV2xUAA by HBsAg and L-HDAg trans-complementation (Figure 3.30D), as performed for WoDV and DeDV. To assess the infectivity of HDV 2xUAA pseudo particles, HuH7^{NTCP} cells were infected. Similar to what was observed for WoDV and DeDV, the production of infectious particles was facilitated by L-HDAg trans complementation during virus production (Figure 3.30E). Interestingly, the use of HDV 2xUAA mutant led to a substantial increase in HDAg-positive cells compared to HDV WT, confirming the

inhibitory effect of L-HDAg expression on HDV replication (Modahl & Lai, 2000; Sato et al., 2004).

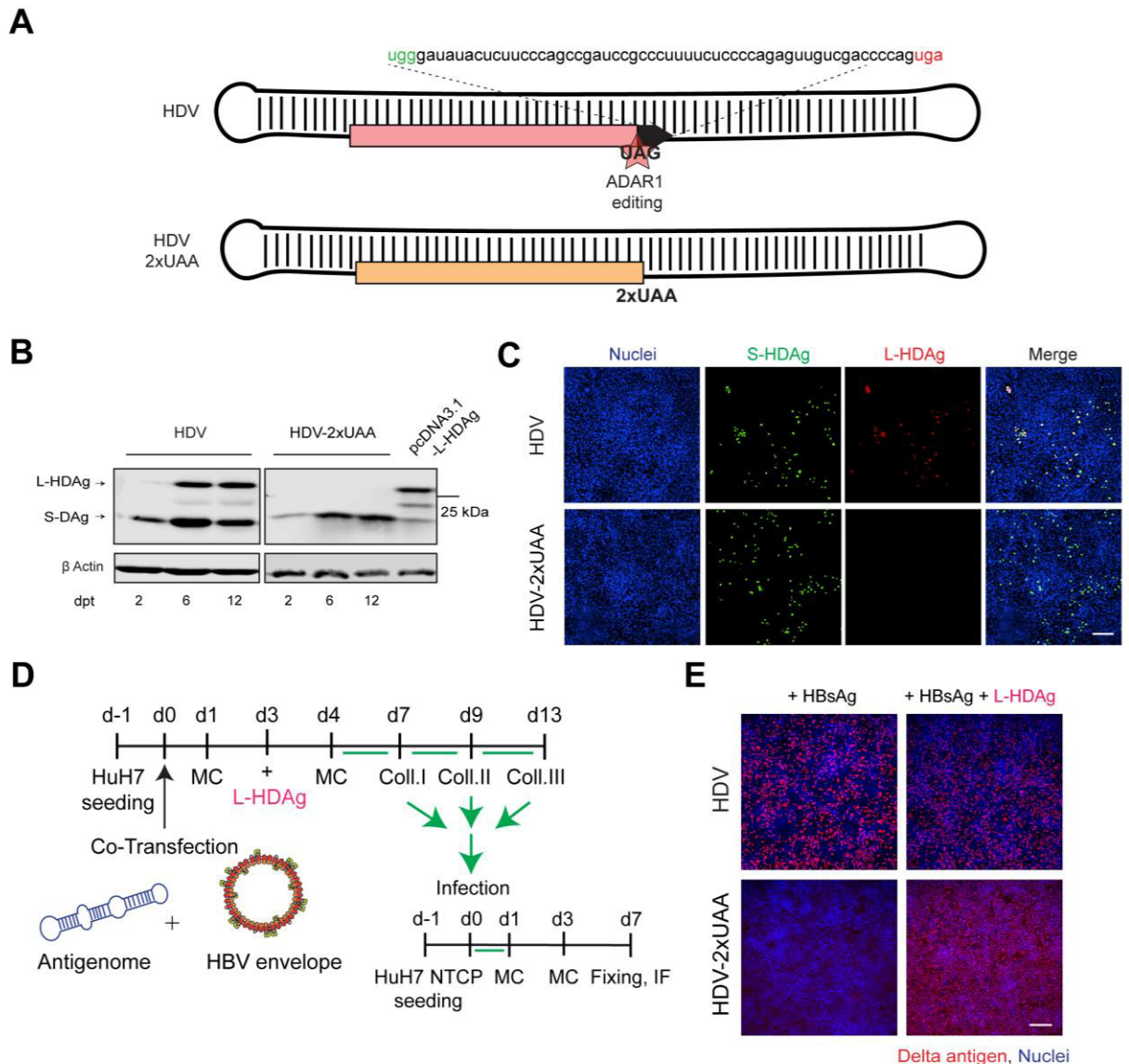


Figure 3.30. Characterization of HDV L-HDAg deficient mutant and packaging by HBV envelope proteins. (A) Schematic representation of HDV 2xUAA genome and absence of ADAR1 editing site, resulting in the lack of L-HDAg expression. HuH7 cells were transfected with HDV WT and HDV 2xUAA antigenome constructs, and after 2, 6- and 12-days, antigen expression was evaluated via WB (B). Transfected cells were also fixed 7 days post-transfection and staining using antibodies against S- and L-HDAg (C). HDV WT and HDV 2UAA antigenome constructs were transfected with an HBsAg plasmid with or without L-HDAg trans-complementation (D). Supernatant from transfection was collected and, after PEG

precipitation, was used to infect HuH7^{NTCP} cells. After 7 days, cells were fixed and stained for D-Ag visualization (E). Scale bar: 200 μ m.

Replication and CDMS of the HDV 2xUAA mutant were tested in innate immune-incompetent (HuH7^{NTCP}) and innate immune-competent (HepaRG^{NTCP}NT) hepatoma cells (Figure 3.31A). The infection rate between HDV WT and HDV 2xUAA appeared comparable, as indicated by IF staining of infected cells, on day 6 pi (Figure 3.31B). CDMAA showed that HDV WT and HDV 2xUAA propagated effectively through cell division in HuH7^{NTCP} due to the lack of innate immunity induction (Figure 3.31C left panel). In HepaRG^{NTCP}NT cells, a substantial reduction in CDMS for HDV WT was observed (Figure 3.30C-right panel). Notably, CMDS of HDV 2xUAA mutant seemed not resistant to virus-induced IFN, as indicated by single DAg-positive cells and lack of cluster formation in both dilution factors.

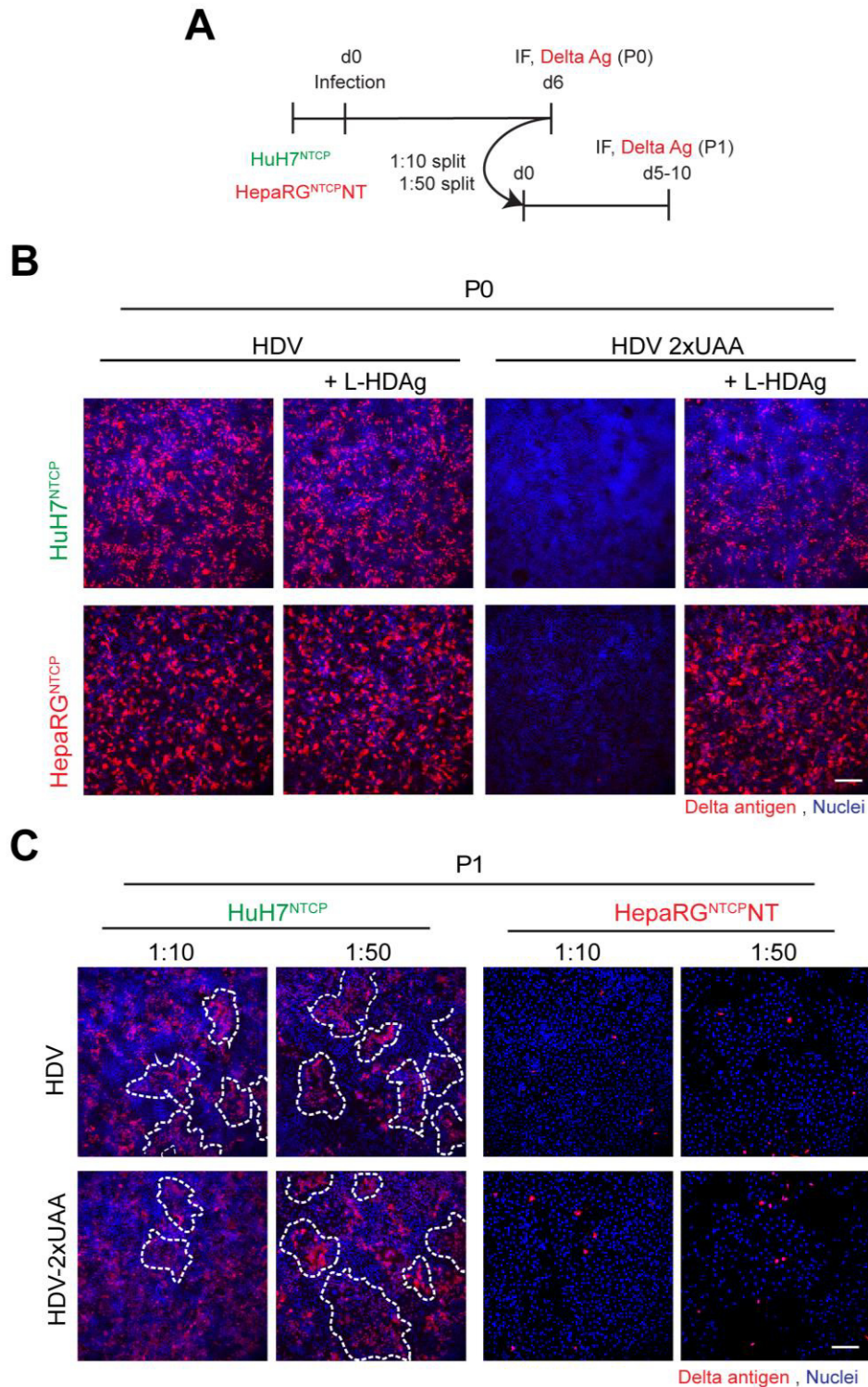


Figure 3.31. HDV interferon sensitivity is not conferred by L-HDAg expression. PEG precipitated virus was used to infect HuH7-NTCP and HepaRG^{NTCP}NT cells (A), and after 5 days, cells were fixed and stained for D- Ag visualization (B). In parallel, infected cells were split (1:10 or 1:50 dilution factor), and after 5 days delta antigen-positive cells were visualized by IF staining of Dag (C). Scale bar: 200 μ m.

These findings suggest that the sensitivity of human HDV to IFN stimulation is not reliant on the emergence of the L-HDAg.

Given the lack of IFN sensitivity of WoDV and DeDV in the presence of L-HDAg and the inhibition of CMDS for HDV L-HDAg deficient mutant, other viral factors that could facilitate IFN resistance were evaluated.

3.3.6 The predominant nuclear localization of HDAg is not conserved among WoDV and DeDV

The S-HDAg of the human HDV is localizing predominantly in the nuclei of transfected and infected cells (Alves et al., 2008; Chang et al., 1992; Chou et al., 1998; Tavanez et al., 2002). In contrast, transfection and infection experiments show ubiquitous WoDV and DeDV Ag localization within the cell, suggesting possible differences in replication strategies between HDV and DLAs. To achieve a more representative and intuitive image of Ag distribution within cells, HepaRG^{NTCP}NT cells were infected with HDV, WoDV, and DeDV. 6 days pi, cells were fixed and stained using FD3A7 antibody to visualize DAg together with an antibody directed against *wheat germ agglutinin* (WGA), to define membrane rims (Figure 3.32).

HDAg localized in the nuclei of infected cells, as indicated by co-localization with Hoechst staining (Figure 3.32A&B). Interestingly, WoDV and DeDV DAg localized in both nuclei and cytoplasm, having a more diffuse subcellular localization. Interestingly, DeDAg was even observed to have a predominant localization in the cytoplasm of infected cells (DeDVAg FOV2).

Considering the role of S-HDAg in HDV replication, this phenotype might indicate a different RNA replication mechanism adopted by DLAs, that could circumvent innate immunity recognition and affect sensitivity to antiviral state. The potential implications of the different viral DAg localization are currently under investigation.

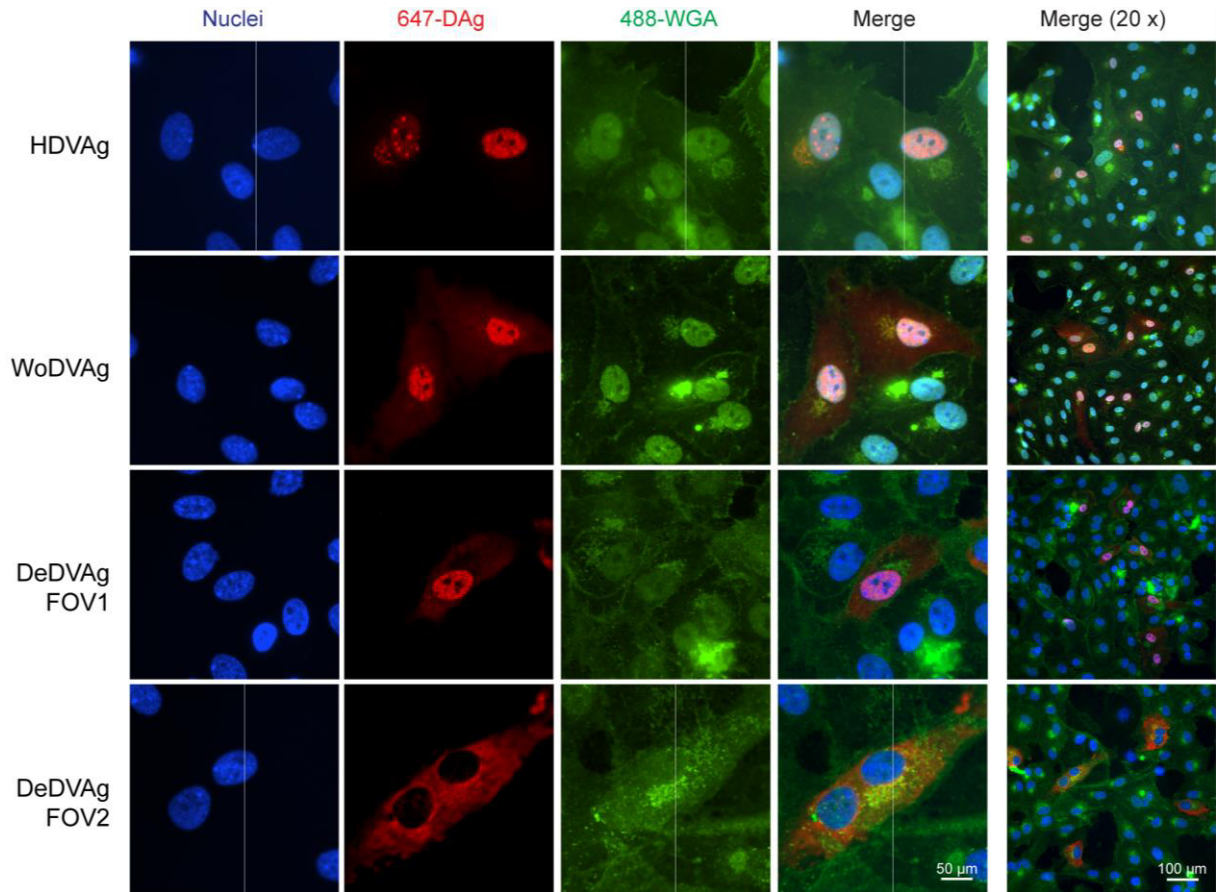


Figure 3.32. Subcellular localization of WoDV and DeDV in infected HepaRG^{NTCP}NT cells. HepaRG^{NTCP}NT cells were infected with HDV, WoDV, and DeDV pseudo particles and 6 days pi, cells were fixed and stained for DAG and wheat germ agglutinin (WGA) to define cellular rims (A). DAG signal was quantified and represented as a percentage of nuclear or extranuclear. Scale bar: 100 μm, with 20x magnification objective, 50 μm, zoom-in sections.

3.3.7 Study of Innate Immune Responses Upon Infection of Lung Carcinoma Epithelial Cells of HDV and HDV-Like Agents

Until now, the investigation of HDV replication has been primarily restricted to liver-derived cell lines (Heuschkel et al., 2021), limiting the availability of infection models. Nevertheless, with the identification of HDV-like agents and their putative expanded tissue and organ tropism, new non-hepato-derived infection cell culture models must be generated. To this purpose, the A549 lung carcinoma cell line was examined to further characterize the infection, replication, and induction of innate immunity in a novel cell culture model.

Pseudo particles with HBsAg as packaging protein were used for infection, requiring the generation of susceptible A549 cell lines through human NTCP transduction and subsequent expression validation. Immune-competent A549 cells were transduced with hNTCP to ensure susceptibility to HDV and HDV-like agents' pseudo particles. Additionally, A549 MDA5 KO transduction was carried out, considering the crucial role of MDA5 in HDV sensing and recognition. NTCP expression was validated via MyrB-Atto565 binding (Figure 3.33A). MyrB-Atto565 binding was blocked by pretreatment with unlabeled MyrB, suggesting specific binding of the labelled peptide to NTCP (Figure 3.33B). As a positive control for NTCP expression, a peptide binding assay was carried out using well-established HuH7^{NTCP} and HepaRG^{NTCP}NT cells. Atto565 magenta signal of bound peptide indicated a comparable NTCP expression level upon transduction between A549^{NTCP}WT and MDA5KO and the already established HuH7^{NTCP} and HepaRG^{NTCP}NT cells (Figure 3.33B).

After confirmation of the NTCP expression and membrane localization, A549^{NTCP} WT and MDA5KO were evaluated regarding susceptibility to viral infection and ISGs upregulation.

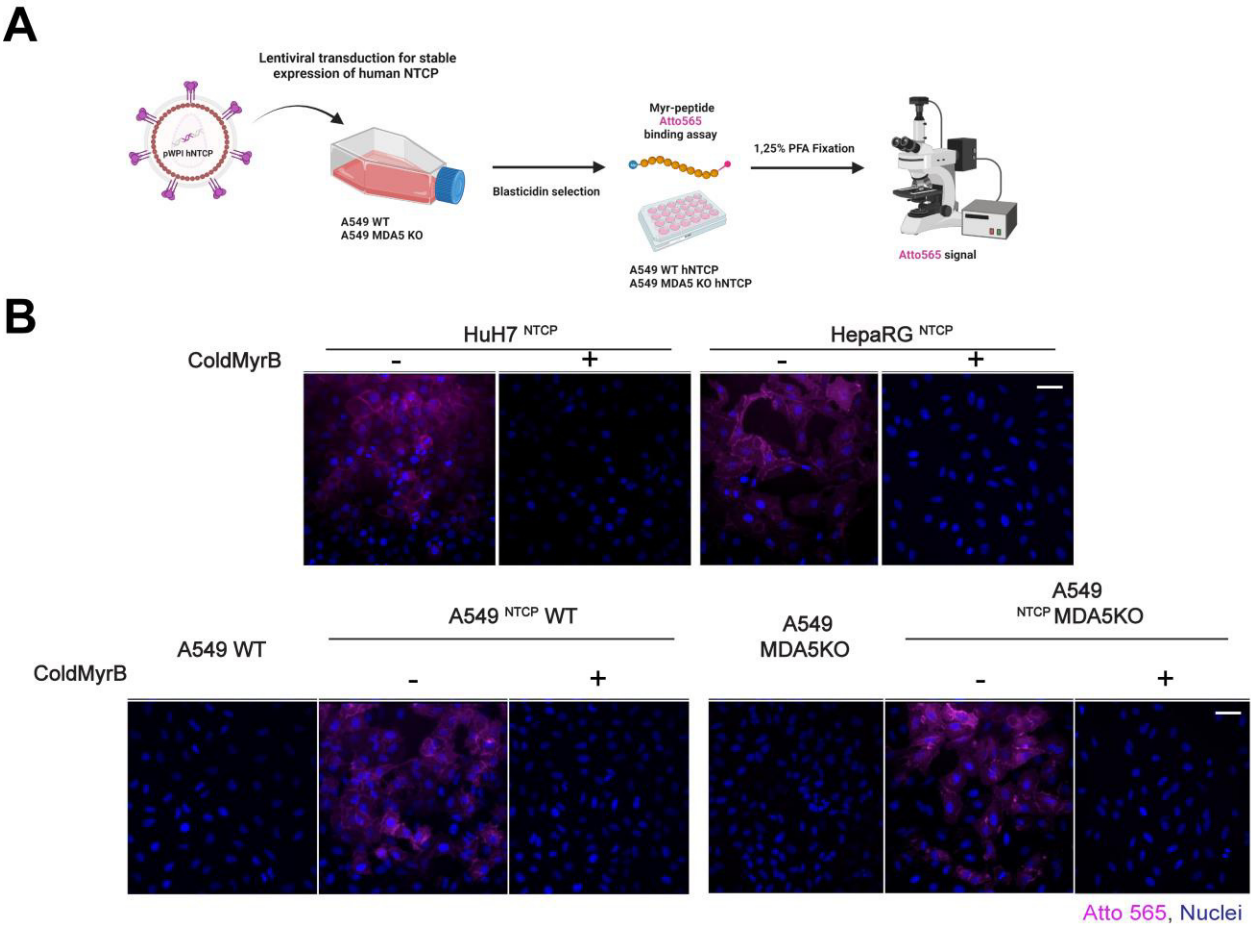


Figure 3.33. Validation of NTCP expression of newly generated cell lines. A549 WT and A549 MDA5 KO were transduced for human NTCP stable expression and selection with Blasticidin antibiotic (A). NTCP expression was validated via myristoylated peptide binding coupled with ATTO565 fluorescent dye. Cells were optionally pretreated with unlabeled MyrcludexB (cold MyrB), blocking the further binding of MyrB-ATTO565 staining and displaying specificity. ATTO565-hNTCP staining on commonly used cell lines, HuH7^{NTCP} and HepaRG^{NTCP}, compared to A549 and A549 MDA5 KO parental cell lines and newly generated A549^{NTCP} and A549^{NTCP} MDA5 KO (B). Scale bar: 200 μ m.

Next, the efficiency of MDA5 KO was evaluated. While MDA5 was present in A549^{NTCP} WT cells and could be increased by IFN α treatment, in A549^{NTCP} MDA5KO cells, the PRR expression was completely abolished (Figure 3.34A)

Newly generated A549^{NTCP} were mono-infected with HDV, WoDV, or DeDV and 6 dpi, DAg was visualized by IF (Figure 3.33B). In parallel, on days 1 and 6 pi, RNA was extracted to detect viral genomes via RT-qPCR (Figure 3.34C).

IF analysis revealed a lower infection rate for WoDV and DeDV compared to HDV (Figure 3.34B). However, the increase in viral RNA indicated the establishment of replication for all agents tested and in both cell lines (Figure 3.34C). Therefore, host responses to HDV and HDV-like agents infection were further evaluated by measuring the mRNA level of ISG15 and Mx1 ISGs.

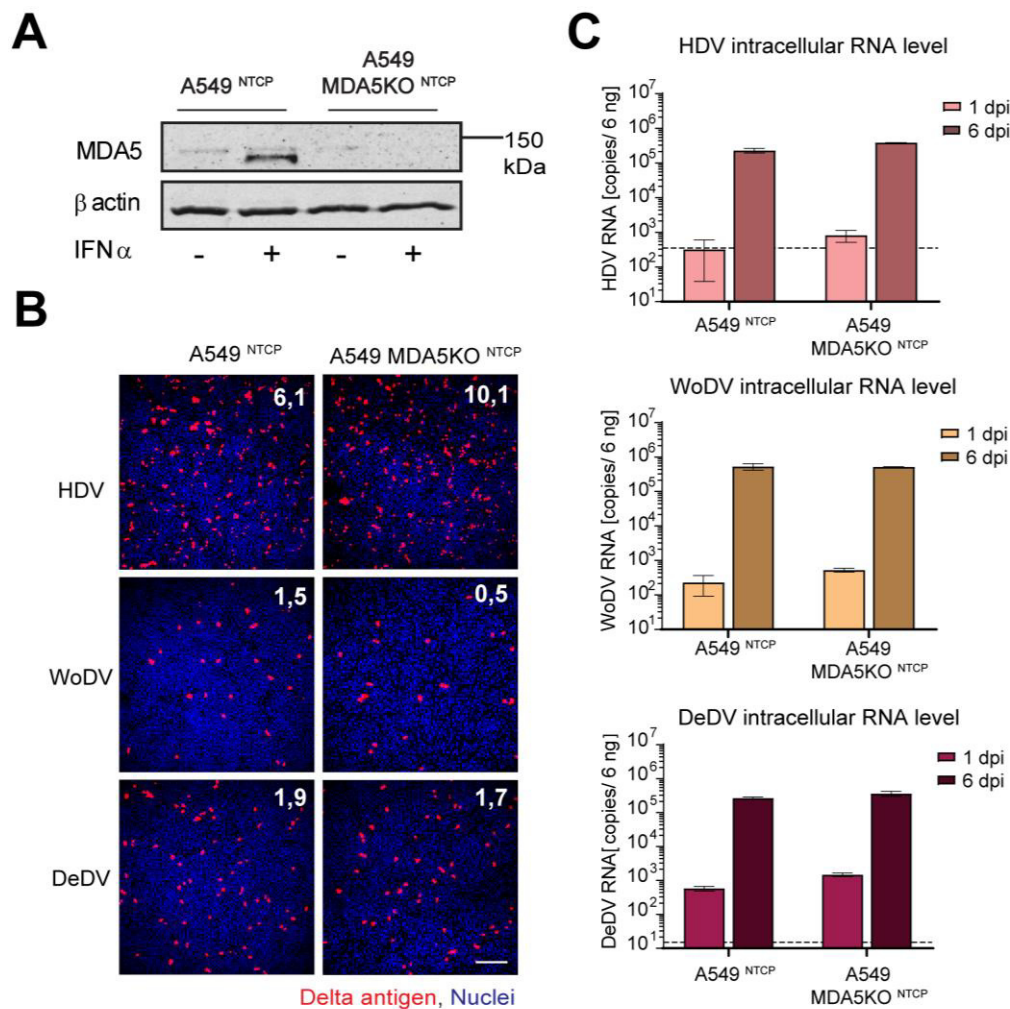


Figure 3.34. Quantification of intracellular viral RNA delta antigen-positive cells upon infection of A549^{NTCP}. MDA5 KO efficiency was assessed upon 24 hours of IFN α 2A treatment (A). DAg-positive cells were visualized via IF after FD3A7 staining at day 6 pi (B). Viral copy numbers in A549^{NTCP} WT and A549^{NTCP}

MDA5KO cell lines infected with HDV, WoDV, or DeDV were measured on 1 and 6 dpi by RT-qPCR. Viral RNA was quantified along a plasmid standard and is displayed in reference to uninfected conditions (C). Values are shown as mean \pm SD. Scale bar: 200 μ m.

A549^{NTCP} cells and HepaRG^{NTCP}NT cells were infected, and ISG induction was measured on days 1 and 6 pi. Interestingly, although the infection rate was comparable between HepaRG^{NTCP}NT and A549^{NTCP} WT cells (data not shown), HDV induced significantly less upregulation of Mx1 mRNA in A549 WT compared to HepaRG^{NTCP}NT (Figure 3.35A). Moreover, no ISG15 upregulation was observed in HDV-infected A549^{NTCP} WT cells, hinting that the innate immune sensing of HDV replication in A549 might differ from hepato-derived HepaRG^{NTCP}NT cells (Figure 3.35B).

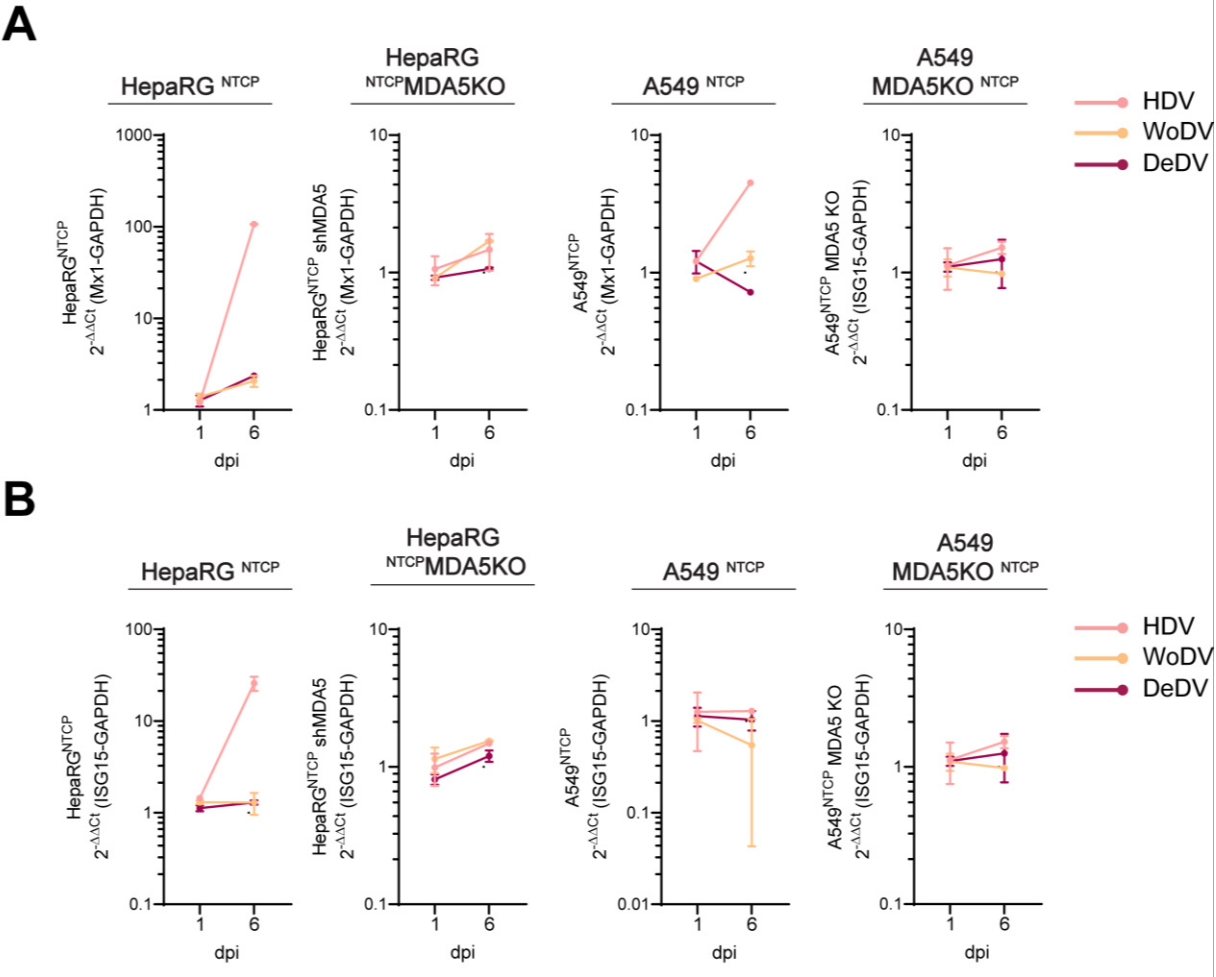


Figure 3.35. ISGs upregulation in infected A549^{NTCP} cells. Mx1 (A) and ISG15 (B) expression in HepaRG^{NTCP}NT and A549^{NTCP}WT and MDA5KO cell lines were measured on day 1 and 6 pi. Data are normalized to GAPDH and displayed as fold change to uninfected condition. Values are shown as mean \pm SD.

The next step was to evaluate CDMS by splitting infected cells and staining for DAg when cellular confluency was reached after clonal expansion (Figure 3.36A).

Despite transfection experiments showing a lack of cluster formation in A549 transfected cells, infected A549^{NTCP} cells allow the formation of DAg -positive clusters independently from MDA5 expression (Figure 3.36B). This phenotype was probably a direct consequence of a limited innate immunity stimulation upon HDV and HDV-like agents in A549 cells. Novel infection models are currently under development to better understand the dynamics of innate immune induction upon HDV and HDV-like agents in non-hepatic tissues.

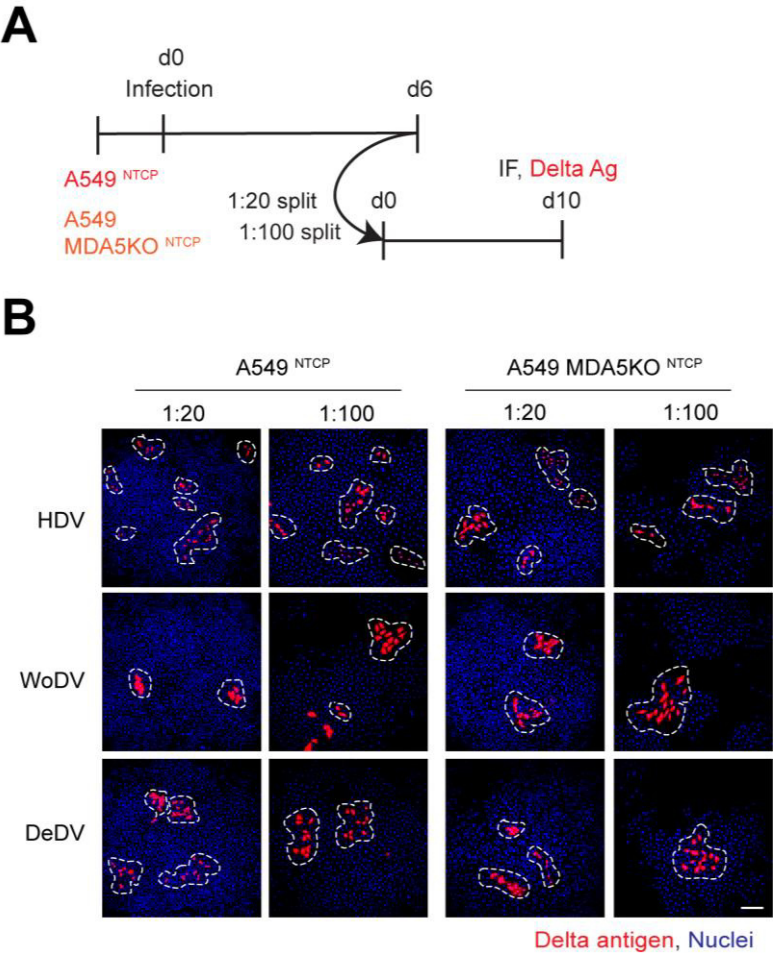


Figure 3.36. A549^{NTCP} cells allow a moderate WoDV and DeDV cell division mediated spread. Innate immune competent A549^{NTCP}WT or MDA5 KO cells were infected, and after 6 days, cells were split at 1:20 or 1:100 dilution factor to allow clonal expansion (A). At confluence, cells were fixed, and clusters of DAG-positive cells were visualized by IF staining of DAG (B). Scale bar: 200 μ m.

In summary, infection of innate immune competent cells revealed a reduced capacity of WoDV and DeDV to activate innate immune response with consequent lack of perturbation of cell division-mediated spread. Furthermore, the CDMS of WoDV and DeDV was not significantly affected by exogenous IFN treatment. Therefore, both agents not only lacked a strong IFN activation but also displayed resistance to IFN treatment. This data shed light on potential evolutionary differences between HDV and HDV-like agents in terms of activation and sensitivity to IFN response in human-derived cell lines.

4. DISCUSSION

The recent discovery of HDV-like agents in different vertebrate and invertebrate species provides the tools for a better understanding of how the human HDV evolved to be the pathogen that we know nowadays and its close relationship with its helper virus HBV.

4.1 HDV-like agents replication, host range, and tissue permissiveness

Due to the newness of the discovery of HDV-like agents, tools to investigate their replication in vitro and in vivo needed to be generated. Therefore, to identify viral markers, such as viral RNA and viral antigen, indicators of in vitro replication of HDV-like agents, were assessed via specific assays and techniques. DLAs found in woodchucks (WoDV), deer (DeDV), bats (BaDV), and various duck species (AvDV), showed distinct replication and spread rates, hinting at important genome differences reflecting distinct persistence outcomes. Knowing these differences provides an important tool for evaluating how virus variation affects viral and host survival and to understand virus-associated pathogenesis.

4.1.1 Function and conservation of delta antigen among HDV-like agents

Considering the novelty of HDV-like agents, tools needed to be established to investigate and comprehensively understand the replication capacity of infectious clones. Due to the amino acid diversity of various viral antigens, the commercial antibody FD3A7 directed against human S-HDAg was not optimal for all agents studied. Antigen expression analysis demonstrated elevated species cross-reactivity with viral antigens from mammalian HDV-like agents, namely WoDV, DeDV, and BaDV (Figure 3.2). This observation indicated a more conserved S-DAg sequence between HDV and other mammals DLAs, thus confirming the in-silico prediction data and alpha-fold prediction modeling (Figure 4.1).

FD3A7 antibody failed to detect AvDAg, likely due to the phylogenetic distance between AvDV and HDV. Additionally, the antibody developed for detecting AvDAg demonstrated high specificity, as no other DAg was detectable using this antibody (Figure 3.3). This constitutes essential information on the evolution and viral host adaptation. One could speculate that the replication might occur similarly, considering the extreme similarities between the antigens of HDV and HDV-like agents and their similar genome characteristics. The S-HDAg of HDV plays an important, yet not fully understood role, in viral RNA replication. It presents structural similarities to transcription factors and can undergo acetylation and methylation as other transcription regulatory proteins (Lee & Sheu, 2008; Mu et al., 2004; Payne et al., 1999).

Moreover, S-HDAg has been shown to bind RNA Pol II and enhance viral RNA transcription (Cao et al., 2009; Yamaguchi et al., 2001). For its function in RNA replication, S-HDAg must be phosphorylated. Specifically, phosphorylation of serine in position 177 of the S-HDAg is essential for viral replication, possibly enhancing the interaction between Pol II and HDV RNA (Chen et al., 2008; Mu et al., 2001; Mu et al., 1999). On this line, it is necessary to mention that serine 177 is conserved among the mammalian HDV-like agents tested (Figure 1.11 & 4.1A - indicated in position 179) but is lost in the AvDAg (Figure 1.11). This might indicate a different replication strategy adopted by this phylogenetically distant agent. Among the HDV-like agents tested, AvDV is the most phylogenetically distant from the human HDV. Upon AvDV cDNA transfection of human HuH7 cells, no efficient replication was established for this agent. This might indicate a specific adaptation to exploit avian-related host machinery for replication.

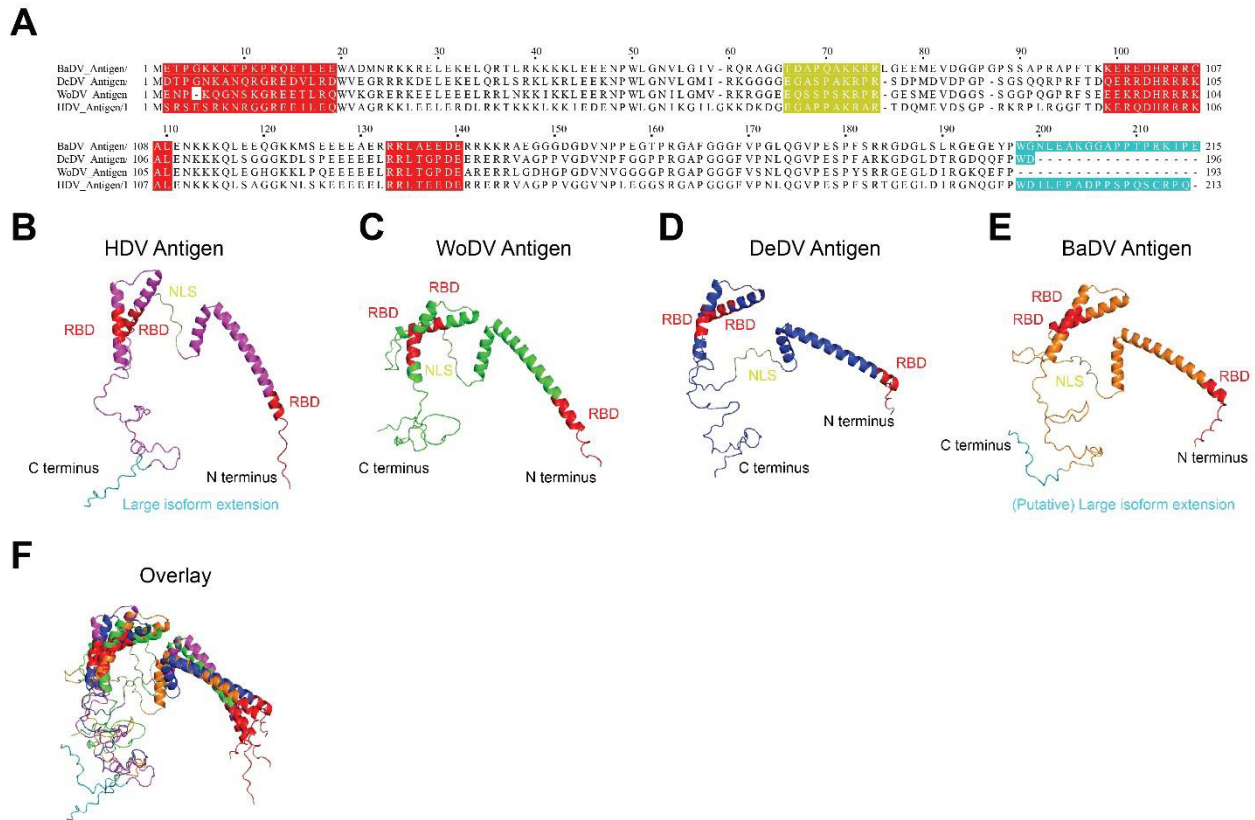


Figure 4.1. Comparison of HDV and HDV-like agents' antigens. (A) Alignment of the human HDV L-HDAg and the putative L-DAg sequences of the HDV-like agents. The translated genome of human HDV is compared with the putative L-DAg of newly discovered delta viruses. The translations of the L-DAg proteins were aligned using MUSCLE and visualized using Jalview. Highlighted in the alignment sequence are the RNA binding domains (RBD, red), the nuclear localization signal (NLS, smudge green) and putative large delta antigen extension (light blue) generated by ADAR1 editing of AUG stop codon present in HDV, DeDV and BaDV sequences. Prediction of the secondary structure of HDV (B), WoDV (C), DeDV (D) and BaDV (E) antigens and overlapping comparison (F) generated using Alpha Fold software.

4.1.2 HDV-like agents do not express a farnesylated large delta antigen during replication

Both *in silico* prediction data and *in vitro* investigations have shown that HDV-like agents share genome features with the human HDV, such as the ORF resembling S-HDAg, highly base-paired genomes and ribozyme sequences (Bergner et al., 2021; Chang et al., 2019; Szirovicza et al., 2022). However, HDV-like agents do not encode for a farnesylated L-DAg expression. L-HDAg, when farnesylated by cellular enzymes, ensures the packaging of the

human HDV RNP complex by HBsAg (Glenn et al., 1992; Lee et al., 1994; Sureau et al., 1993). After transfecting cDNAs of WoDV, DeDV, and BaDV into HuH7 cells, only the respective small delta antigens were expressed (Figure 3.5). This implied that the stop codons of the S-DAG ORFs cannot be edited by ADAR1, as observed in HDV.

Among the HDV-like agents tested, only DeDV and BaDV have a UAG stop codon at the end of its antigen ORF (Figure 3.6). If edited, it could lead to the extension of the S-DAG by 2 and 18 amino acids, respectively, but without a farnesylation signal present (Figure 1.11 & 4.1). However, replication and S-BaDAG expression were low in human hepatoma cell line (HuH7 cells). A low replication rate would not allow the expression of a putative large delta antigen, even if the genome sequence would permit it.

Additionally, the conservation level of ADAR1 among the host species and their respective expression levels has to be considered (Figure 3.7). Nevertheless, it is tempting to speculate that the genome of BaDV and other HDV-like agents tested, could be edited via alternative pathways (i.e., enzymes other than ADAR1) or a different editing site along the viral genome. It is already known how during translation of viral proteins a frame shift can occur (Loughran et al., 2011; Park & Hahn, 2021; Yan et al., 2023). This event takes place at specific locations in the nucleotide sequence known as frameshift sites. Here, some ribosomes translating the RNA will shift back or forward one nucleotide, causing them to start decoding a different reading frame. Meanwhile, the remaining ribosomes continue reading the original frame. This allows the same segment of an RNA molecule to be read in two different ways, producing two distinct protein molecules with different amino acid sequences. Although it is not yet clear why viruses use this ribosomal frameshifting, it has been observed that it could play a role in viral antibiotic resistance. (Park & Hahn, 2021). Moreover, this strategy can be extremely useful expectably in the context of viruses with a small genome, with a limited coding capacity. HDV and HDV-like agents would fall into this category.

4.1.3 *Envelopment-independent spreading pathways of HDV and HDV-like agent*

A cell division-mediated viral amplification assay demonstrated the capability of these HDV-like agents to amplify their genome via clonal expansion (Figure 3.10), indicating that this spreading pathway is evolutionarily conserved among the *Deltavirus* genus.

WoDV and DeDV might still be able to spread via cell division once infection is established and considering the lack of apparent association with a respective helper virus, this spreading pathway might have a critical role in the epidemiology and persistence of these agents. One could speculate that once host-to-host transmission occurred via undefined routes, HDV-like agents could amplify and persist via this pathway. This also highlights the importance of cell division-mediated spread not only for HDV persistence but for the whole viral family (Giersch et al., 2019; Zhang et al., 2018). The replication of HDV occurs via a rolling circle mechanism, which is also shared with plant-infecting viruses known as viroids. Similar to HDV, viroids have a small RNA genome, encoding for ribozyme sequences. All these common characteristics between HDV and viroids led to the theory that HDV may have originated from viroids and later acquired protein-coding capacity (Flores et al., 2011; Gudima et al., 2000; Netter et al., 2021; Taylor & Pelchat, 2010). Moreover, the similarities between HDV and HDV-like agents suggest that they may have the ability to spread and amplify like viroids through the induction of intercellular membrane channels (Kumar et al., 2015). However, co-culture system did not show evidence of cell-to-cell spread (Figure 3.11), which is consistent with an earlier study investigating the envelope-free cell-to-cell spread of HDV (Giersch et al., 2019).

Importantly, the lack of cell-to-cell spread in my co-culture system does not necessarily mean that HDV and HDV-like agents cannot spread like viroids *in vivo*. Indeed, cell culture models might not fully recapitulate the intercellular membrane channels. Therefore,

further studies are required to investigate the possibility of viroid-like spread by HDV and HDV-like agents in naturally occurring scenarios.

Moreover, it is also possible that these agents may use alternative spreading pathways, such as an autonomous or envelope protein-driven extracellular spreading pathway. These pathways potentially have a pivotal role in spreading HDV-like agents *in vivo*, necessitating additional research to comprehensively grasp the pathogenesis of HDV and HDV-like agents.

4.1.4 Replication and cell division-mediated spread of HDV-like agents is not limited to human or hepatic cells

The discovery of HDV-like agents highlighted the possibility of host-shifting and adaptation to a broad range of species (Bergner et al., 2021).

To better understand the dynamics of this aspect, replication and CDMS were evaluated in non-human derived cell lines. Antigenomic transfection studies in different animal-derived cell lines showed strong antigen expression and CDMS for HDV, WoDV and DeDV in primate (VeroE6) and rodent (CHO)-derived cell lines but not in galliform (LMH) and chiroptera (PaKi)-derived cell lines (Figure 3.8&3.2) indicating an adaptation only within specific mammalian species. The lack of replication of HDV in avian cells was previously observed in two independent studies (Chang et al., 2000; Liu et al., 2001), identifying the absence of a specific host factor indispensable for HDV replication in LMH cells. On the same line, AvDV replication and cell division-mediated spread were observed to be efficient only in LMH cells among all the human and non-human cell lines tested (Figure 3.5&3.8). This high replication rate allowed the expression of a second viral antigen, approximately 20 amino acids bigger than S-AvDAg (Figure 3.5&3.8). Although the AvDV genome does not encode the possibility of the emergence of a large delta antigen, a higher replication rate established in a more suitable host (i.e., chicken) could favor other types of genome modification. Indeed, a + 1 frameshift after the S-AvDAg could lead to

the extension of the ORF by 17 amino acids. It would be tempting to speculate that this extension would serve as a factor for the packaging by the hepadnavirus identified in ducks (DHBV). Considering the high difference between human HBV and DHBV, farnesylation might not be involved in the packaging.

One of the main reasons for evaluating different non-human cell lines was the lack of efficient replication of BaDV in human hepatoma cells (Figure 3.4&3.5).

However, BaDV could not efficiently replicate even in a bat cell line (Figure 3.8 & 3.12). To fully assess if the lack of efficient replication is due to the lack of essential factors and to exclude a possible replication defect in the clone used, a broader cell line selection and different BaDV clones need to be evaluated. Nevertheless, the diversity of bat species might play a crucial role in the adaptation and evolution of viral genomes.

Metagenome analysis has shown that these novel HDV-like agents are not exclusively detected in liver tissues (Bergner et al., 2021; Chang et al., 2019). HDV is mainly regarded as a hepatotropic virus due to its dependence on HBsAg/NTCP interaction for target cells entry (Ni et al., 2014). However, HDV alone has been shown to replicate in non-hepatic tissues (Polo et al., 1995; Taylor, 2009). Moreover, a recent study identified HDV-like sequences in the salivary glands of Sjogren's patients (Hesterman et al., 2023). Whether these sequences are HDV or HDV-like agents, it is still unclear.

Intracellular antigen levels were comparable for HDAg, WoAg, and DeAg in non-liver-derived cells, such as HeLa and HEK293T (Figure 3.9). However, CDMS was higher in terms of cluster number and size for WoDV and DeDV compared to HDV, indicating a more robust spreading capability in non-hepatic tissues (Figure 3.13).

In A549 cells, HDV-like agents did not replicate efficiently. Given HDV's sensitivity to interferon induction, the innate immune system may be involved in this inefficiency. To test this possibility, A549 cells were transfected with HDV-like agents genome constructs and treated with the JAK1/JAK2 inhibitor Ruxolitinib (Becker et al., 2014; Zhang et al., 2022) to suppress intrinsic immune induction. As a result of Ruxolitinib treatment, ISG

upregulation was successfully reduced in transfected cells (Figure 3.14). Subsequently, upon splitting, CDMS of HDV and HDV-like agents increased in A549 cells although the cluster size remained limited.

This phenotype could imply a combination of innate immunity counteraction and a possible lack of cellular factors that enable successful replication and consequential CDMS in A549 cells. To further study and characterize natural immunity stimulation and sensitivity to interferon of HDV-like agents, an infection system was implemented, starting from finding a putative helper virus that could envelope the RNP of highly replicating WoDV and DeDV.

In summary, I investigated the intracellular replication and cell division-mediated spread, of recently discovered HDV-like agents in cells from different hosts and tissues. Results give novel insights into the evolution of HDV-like agents regarding genome diversity and host adaptation. Data also sheds light on the importance of cell division-mediated spread for HDV persistence, which should be considered for developing a curative or preventing treatment.

4.1.5 *Future perspectives*

The unanswered question remains whether an active restriction factor or a lacking dependency factor is responsible for the inefficient viral replication in some of the cell lines tested. To further investigate this aspect, I will conduct cell fusion experiments. Cells which were shown to generally be permissive for HDV and HDV-like agents replication (e.g., HuH7, CHO) will be fused with cells that show low permissiveness for viral replication (e.g., LMH) via treatment with already known fusogens (e.g. PEG) (Lempp et al., 2016). Fusion and syncytia formation between different cell types will allow sharing of cellular factors. In the absence of viral replication, a limiting factor expressed in non-permissive cell lines might actively inhibit the replication, whereas viral replication in fused cells would indicate a missing host factor.

Furthermore, replication in primary hepatoma cell lines obtained from woodchuck, deer and duck species will be assessed. This could add further information on the original and most suitable host for the replication of these HDV-like agents.

4.2 Establishment of an infection system and characterization of extracellular spread

Till now, little is known about the natural occurring spreading pathways of non-human HDV-like agents. However, this knowledge could provide valuable information for understanding the spread and transmission dynamics of HDV and HDV-like agents. Genomic characteristics of DLAs hinted to the possibilities of diverse extracellular spreading pathways, such as exploiting helper viruses glycoproteins without a functional farnesylated L-DAG. Different pseudotyping strategies (e.g. using different viral envelope proteins or trans complementation techniques) indicated the possibilities for WoDV and DeDV to spread extracellularly and establish infection in target cells. This is an important aspect for understanding and controlling potential emerging infectious diseases and monitoring differential and potentially overlooked transmission pathways.

4.2.1 Pseudo-typing of HDV and HDV-like agents using selected envelope proteins from hepadna- and non-hepadnaviruses

A recent study reported that HDV might be packaged by envelope glycoproteins of diverse non-hepadnaviruses (Perez-Vargas et al., 2019). This observation raises interesting possibilities in the field of epidemiology, particularly with regards to the prevalence and mortality rate of Hepatitis C virus (HCV) infection. However, there is a lack of epidemiological evidence to support this potential transmission, as only one patient has been reported with circulating HDV RNA without any accompanying HBV infection markers. (Chemin et al., 2021). Further studies were conducted to investigate this observation, but no evidence of this phenomenon was found in the considered cohort (Cappy et al., 2021; Pfluger et al., 2021; Roggenbach et al., 2021).

The HDV-like agents investigated in this study have not been identified as satellite agents of any known helper virus (Bergner et al., 2021; Iwamoto et al., 2021).

Given the broad range of cellular replication and the absence of L-DAG expression, HDV-like agents could exploit hepadna- and non-hepadnavirus envelope glycoproteins for extracellular propagation. To this purpose, clones of HDV-like agents were co-transfected with plasmids encoding envelope proteins derived from Hepatitis C virus (HCV-E1E2), Dengue virus (DENV-PrME) and Vesicular stomatitis virus (VSV-g).

For HCV-E1E2 and DENV-PrME co-transfection, RT-qPCR analysis did not show a significant increase in the viral RNA level in the supernatant compared to antigenome-only transfection (Figure 3.15), indicating a lack of efficient pseudo-typing using these envelope proteins. Interestingly, VSV-g could support a more efficient RNA release, as indicated by a moderate increase in extracellular RNA levels. Moreover, IF analysis showed delta antigen-positive HuH7^{NTCP} cells infected with pseudo-type WoDV/VSV-g and DeDV/VSV-g particles (Figure 3.15). VSV-g was reported to be able to package HDV RNP (Perez-Vargas et al., 2019). However, the packaging of WoDV and DeDV was even more efficient when compared to HDV. This might indicate differences and advantages in the replication of HDV-like agents, making them more prone to being packed by VSV envelope proteins. Interestingly, this packaging could occur without the expression of a farnesylated L-DAG, excluding the possible involvement of farnesylation in the process. Nevertheless, its flexibility makes VSV-g widely used as an envelope protein for pseudo-particle formation (Mendenhall et al., 2012; Yoshida et al., 1997). Therefore, the packaging observed using this envelope protein might not be specific for WoDV, and DeDV as the packaging of HDV by HBV. However, this finding provided proof of an artificial pseudo-typing without L-HDAG expression.

4.2.2 Trans-complemented L-HDAG promotes the packaging of WoDV and DeDV RNP by HBsAg

It remains unclear how these HDV-like agents could spread extracellularly, as they lack the L-DAG expression, which is a critical feature for efficient host-to-host spread for the human HDV. Considering the highly conserved regions between HDV and the DAG of

WoDV and DeDV, I hypothesized that the human L-HDAg could also assist the packaging of WoDV and DeDV RNP by HBsAg. Trans-complementation with the human L-HDAg enhanced the extracellular viral RNA release of WoDV and DeDV (Figure 3.20), indicating an interaction between L-HDAg and the RNP of HDV-like agents. This interaction was dependent on the farnesylation of the artificially provided L-HDAg since the farnesylation inhibitor LNF could notably decrease extracellular RNA release. L-HDAg mediated an efficient packaging of WoDV and DeDV RNP by HBsAg, resulting in the pseudo-typing of HDV-like agents and infection of hepatocytes in an NTCP-dependent manner.

The inhibitory effect of farnesylated L-HDAg expression on HDV replication is already well-characterized (Modahl & Lai, 2000; Sato et al., 2004). Given the gain-of-function role of L-HDAg in the packaging of WoDV and DeDV by HBsAg, the effects of its expression on viral replication were investigated. For HDV and all the HDV-like agents tested, co-expression of wild-type L-HDAg resulted in a reduced intracellular viral RNA replication, indicating an active inhibitory effect (Figure 3.16). As expected, the abrogation of farnesylation reversed the inhibitory effect on HDV replication. Furthermore, the presence of non-farnesylated L-HDAg had a more pronounced negative effect on the replication of WoDV and DeDV when compared to HDV (Figure 3.17).

These results hint at the interchangeable role of the viral antigens of HDV, WoDV, and DeDV, providing important information on antigen conservation and mechanism in putative co-infection scenarios.

From an evolutionary point of view, it would be interesting to speculate that the human HDV gained the capability to express a large, farnesylated DA_g, probably in co-existence with the human HBV in the human liver. This interaction permitted an efficient adaptation of the human HDV as a hepatotropic virus. On the other hand, L-HDAg restricts intracellular HDV replication. Maintaining a balance between L-HDAg-mediated HDV release and intracellular replication may be critical for establishing a chronic infection in the liver. However, a limitation of this cell culture system is the production of chimeric

pseudo-particles. Co-infection with their actual helper virus would mimic more realistic infection conditions.

4.2.3 Open questions and future directions

The identification of an efficient extracellular spread for HDV-like agents remains elusive. As mentioned above, HDV-like agents could spread extracellularly even without a helper virus (Figure 4.2). Although this is not the main route of the spread of HDV, things might have been different before the co-evolution that allowed HDV to exploit the HBV surface protein to egress and de novo infect hepatocytes.

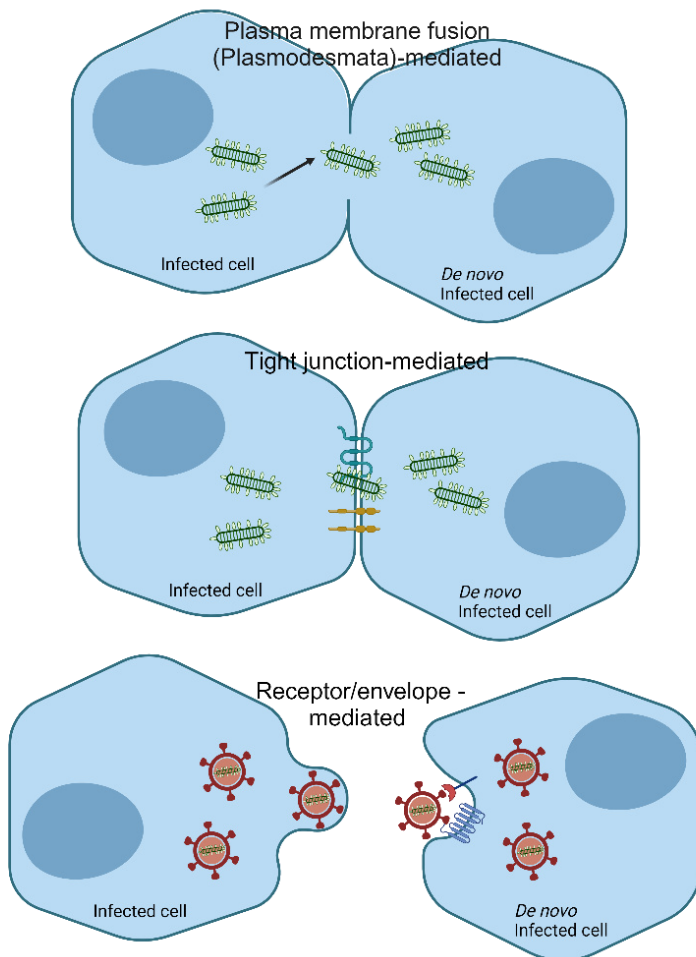


Figure 4.2. Models of putative cell-to-cell transmission pathways of HDV-like agents. (A) Cell-cell plasma-membrane fusion promotes the movement of infectious viral RNPs into the uninfected target cell. Cell-to-cell spread could result in syncytium formation and de novo infection without extracellular spread. Plant viruses can spread from cell to cell through nanochannels called plasmodesmata. (B) Viruses can pass through tight junctions by exiting basolaterally from an infected cell and becoming trapped between the infected and uninfected cell membranes. To penetrate the uninfected target cell, virions use viral entry receptors within tight junctions to fuse with it. Herpes viruses can spread across tight junctions. (C) Viral RNA could be enveloped in glycoproteins provided from a helper virus and enter the target cell via receptor-mediated binding.

The ability of many viruses to spread between infected and uninfected target cells by exploiting physiological cell-cell contacts or by establishing de novo contacts by

subverting the cellular adhesion machinery has been described (Sattentau, 2008). For example, HCV can spread in the presence of neutralizing antibodies that block both the viral glycoprotein and the cellular receptor required for cell attachment and entry (Timpe et al., 2008). Measles virus can induce cell-cell fusion and syncytia formation as an alternative to cell-free spread (Duprex et al., 1999). HIV requires CD4 as a primary receptor on the surface of immune cells but can also use virological synapsis to spread between neighboring cells (Groot et al., 2008). The strategy of spreading through direct cell-to-cell infection offers several advantages. It allows for rapid transmission without binding to a specific receptor on the target cell surface, simplifying the entry process. Additionally, this method may require a lower level of viral replication to establish a new infection. Finally, movement without exiting into the extracellular *milieu* could protect the virus from external factors (Sattentau, 2008).

Moreover, HBV has been shown to localize in exosome vesicles and exploit ESCRT secretory pathways (Kakizaki et al., 2020; Prange, 2022; Sanada et al., 2017; Yang et al., 2017).

To test whether this mechanism could also apply to HDV and HDV-like agents, I will evaluate the viral RNA localization within the exosomal/ endosomal compartment.

The routes of transmission and pathogenicity to animals and humans must be considered, to assess the potential for cross-species transmission or even spillover to humans. In rodents, HDV-like RNA has been detected primarily in blood, suggesting a blood-borne rather than a fecal-oral route, as with HDV. However, HDV-like agents in bat saliva, which feed on humans and domestic animals, provide an ecological opportunity for interspecies transmission. Given the ability of viruses to shift from host to host, investigating this process in the context of HDV-like agents could also offer valuable insights into the origin of human HDV and on the specific adaptation as hepatotropic virus.

4.3 Characterization of the interplay between HDV-like agents and the innate immune response

To date, the interaction between HDV-like agents and the host immune system is still unclear. However, based on what we discussed previously for HDV, I evaluated the replication and persistence of HDV-like agents in the context of infection.

An *in vitro* infection cell culture system was established to study the interplay between HDV-like agents and innate immune activation in human hepatoma cells. Infectious pseudo-particles generated by L-HDAg trans-complementation were used to elucidate viral tropism, spread and cellular defense immunity in the context of infection. As significant advantage, this methodology provides a BSL-2 safety-approved infection setting and can be used to address many questions, like how the absence of L-DAg or helper virus affects viral replication, sensing, innate immune induction, and spread via CDMS.

4.3.1 Infection and cell division-mediated spread of WoDV and DeDV in HepaRG^{NTCP} cells

WoDV and DeDV infection in HepaRG^{NTCP} cells resulted in a successful replication establishment. Notably, WoDV and DeDV infection induced lower ISGs upregulation when compared to HDV (Figure 3.25). Moreover, WoDV and DeDV could spread via cell division independent of the MDA5 or LGP2 expression level. Most interestingly, CDMS of WoDV and DeDV did not seem to be affected by exogenous IFN treatment upon infection of HuH7^{NTCP} cells (Figure 3.27). This phenotype could be explained by different factors.

As viruses adapt to new hosts for replication, *vice versa*, the host can evolve to optimize viral recognition and clearance (Banerjee et al., 2018; Bean et al., 2013; Mandl et al., 2015). Since these HDV-like agents were identified in hosts not so phylogenetically related to humans, the host innate immune system could play an essential and decisive role in the

recognition. Along this line, it is important to mention that PRR such as MDA5 or LGP2, crucial for the optimal recognition of HDV by the human innate immune system, could be structurally and functionally very distant from the ones found in woodchuck or deer natural immune system (Lemos de Matos et al., 2013). Previously investigation highlighted similarities between the complexity of innate immune induction in humans and innate immunity in bats and rodent species (Banerjee et al., 2018; Clayton & Munir, 2020; De La Cruz-Rivera et al., 2018; Lu et al., 2002; Sarkis et al., 2018). Nevertheless, diversity in the recognition by the natural immune system could lead to possible spill-over events. This could have been the case for two phylogenetically very close HDV-like agents. Indeed, the HDV-like agents identified in spiny rats (Paraskevopoulou et al., 2020) and in a species of bat (Bergner et al., 2021) share 98% of genome identity. This could hint at a possible host-to-host transmission, possibly after evasion of the innate immune system of the recipient host (Bergner et al., 2021).

The S-DAG could counteract the innate immune responses upon infection as the only viral protein expressed during HDV-like agents replication. It has already been shown how viral protein can interact with direct factors involved in innate immunity regulation and signaling (Pugnale et al., 2009; Roca Suarez et al., 2018; Xu et al., 2021). PrM, a structural protein of several Flaviviruses, can bind MDA5 and prevent interaction with MAVS from initiating interferon signaling (Sui et al., 2023). Moreover, hepatitis viruses such as HAV or HEV can interact with different JAK signaling effectors and mitigate the response (Xu et al., 2021).

Following this hypothesis, it is essential to notice the differential antigen localization between HDV and HDV-like agents in infected HepaRG^{NTCP} cells (Figure 3.31). While HDV S-HDAg was observed to localize predominantly in the nuclei of infected cells, with the typical antigen aggregation in hubs within the nuclei, WoDV and DeDV DAg was ubiquitously express. The cytoplasmic localization of WoDV and DeDV Ags could indicate active countermeasures to either block MDA5 from sensing viral replication or shield viral RNA from degradation.

A model of a putative mode of immune evasion is depicted in Figure 4.3.

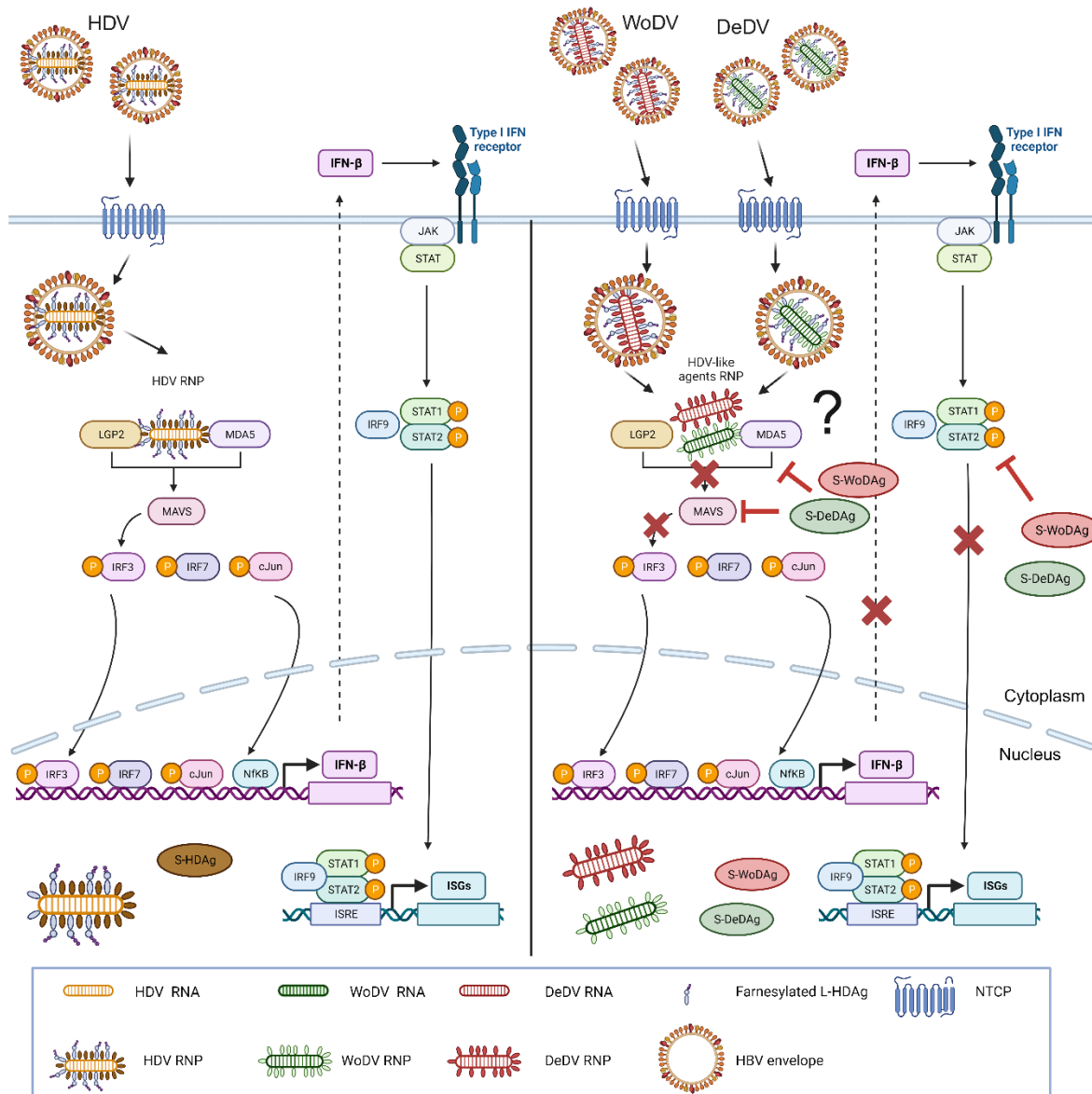


Figure 4.3: Model for innate immunity evasion by WoDV and DeDV in human hepatoma cells.

Putative HDV-like agents suppression of type I IFN response (T-arrows in red indicate blocking the targets). S-DAg interferes with MDA5 or LGP2 physiological function interfering with MAVS pathways, thereby inhibiting the type I IFN response. This counteraction affects the function of IRF3 and IRF7 kinases inhibiting production of IF-β and consequentially suppressing ISGs upregulation. Moreover, S-WoDAg and S-DeDAg could directly bind factors involved downstream in the innate immune signaling cascade, such as STAT1/STAT2, leading to inhibition of innate immune responses.

4.3.2 The role of L-HDAg expression in HDV interferon sensitivity

When HDV replication is well established, L-HDAg is expressed via the editing by the host enzyme ADAR1 (Wong & Lazinski, 2002). Hartwig et al. demonstrated that the activity of the IFN-induced ADAR1-L isoform could enhance the editing of the S-HDAg into L-HDAg (Hartwig et al., 2004; Hartwig et al., 2006), leading to the consequential reduction of HDV replication. Moreover, L-HDAg has been shown to induce the NF- κ B pathway, inhibiting HDV infectivity (Michelet et al., 2022; Williams et al., 2012).

Results using an HDV mutant, defective for L-HDAg expression, showed no advantage of lacking the L-HDAg expression since CDMS of this HDV mutant was also highly inhibited by replication-induced endogenous IFN in infected HepaRG^{NTCP} (Figure 3.30). This finding aligns with a previous work from my group showing no upregulation in HDV genome editing upon IFN treatment (Zhang et al., 2022). Due to the lack of inhibition by L-HDAg, replication of this HDV mutant was higher compared to WT HDV. This led to higher ISG upregulation, probably causing a more efficient viral clearance.

The scenario seemed to be different in the context of WoDV and DeDV infection. Indeed, even when viral replication was higher when compared to HDV, the innate immune response was non efficiently mounted, hinting at the complexity of factors involved.

Moreover, the artificial expression of L-HDAg did not influence WoDV and DeDV sensitivity to IFN treatment (Figure 3.28).

4.3.3 Replication and Innate Immunity Induction in Non-hepatic Cells

Given their broad tropism, it was crucial to investigate infection of HDV and HDV-like agents in non-hepatic derived models to better comprehend factors that allow viral persistence.

Infection in lung epithelial-derived cells, A549^{NTCP}, showed a moderate increase in ISG expression upon establishment of viral replication (Figure 3.34). This phenotype might be

explained by the low LGP2 expression in A549 cells (HPAP, 2023), confirming the critical role of this specific PRR in HDV sensing. Although innate immune activation was not high, cell division-mediated spread was still limited in terms of cluster size, probably indicating a lack of specific host factors required for efficient spreading. Although the initial infection rate for WoDV and DeDV was lower compared to HDV, cell division-mediated spread seemed more efficient for HDV-like agents, indicating a putative less strict liver adaptation.

In conclusion, a robust infection system was established for the WoDV and DeDV DLAs, overcoming the challenge that they do not express a farnesylated L-DAG and cannot be packaged by HBsAg. HDV replication led to IFN activation in HepaRG^{NTCP} cells, accompanied by a restriction of CDMS, whereas infection with WoDV and DeDV induced a low IFN response in HepaRG^{NTCP} cells and the CDMS of these agents remained efficient independent of MDA5/LGP2 expression. Furthermore, the CDMS of WoDV and DeDV was not significantly affected by exogenous IFN treatment. Thus, not only do both agents lack strong IFN activation, but they also exhibit resistance to IFN treatment. These data highlight potential evolutionary differences between HDV and HDV-like agents in terms of activation and sensitivity to IFN response.

4.3.4 Approaches to Unveil Recognition Mechanisms

HDV replicates in the nucleus of infected cells, but little is known about the replication site of HDV-like agents. To identify the replication site of WoDV and DeDV, I will optimize an RNA Scope protocol with genome strand-specific probes. To obtain a bulk measurement of RNA localization during replication, lysates from infected cells will be fractionated to separate nuclei from the cytoplasmic compartment. The viral RNA content of each fraction will be assessed by RT-qPCR. This could provide information on viral RNA localization and putative replication sites.

Additionally, I will take advantages of cells derived from woodchuck and deer will be included to identify their sensing PRR and compare it to human innate immunity.

Several approaches will be implemented to further evaluate the role of DAg in the counteraction of immune recognition: (i) Transfection of viral IVT RNA in innate immune competent cells and evaluation of ISGs induction, in the absence of viral antigen expression, to potentially shield the recognition (ii) Generation of stable cell lines expressing DAg of WoDV and DeDV (and HDV, as positive control), and evaluation of ISG induction in the context of HDV infection in these cell lines. If the HDV-like agent antigen plays a role in preventing the recognition of viral RNA by the innate immune system, a difference in ISGs upregulation will be observed. (iii) Co-immunoprecipitation protocols will be established to confirm the active interaction between viral antigens and factors involved in the innate immunity cascade, beginning with factors already known in the literature to be targets of viral proteins (i.e., MDA5, LGP2). Moreover, approaches of interactome analysis via mass spectrometry will be applied to broaden the selection of factors interacting with HDV and HDV-like agents viral antigens.

4.4 Final Conclusions

During my PhD I investigated how recently discovered HDV-like agents replicate, spread and persist in different hosts and tissues. Cell division-mediated spread was found to be a conserved spread pathway among DLAs. In particular, WoDV and DeDV were shown to spread efficiently in human and non-human cell lines and independently of tissue type.

In the search for helper viruses for these pathogens, VSVg could provide an envelope for WoDV and DeDV without the need for antigen farnesylation. Interestingly, WoDV and DeDV DAg could form complexes with human HDV L-HDAg and use it for packaging by HBsAg, resulting in pseudotyping and formation of infectious viral particles.

These results provide new insights into the evolution of HDV-like pathogens in terms of genome diversity, host adaptation and helper virus selection. The study also highlights the importance of cell division-mediated spread for the persistence of HDV and HDV-like agents, which is critical for the development of curative treatments.

To assess the possibility of cross-species transmission or spillover to humans, it is important to consider putative spreading routes and pathogenicity to animals and humans. In addition, interactions with other possible helper viruses must be investigated to better understand the factors promoting host-switching. The evolution of HDV-like agents also sheds light on the origin of HDV and the functionality of its farnesylated L-HDAg. Indeed, human HDV remains the only delta virus identified to date that naturally expresses a farnesylated L-HDAg that interacts with HBV envelope proteins as a helper function. Further studies are needed to understand how the other members of the Kalmoviridae family can spread extracellularly or from host to host, and whether this process involves the use of other viruses as helpers. Indeed, co-infection with their "natural" helper virus would mimic more realistic infection conditions.

Nevertheless, HDV-like agents constituted valuable tools for exploring the potential role of L-HDAg sensitivity to IFN induction and cell division-mediated spread. The results show

that HDV-like agents can replicate and spread via cell division in human hepatoma cell lines with only low detection by MDA5 or induction of ISG expression. Most importantly, exogenous IFN treatment did not significantly affect the intracellular cell division-mediated spread of DLAs, shedding light on a possible evasion mechanism that these agents employ to better counteract innate immune responses. This established cell culture system provides a basis for investigating the nature of HDV-like agents and contributes to a better understanding of the evolution, spread, and interaction with the innate immune system of this unique group of viral agents.

5. APPENDIX

5.1 FUNCTIONAL ANALYSES OF MUTATIONS OF PUTATIVE PHOSPHORYLATION SITES IN THE PRE_{S1} DOMAIN OF HEPATITIS B VIRUS LARGE ENVELOPE PROTEIN

In the initial phase of my PhD, I focused my research on functional analyses of mutations of putative phosphorylation sites in the preS₁ domain of the Hepatitis B Virus large envelope protein (L-HBsAg). Using a cell-free-based expression system, three potential phosphorylation sites within the HBV preS-domain were identified: S6, S67, and S98. To investigate the role of the identified serine residues in infection, I constructed 6 mutants with substitutions of serine to alanine or aspartic acid (S6A, S67A, S98A, S6D, S67D, S98D). These mutants were evaluated with regard to L-HBsAg expression, secretion of viral particles and virion production after transfection of HuH7 cells. Infection of L-HBsAg mutated HBV particles was assayed in susceptible HepG2 NTCP cell line. All substitutions supported the assembly and secretion of viral particles. While mutations at positions 67 and 98 had no effect, substituting serine 6 with aspartic acid resulted in a strong reduction of infectivity. We used HDV to investigate whether the effect is associated with viral entry. Abrogation of infectivity was also observed in the context of HDV infection, confirming the involvement of this specific mutation in the early phase of viral infection. Since serine 6 possibly plays an important role in the myristoylation of the L-protein, I am presently investigating if a modification at this site regulates myristoylation and viral infectivity. My perspectives for this side project are to finish the ongoing validation experiments and focus on writing a small paper.

5.2 JOINT HOST-PATHOGEN GENOMIC ANALYSIS IDENTIFIES HEPATITIS B VIRUS MUTATIONS ASSOCIATED WITH HUMAN *NTCP* AND HLA CLASS I VARIATION

Results contained in this paragraph are a joint study in collaboration with the group of Prof. Jacques Fellay, MD PhD (EPFL-Lausanne). The manuscript have been submitted to Cell Genomics and is currently under revision.

Evolutionary changes in the hepatitis B virus (HBV) genome might reflect adaptation to host-induced selective pressure. Leveraging paired host exome and ultra-deep HBV genome sequencing data from 567 chronic hepatitis B patients, the study aims to identify the signatures of this evolutionary process by conducting genome-to-genome (G2G) association tests between all pairs of viral mutations and human genetic variants. A significant association was identified between an Asian-specific missense variant in the gene encoding the HBV entry receptor *NTCP* (rs2296651; S267F), and amino acid mutations within the receptor-binding region of the HBV preS1 domain. The results suggest the emergence of HBV escape mutations that might alter the interaction between HBV PreS1 and its cellular receptor *NTCP* during viral entry into hepatocytes and confirm the role of HLA class I restriction in inducing HBV epitope variations.

The positive association between the *NTCP* S267F variant and three preS1 residues (17A, 35R, 51P), along with evidence of intra-host selection, suggests that the mutations may confer a fitness advantage for HBV within carriers of the *NTCP* variant. However, results from peptide binding assays suggest that compared to preS1 peptides derived from wildtype genotype C sequences (Myr-WT), peptides that carry the mutations (Myr-ARP) only display a minor increase in binding to *NTCP* S267F. Nonetheless, it is possible that the preS1 mutations could also play a role in downstream processes that are essential for preS1-*NTCP* internalization. For example, it has been shown that the presence of preS1 is required for *NTCP* oligomerization and that *NTCP* oligomerization is essential for preS1-*NTCP* internalization. Furthermore, the *NTCP* S267F variant has been shown to reduce

NTCP oligomerization. It is thus possible that the preS1 mutations improve the oligomerization efficiency of NTCP S267F-WT heterodimers or NTCP S267F homodimers. Further studies are needed to uncover the exact mechanism.

6. REFERENCES

- Abou-Jaoude, G., Molina, S., Maurel, P., & Sureau, C. (2007). Myristoylation signal transfer from the large to the middle or the small HBV envelope protein leads to a loss of HDV particles infectivity. *Virology*, *365*(1), 204-209. <https://doi.org/10.1016/j.virol.2007.03.030>
- Aghazadeh, M., Shi, M., Barrs, V. R., McLuckie, A. J., Lindsay, S. A., Jameson, B., Hampson, B., Holmes, E. C., & Beatty, J. A. (2018). A Novel Hepadnavirus Identified in an Immunocompromised Domestic Cat in Australia. *Viruses*, *10*(5). <https://doi.org/10.3390/v10050269>
- Aliasi-Sinai, L., Worthington, T., Lange, M., & Kushner, T. (2023). Maternal-to-Child Transmission of Hepatitis B Virus and Hepatitis Delta Virus. *Clin Liver Dis*, *27*(4), 917-935. <https://doi.org/10.1016/j.cld.2023.05.007>
- Alter, H. J., Purcell, R. H., Holland, P. V., & Popper, H. (1978). Transmissible agent in non-A, non-B hepatitis. *Lancet*, *1*(8062), 459-463. [https://doi.org/10.1016/s0140-6736\(78\)90131-9](https://doi.org/10.1016/s0140-6736(78)90131-9)
- Alvarado-Mora, M. V., Romano, C. M., Gomes-Gouvea, M. S., Gutierrez, M. F., Carrilho, F. J., & Pinho, J. R. (2011). Dynamics of hepatitis D (delta) virus genotype 3 in the Amazon region of South America. *Infect Genet Evol*, *11*(6), 1462-1468. <https://doi.org/10.1016/j.meegid.2011.05.020>
- Alves, C., Freitas, N., & Cunha, C. (2008). Characterization of the nuclear localization signal of the hepatitis delta virus antigen. *Virology*, *370*(1), 12-21. <https://doi.org/10.1016/j.virol.2007.07.034>
- Anthony, S. J., St Leger, J. A., Liang, E., Hicks, A. L., Sanchez-Leon, M. D., Jain, K., Lefkowitz, J. H., Navarrete-Macias, I., Knowles, N., Goldstein, T., Pugliares, K., Ip, H. S., Rowles, T., & Lipkin, W. I. (2015). Discovery of a Novel Hepatovirus (Phopivirus of Seals) Related to Human Hepatitis A Virus. *mBio*, *6*(4). <https://doi.org/10.1128/mBio.01180-15>
- Aslan, A. T., & Balaban, H. Y. (2020). Hepatitis E virus: Epidemiology, diagnosis, clinical manifestations, and treatment. *World J Gastroenterol*, *26*(37), 5543-5560. <https://doi.org/10.3748/wjg.v26.i37.5543>
- Balayan, M. S., Andjaparidze, A. G., Savinskaya, S. S., Ketiladze, E. S., Braginsky, D. M., Savinov, A. P., & Poleschuk, V. F. (1983). Evidence for a virus in non-A, non-B hepatitis transmitted via the fecal-oral route. *Intervirology*, *20*(1), 23-31. <https://doi.org/10.1159/000149370>
- Banerjee, A., Misra, V., Schountz, T., & Baker, M. L. (2018). Tools to study pathogen-host interactions in bats. *Virus Res*, *248*, 5-12. <https://doi.org/10.1016/j.virusres.2018.02.013>
- Barros, L. M., Gomes-Gouvea, M. S., Pinho, J. R., Alvarado-Mora, M. V., Dos Santos, A., Mendes-Correa, M. C., Caldas, A. J., Sousa, M. T., Santos, M. D., & Ferreira, A. S. (2011). Hepatitis Delta virus genotype 8 infection in Northeast Brazil: inheritance
-

- from African slaves? *Virus Res*, 160(1-2), 333-339. <https://doi.org/10.1016/j.virusres.2011.07.006>
- Bazinet, M., Pantea, V., Cebotarescu, V., Cojuhari, L., Jimbei, P., Albrecht, J., Schmid, P., Le Gal, F., Gordien, E., Krawczyk, A., Mijocevic, H., Karimzadeh, H., Roggendorf, M., & Vaillant, A. (2017). Safety and efficacy of REP 2139 and pegylated interferon alfa-2a for treatment-naïve patients with chronic hepatitis B virus and hepatitis D virus co-infection (REP 301 and REP 301-LTF): a non-randomised, open-label, phase 2 trial. *Lancet Gastroenterol Hepatol*, 2(12), 877-889. [https://doi.org/10.1016/S2468-1253\(17\)30288-1](https://doi.org/10.1016/S2468-1253(17)30288-1)
- Bean, A. G., Baker, M. L., Stewart, C. R., Cowled, C., Deffrasnes, C., Wang, L. F., & Lowenthal, J. W. (2013). Studying immunity to zoonotic diseases in the natural host - keeping it real. *Nat Rev Immunol*, 13(12), 851-861. <https://doi.org/10.1038/nri3551>
- Becker, H., Engelhardt, M., von Bubnoff, N., & Wäsch, R. (2014). Ruxolitinib. *Recent Results Cancer Res*, 201, 249-257. https://doi.org/10.1007/978-3-642-54490-3_16
- Bergner, L. M., Orton, R. J., Broos, A., Tello, C., Becker, D. J., Carrera, J. E., Patel, A. H., Biek, R., & Streicker, D. G. (2021). Diversification of mammalian deltaviruses by host shifting. *Proc Natl Acad Sci U S A*, 118(3). <https://doi.org/10.1073/pnas.2019907118>
- Blanchet, M., & Sureau, C. (2007). Infectivity determinants of the hepatitis B virus pre-S domain are confined to the N-terminal 75 amino acid residues. *J Virol*, 81(11), 5841-5849. <https://doi.org/10.1128/JVI.00096-07>
- Blumberg, B. S., Alter, H. J., & Visnich, S. (1965). A "New" Antigen in Leukemia Sera. *JAMA*, 191, 541-546. <https://doi.org/10.1001/jama.1965.03080070025007>
- Bogomolov, P., Alexandrov, A., Voronkova, N., Macievich, M., Kokina, K., Petrachenkova, M., Lehr, T., Lempp, F. A., Wedemeyer, H., Haag, M., Schwab, M., Haefeli, W. E., Blank, A., & Urban, S. (2016). Treatment of chronic hepatitis D with the entry inhibitor myrcludex B: First results of a phase Ib/IIa study. *J Hepatol*, 65(3), 490-498. <https://doi.org/10.1016/j.jhep.2016.04.016>
- Bordier, B. B., Marion, P. L., Ohashi, K., Kay, M. A., Greenberg, H. B., Casey, J. L., & Glenn, J. S. (2002). A prenylation inhibitor prevents production of infectious hepatitis delta virus particles. *J Virol*, 76(20), 10465-10472. <https://doi.org/10.1128/jvi.76.20.10465-10472.2002>
- Bradley, D. W., & Balayan, M. S. (1988). Virus of enterically transmitted non-A, non-B hepatitis. *Lancet*, 1(8589), 819. [https://doi.org/10.1016/s0140-6736\(88\)91674-1](https://doi.org/10.1016/s0140-6736(88)91674-1)
- Bradley, D. W., McCaustland, K. A., Cook, E. H., Schable, C. A., Ebert, J. W., & Maynard, J. E. (1985). Posttransfusion non-A, non-B hepatitis in chimpanzees. Physicochemical evidence that the tubule-forming agent is a small, enveloped virus. *Gastroenterology*, 88(3), 773-779. <https://www.ncbi.nlm.nih.gov/pubmed/2981754>
- Braga, W. S., Castilho Mda, C., Borges, F. G., Leao, J. R., Martinho, A. C., Rodrigues, I. S., Azevedo, E. P., Barros Junior, G. M., & Parana, R. (2012). Hepatitis D virus infection

- in the Western Brazilian Amazon - far from a vanishing disease. *Rev Soc Bras Med Trop*, 45(6), 691-695. <https://doi.org/10.1590/s0037-86822012000600007>
- Brazas, R., & Ganem, D. (1996). A cellular homolog of hepatitis delta antigen: implications for viral replication and evolution. *Science*, 274(5284), 90-94. <https://doi.org/10.1126/science.274.5284.90>
- Cao, D., Haussecker, D., Huang, Y., & Kay, M. A. (2009). Combined proteomic-RNAi screen for host factors involved in human hepatitis delta virus replication. *RNA*, 15(11), 1971-1979. <https://doi.org/10.1261/rna.1782209>
- Cappy, P., Lucas, Q., Kankarafou, N., Sureau, C., & Laperche, S. (2021). No Evidence of Hepatitis C Virus (HCV)-Assisted Hepatitis D Virus Propagation in a Large Cohort of HCV-Positive Blood Donors. *J Infect Dis*, 223(8), 1376-1380. <https://doi.org/10.1093/infdis/jiaa517>
- Casey, J. L. (2002). RNA editing in hepatitis delta virus genotype III requires a branched double-hairpin RNA structure. *J Virol*, 76(15), 7385-7397. <https://doi.org/10.1128/jvi.76.15.7385-7397.2002>
- Casey, J. L., Brown, T. L., Colan, E. J., Wignall, F. S., & Gerin, J. L. (1993). A genotype of hepatitis D virus that occurs in northern South America. *Proc Natl Acad Sci U S A*, 90(19), 9016-9020. <https://doi.org/10.1073/pnas.90.19.9016>
- Casey, J. L., & Gerin, J. L. (1995). Hepatitis D virus RNA editing: specific modification of adenosine in the antigenomic RNA. *J Virol*, 69(12), 7593-7600. <https://doi.org/10.1128/JVI.69.12.7593-7600.1995>
- Castaneda, D., Gonzalez, A. J., Alomari, M., Tandon, K., & Zervos, X. B. (2021). From hepatitis A to E: A critical review of viral hepatitis. *World J Gastroenterol*, 27(16), 1691-1715. <https://doi.org/10.3748/wjg.v27.i16.1691>
- Catanese, M. T., Ansuini, H., Graziani, R., Huby, T., Moreau, M., Ball, J. K., Paonessa, G., Rice, C. M., Cortese, R., Vitelli, A., & Nicosia, A. (2010). Role of scavenger receptor class B type I in hepatitis C virus entry: kinetics and molecular determinants. *J Virol*, 84(1), 34-43. <https://doi.org/10.1128/JVI.02199-08>
- Chang, J., Moraleda, G., & Taylor, J. (2000). Limitations to replication of hepatitis delta virus in avian cells. *J Virol*, 74(19), 8861-8866. <https://doi.org/10.1128/jvi.74.19.8861-8866.2000>
- Chang, M. F., Chang, S. C., Chang, C. I., Wu, K., & Kang, H. Y. (1992). Nuclear localization signals, but not putative leucine zipper motifs, are essential for nuclear transport of hepatitis delta antigen. *Journal of Virology*, 66(10), 6019-6027. <https://doi.org/doi:10.1128/jvi.66.10.6019-6027.1992>
- Chang, W. S., Pettersson, J. H., Le Lay, C., Shi, M., Lo, N., Wille, M., Eden, J. S., & Holmes, E. C. (2019). Novel hepatitis D-like agents in vertebrates and invertebrates. *Virus Evol*, 5(2), vez021. <https://doi.org/10.1093/ve/vez021>
- Chao, M., Hsieh, S. Y., & Taylor, J. (1990). Role of two forms of hepatitis delta virus antigen: evidence for a mechanism of self-limiting genome replication. *J Virol*, 64(10), 5066-5069. <https://doi.org/10.1128/JVI.64.10.5066-5069.1990>

-
- Charnay, P., Pourcel, C., Louise, A., Fritsch, A., & Tiollais, P. (1979). Cloning in *Escherichia coli* and physical structure of hepatitis B virion DNA. *Proc Natl Acad Sci U S A*, 76(5), 2222-2226. <https://doi.org/10.1073/pnas.76.5.2222>
- Chemin, I., Pujol, F. H., Scholtès, C., Loureiro, C. L., Amirache, F., Levrero, M., Zoulim, F., Pérez-Vargas, J., & Cosset, F. L. (2021). Preliminary Evidence for Hepatitis Delta Virus Exposure in Patients Who Are Apparently Not Infected With Hepatitis B Virus. *Hepatology*, 73(2), 861-864. <https://doi.org/10.1002/hep.31453>
- Chen, P. J., Kalpana, G., Goldberg, J., Mason, W., Werner, B., Gerin, J., & Taylor, J. (1986). Structure and replication of the genome of the hepatitis delta virus. *Proc Natl Acad Sci U S A*, 83(22), 8774-8778. <https://doi.org/10.1073/pnas.83.22.8774>
- Chen, Y. S., Huang, W. H., Hong, S. Y., Tsay, Y. G., & Chen, P. J. (2008). ERK1/2-mediated phosphorylation of small hepatitis delta antigen at serine 177 enhances hepatitis delta virus antigenomic RNA replication. *J Virol*, 82(19), 9345-9358. <https://doi.org/10.1128/JVI.00656-08>
- Childs, K. S., Andrejeva, J., Randall, R. E., & Goodbourn, S. (2009). Mechanism of mda-5 Inhibition by paramyxovirus V proteins. *J Virol*, 83(3), 1465-1473. <https://doi.org/10.1128/JVI.01768-08>
- Choo, Q. L., Kuo, G., Weiner, A. J., Overby, L. R., Bradley, D. W., & Houghton, M. (1989). Isolation of a cDNA clone derived from a blood-borne non-A, non-B viral hepatitis genome. *Science*, 244(4902), 359-362. <https://doi.org/10.1126/science.2523562>
- Chou, H. C., Hsieh, T. Y., Sheu, G. T., & Lai, M. M. (1998). Hepatitis delta antigen mediates the nuclear import of hepatitis delta virus RNA. *J Virol*, 72(5), 3684-3690. <https://doi.org/10.1128/JVI.72.5.3684-3690.1998>
- Cibangu, K., & Onoya Onaluwa, P. (2021). Epidemiology of Hepatitis B Virus. In R. Luis (Ed.), *Hepatitis B* (pp. Ch. 1). IntechOpen. <https://doi.org/10.5772/intechopen.101097>
- Clayton, E., & Munir, M. (2020). Fundamental Characteristics of Bat Interferon Systems. *Front Cell Infect Microbiol*, 10, 527921. <https://doi.org/10.3389/fcimb.2020.527921>
- Corman, V. M., Grundhoff, A., Baechlein, C., Fischer, N., Gmyl, A., Wollny, R., Dei, D., Ritz, D., Binger, T., Adankwah, E., Marfo, K. S., Annison, L., Annan, A., Adu-Sarkodie, Y., Oppong, S., Becher, P., Drosten, C., & Drexler, J. F. (2015). Highly divergent hepaciviruses from African cattle. *J Virol*, 89(11), 5876-5882. <https://doi.org/10.1128/JVI.00393-15>
- Cornberg, M., & Manns, M. P. (2022). The curing regimens of HCV: A SWOT analysis. *Antiviral Therapy*, 27(2), 13596535211072672. <https://doi.org/10.1177/13596535211072672>
- Cui, F., Liang, X., Wang, F., Zheng, H., Hutin, Y. J., & Yang, W. (2014). Development, production, and postmarketing surveillance of hepatitis A vaccines in China. *J Epidemiol*, 24(3), 169-177. <https://doi.org/10.2188/jea.je20130022>
- Dane, D. S., Cameron, C. H., & Briggs, M. (1970). Virus-like particles in serum of patients with Australia-antigen-associated hepatitis. *Lancet*, 1(7649), 695-698. [https://doi.org/10.1016/s0140-6736\(70\)90926-8](https://doi.org/10.1016/s0140-6736(70)90926-8)
-

-
- Das, A., Hirai-Yuki, A., Gonzalez-Lopez, O., Rhein, B., Moller-Tank, S., Brouillette, R., Hensley, L., Misumi, I., Lovell, W., Cullen, J. M., Whitmire, J. K., Maury, W., & Lemon, S. M. (2017). TIM1 (HAVCR1) Is Not Essential for Cellular Entry of Either Quasi-enveloped or Naked Hepatitis A Virions. *mBio*, 8(5). <https://doi.org/10.1128/mBio.00969-17>
- De La Cruz-Rivera, P. C., Kanchwala, M., Liang, H., Kumar, A., Wang, L. F., Xing, C., & Schoggins, J. W. (2018). The IFN Response in Bats Displays Distinctive IFN-Stimulated Gene Expression Kinetics with Atypical RNASEL Induction. *J Immunol*, 200(1), 209-217. <https://doi.org/10.4049/jimmunol.1701214>
- de la Pena, M., Ceprian, R., Casey, J. L., & Cervera, A. (2021). Hepatitis delta virus-like circular RNAs from diverse metazoans encode conserved hammerhead ribozymes. *Virus Evol*, 7(1), veab016. <https://doi.org/10.1093/ve/veab016>
- de la Pena, M., & Gago-Zachert, S. (2022). A life of research on circular RNAs and ribozymes: towards the origin of viroids, deltaviruses and life. *Virus Res*, 314, 198757. <https://doi.org/10.1016/j.virusres.2022.198757>
- de Oliveira Carneiro, I., Sander, A. L., Silva, N., Moreira-Soto, A., Normann, A., Flehmig, B., Lukashev, A. N., Dotzauer, A., Wieseke, N., Franke, C. R., & Drexler, J. F. (2018). A Novel Marsupial Hepatitis A Virus Corroborates Complex Evolutionary Patterns Shaping the Genus Hepatovirus. *J Virol*, 92(13). <https://doi.org/10.1128/JVI.00082-18>
- Diakoudi, G., Capozza, P., Lanave, G., Pellegrini, F., Di Martino, B., Elia, G., Decaro, N., Camero, M., Ghergo, P., Stasi, F., Cavalli, A., Tempesta, M., Barrs, V. R., Beatty, J., Banyai, K., Catella, C., Lucente, M. S., Buonavoglia, A., Fusco, G., & Martella, V. (2022). A novel hepadnavirus in domestic dogs. *Sci Rep*, 12(1), 2864. <https://doi.org/10.1038/s41598-022-06842-z>
- Dias, A. A., Silva, C. A. d. M. e., Silva, C. O. d., Linhares, N. R. C., Santos, J. P. S., Vivarini, A. d. C., Marques, M. Â. d. M., Rosa, P. S., Lopes, U. G., Berrêdo-Pinho, M., & Pessolani, M. C. V. (2021). TLR-9 Plays a Role in Mycobacterium leprae-Induced Innate Immune Activation of A549 Alveolar Epithelial Cells [Original Research]. *Frontiers in Immunology*, 12. <https://doi.org/10.3389/fimmu.2021.657449>
- Dill, J. A., Camus, A. C., Leary, J. H., Di Giallonardo, F., Holmes, E. C., & Ng, T. F. (2016). Distinct Viral Lineages from Fish and Amphibians Reveal the Complex Evolutionary History of Hepadnaviruses. *J Virol*, 90(17), 7920-7933. <https://doi.org/10.1128/JVI.00832-16>
- Ding, B. (2009). The biology of viroid-host interactions. *Annu Rev Phytopathol*, 47, 105-131. <https://doi.org/10.1146/annurev-phyto-080508-081927>
- Drexler, J. F., Corman, V. M., Muller, M. A., Lukashev, A. N., Gmyl, A., Coutard, B., Adam, A., Ritz, D., Leijten, L. M., van Riel, D., Kallies, R., Klose, S. M., Gloza-Rausch, F., Binger, T., Annan, A., Adu-Sarkodie, Y., Oppong, S., Bourgarel, M., Rupp, D., . . . Drosten, C. (2013). Evidence for novel hepaciviruses in rodents. *PLoS Pathog*, 9(6), e1003438. <https://doi.org/10.1371/journal.ppat.1003438>
-

-
- Drexler, J. F., Geipel, A., König, A., Corman, V. M., van Riel, D., Leijten, L. M., Bremer, C. M., Rasche, A., Cottontail, V. M., Maganga, G. D., Schlegel, M., Müller, M. A., Adam, A., Klose, S. M., Carneiro, A. J., Stocker, A., Franke, C. R., Gloza-Rausch, F., Geyer, J., . . . Drosten, C. (2013). Bats carry pathogenic hepadnaviruses antigenically related to hepatitis B virus and capable of infecting human hepatocytes. *Proc Natl Acad Sci U S A*, *110*(40), 16151-16156. <https://doi.org/10.1073/pnas.1308049110>
- Drexler, J. F., Seelen, A., Corman, V. M., Fumie Tateno, A., Cottontail, V., Melim Zerbinati, R., Gloza-Rausch, F., Klose, S. M., Adu-Sarkodie, Y., Oppong, S. K., Kalko, E. K., Osterman, A., Rasche, A., Adam, A., Müller, M. A., Ulrich, R. G., Leroy, E. M., Lukashev, A. N., & Drosten, C. (2012). Bats worldwide carry hepatitis E virus-related viruses that form a putative novel genus within the family Hepeviridae. *J Virol*, *86*(17), 9134-9147. <https://doi.org/10.1128/JVI.00800-12>
- Duprex, W. P., McQuaid, S., Hangartner, L., Billeter, M. A., & Rima, B. K. (1999). Observation of measles virus cell-to-cell spread in astrocytoma cells by using a green fluorescent protein-expressing recombinant virus. *J Virol*, *73*(11), 9568-9575. <https://doi.org/10.1128/JVI.73.11.9568-9575.1999>
- Elena, S. F., Dopazo, J., Flores, R., Diener, T. O., & Moya, A. (1991). Phylogeny of viroids, viroidlike satellite RNAs, and the viroidlike domain of hepatitis delta virus RNA. *Proc Natl Acad Sci U S A*, *88*(13), 5631-5634. <https://doi.org/10.1073/pnas.88.13.5631>
- Feinstone, S. M., Kapikian, A. Z., & Purceli, R. H. (1973). Hepatitis A: detection by immune electron microscopy of a viruslike antigen associated with acute illness. *Science*, *182*(4116), 1026-1028. <https://doi.org/10.1126/science.182.4116.1026>
- Filipovska, J., & Konarska, M. M. (2000). Specific HDV RNA-templated transcription by pol II in vitro. *RNA*, *6*(1), 41-54. <https://doi.org/10.1017/s1355838200991167>
- Findlay, G. M., & Willcox, R. R. (1945). Infective hepatitis; transmission by faeces and urine. *Lancet*, *2*(6378), 594-597. [https://doi.org/10.1016/s0140-6736\(45\)91612-6](https://doi.org/10.1016/s0140-6736(45)91612-6)
- Flores, R., Gago-Zachert, S., Serra, P., Sanjuan, R., & Elena, S. F. (2014). Viroids: survivors from the RNA world? *Annu Rev Microbiol*, *68*, 395-414. <https://doi.org/10.1146/annurev-micro-091313-103416>
- Flores, R., Grubb, D., Elleuch, A., Nohales, M. A., Delgado, S., & Gago, S. (2011). Rolling-circle replication of viroids, viroid-like satellite RNAs and hepatitis delta virus: variations on a theme. *RNA Biol*, *8*(2), 200-206. <https://doi.org/10.4161/rna.8.2.14238>
- Freitas, N., Cunha, C., Menne, S., & Gudima, S. O. (2014). Envelope proteins derived from naturally integrated hepatitis B virus DNA support assembly and release of infectious hepatitis delta virus particles. *J Virol*, *88*(10), 5742-5754. <https://doi.org/10.1128/JVI.00430-14>
- Gabrielli, F., Alberti, F., Russo, C., Cursaro, C., Seferi, H., Margotti, M., & Andreone, P. (2023). Treatment Options for Hepatitis A and E: A Non-Systematic Review. *Viruses*, *15*(5). <https://doi.org/10.3390/v15051080>
- George, C. X., Wagner, M. V., & Samuel, C. E. (2005). Expression of interferon-inducible RNA adenosine deaminase ADAR1 during pathogen infection and mouse embryo
-

- development involves tissue-selective promoter utilization and alternative splicing. *J Biol Chem*, 280(15), 15020-15028. <https://doi.org/10.1074/jbc.M500476200>
- Giersch, K., Bhadra, O. D., Volz, T., Allweiss, L., Riecken, K., Fehse, B., Lohse, A. W., Petersen, J., Sureau, C., Urban, S., Dandri, M., & Lutgehetmann, M. (2019). Hepatitis delta virus persists during liver regeneration and is amplified through cell division both in vitro and in vivo. *Gut*, 68(1), 150-157. <https://doi.org/10.1136/gutjnl-2017-314713>
- Giguere, T., & Perreault, J. P. (2017). Classification of the Pospiviroidae based on their structural hallmarks. *PLoS One*, 12(8), e0182536. <https://doi.org/10.1371/journal.pone.0182536>
- Gillich, N., Zhang, Z., Binder, M., Urban, S., & Bartenschlager, R. (2023). Effect of variants in LGP2 on MDA5-mediated activation of interferon response and suppression of hepatitis D virus replication. *J Hepatol*, 78(1), 78-89. <https://doi.org/10.1016/j.jhep.2022.08.041>
- Glenn, J. S., Watson, J. A., Havel, C. M., & White, J. M. (1992). Identification of a prenylation site in delta virus large antigen. *Science*, 256(5061), 1331-1333. <https://doi.org/10.1126/science.1598578>
- Goldsmith, R., Yarbough, P. O., Reyes, G. R., Fry, K. E., Gabor, K. A., Kamel, M., Zakaria, S., Amer, S., & Gaffar, Y. (1992). Enzyme-linked immunosorbent assay for diagnosis of acute sporadic hepatitis E in Egyptian children. *Lancet*, 339(8789), 328-331. [https://doi.org/10.1016/0140-6736\(92\)91647-q](https://doi.org/10.1016/0140-6736(92)91647-q)
- Groot, F., Welsch, S., & Sattentau, Q. J. (2008). Efficient HIV-1 transmission from macrophages to T cells across transient virological synapses. *Blood*, 111(9), 4660-4663. <https://doi.org/10.1182/blood-2007-12-130070>
- Gudima, S., Wu, S. Y., Chiang, C. M., Moraleta, G., & Taylor, J. (2000). Origin of hepatitis delta virus mRNA. *J Virol*, 74(16), 7204-7210. <https://doi.org/10.1128/jvi.74.16.7204-7210.2000>
- Hahn, C. M., Iwanowicz, L. R., Cornman, R. S., Conway, C. M., Winton, J. R., & Blazer, V. S. (2015). Characterization of a Novel Hepadnavirus in the White Sucker (*Catostomus commersonii*) from the Great Lakes Region of the United States. *J Virol*, 89(23), 11801-11811. <https://doi.org/10.1128/JVI.01278-15>
- Han, Z., Nogusa, S., Nicolas, E., Balachandran, S., & Taylor, J. (2011). Interferon impedes an early step of hepatitis delta virus infection. *PLoS One*, 6(7), e22415. <https://doi.org/10.1371/journal.pone.0022415>
- Hartman, Z. C., Black, E. P., & Amalfitano, A. (2007). Adenoviral infection induces a multifaceted innate cellular immune response that is mediated by the toll-like receptor pathway in A549 cells. *Virology*, 358(2), 357-372. <https://doi.org/https://doi.org/10.1016/j.virol.2006.08.041>
- Hartwig, D., Schoeneich, L., Greeve, J., Schutte, C., Dorn, I., Kirchner, H., & Hennig, H. (2004). Interferon-alpha stimulation of liver cells enhances hepatitis delta virus RNA editing in early infection. *J Hepatol*, 41(4), 667-672. <https://doi.org/10.1016/j.jhep.2004.06.025>

-
- Hartwig, D., Schutte, C., Warnecke, J., Dorn, I., Hennig, H., Kirchner, H., & Schlenke, P. (2006). The large form of ADAR 1 is responsible for enhanced hepatitis delta virus RNA editing in interferon-alpha-stimulated host cells. *J Viral Hepat*, *13*(3), 150-157. <https://doi.org/10.1111/j.1365-2893.2005.00663.x>
- Harvey, E., Mifsud, J. C. O., Holmes, E. C., & Mahar, J. E. (2023). Divergent hepaciviruses, delta-like viruses, and a chu-like virus in Australian marsupial carnivores (dasyurids). *Virus Evol*, *9*(2), vead061. <https://doi.org/10.1093/ve/vead061>
- He, B., Zhang, F., Xia, L., Hu, T., Chen, G., Qiu, W., Fan, Q., Feng, Y., Guo, H., & Tu, C. (2015). Identification of a novel Orthohepadnavirus in pomona roundleaf bats in China. *Arch Virol*, *160*(1), 335-337. <https://doi.org/10.1007/s00705-014-2222-0>
- Heidrich, B., Yurdaydin, C., Kabacam, G., Ratsch, B. A., Zachou, K., Bremer, B., Dalekos, G. N., Erhardt, A., Tabak, F., Yalcin, K., Gurel, S., Zeuzem, S., Cornberg, M., Bock, C. T., Manns, M. P., Wedemeyer, H., & Group, H.-S. (2014). Late HDV RNA relapse after peginterferon alpha-based therapy of chronic hepatitis delta. *Hepatology*, *60*(1), 87-97. <https://doi.org/10.1002/hep.27102>
- Hepatitis B vaccines: WHO position paper – July 2017. (2017). *Wkly Epidemiol Rec*, *92*(27), 369-392. (Vaccins anti-hépatite B: note de synthèse de l’OMS – juillet 2017.)
- Herzog, C., Van Herck, K., & Van Damme, P. (2021). Hepatitis A vaccination and its immunological and epidemiological long-term effects - a review of the evidence. *Hum Vaccin Immunother*, *17*(5), 1496-1519. <https://doi.org/10.1080/21645515.2020.1819742>
- Hesterman, M. C., Furrer, S. V., Fallon, B. S., & Weller, M. L. (2023). Analysis of Hepatitis D Virus in Minor Salivary Gland of Sjogren's Disease. *J Dent Res*, *102*(11), 1272-1279. <https://doi.org/10.1177/00220345231186394>
- Hetzel, U., Szirovicza, L., Smura, T., Prahauer, B., Vapalahti, O., Kipar, A., & Hepojoki, J. (2019). Identification of a Novel Deltavirus in Boa Constrictors. *mBio*, *10*(2). <https://doi.org/10.1128/mBio.00014-19>
- Heuschkel, M. J., Baumert, T. F., & Verrier, E. R. (2021). Cell Culture Models for the Study of Hepatitis D Virus Entry and Infection. *Viruses*, *13*(8). <https://doi.org/10.3390/v13081532>
- Hirschman, S. Z., Vernace, S. J., & Schaffner, F. (1971). D.N.A. polymerase in preparations containing Australia antigen. *Lancet*, *1*(7709), 1099-1103. [https://doi.org/10.1016/s0140-6736\(71\)91839-3](https://doi.org/10.1016/s0140-6736(71)91839-3)
- Hou, J., Liu, Z., & Gu, F. (2005). Epidemiology and Prevention of Hepatitis B Virus Infection. *Int J Med Sci*, *2*(1), 50-57. <https://doi.org/10.7150/ijms.2.50>
- HPAP. (2023, 2023). *DHX58*. HPAP. Retrieved 10 December 23 from <https://www.proteinatlas.org/ENSG00000108771-DHX58/subcellular>
- Hwang, S. B., & Lai, M. M. (1993). Isoprenylation mediates direct protein-protein interactions between hepatitis large delta antigen and hepatitis B virus surface antigen. *J Virol*, *67*(12), 7659-7662. <https://doi.org/10.1128/JVI.67.12.7659-7662.1993>
-

-
- Hwang, S. B., & Lai, M. M. (1994). Isoprenylation masks a conformational epitope and enhances trans-dominant inhibitory function of the large hepatitis delta antigen. *J Virol*, 68(5), 2958-2964. <https://doi.org/10.1128/JVI.68.5.2958-2964.1994>
- Ivaniushina, V., Radjef, N., Alexeeva, M., Gault, E., Semenov, S., Salhi, M., Kiselev, O., & Deny, P. (2001). Hepatitis delta virus genotypes I and II cocirculate in an endemic area of Yakutia, Russia. *J Gen Virol*, 82(Pt 11), 2709-2718. <https://doi.org/10.1099/0022-1317-82-11-2709>
- Iwamoto, M., Saso, W., Sugiyama, R., Ishii, K., Ohki, M., Nagamori, S., Suzuki, R., Aizaki, H., Ryo, A., Yun, J. H., Park, S. Y., Ohtani, N., Muramatsu, M., Iwami, S., Tanaka, Y., Sureau, C., Wakita, T., & Watashi, K. (2019). Epidermal growth factor receptor is a host-entry cofactor triggering hepatitis B virus internalization. *Proc Natl Acad Sci U S A*, 116(17), 8487-8492. <https://doi.org/10.1073/pnas.1811064116>
- Iwamoto, M., Shibata, Y., Kawasaki, J., Kojima, S., Li, Y. T., Iwami, S., Muramatsu, M., Wu, H. L., Wada, K., Tomonaga, K., Watashi, K., & Horie, M. (2021). Identification of novel avian and mammalian deltaviruses provides new insights into deltavirus evolution. *Virus Evol*, 7(1), veab003. <https://doi.org/10.1093/ve/veab003>
- Johne, R., Heckel, G., Plenge-Bonig, A., Kindler, E., Maresch, C., Reetz, J., Schielke, A., & Ulrich, R. G. (2010). Novel hepatitis E virus genotype in Norway rats, Germany. *Emerg Infect Dis*, 16(9), 1452-1455. <https://doi.org/10.3201/eid1609.100444>
- Kakizaki, M., Yamamoto, Y., Otsuka, M., Kitamura, K., Ito, M., Kawai, H. D., Muramatsu, M., Kagawa, T., & Kotani, A. (2020). Extracellular vesicles secreted by HBV-infected cells modulate HBV persistence in hydrodynamic HBV transfection mouse model. *J Biol Chem*, 295(35), 12449-12460. <https://doi.org/10.1074/jbc.RA120.014317>
- Kang, C., & Syed, Y. Y. (2020). Bulevirtide: First Approval. *Drugs*, 80(15), 1601-1605. <https://doi.org/10.1007/s40265-020-01400-1>
- Kato, N., Hijikata, M., Ootsuyama, Y., Nakagawa, M., Ohkoshi, S., Sugimura, T., & Shimotohno, K. (1990). Molecular cloning of the human hepatitis C virus genome from Japanese patients with non-A, non-B hepatitis. *Proc Natl Acad Sci U S A*, 87(24), 9524-9528. <https://doi.org/10.1073/pnas.87.24.9524>
- Khalfi, P., Denis, Z., Merolla, G., Chavey, C., Ursic-Bedoya, J., Soppa, L., Szirovicza, L., Hetzel, U., Dufourt, J., Leyrat, C., Goldmann, N., Goto, K., Verrier, E., Baumert, T. F., Glebe, D., Courgnaud, V., Grégoire, D., Hepojoki, J., & Majzoub, K. (2023). Unraveling human, rodent and snake *Kolmioviridae* replication to anticipate cross-species transmission. *bioRxiv*, 2023.2005.2017.541162. <https://doi.org/10.1101/2023.05.17.541162>
- Khuroo, M. S. (1980). Study of an epidemic of non-A, non-B hepatitis. Possibility of another human hepatitis virus distinct from post-transfusion non-A, non-B type. *Am J Med*, 68(6), 818-824. [https://doi.org/10.1016/0002-9343\(80\)90200-4](https://doi.org/10.1016/0002-9343(80)90200-4)
- Khuroo, M. S., Teli, M. R., Skidmore, S., Sofi, M. A., & Khuroo, M. I. (1981). Incidence and severity of viral hepatitis in pregnancy. *Am J Med*, 70(2), 252-255. [https://doi.org/10.1016/0002-9343\(81\)90758-0](https://doi.org/10.1016/0002-9343(81)90758-0)
-

-
- Koh, C., Canini, L., Dahari, H., Zhao, X., Uprichard, S. L., Haynes-Williams, V., Winters, M. A., Subramanya, G., Cooper, S. L., Pinto, P., Wolff, E. F., Bishop, R., Ai Thanda Han, M., Cotler, S. J., Kleiner, D. E., Keskin, O., Idilman, R., Yurdaydin, C., Glenn, J. S., & Heller, T. (2015). Oral prenylation inhibition with lonafarnib in chronic hepatitis D infection: a proof-of-concept randomised, double-blind, placebo-controlled phase 2A trial. *Lancet Infect Dis*, *15*(10), 1167-1174. [https://doi.org/10.1016/S1473-3099\(15\)00074-2](https://doi.org/10.1016/S1473-3099(15)00074-2)
- Kos, A., Dijkema, R., Arnberg, A. C., van der Meide, P. H., & Schellekens, H. (1986). The hepatitis delta (delta) virus possesses a circular RNA. *Nature*, *323*(6088), 558-560. <https://doi.org/10.1038/323558a0>
- Krugman, S., Giles, J. P., & Hammond, J. (1967). Infectious hepatitis. Evidence for two distinctive clinical, epidemiological, and immunological types of infection. *JAMA*, *200*(5), 365-373. <https://doi.org/10.1001/jama.200.5.365>
- Kumar, D., Kumar, R., Hyun, T. K., & Kim, J. Y. (2015). Cell-to-cell movement of viruses via plasmodesmata. *J Plant Res*, *128*(1), 37-47. <https://doi.org/10.1007/s10265-014-0683-6>
- Kuo, M. Y., Goldberg, J., Coates, L., Mason, W., Gerin, J., & Taylor, J. (1988). Molecular cloning of hepatitis delta virus RNA from an infected woodchuck liver: sequence, structure, and applications. *J Virol*, *62*(6), 1855-1861. <https://doi.org/10.1128/JVI.62.6.1855-1861.1988>
- Lai, M. M. (2005). RNA replication without RNA-dependent RNA polymerase: surprises from hepatitis delta virus. *J Virol*, *79*(13), 7951-7958. <https://doi.org/10.1128/JVI.79.13.7951-7958.2005>
- Lamas Longarela, O., Schmidt, T. T., Schoneweis, K., Romeo, R., Wedemeyer, H., Urban, S., & Schulze, A. (2013). Proteoglycans act as cellular hepatitis delta virus attachment receptors. *PLoS One*, *8*(3), e58340. <https://doi.org/10.1371/journal.pone.0058340>
- Lampertico, P., Roulot, D., & Wedemeyer, H. (2022). Bulevirtide with or without pegIFN α for patients with compensated chronic hepatitis delta: From clinical trials to real-world studies. *J Hepatol*, *77*(5), 1422-1430. <https://doi.org/10.1016/j.jhep.2022.06.010>
- Lancet, T. (2022). Viral hepatitis elimination: a challenge, but within reach. *Lancet*, *400*(10348), 251. [https://doi.org/10.1016/S0140-6736\(22\)01377-0](https://doi.org/10.1016/S0140-6736(22)01377-0)
- Lanford, R. E., Chavez, D., Brasky, K. M., Burns, R. B., 3rd, & Rico-Hesse, R. (1998). Isolation of a hepadnavirus from the woolly monkey, a New World primate. *Proc Natl Acad Sci U S A*, *95*(10), 5757-5761. <https://doi.org/10.1073/pnas.95.10.5757>
- Lasda, E., & Parker, R. (2014). Circular RNAs: diversity of form and function. *RNA*, *20*(12), 1829-1842. <https://doi.org/10.1261/rna.047126.114>
- Lauber, C., Seitz, S., Mattei, S., Suh, A., Beck, J., Herstein, J., Borold, J., Salzburger, W., Kaderali, L., Briggs, J. A. G., & Bartenschlager, R. (2017). Deciphering the Origin and Evolution of Hepatitis B Viruses by Means of a Family of Non-enveloped Fish
-

- Viruses. *Cell Host Microbe*, 22(3), 387-399 e386. <https://doi.org/10.1016/j.chom.2017.07.019>
- Le Gal, F., Brichtler, S., Drugan, T., Alloui, C., Roulot, D., Pawlotsky, J. M., Deny, P., & Gordien, E. (2017). Genetic diversity and worldwide distribution of the deltavirus genus: A study of 2,152 clinical strains. *Hepatology*, 66(6), 1826-1841. <https://doi.org/10.1002/hep.29574>
- Lee, C. H., Chang, S. C., Wu, C. H., & Chang, M. F. (2001). A novel chromosome region maintenance 1-independent nuclear export signal of the large form of hepatitis delta antigen that is required for the viral assembly. *J Biol Chem*, 276(11), 8142-8148. <https://doi.org/10.1074/jbc.M004477200>
- Lee, C. Z., Chen, P. J., Lai, M. M., & Chen, D. S. (1994). Isoprenylation of large hepatitis delta antigen is necessary but not sufficient for hepatitis delta virus assembly. *Virology*, 199(1), 169-175. <https://doi.org/10.1006/viro.1994.1109>
- Lee, C. Z., & Sheu, J. C. (2008). Histone H1e interacts with small hepatitis delta antigen and affects hepatitis delta virus replication. *Virology*, 375(1), 197-204. <https://doi.org/10.1016/j.virol.2008.02.003>
- Leistner, C. M., Gruen-Bernhard, S., & Glebe, D. (2008). Role of glycosaminoglycans for binding and infection of hepatitis B virus. *Cell Microbiol*, 10(1), 122-133. <https://doi.org/10.1111/j.1462-5822.2007.01023.x>
- Lemon, S. M., Ott, J. J., Van Damme, P., & Shouval, D. (2017). Type A viral hepatitis: A summary and update on the molecular virology, epidemiology, pathogenesis and prevention. *J Hepatol*. <https://doi.org/10.1016/j.jhep.2017.08.034>
- Lemos de Matos, A., McFadden, G., & Esteves, P. J. (2013). Positive evolutionary selection on the RIG-I-like receptor genes in mammals. *PLoS One*, 8(11), e81864. <https://doi.org/10.1371/journal.pone.0081864>
- Lempp, F. A., Mutz, P., Lipps, C., Wirth, D., Bartenschlager, R., & Urban, S. (2016). Evidence that hepatitis B virus replication in mouse cells is limited by the lack of a host cell dependency factor. *J Hepatol*, 64(3), 556-564. <https://doi.org/10.1016/j.jhep.2015.10.030>
- Liu, Y. T., Brazas, R., & Ganem, D. (2001). Efficient hepatitis delta virus RNA replication in avian cells requires a permissive factor(s) from mammalian cells. *J Virol*, 75(16), 7489-7493. <https://doi.org/10.1128/JVI.75.16.7489-7493.2001>
- Lo, K., Hwang, S. B., Duncan, R., Trousdale, M., & Lai, M. M. (1998). Characterization of mRNA for hepatitis delta antigen: exclusion of the full-length antigenomic RNA as an mRNA. *Virology*, 250(1), 94-105. <https://doi.org/10.1006/viro.1998.9364>
- Loader, M., Moravek, R., Witowski, S. E., & Driscoll, L. M. (2019). A clinical review of viral hepatitis. *JAAPA*, 32(11), 15-20. <https://doi.org/10.1097/01.JAA.0000586300.88300.84>
- Loo, Y. M., & Gale, M., Jr. (2011). Immune signaling by RIG-I-like receptors. *Immunity*, 34(5), 680-692. <https://doi.org/10.1016/j.immuni.2011.05.003>
- Loughran, G., Firth, A. E., & Atkins, J. F. (2011). Ribosomal frameshifting into an overlapping gene in the 2B-encoding region of the cardiovirus genome.

- Proceedings of the National Academy of Sciences*, 108(46), E1111-E1119. <https://doi.org/doi:10.1073/pnas.1102932108>
- Lu, M., Lohrengel, B., Hilken, G., Kemper, T., & Roggendorf, M. (2002). Woodchuck gamma interferon upregulates major histocompatibility complex class I transcription but is unable to deplete woodchuck hepatitis virus replication intermediates and RNAs in persistently infected woodchuck primary hepatocytes. *J Virol*, 76(1), 58-67. <https://doi.org/10.1128/jvi.76.1.58-67.2002>
- Lucifora, J., Alfaiate, D., Pons, C., Michelet, M., Ramirez, R., Fusil, F., Amirache, F., Rossi, A., Legrand, A. F., Charles, E., Vegna, S., Farhat, R., Rivoire, M., Passot, G., Gadot, N., Testoni, B., Bach, C., Baumert, T. F., Hyrina, A., . . . Durantel, D. (2023). Hepatitis D virus interferes with hepatitis B virus RNA production via interferon-dependent and -independent mechanisms. *J Hepatol*, 78(5), 958-970. <https://doi.org/10.1016/j.jhep.2023.01.005>
- Luo, G. X., Chao, M., Hsieh, S. Y., Sureau, C., Nishikura, K., & Taylor, J. (1990). A specific base transition occurs on replicating hepatitis delta virus RNA. *J Virol*, 64(3), 1021-1027. <https://doi.org/10.1128/JVI.64.3.1021-1027.1990>
- Lyons, S., Kapoor, A., Schneider, B. S., Wolfe, N. D., Culshaw, G., Corcoran, B., Durham, A. E., Burden, F., McGorum, B. C., & Simmonds, P. (2014). Viraemic frequencies and seroprevalence of non-primate hepacivirus and equine pegiviruses in horses and other mammalian species. *J Gen Virol*, 95(Pt 8), 1701-1711. <https://doi.org/10.1099/vir.0.065094-0>
- Macnaughton, T. B., Shi, S. T., Modahl, L. E., & Lai, M. M. (2002). Rolling circle replication of hepatitis delta virus RNA is carried out by two different cellular RNA polymerases. *J Virol*, 76(8), 3920-3927. <https://doi.org/10.1128/jvi.76.8.3920-3927.2002>
- Makino, S., Chang, M. F., Shieh, C. K., Kamahora, T., Vannier, D. M., Govindarajan, S., & Lai, M. M. (1987). Molecular cloning and sequencing of a human hepatitis delta (delta) virus RNA. *Nature*, 329(6137), 343-346. <https://doi.org/10.1038/329343a0>
- Mandl, J. N., Ahmed, R., Barreiro, L. B., Daszak, P., Epstein, J. H., Virgin, H. W., & Feinberg, M. B. (2015). Reservoir host immune responses to emerging zoonotic viruses. *Cell*, 160(1-2), 20-35. <https://doi.org/10.1016/j.cell.2014.12.003>
- Mason, W. S., Seal, G., & Summers, J. (1980). Virus of Pekin ducks with structural and biological relatedness to human hepatitis B virus. *J Virol*, 36(3), 829-836. <https://doi.org/10.1128/JVI.36.3.829-836.1980>
- Mederacke, I., Filmann, N., Yurdaydin, C., Bremer, B., Puls, F., Zacher, B. J., Heidrich, B., Tillmann, H. L., Rosenau, J., Bock, C. T., Savas, B., Helfritz, F., Lehner, F., Strassburg, C. P., Klempnauer, J., Wursthorn, K., Lehmann, U., Manns, M. P., Herrmann, E., & Wedemeyer, H. (2012). Rapid early HDV RNA decline in the peripheral blood but prolonged intrahepatic hepatitis delta antigen persistence after liver transplantation. *J Hepatol*, 56(1), 115-122. <https://doi.org/10.1016/j.jhep.2011.06.016>

-
- Mendenhall, A., Lesnik, J., Mukherjee, C., Antes, T., & Sengupta, R. (2012). Packaging HIV- or FIV-based lentivector expression constructs and transduction of VSV-G pseudotyped viral particles. *J Vis Exp*(62), e3171. <https://doi.org/10.3791/3171>
- Meng, X. J., Halbur, P. G., Shapiro, M. S., Govindarajan, S., Bruna, J. D., Mushahwar, I. K., Purcell, R. H., & Emerson, S. U. (1998). Genetic and experimental evidence for cross-species infection by swine hepatitis E virus. *J Virol*, *72*(12), 9714-9721. <https://doi.org/10.1128/JVI.72.12.9714-9721.1998>
- Mentha, N., Clement, S., Negro, F., & Alfaiate, D. (2019). A review on hepatitis D: From virology to new therapies. *J Adv Res*, *17*, 3-15. <https://doi.org/10.1016/j.jare.2019.03.009>
- Michelet, M., Alfaiate, D., Chardes, B., Pons, C., Faure-Dupuy, S., Engleitner, T., Farhat, R., Riedl, T., Legrand, A. F., Rad, R., Rivoire, M., Zoulim, F., Heikenwalder, M., Salvetti, A., Durantel, D., & Lucifora, J. (2022). Inducers of the NF-kappaB pathways impair hepatitis delta virus replication and strongly decrease progeny infectivity in vitro. *JHEP Rep*, *4*(3), 100415. <https://doi.org/10.1016/j.jhepr.2021.100415>
- Migueres, M., Lhomme, S., & Izopet, J. (2021). Hepatitis A: Epidemiology, High-Risk Groups, Prevention and Research on Antiviral Treatment. *Viruses*, *13*(10). <https://doi.org/10.3390/v13101900>
- Modahl, L. E., & Lai, M. M. (2000). The large delta antigen of hepatitis delta virus potently inhibits genomic but not antigenomic RNA synthesis: a mechanism enabling initiation of viral replication. *J Virol*, *74*(16), 7375-7380. <https://doi.org/10.1128/jvi.74.16.7375-7380.2000>
- Modahl, L. E., Macnaughton, T. B., Zhu, N., Johnson, D. L., & Lai, M. M. (2000). RNA-Dependent replication and transcription of hepatitis delta virus RNA involve distinct cellular RNA polymerases. *Mol Cell Biol*, *20*(16), 6030-6039. <https://doi.org/10.1128/MCB.20.16.6030-6039.2000>
- Mothes, W., Sherer, N. M., Jin, J., & Zhong, P. (2010). Virus cell-to-cell transmission. *J Virol*, *84*(17), 8360-8368. <https://doi.org/10.1128/JVI.00443-10>
- Mu, J. J., Chen, D. S., & Chen, P. J. (2001). The conserved serine 177 in the delta antigen of hepatitis delta virus is one putative phosphorylation site and is required for efficient viral RNA replication. *J Virol*, *75*(19), 9087-9095. <https://doi.org/10.1128/JVI.75.19.9087-9095.2001>
- Mu, J. J., Tsay, Y. G., Juan, L. J., Fu, T. F., Huang, W. H., Chen, D. S., & Chen, P. J. (2004). The small delta antigen of hepatitis delta virus is an acetylated protein and acetylation of lysine 72 may influence its cellular localization and viral RNA synthesis. *Virology*, *319*(1), 60-70. <https://doi.org/10.1016/j.virol.2003.10.024>
- Mu, J. J., Wu, H. L., Chiang, B. L., Chang, R. P., Chen, D. S., & Chen, P. J. (1999). Characterization of the phosphorylated forms and the phosphorylated residues of hepatitis delta virus delta antigens. *J Virol*, *73*(12), 10540-10545. <https://doi.org/10.1128/JVI.73.12.10540-10545.1999>
- Muir, A. J., Arora, S., Everson, G., Flisiak, R., George, J., Ghalib, R., Gordon, S. C., Gray, T., Greenbloom, S., Hassanein, T., Hillson, J., Horga, M. A., Jacobson, I. M., Jeffers,
-

-
- L., Kowdley, K. V., Lawitz, E., Lueth, S., Rodriguez-Torres, M., Rustgi, V., . . . group, E. s. (2014). A randomized phase 2b study of peginterferon lambda-1a for the treatment of chronic HCV infection. *J Hepatol*, 61(6), 1238-1246. <https://doi.org/10.1016/j.jhep.2014.07.022>
- Mutz, P., Metz, P., Lempp, F. A., Bender, S., Qu, B., Schoneweis, K., Seitz, S., Tu, T., Restuccia, A., Frankish, J., Dachert, C., Schusser, B., Koschny, R., Polychronidis, G., Schemmer, P., Hoffmann, K., Baumert, T. F., Binder, M., Urban, S., & Bartenschlager, R. (2018). HBV Bypasses the Innate Immune Response and Does Not Protect HCV From Antiviral Activity of Interferon. *Gastroenterology*, 154(6), 1791-1804 e1722. <https://doi.org/10.1053/j.gastro.2018.01.044>
- Nainan, O. V., Margolis, H. S., Robertson, B. H., Balayan, M., & Brinton, M. A. (1991). Sequence analysis of a new hepatitis A virus naturally infecting cynomolgus macaques (*Macaca fascicularis*). *J Gen Virol*, 72 (Pt 7), 1685-1689. <https://doi.org/10.1099/0022-1317-72-7-1685>
- Neefe, J. R., Stokes, J., Reinhold, J. G., & Lukens, F. D. (1944). Hepatitis Due to the Injection of Homologous Blood Products in Human Volunteers. *J Clin Invest*, 23(5), 836-855. <https://doi.org/10.1172/JCI101557>
- Netter, H. J., Barrios, M. H., Littlejohn, M., & Yuen, L. K. W. (2021). Hepatitis Delta Virus (HDV) and Delta-Like Agents: Insights Into Their Origin. *Front Microbiol*, 12, 652962. <https://doi.org/10.3389/fmicb.2021.652962>
- Ni, Y., Lempp, F. A., Mehrle, S., Nkongolo, S., Kaufman, C., Fälth, M., Stindt, J., Königer, C., Nassal, M., Kubitz, R., Sülthmann, H., & Urban, S. (2014). Hepatitis B and D viruses exploit sodium taurocholate co-transporting polypeptide for species-specific entry into hepatocytes. *Gastroenterology*, 146(4), 1070-1083. <https://doi.org/10.1053/j.gastro.2013.12.024>
- Nohales, M. A., Flores, R., & Daros, J. A. (2012). Viroid RNA redirects host DNA ligase 1 to act as an RNA ligase. *Proc Natl Acad Sci U S A*, 109(34), 13805-13810. <https://doi.org/10.1073/pnas.1206187109>
- Oon, G. C. (2012). Viral hepatitis--the silent killer. *Ann Acad Med Singap*, 41(7), 279-280. <https://www.ncbi.nlm.nih.gov/pubmed/22892603>
- Organization, W. H. (2023a). *Hepatitis A*. WHO. Retrieved 11 December 2023 from <https://www.who.int/news-room/fact-sheets/detail/hepatitis-a>
- Organization, W. H. (2023b). *Hepatitis E*. WHO. Retrieved 11 December from <https://www.who.int/news-room/fact-sheets/detail/hepatitis-e>
- Pacin-Ruiz, B., Cortese, M. F., Taberner, D., Sopena, S., Gregori, J., Garcia-Garcia, S., Casillas, R., Najarro, A., Aldama, U., Palom, A., Rando-Segura, A., Galan, A., Vila, M., Riveiro-Barciela, M., Quer, J., Gonzalez-Asequinolaza, G., Buti, M., & Rodriguez-Frias, F. (2022). Inspecting the Ribozyme Region of Hepatitis Delta Virus Genotype 1: Conservation and Variability. *Viruses*, 14(2). <https://doi.org/10.3390/v14020215>
- Paganelli, M., Stephenne, X., & Sokal, E. M. (2012). Chronic hepatitis B in children and adolescents. *J Hepatol*, 57(4), 885-896. <https://doi.org/10.1016/j.jhep.2012.03.036>
-

-
- Pan, Y., Xia, H., He, Y., Zeng, S., Shen, Z., & Huang, W. (2023). The progress of molecules and strategies for the treatment of HBV infection. *Front Cell Infect Microbiol*, *13*, 1128807. <https://doi.org/10.3389/fcimb.2023.1128807>
- Paraskevopoulou, S., Pirzer, F., Goldmann, N., Schmid, J., Corman, V. M., Gottula, L. T., Schroeder, S., Rasche, A., Muth, D., Drexler, J. F., Heni, A. C., Eibner, G. J., Page, R. A., Jones, T. C., Muller, M. A., Sommer, S., Glebe, D., & Drosten, C. (2020). Mammalian deltavirus without hepadnavirus coinfection in the neotropical rodent *Proechimys semispinosus*. *Proc Natl Acad Sci U S A*, *117*(30), 17977-17983. <https://doi.org/10.1073/pnas.2006750117>
- Park, D., & Hahn, Y. (2021). Rapid protein sequence evolution via compensatory frameshift is widespread in RNA virus genomes. *BMC Bioinformatics*, *22*(1), 251. <https://doi.org/10.1186/s12859-021-04182-9>
- Pascarella, S., & Negro, F. (2011). Hepatitis D virus: an update. *Liver Int*, *31*(1), 7-21. <https://doi.org/10.1111/j.1478-3231.2010.02320.x>
- Patterson, J. B., & Samuel, C. E. (1995). Expression and regulation by interferon of a double-stranded-RNA-specific adenosine deaminase from human cells: evidence for two forms of the deaminase. *Mol Cell Biol*, *15*(10), 5376-5388. <https://doi.org/10.1128/mcb.15.10.5376>
- Payne, C. J., Ellis, T. M., Plant, S. L., Gregory, A. R., & Wilcox, G. E. (1999). Sequence data suggests big liver and spleen disease virus (BLSV) is genetically related to hepatitis E virus. *Vet Microbiol*, *68*(1-2), 119-125. [https://doi.org/10.1016/s0378-1135\(99\)00067-x](https://doi.org/10.1016/s0378-1135(99)00067-x)
- Perez-Vargas, J., Amirache, F., Boson, B., Mialon, C., Freitas, N., Sureau, C., Fusil, F., & Cosset, F. L. (2019). Enveloped viruses distinct from HBV induce dissemination of hepatitis D virus in vivo. *Nat Commun*, *10*(1), 2098. <https://doi.org/10.1038/s41467-019-10117-z>
- Perez-Vargas, J., Pereira de Oliveira, R., Jacquet, S., Pontier, D., Cosset, F. L., & Freitas, N. (2021). HDV-Like Viruses. *Viruses*, *13*(7). <https://doi.org/10.3390/v13071207>
- Pfluger, L. S., Schulze Zur Wiesch, J., Polywka, S., & Lutgehetmann, M. (2021). Hepatitis delta virus propagation enabled by hepatitis C virus-Scientifically intriguing, but is it relevant to clinical practice? *J Viral Hepat*, *28*(1), 213-216. <https://doi.org/10.1111/jvh.13385>
- Piewbang, C., Dankaona, W., Poonsin, P., Yostawonkul, J., Lacharoje, S., Sirivisoot, S., Kasantikul, T., Tummaruk, P., & Techangamsuwan, S. (2022). Domestic cat hepadnavirus associated with hepatopathy in cats: A retrospective study. *J Vet Intern Med*, *36*(5), 1648-1659. <https://doi.org/10.1111/jvim.16525>
- Pileri, P., Uematsu, Y., Campagnoli, S., Galli, G., Falugi, F., Petracca, R., Weiner, A. J., Houghton, M., Rosa, D., Grandi, G., & Abrignani, S. (1998). Binding of hepatitis C virus to CD81. *Science*, *282*(5390), 938-941. <https://doi.org/10.1126/science.282.5390.938>
-

-
- Pischke, S., Behrendt, P., Bock, C. T., Jilg, W., Manns, M. P., & Wedemeyer, H. (2014). Hepatitis E in Germany--an under-reported infectious disease. *Dtsch Arztebl Int*, *111*(35-36), 577-583. <https://doi.org/10.3238/arztebl.2014.0577>
- Polo, J. M., Jeng, K. S., Lim, B., Govindarajan, S., Hofman, F., Sangiorgi, F., & Lai, M. M. (1995). Transgenic mice support replication of hepatitis delta virus RNA in multiple tissues, particularly in skeletal muscle. *J Virol*, *69*(8), 4880-4887. <https://doi.org/10.1128/JVI.69.8.4880-4887.1995>
- Polson, A. G., Ley, H. L., 3rd, Bass, B. L., & Casey, J. L. (1998). Hepatitis delta virus RNA editing is highly specific for the amber/W site and is suppressed by hepatitis delta antigen. *Mol Cell Biol*, *18*(4), 1919-1926. <https://doi.org/10.1128/mcb.18.4.1919>
- Prange, R. (2022). Hepatitis B virus movement through the hepatocyte: An update. *Biol Cell*, *114*(12), 325-348. <https://doi.org/10.1111/boc.202200060>
- Provost, P. J., & Hilleman, M. R. (1979). Propagation of human hepatitis A virus in cell culture in vitro. *Proc Soc Exp Biol Med*, *160*(2), 213-221. <https://doi.org/10.3181/00379727-160-40422>
- Provost, P. J., Hughes, J. V., Miller, W. J., Giesa, P. A., Banker, F. S., & Emini, E. A. (1986). An inactivated hepatitis A viral vaccine of cell culture origin. *J Med Virol*, *19*(1), 23-31. <https://doi.org/10.1002/jmv.1890190105>
- Pugnale, P., Paziienza, V., Guilloux, K., & Negro, F. (2009). Hepatitis delta virus inhibits alpha interferon signaling. *Hepatology*, *49*(2), 398-406. <https://doi.org/10.1002/hep.22654>
- Quan, P. L., Firth, C., Conte, J. M., Williams, S. H., Zambrana-Torrel, C. M., Anthony, S. J., Ellison, J. A., Gilbert, A. T., Kuzmin, I. V., Niezgod, M., Osinubi, M. O., Recuenco, S., Markotter, W., Breiman, R. F., Kalemba, L., Malekani, J., Lindblade, K. A., Rostal, M. K., Ojeda-Flores, R., . . . Lipkin, W. I. (2013). Bats are a major natural reservoir for hepaciviruses and pegiviruses. *Proc Natl Acad Sci U S A*, *110*(20), 8194-8199. <https://doi.org/10.1073/pnas.1303037110>
- Radjef, N., Gordien, E., Ivaniushina, V., Gault, E., Anais, P., Drugan, T., Trinchet, J. C., Roulot, D., Tamby, M., Milinkovitch, M. C., & Deny, P. (2004). Molecular phylogenetic analyses indicate a wide and ancient radiation of African hepatitis delta virus, suggesting a deltavirus genus of at least seven major clades. *J Virol*, *78*(5), 2537-2544. <https://doi.org/10.1128/jvi.78.5.2537-2544.2004>
- Raj, V. S., Smits, S. L., Pas, S. D., Provacia, L. B., Moorman-Roest, H., Osterhaus, A. D., & Haagmans, B. L. (2012). Novel hepatitis E virus in ferrets, the Netherlands. *Emerg Infect Dis*, *18*(8), 1369-1370. <https://doi.org/10.3201/eid1808.111659>
- Rasche, A., Sander, A. L., Corman, V. M., & Drexler, J. F. (2019). Evolutionary biology of human hepatitis viruses. *J Hepatol*, *70*(3), 501-520. <https://doi.org/10.1016/j.jhep.2018.11.010>
- Rasche, A., Saqib, M., Liljander, A. M., Bornstein, S., Zohaib, A., Renneker, S., Steinhagen, K., Wernery, R., Younan, M., Gluecks, I., Hilali, M., Musa, B. E., Jores, J., Wernery, U., Drexler, J. F., Drosten, C., & Corman, V. M. (2016). Hepatitis E Virus Infection in
-

- Dromedaries, North and East Africa, United Arab Emirates, and Pakistan, 1983-2015. *Emerg Infect Dis*, 22(7), 1249-1252. <https://doi.org/10.3201/eid2207.160168>
- Ratti, G., Stranieri, A., Scavone, D., Cafiso, A., Meazzi, S., Luzzago, C., Dall'Ara, P., Tagliasacchi, F., Cavicchioli, L., Ferrari, F., Giordano, A., Paltrinieri, S., & Lauzi, S. (2023). Detection and genetic characterization of domestic cat hepatitis virus in cats with cavitory effusions. *Vet Microbiol*, 284, 109828. <https://doi.org/10.1016/j.vetmic.2023.109828>
- Reyes, G. R., Purdy, M. A., Kim, J. P., Luk, K. C., Young, L. M., Fry, K. E., & Bradley, D. W. (1990). Isolation of a cDNA from the virus responsible for enterically transmitted non-A, non-B hepatitis. *Science*, 247(4948), 1335-1339. <https://doi.org/10.1126/science.2107574>
- Rizzetto, M. (2020). The Discovery of the Hepatitis D Virus: Three Princes of Serendip and the Recognition of Autoantibodies to Liver-Kidney Microsomes. *Clin Liver Dis (Hoboken)*, 16(Suppl 1), 1-11. <https://doi.org/10.1002/cld.1033>
- Rizzetto, M., Canese, M. G., Arico, S., Crivelli, O., Trepo, C., Bonino, F., & Verme, G. (1977). Immunofluorescence detection of new antigen-antibody system (delta/anti-delta) associated to hepatitis B virus in liver and in serum of HBsAg carriers. *Gut*, 18(12), 997-1003. <https://doi.org/10.1136/gut.18.12.997>
- Robertson, B. H. (2001). Viral hepatitis and primates: historical and molecular analysis of human and nonhuman primate hepatitis A, B, and the GB-related viruses. *J Viral Hepat*, 8(4), 233-242. <https://doi.org/10.1046/j.1365-2893.2001.00295.x>
- Robinson, W. S., & Greenman, R. L. (1974). DNA polymerase in the core of the human hepatitis B virus candidate. *J Virol*, 13(6), 1231-1236. <https://doi.org/10.1128/JVI.13.6.1231-1236.1974>
- Roca Suarez, A. A., Van Renne, N., Baumert, T. F., & Lupberger, J. (2018). Viral manipulation of STAT3: Evade, exploit, and injure. *PLoS Pathog*, 14(3), e1006839. <https://doi.org/10.1371/journal.ppat.1006839>
- Roggenbach, I., Chi, X., Lempp, F. A., Qu, B., Walter, L., Wu, R., Gao, X., Schnitzler, P., Ding, Y., Urban, S., & Niu, J. (2021). HDV Seroprevalence in HBsAg-Positive Patients in China Occurs in Hotspots and Is Not Associated with HCV Mono-Infection. *Viruses*, 13(9). <https://doi.org/10.3390/v13091799>
- Sakugawa, H., Nakasone, H., Nakayoshi, T., Kawakami, Y., Miyazato, S., Kinjo, F., Saito, A., Ma, S. P., Hotta, H., & Kinoshita, M. (1999). Hepatitis delta virus genotype 11b predominates in an endemic area, Okinawa, Japan. *J Med Virol*, 58(4), 366-372. [https://doi.org/10.1002/\(sici\)1096-9071\(199908\)58:4<366::aid-jmv8>3.0.co;2-x](https://doi.org/10.1002/(sici)1096-9071(199908)58:4<366::aid-jmv8>3.0.co;2-x)
- Salehi-Ashtiani, K., Luptak, A., Litovchick, A., & Szostak, J. W. (2006). A genomewide search for ribozymes reveals an HDV-like sequence in the human CPEB3 gene. *Science*, 313(5794), 1788-1792. <https://doi.org/10.1126/science.1129308>
- Samuel, D., Zignego, A. L., Reynes, M., Feray, C., Arulnaden, J. L., David, M. F., Gigou, M., Bismuth, A., Mathieu, D., Gentilini, P., & et al. (1995). Long-term clinical and virological outcome after liver transplantation for cirrhosis caused by chronic delta hepatitis. *Hepatology*, 21(2), 333-339.

-
- Sanada, T., Hirata, Y., Naito, Y., Yamamoto, N., Kikkawa, Y., Ishida, Y., Yamasaki, C., Tateno, C., Ochiya, T., & Kohara, M. (2017). Transmission of HBV DNA Mediated by Ceramide-Triggered Extracellular Vesicles. *Cell Mol Gastroenterol Hepatol*, 3(2), 272-283. <https://doi.org/10.1016/j.jcmgh.2016.10.003>
- Sarkis, S., Dabo, S., Lise, M. C., Neuveut, C., Meurs, E. F., Lacoste, V., & Lavergne, A. (2018). A potential robust antiviral defense state in the common vampire bat: Expression, induction and molecular characterization of the three interferon-stimulated genes -OAS1, ADAR1 and PKR. *Dev Comp Immunol*, 85, 95-107. <https://doi.org/10.1016/j.dci.2018.04.006>
- Sato, S., Cornillez-Ty, C., & Lazinski, D. W. (2004). By inhibiting replication, the large hepatitis delta antigen can indirectly regulate amber/W editing and its own expression. *J Virol*, 78(15), 8120-8134. <https://doi.org/10.1128/jvi.78.15.8120-8134.2004>
- Satoh, T., Kato, H., Kumagai, Y., Yoneyama, M., Sato, S., Matsushita, K., Tsujimura, T., Fujita, T., Akira, S., & Takeuchi, O. (2010). LGP2 is a positive regulator of RIG-I- and MDA5-mediated antiviral responses. *Proc Natl Acad Sci U S A*, 107(4), 1512-1517. <https://doi.org/10.1073/pnas.0912986107>
- Sattentau, Q. (2008). Avoiding the void: cell-to-cell spread of human viruses. *Nat Rev Microbiol*, 6(11), 815-826. <https://doi.org/10.1038/nrmicro1972>
- Savva, Y. A., Rieder, L. E., & Reenan, R. A. (2012). The ADAR protein family. *Genome Biol*, 13(12), 252. <https://doi.org/10.1186/gb-2012-13-12-252>
- Schulze, A., Gripon, P., & Urban, S. (2007). Hepatitis B virus infection initiates with a large surface protein-dependent binding to heparan sulfate proteoglycans. *Hepatology*, 46(6), 1759-1768. <https://doi.org/10.1002/hep.21896>
- Shakil, A. O., Hadziyannis, S., Hoofnagle, J. H., Di Bisceglie, A. M., Gerin, J. L., & Casey, J. L. (1997). Geographic distribution and genetic variability of hepatitis delta virus genotype I. *Virology*, 234(1), 160-167. <https://doi.org/10.1006/viro.1997.8644>
- Sharmeen, L., Kuo, M. Y., Dinter-Gottlieb, G., & Taylor, J. (1988). Antigenomic RNA of human hepatitis delta virus can undergo self-cleavage. *J Virol*, 62(8), 2674-2679. <https://doi.org/10.1128/JVI.62.8.2674-2679.1988>
- Sharmeen, L., Kuo, M. Y., & Taylor, J. (1989). Self-ligating RNA sequences on the antigenome of human hepatitis delta virus. *J Virol*, 63(3), 1428-1430. <https://doi.org/10.1128/JVI.63.3.1428-1430.1989>
- Simons, J. N., Pilot-Matias, T. J., Leary, T. P., Dawson, G. J., Desai, S. M., Schlauder, G. G., Muerhoff, A. S., Erker, J. C., Buijk, S. L., Chalmers, M. L., & et al. (1995). Identification of two flavivirus-like genomes in the GB hepatitis agent. *Proc Natl Acad Sci U S A*, 92(8), 3401-3405. <https://doi.org/10.1073/pnas.92.8.3401>
- Sninsky, J. J., Siddiqui, A., Robinson, W. S., & Cohen, S. N. (1979). Cloning and endonuclease mapping of the hepatitis B viral genome. *Nature*, 279(5711), 346-348. <https://doi.org/10.1038/279346a0>
- Stockdale, A. J., Kreuels, B., Henrion, M. Y. R., Giorgi, E., Kyomuhangi, I., de Martel, C., Hutin, Y., & Geretti, A. M. (2020). The global prevalence of hepatitis D virus
-

- infection: Systematic review and meta-analysis. *J Hepatol*, 73(3), 523-532. <https://doi.org/10.1016/j.jhep.2020.04.008>
- Suarez-Amaran, L., Usai, C., Di Scala, M., Godoy, C., Ni, Y., Hommel, M., Palomo, L., Segura, V., Olague, C., Vales, A., Ruiz-Ripa, A., Buti, M., Salido, E., Prieto, J., Urban, S., Rodriguez-Frias, F., Aldabe, R., & Gonzalez-Aseguinolaza, G. (2017). A new HDV mouse model identifies mitochondrial antiviral signaling protein (MAVS) as a key player in IFN-beta induction. *J Hepatol*, 67(4), 669-679. <https://doi.org/10.1016/j.jhep.2017.05.010>
- Sui, L., Zhao, Y., Wang, W., Chi, H., Tian, T., Wu, P., Zhang, J., Zhao, Y., Wei, Z. K., Hou, Z., Zhou, G., Wang, G., Wang, Z., & Liu, Q. (2023). Flavivirus prM interacts with MDA5 and MAVS to inhibit RLR antiviral signaling. *Cell Biosci*, 13(1), 9. <https://doi.org/10.1186/s13578-023-00957-0>
- Summers, J., Smolec, J. M., & Snyder, R. (1978). A virus similar to human hepatitis B virus associated with hepatitis and hepatoma in woodchucks. *Proc Natl Acad Sci U S A*, 75(9), 4533-4537. <https://doi.org/10.1073/pnas.75.9.4533>
- Sureau, C., Guerra, B., & Lanford, R. E. (1993). Role of the large hepatitis B virus envelope protein in infectivity of the hepatitis delta virion. *J Virol*, 67(1), 366-372. <https://doi.org/10.1128/JVI.67.1.366-372.1993>
- Sureau, C., & Salisse, J. (2013). A conformational heparan sulfate binding site essential to infectivity overlaps with the conserved hepatitis B virus a-determinant. *Hepatology*, 57(3), 985-994. <https://doi.org/10.1002/hep.26125>
- Szirovicza, L., Hetzel, U., Kipar, A., & Hepojoki, J. (2022). Short '1.2x Genome' Infectious Clone Initiates Kolmiovirid Replication in Boa constrictor Cells. *Viruses*, 14(1). <https://doi.org/10.3390/v14010107>
- Szirovicza, L., Hetzel, U., Kipar, A., Martinez-Sobrido, L., Vapalahti, O., & Hepojoki, J. (2020). Snake Deltavirus Utilizes Envelope Proteins of Different Viruses To Generate Infectious Particles. *mBio*, 11(2). <https://doi.org/10.1128/mBio.03250-19>
- Tam, A. W., Smith, M. M., Guerra, M. E., Huang, C. C., Bradley, D. W., Fry, K. E., & Reyes, G. R. (1991). Hepatitis E virus (HEV): molecular cloning and sequencing of the full-length viral genome. *Virology*, 185(1), 120-131. [https://doi.org/10.1016/0042-6822\(91\)90760-9](https://doi.org/10.1016/0042-6822(91)90760-9)
- Tavanez, J. P., Cunha, C., Silva, M. C., David, E., Monjardino, J., & Carmo-Fonseca, M. (2002). Hepatitis delta virus ribonucleoproteins shuttle between the nucleus and the cytoplasm. *RNA*, 8(5), 637-646. <https://doi.org/10.1017/s1355838202026432>
- Taylor, J., & Pelchat, M. (2010). Origin of hepatitis delta virus. *Future Microbiol*, 5(3), 393-402. <https://doi.org/10.2217/fmb.10.15>
- Taylor, J. M. (2006). Structure and replication of hepatitis delta virus RNA. *Curr Top Microbiol Immunol*, 307, 1-23. https://doi.org/10.1007/3-540-29802-9_1
- Taylor, J. M. (2009). Chapter 3 Replication of the Hepatitis Delta Virus RNA Genome. In *Advances in Virus Research* (Vol. 74, pp. 103-121). Academic Press. [https://doi.org/https://doi.org/10.1016/S0065-3527\(09\)74003-5](https://doi.org/https://doi.org/10.1016/S0065-3527(09)74003-5)

-
- Taylor, J. M. (2014). Host RNA circles and the origin of hepatitis delta virus. *World J Gastroenterol*, 20(11), 2971-2978. <https://doi.org/10.3748/wjg.v20.i11.2971>
- Ticehurst, J. R., Racaniello, V. R., Baroudy, B. M., Baltimore, D., Purcell, R. H., & Feinstone, S. M. (1983). Molecular cloning and characterization of hepatitis A virus cDNA. *Proc Natl Acad Sci U S A*, 80(19), 5885-5889. <https://doi.org/10.1073/pnas.80.19.5885>
- Timpe, J. M., Stamataki, Z., Jennings, A., Hu, K., Farquhar, M. J., Harris, H. J., Schwarz, A., Desombere, I., Roels, G. L., Balfe, P., & McKeating, J. A. (2008). Hepatitis C virus cell-cell transmission in hepatoma cells in the presence of neutralizing antibodies. *Hepatology*, 47(1), 17-24. <https://doi.org/10.1002/hep.21959>
- Urban, C., Welsch, H., Heine, K., Wüst, S., Haas, D. A., Dächert, C., Pandey, A., Pichlmair, A., & Binder, M. (2020). Persistent Innate Immune Stimulation Results in IRF3-Mediated but Caspase-Independent Cytostasis. *Viruses*, 12(6), 635. <https://www.mdpi.com/1999-4915/12/6/635>
- Vaudin, M., Wolstenholme, A. J., Tsiquaye, K. N., Zuckerman, A. J., & Harrison, T. J. (1988). The complete nucleotide sequence of the genome of a hepatitis B virus isolated from a naturally infected chimpanzee. *J Gen Virol*, 69 (Pt 6), 1383-1389. <https://doi.org/10.1099/0022-1317-69-6-1383>
- Verrier, E. R., Colpitts, C. C., Bach, C., Heydmann, L., Weiss, A., Renaud, M., Durand, S. C., Habersetzer, F., Durantel, D., Abou-Jaoude, G., Lopez Ledesma, M. M., Felmlee, D. J., Soumillon, M., Croonenborghs, T., Pochet, N., Nassal, M., Schuster, C., Brino, L., Sureau, C., . . . Baumert, T. F. (2016). A targeted functional RNA interference screen uncovers glypican 5 as an entry factor for hepatitis B and D viruses. *Hepatology*, 63(1), 35-48. <https://doi.org/10.1002/hep.28013>
- Viana, S., Parana, R., Moreira, R. C., Compri, A. P., & Macedo, V. (2005). High prevalence of hepatitis B virus and hepatitis D virus in the western Brazilian Amazon. *Am J Trop Med Hyg*, 73(4), 808-814. <https://www.ncbi.nlm.nih.gov/pubmed/16222030>
- Viruses, I. C. o. T. o. (2020). *Family : Kolmioviridae*. ICTV. Retrieved 1 December 2023 from https://ictv.global/taxonomy/taxondetails?taxnode_id=202209293&taxon_name=Kolmioviridae
- Walter, S., Rasche, A., Moreira-Soto, A., Pfaender, S., Bletsa, M., Corman, V. M., Aguilar-Setien, A., Garcia-Lacy, F., Hans, A., Todt, D., Schuler, G., Shnaiderman-Torban, A., Steinman, A., Roncoroni, C., Veneziano, V., Rusenova, N., Sandev, N., Rusenov, A., Zapryanova, D., . . . Drexler, J. F. (2017). Differential Infection Patterns and Recent Evolutionary Origins of Equine Hepaciviruses in Donkeys. *J Virol*, 91(1). <https://doi.org/10.1128/JVI.01711-16>
- Wang, K. S., Choo, Q. L., Weiner, A. J., Ou, J. H., Najarian, R. C., Thayer, R. M., Mullenbach, G. T., Denniston, K. J., Gerin, J. L., & Houghton, M. (1986). Structure, sequence and expression of the hepatitis delta (delta) viral genome. *Nature*, 323(6088), 508-514. <https://doi.org/10.1038/323508a0>
- Wang, W., Lempp, F. A., Schlund, F., Walter, L., Decker, C. C., Zhang, Z., Ni, Y., & Urban, S. (2021). Assembly and infection efficacy of hepatitis B virus surface protein
-

- exchanges in 8 hepatitis D virus genotype isolates. *J Hepatol*, 75(2), 311-323. <https://doi.org/10.1016/j.jhep.2021.03.025>
- Wang, Y. (2021). Current view and perspectives in viroid replication. *Curr Opin Virol*, 47, 32-37. <https://doi.org/10.1016/j.coviro.2020.12.004>
- Wang, Y. C., Huang, C. R., Chao, M., & Lo, S. J. (2009). The C-terminal sequence of the large hepatitis delta antigen is variable but retains the ability to bind clathrin. *Virology*, 6, 31. <https://doi.org/10.1186/1743-422X-6-31>
- Webb, C. H., & Luptak, A. (2011). HDV-like self-cleaving ribozymes. *RNA Biol*, 8(5), 719-727. <https://doi.org/10.4161/rna.8.5.16226>
- Webster, D. P., Klennerman, P., & Dusheiko, G. M. (2015). Hepatitis C. *Lancet*, 385(9973), 1124-1135. [https://doi.org/10.1016/S0140-6736\(14\)62401-6](https://doi.org/10.1016/S0140-6736(14)62401-6)
- Wedemeyer, H., & Negro, F. (2019). Devil hepatitis D: an orphan disease or largely underdiagnosed? *Gut*, 68(3), 381-382. <https://doi.org/10.1136/gutjnl-2018-317403>
- Wedemeyer, H., Yurdaydin, C., Dalekos, G. N., Erhardt, A., Cakaloglu, Y., Degertekin, H., Gurel, S., Zeuzem, S., Zachou, K., Bozkaya, H., Koch, A., Bock, T., Dienes, H. P., Manns, M. P., & Group, H. S. (2011). Peginterferon plus adefovir versus either drug alone for hepatitis delta. *N Engl J Med*, 364(4), 322-331. <https://doi.org/10.1056/NEJMoa0912696>
- WHO. (2023). *Hepatitis*. WHO. Retrieved 5 December 2023 from https://www.who.int/health-topics/hepatitis#tab=tab_1
- Wieland, S., Thimme, R., Purcell, R. H., & Chisari, F. V. (2004). Genomic analysis of the host response to hepatitis B virus infection. *Proc Natl Acad Sci U S A*, 101(17), 6669-6674. <https://doi.org/10.1073/pnas.0401771101>
- Wille, M., Netter, H. J., Littlejohn, M., Yuen, L., Shi, M., Eden, J. S., Klaassen, M., Holmes, E. C., & Hurt, A. C. (2018). A Divergent Hepatitis D-Like Agent in Birds. *Viruses*, 10(12). <https://doi.org/10.3390/v10120720>
- Williams, V., Brichtler, S., Khan, E., Chami, M., Deny, P., Kremsdorf, D., & Gordien, E. (2012). Large hepatitis delta antigen activates STAT-3 and NF-kappaB via oxidative stress. *J Viral Hepat*, 19(10), 744-753. <https://doi.org/10.1111/j.1365-2893.2012.01597.x>
- Wong, S. K., & Lazinski, D. W. (2002). Replicating hepatitis delta virus RNA is edited in the nucleus by the small form of ADAR1. *Proc Natl Acad Sci U S A*, 99(23), 15118-15123. <https://doi.org/10.1073/pnas.232416799>
- Woo, P. C., Lau, S. K., Teng, J. L., Tsang, A. K., Joseph, M., Wong, E. Y., Tang, Y., Sivakumar, S., Xie, J., Bai, R., Wernery, R., Wernery, U., & Yuen, K. Y. (2014). New hepatitis E virus genotype in camels, the Middle East. *Emerg Infect Dis*, 20(6), 1044-1048. <https://doi.org/10.3201/eid2006.140140>
- Wu, H. N., Lin, Y. J., Lin, F. P., Makino, S., Chang, M. F., & Lai, M. M. (1989). Human hepatitis delta virus RNA subfragments contain an autocleavage activity. *Proc Natl Acad Sci U S A*, 86(6), 1831-1835. <https://doi.org/10.1073/pnas.86.6.1831>
- Wu, J. C., Chiang, T. Y., & Sheen, I. J. (1998). Characterization and phylogenetic analysis of a novel hepatitis D virus strain discovered by restriction fragment length

- polymorphism analysis. *J Gen Virol*, 79 (Pt 5), 1105-1113. <https://doi.org/10.1099/0022-1317-79-5-1105>
- Xu, C., Chen, J., & Chen, X. (2021). Host Innate Immunity Against Hepatitis Viruses and Viral Immune Evasion. *Front Microbiol*, 12, 740464. <https://doi.org/10.3389/fmicb.2021.740464>
- Yamaguchi, Y., Filipovska, J., Yano, K., Furuya, A., Inukai, N., Narita, T., Wada, T., Sugimoto, S., Konarska, M. M., & Handa, H. (2001). Stimulation of RNA polymerase II elongation by hepatitis delta antigen. *Science*, 293(5527), 124-127. <https://doi.org/10.1126/science.1057925>
- Yamamoto, S., Fukuhara, T., Ono, C., Uemura, K., Kawachi, Y., Shiokawa, M., Mori, H., Wada, M., Shima, R., Okamoto, T., Hiraga, N., Suzuki, R., Chayama, K., Wakita, T., & Matsuura, Y. (2016). Lipoprotein Receptors Redundantly Participate in Entry of Hepatitis C Virus. *PLoS Pathog*, 12(5), e1005610. <https://doi.org/10.1371/journal.ppat.1005610>
- Yan, H., Peng, B., He, W., Zhong, G., Qi, Y., Ren, B., Gao, Z., Jing, Z., Song, M., Xu, G., Sui, J., & Li, W. (2013). Molecular determinants of hepatitis B and D virus entry restriction in mouse sodium taurocholate cotransporting polypeptide. *J Virol*, 87(14), 7977-7991. <https://doi.org/10.1128/JVI.03540-12>
- Yan, H., Peng, B., Liu, Y., Xu, G., He, W., Ren, B., Jing, Z., Sui, J., & Li, W. (2014). Viral entry of hepatitis B and D viruses and bile salts transportation share common molecular determinants on sodium taurocholate cotransporting polypeptide. *J Virol*, 88(6), 3273-3284. <https://doi.org/10.1128/JVI.03478-13>
- Yan, H., Zhong, G., Xu, G., He, W., Jing, Z., Gao, Z., Huang, Y., Qi, Y., Peng, B., Wang, H., Fu, L., Song, M., Chen, P., Gao, W., Ren, B., Sun, Y., Cai, T., Feng, X., Sui, J., & Li, W. (2012). Sodium taurocholate cotransporting polypeptide is a functional receptor for human hepatitis B and D virus. *Elife*, 1, e00049. <https://doi.org/10.7554/eLife.00049>
- Yan, S., Zhu, Q., Hohl, J., Dong, A., & Schlick, T. (2023). Evolution of coronavirus frameshifting elements: Competing stem networks explain conservation and variability. *Proc Natl Acad Sci U S A*, 120(20), e2221324120. <https://doi.org/10.1073/pnas.2221324120>
- Yang, H.-I., Lee, M.-H., Liu, J., & Hu, H.-H. (2019). Epidemiology of Viral Hepatitis B, C, and D: A Global View. In M.-H. Chang & K. B. Schwarz (Eds.), *Viral Hepatitis in Children: Prevention and Management* (pp. 33-53). Springer Singapore. https://doi.org/10.1007/978-981-13-0050-9_3
- Yang, Y., Han, Q., Hou, Z., Zhang, C., Tian, Z., & Zhang, J. (2017). Exosomes mediate hepatitis B virus (HBV) transmission and NK-cell dysfunction. *Cell Mol Immunol*, 14(5), 465-475. <https://doi.org/10.1038/cmi.2016.24>
- Yoshida, Y., Emi, N., & Hamada, H. (1997). VSV-G-pseudotyped retroviral packaging through adenovirus-mediated inducible gene expression. *Biochem Biophys Res Commun*, 232(2), 379-382. <https://doi.org/10.1006/bbrc.1996.5976>

- Zhang, H. L., Ye, H. Q., Liu, S. Q., Deng, C. L., Li, X. D., Shi, P. Y., & Zhang, B. (2017). West Nile Virus NS1 Antagonizes Interferon Beta Production by Targeting RIG-I and MDA5. *J Virol*, 91(18). <https://doi.org/10.1128/JVI.02396-16>
- Zhang, Z., Filzmayer, C., Ni, Y., Sultmann, H., Mutz, P., Hiet, M. S., Vondran, F. W. R., Bartenschlager, R., & Urban, S. (2018). Hepatitis D virus replication is sensed by MDA5 and induces IFN-beta/lambda responses in hepatocytes. *J Hepatol*, 69(1), 25-35. <https://doi.org/10.1016/j.jhep.2018.02.021>
- Zhang, Z., Ni, Y., Lempp, F. A., Walter, L., Mutz, P., Bartenschlager, R., & Urban, S. (2022). Hepatitis D virus-induced interferon response and administered interferons control cell division-mediated virus spread. *J Hepatol*, 77(4), 957-966. <https://doi.org/10.1016/j.jhep.2022.05.023>
- Zhang, Z., & Urban, S. (2020). Interplay between Hepatitis D Virus and the Interferon Response. *Viruses*, 12(11). <https://doi.org/10.3390/v12111334>
- Zhang, Z., & Urban, S. (2021). New insights into HDV persistence: The role of interferon response and implications for upcoming novel therapies. *J Hepatol*, 74(3), 686-699. <https://doi.org/10.1016/j.jhep.2020.11.032>

7. PUBLICATIONS

Xu, Z. M., **Gnouamozi,G.E** ..., Urban S.,Fellay J. Joint host-pathogen genomic analysis identifies hepatitis B virus mutations associated with human *NTCP* and HLA class I variation. *Submitted to Nature Genetics*

ORAL PRESENTATIONS

Gnouamozi,G.E , Zhang, Z., Urban, S. ' Investigation of replication, pseudotyping and IFN responses of woodchuck and deer HDV-like agents in human hepatoma cell lines'. *International HBV Meeting*, Kobe, Japan, September 19-23, 2023.

Gnouamozi,G.E , Seitz, S. , Urban, S. ' Effects of HDV-LHDAG expression and prenylation on replication of HDV and delta- like agents' *International HBV Meeting*, Paris, France, September 18-22, 2022.

Gnouamozi,G.E, Zhang, Z., Lauber, C., Seitz, S. , Urban, S. 'Analysis of replication, cell division-mediated spread and pseudo-typing of the novel mammalian delta-like agents'. *GfV workshop One Health and Zoonotic Viruses*, Goslar, Germany, July 27-29, 2022

Gnouamozi,G.E, Zhang, Z., Lauber, C., Seitz, S. , Urban, S. 'Analysis of replication, cell division-mediated spread and pseudo-typing of the novel mammalian delta-like agents'. *Annual Meeting of the German Society for Virology (GfV)*, Munich, Germany, 30 March – 2 April 2022.

Gnouamozi,G.E , Zhang, Z., Lauber, C., Seitz, S. , Urban, S. ' Analysis of replication, cell division-mediated spread and pseudo-typing of the novel mammalian delta-like agents'. *Workshop 'Recent developments in HDV research '*, Munich, Germany, November 13, 2021, (Invited speaker).

Gnouamozi,G.E , Zhang, Z., Lauber, C., Seitz, S. , Urban, S. ' Analysis of replication, cell division-mediated spread and pseudo-typing of the novel mammalian delta-like agents'. *International HBV Meeting*, Toronto, Canada, September 27-30, 2021.

Gnouamozi,G.E , Zhang, Z., Lauber, C., Seitz, S. , Urban, S. ' Novel mammalian HDV-like agents show distinct cellular tropism and infection pathways independent of hepadnaviruses'. *Virus Genomics and Evolution*, Virtual, September 13-15, 2021.

POSTER PRESENTATIONS

Gnouamozi, G.E. , Seitz, S. , Urban, S. ' Effects of HDV-LHDAG expression and prenylation on replication of HDV and delta- like agents' Annual Meeting of the German Society for Virology (GfV), Ulm, Germany, 28 March – 31 March, 2023.

Gnouamozi, G.E. , Zhang, Z., Lauber, C., Seitz, S. , Urban, S. ' Analysis of replication, cell division-mediated spread and pseudo-typing of the novel mammalian delta-like agents'. International Symposium on Translational Research in Viral Hepatitis, Grainau, Germany, scheduled for April 24-26, 2022.

Gnouamozi, G.E., Fogeron ,M.L., Montserret, R. , Ni, Y. , Böckman, A., Urban, S. 'Functional analyses of mutations of putative phosphorylation sites in the preS1 domain of Hepatitis B Virus large envelope protein'. Annual Meeting of the German Society for Virology (GfV), Berlin, Germany, March 25-27, 2020, (Cancelled due to Covid-19 pandemic).

8. ACKNOWLEDGMENTS

First and foremost, I would like to express my sincere gratitude to my supervisor, Stephan. Your passion for knowledge and insightful guidance have been the foundation for this research and my personal and scientific growth. Thank you for taking the leap of faith five years ago and welcoming me into your research group.

I would also like to thank the members of my thesis committee, Ursula Klingmüller, Loan Dao Thi, and Fredy Frischknecht. Thank you for deciding without hesitation to join this adventure and for your willingness to share your expertise and invaluable suggestions with me.

Thanks to my present and former colleagues, the "AGUs", who have left a lasting impression on my scientific and profane life: Talisa, Angga, Lea, Kuno, Zhenfeng, Lisa, Julius, Franz, Yi, Martina and a special thanks goes to Benno for taking on the burden of proofreading this thesis. Thank you all for your patience, the countless discussions, and the laughter. Each of you has taught me something, and I am grateful for that. A special mention goes to Stefan Seitz, whom I thank for insightful and lively discussions.

This journey would not have been the same without the friendship of two special people: Ombretta and Laura. My greatest gratitude goes to you, who made me feel at home even when home was far away.

My most special acknowledgement goes to my partner in crime, Thore. Your unconditional love, support and understanding have pushed me through so many challenges. I count myself lucky.

Finally, my biggest, warmest, and heartfelt thank you goes to my Mami and Papo. Your sacrifices and belief in my abilities have been my true driving force, especially in the darkest moments. This work is dedicated to you.

